

University of Windsor

## Scholarship at UWindor

---

Electronic Theses and Dissertations

Theses, Dissertations, and Major Papers

---

10-30-2020

# New Designs for Wearable Technologies: Stretchable e-Textiles and e-Skin

Yunyun Wu  
*University of Windsor*

Follow this and additional works at: <https://scholar.uwindsor.ca/etd>

---

### Recommended Citation

Wu, Yunyun, "New Designs for Wearable Technologies: Stretchable e-Textiles and e-Skin" (2020).  
*Electronic Theses and Dissertations*. 8493.  
<https://scholar.uwindsor.ca/etd/8493>

This online database contains the full-text of PhD dissertations and Masters' theses of University of Windsor students from 1954 forward. These documents are made available for personal study and research purposes only, in accordance with the Canadian Copyright Act and the Creative Commons license—CC BY-NC-ND (Attribution, Non-Commercial, No Derivative Works). Under this license, works must always be attributed to the copyright holder (original author), cannot be used for any commercial purposes, and may not be altered. Any other use would require the permission of the copyright holder. Students may inquire about withdrawing their dissertation and/or thesis from this database. For additional inquiries, please contact the repository administrator via email ([scholarship@uwindsor.ca](mailto:scholarship@uwindsor.ca)) or by telephone at 519-253-3000ext. 3208.

**New Designs for Wearable Technologies: Stretchable e-Textiles and e-Skin**

By

**Yunyun Wu**

A Dissertation  
Submitted to the Faculty of Graduate Studies  
through the Department of Chemistry and Biochemistry  
in Partial Fulfillment of the Requirements for  
the Degree of Doctor of Philosophy  
at the University of Windsor

Windsor, Ontario, Canada

2020

© 2020 Yunyun Wu

**New Designs for Wearable Technologies: Stretchable e-Textiles and e-Skin**

by

**Yunyun Wu**

APPROVED BY:

---

H.-J. Chung, External Examiner  
University of Alberta

---

B. Zhou  
Department of Mechanical, Automotive and Materials Engineering

---

S. Rondeau-Gagné  
Department of Chemistry and Biochemistry

---

J. Rawson  
Department of Chemistry and Biochemistry

---

T. Carmichael, Advisor  
Department of Chemistry and Biochemistry

September 10, 2020

## DECLARATION OF CO-AUTHORSHIP/PREVIOUS PUBLICATION

### I. Co-Authorship

I hereby declare that this dissertation incorporates material that is result of joint research, with contributions assessed using Contributor Roles Taxonomy (CRediT) as follows:

*Chapter 2 of the dissertation was co-authored with Sara S. Mechael, Yiting Chen, and Tricia Breen Carmichael. Author contributions are listed below: Conceptualization, Y.W. and T.B.C.; Methodology, Y.W., S.S.M., Y.C., and T.B.C.; Investigation, Y.W., S.S.M., and Y.C.; Writing, Y.W. and T.B.C.; Supervision, T.B.C.*

*Chapter 3 of the dissertation was co-authored with Sara S. Mechael, Cecilia Lerma, R. Stephen Carmichael, and Tricia Breen Carmichael. Author contributions are listed below: Conceptualization, Y.W. and T.B.C.; Methodology, Y.W., S.S.M., and T.B.C.; Investigation, Y.W., C.L., S.S.M., and R.S.C.; Writing, Y.W., T.B.C, and R.S.C.; Supervision, T.B.C.*

*Chapter 4 of the dissertation was co-authored with Sara S. Mechael, Yiting Chen and Tricia Breen Carmichael. Author contributions are listed below: Conceptualization, Y.W. S.S.M. and T.B.C.; Methodology, Y.W., S.S.M., Y.C. and T.B.C.; Investigation, Y.W. and S.S.M; Writing, Y.W. and T.B.C.; Supervision, T.B.C.*

*Chapter 5 of the dissertation was co-authored with Kory Schlingman, Sara S. Mechael, Yiting Chen, and Tricia Breen Carmichael. Author contributions are listed below: Conceptualization, Y.W. and T.B.C.; Methodology, Y.W. and T.B.C.; Investigation, Y.W., K.S., S.S.M. and Y.C.; Writing, Y.W. and T.B.C.; Supervision, T.B.C.*

I am aware of the University of Windsor Senate Policy on Authorship and I certify that I have properly acknowledged the contribution of other researchers to my dissertation, and have obtained written permission from each of the co-author(s) to include the above material(s) in my dissertation.

I certify that, with the above qualification, this dissertation, and the research to which it refers, is the product of my own work.

## II. Previous Publication

This dissertation includes *three* original papers that have been previously published/submitted for publication in peer reviewed journals and *one* original paper that is to be submitted, as follows:

Thesis Chapter	Publication title/full citation	Publication status*
<i>Chapter 2</i>	<i>Yunyun Wu, Sara S. Mechael, Yiting Chen, and Tricia Breen Carmichael. "Solution Deposition of Conformal Gold Coatings on Knitted Fabric for E-textiles and Electroluminescent Clothing" Advanced Materials Technologies 2018, 3, 1700292.</i>	<i>Published</i>
<i>Chapter 3</i>	<i>Yunyun Wu, Sara S. Mechael, Cecilia Lerma, R. Stephen Carmichael and Tricia Breen Carmichael. "Stretchable Ultrasheer Fabrics as Semitransparent Electrodes for Wearable Light-emitting e-Textiles with Changeable Display Patterns" Matter 2020, 2, 882-895.</i>	<i>Published</i>
<i>Chapter 4</i>	<i>"Velour Fabric as an Island-Bridge Architectural Design for Stretchable Textile-Based Lithium-Ion Battery Electrodes"</i>	<i>Submitted</i>
<i>Chapter 5</i>	<i>"Engineering the Cracking Patterns in Stretchable Copper Films Using Acid-Oxidized Poly(dimethylsiloxane) Substrates"</i>	<i>To be Submitted</i>

I certify that I have obtained a written permission from the copyright owner(s) to include the above published material(s) in my dissertation. I certify that the above material describes work completed during my registration as a graduate student at the University of Windsor.

### III. General

I declare that, to the best of my knowledge, my dissertation does not infringe upon anyone's copyright nor violate any proprietary rights and that any ideas, techniques, quotations, or any other material from the work of other people included in my dissertation, published or otherwise, are fully acknowledged in accordance with the standard referencing practices. Furthermore, to the extent that I have included copyrighted material that surpasses the bounds of fair dealing within the meaning of the Canada Copyright Act, I certify that I have obtained a written permission from the copyright owner(s) to include such material(s) in my dissertation.

I declare that this is a true copy of my dissertation, including any final revisions, as approved by my dissertation committee and the Graduate Studies office, and that this dissertation has not been submitted for a higher degree to any other University or Institution.

## ABSTRACT

This dissertation comprises research efforts in addressing the challenges of integration of different materials with mechanical mismatches in stretchable e-textiles and e-skin, with a major focus on the design and fabrication of stretchable e-textiles.

**Chapter 2** describes the solution-based metallization of a knitted textile that conformally coats individual fibers with gold, leaving the void structure intact. The resulting gold-coated textile is highly conductive, with a sheet resistance of  $1.07 \Omega/\text{sq}$  in the course direction. The resistance decreases by 80% when the fabric is stretched to 15% strain and remains at this value to 160% strain. This outstanding combination of stretchability and conductivity is accompanied by durability to wearing, sweating, and washing. Low-cost screen printing of a wax resist is demonstrated to produce patterned gold textiles suitable for electrically connecting discrete devices in clothing. The fabrication of electroluminescent fabric by depositing layers of device materials onto the gold-coated textile is furthermore demonstrated, intimately merging device functionality with textiles for imperceptible wearable devices.

**Chapter 3** presents a new textile-centric design paradigm in which we use the textile structure as an integral part of wearable device design. Coating the open framework structure of an ultrasheer knitted textile with a conformal gold film using solution-based metallization forms gold-coated ultrasheer electrodes that are highly conductive ( $3.6 \pm 0.9 \Omega/\text{sq}$ ) and retain conductivity to 200% strain with  $R/R_0 < 2$ . The ultrasheer electrodes produce wearable, highly stretchable light-emitting e-textiles that function to 200% strain. Stencil printing a wax resist provides patterned electrodes for patterned light emission; furthermore, incorporating soft-contact lamination produces light-emitting textiles that exhibit, for the first time, readily changeable patterns of illumination.

**Chapter 4** demonstrates the strategic use of a warp-knitted velour fabric in an “island-bridge” architectural strain-engineering design to prepare stretchable textile-based lithium ion battery (LIB) electrodes. The velour fabric consists of a warp-knitted framework and a cut pile. We integrate the LIB electrode into this

fabric by solution-based metallization to create the warp-knitted framework current collector “bridges”, followed by selectively deposition of the brittle electroactive material CuS on the cut pile “islands”. As the textile electrode is stretched, the warp-knitted framework current collector elongates, while the electroactive cut pile fibers simply ride along at their anchor points on the framework, protecting the brittle CuS coating from strain and subsequent damage. The textile-based stretchable LIB electrode exhibited excellent electrical and electrochemical performance with a current collector sheet resistance of  $0.85 \pm 0.06 \Omega/\text{sq}$  and a specific capacity of 400 mAh/g at 0.5 C for 300 charging-discharging cycles, as well as outstanding rate capability. The electrical performance and charge-discharge cycling stability of the electrode persisted even after 1000 repetitive stretching-releasing cycles, demonstrating the protective functionality of the textile-based island-bridge architectural strain-engineering design.

**Chapter 5** demonstrates the engineering of metal cracking patterns using the topography from acid-oxidized PDMS. Oxidizing the surface of PDMS with aqueous acid mixture created hierarchical topographies. Coating the surface of acid-oxidized PDMS with copper using electroless deposition produced stretchable conductors with a sheet resistance of  $\sim 1.2 \Omega/\text{sq}$ . The cracking patterns of copper films with strain were tuned by simply adjusting the composition of acid mixture to change the topography of PDMS, which affects the resistance change of copper films with strain. The Cu films with an optimal cracking pattern on acid-treated PDMS remain conductive to 85% strain with  $R/R_0$  less than 20.



## DEDICATION

*To my family and people who have inspired, encouraged, and supported me.*

## ACKNOWLEDGEMENTS

First of all, I would like to express my sincere gratitude to my supervisor Dr. Tricia Breen Carmichael for her constant support and guidance. I am especially grateful for her consistent belief in my capabilities, her encouragement, and the freedom she has given me to pursue various research ideas.

I would like to thank my committee members, Dr. Jeremy Rawson and Dr. Simon Rondeau-Gagné, for agreeing to be on my committee and also for providing insightful comments and feedback on my research projects at my committee meetings. I would like to extend further thanks to Dr. Jeremy Rawson for his kind and generous financial support at the beginning of my graduate study. I would also like to thank Dr. Biao Zhou for agreeing to be my outside program reader and Dr. Hyun-Joong Chung for agreeing to be my external examiner.

I would like to thank Steve Carmichael, not only for his contribution to my research, but also for the conversations we have, which help relieve my stress and broaden my knowledge of wine, coffee, and the English language. I extend further thanks to him for preparing delicious food at our group parties.

I would like to thank Dr. Yiting Chen who has been by my side during these past five years as a close and caring friend. Thanks to her for training, helping, and encouraging me in countless situations. I would like to thank Sara S. Mechael not only for her contribution to all of my research projects but also for her being a caring and dependable friend. I would also like to thank Kory Schlingman for always being helpful as a supportive friend.

I would like to thank Cecilia Lerma, Kathy Nguyen, and Aida Gabriela for their assistance with my research projects. I would also like to thank Dr. Akhil Vohra, Dr. Elodie Heyer, Dr. Yassine Beldjoudi, Dr. Alex Stirk, Dr. Jagan Meena and Dr. Bing Liu for their patience and knowledge when I have questions to ask. I would like to thank Brittany Ives, Dominique Leckie, Mitchell Nascimento, Jincheng Xu, Junyang Liu, Ruixue Su, Dalia Kashash, Erica Dionisi, Calum Noade, Lauren Renaud, Nihar Shah, and Rahaf Hussein for their helpful, friendly, and enjoyable conversations. I would also like to thank Sha Zhu, WZ, QLW, JJW and KFS for their companionship.

I would like to thank the staff in the Department of Chemistry, especially Marlene Bezaire, Elizabeth Kickham and Joe Lichaa for their help and support. I would also like to thank Una Lee, Nedhal Al-Nidawy and Dr. Ronan San Juan for the help with teaching in undergraduate labs and their helpful and friendly conversations. I would also like to thank the Academic Writing Advisors at the University of Windsor for their support.

I would like to thank the following people from the Faculty of Engineering: Dr. Xueyuan Nie for access to the battery test system and Tao Li and Chen Zhao for their helpful discussions on batteries. I would also like to thank Sharon Leckie from GLIER for her technical support with taking SEM images.

Last but not least, I would like to thank my family for their unconditional support for all my pursuits.

## TABLE OF CONTENTS

DECLARATION OF CO-AUTHORSHIP/PREVIOUS PUBLICATION .....	iii
ABSTRACT.....	vi
DEDICATION.....	viii
ACKNOWLEDGEMENTS.....	ix
LIST OF FIGURES .....	xiv
LIST OF SUPPLEMENTARY FIGURES.....	xx
LIST OF ABBREVIATIONS/SYMBOLS/UNITS.....	xxiii
Chapter 1 Introduction .....	1
1.1 Development of Electronics: from Rigid to Stretchable .....	2
1.2 Strategies to Stretchable Electronics Design.....	3
1.3 Elastomer-Based Electronics: e-Skin .....	4
1.3.1 Elastomer Substrates.....	4
1.3.2 Elastomer-Based Stretchable Conductors.....	5
1.4 Textile-Based Electronics: e-Textiles.....	12
1.4.1 Textile Structures and Properties .....	13
1.4.2 Conductive Textiles .....	15
1.4.3 Light-Emitting Textiles.....	19
1.4.4 Energy-Storage Textiles.....	22
1.5 Summary and Scope of Dissertation .....	25
1.6 References .....	27
Chapter 2 Solution Deposition of Conformal Gold Coatings on Knitted Fabric for E-Textiles and Electroluminescent Clothing.....	45
2.1 Introduction .....	46
2.2 Results and Discussion .....	48

2.3 Conclusions .....	57
2.4 Experimental.....	57
2.5 References .....	59
2.6 Supporting Information .....	63
Chapter 3 Stretchable Ultrasheer Fabrics as Semitransparent Electrodes for Wearable Light-Emitting e-Textiles with Changeable Display Patterns .....	68
3.1 Introduction .....	69
3.2 Results and Discussion .....	71
3.3 Conclusions .....	84
3.4 Experimental.....	85
3.5 References .....	87
3.6 Supporting Information .....	90
Chapter 4 Velour Fabric as an Island-Bridge Architectural Design for Stretchable Textile-Based Lithium-Ion Battery Electrodes .....	97
4.1 Introduction .....	98
4.2 Results and discussion.....	101
4.3 Conclusions .....	110
4.4 Experimental.....	111
4.5 References .....	113
4.6 Supporting Information .....	119
Chapter 5 Engineering the Cracking Patterns in Stretchable Copper Films Using Acid-Oxidized Poly(dimethylsiloxane) Substrates .....	122
5.1 Introduction .....	123
5.2 Results and Discussion .....	126
5.3 Conclusions .....	134
5.4 Experimental.....	135

5.5 References .....	136
5.6 Supporting Information .....	140
Chapter 6 Conclusion and Outlook .....	143
APPENDICES .....	147
Copyright Permissions.....	147
VITA AUCTORIS .....	162

## LIST OF FIGURES

<b>Figure 1-1</b> A schematic to describe a) "rigid islands" and b) "fully stretchable" approach (adapted with permission from reference [34]).	4
<b>Figure 1-2</b> Schematic to describe a) the rupture of a freestanding metal film caused by local thinning and b) the suppression of local elongation by the substrate for a metal film well bonded to a substrate (adapted with permission from reference [39]). c) Optical microscope image of evaporated gold film on PDMS under 20% strain. The sample was stretched in the vertical direction. Scale bar = 80 $\mu\text{m}$ (adapted with permission from reference [43]. Copyright [2015] American Chemical Society).	6
<b>Figure 1-3</b> Images of wrinkled gold film induced by a) thermal mismatch (adapted with permission from reference [41]), b) uniaxial strain mismatch (adapted with permission from reference [48], copyright [2004] IEEE) and c) omnidirectional strain mismatch (adapted with permission [52]).	7
<b>Figure 1-4</b> Optical microscope images of serpentine gold wires at a) 0% and b) 50% strain. Scale bar = 100 $\mu\text{m}$ (adapted with permission from reference [53]). c) Optical images of "self-similar" serpentine gold wires stretching at 0-300% strain. Inset: illustration of "self-similar" serpentine geometries. Scale bar = 2 mm (adapted with permission from reference [55]).	8
<b>Figure 1-5</b> Optical images of a gold film on rough PDMS at a) 5%, b) 20%, c) 30% and d) 40% strain (adapted with permission from reference [45]). Optical images of a gold film on polymer-coated PDMS at e) 5%, f) 25% and g) 60% strain. Scale bar = 40 $\mu\text{m}$ (adapted with permission from reference [43]. Copyright [2015] American Chemical Society).	10
<b>Figure 1-6</b> SEM of a gold film on PDMS with microcrack morphology at a) 0% and b) 20% strain (adapted with permission from reference [61]). SEM of a gold film on PDMS prepared using ELD of Ni followed by immersion gold at c) 0% and d) 30% strain (adapted with permission from reference [63]. Copyright [2019] American Chemical Society).	11
<b>Figure 1-7</b> Illustration to show that electronic textiles can be used for power sources, information technology, the IoT, artificial intelligence, public health, and space exploration (reproduced with permission from reference [78]).	13

<b>Figure 1-8</b> Schematic to show the textile hierarchy and structures (adapted with permission from reference [73]).	14
<b>Figure 1-9</b> Optical images of metal wires a) woven (adapted with permission from reference [87]) and b) knitted into fabrics (adapted with permission from reference [90]).	16
<b>Figure 1-10</b> SEM images of the a) woven fabric coated with PEDOT:PSS (adapted with permission from reference [114]) and b) knitted fabric printed with the specialized conductive Ag ink. Scale bar = 300 $\mu\text{m}$ (adapted with permission from reference [123]).	17
<b>Figure 1-11</b> a) Optical images of PEDOT-coated textiles and threads pulled from these fabrics after PEDOT coating. b) An illustration showing that only one side of the fabric is coated with PEDOT (adapted with permission from reference [126]).	18
<b>Figure 1-12</b> Photograph of a) LED textile display prototype (adapted with permission from reference [150]). b) Photograph and c) schematic diagram of OLEDs fabricated on fabric substrates (adapted with permission from reference [153]). d) Photograph of a flexible LEC textile during deformation between two fingers (adapted with permission from reference [157]). e) Photographs of the stretchable ACEL fabric at 0-100% strain (adapted with permission from reference [163]).	20
<b>Figure 1-13</b> a) Photographs and SEM images showing durability between the foil-based conventional electrode and the textile battery electrode and b) photograph of solar-charged textile battery (adapted with permission from reference [173]. Copyright [2013] American Chemical Society). SEM images of c) front and d) cross-section of the $\text{LiCoO}_2$ fabric electrode (adapted with permission from reference [185]).	24
<b>Figure 2-1</b> The weft-knitted textile structure. a) Schematic of the weft-knitted textile structure. b) Stereomicroscope image of the pristine textile. Illustrations and optical microscope images of PVD gold-coated textiles stretched in the c,d) course direction and e,f) wale direction, respectively. Red circles show examples of locations where gold deposition was blocked.	49



**Figure 2-2** The weft-knitted textile coated with gold using ENIG. a) Stereomicroscope image of the gold-coated textile. Optical microscope images of the gold-coated textile stretched b) in the wale direction and c) in the course direction under 50% strain. SEM images of d) pristine and e) gold-coated textile. f) Cross-sectional SEM image of the gold-coated textile. ....51

**Figure 2-3** Patterning gold deposition on the knitted textile by wax screen printing. a) Schematic of the patterning process. Optical microscope images of gold lines with widths b) 1000  $\mu\text{m}$ , c) 800  $\mu\text{m}$ , d) 500  $\mu\text{m}$ , e) 300  $\mu\text{m}$ . Optical microscope images of linear gaps in gold with widths f) 1000  $\mu\text{m}$ , g) 800  $\mu\text{m}$ , h) 500  $\mu\text{m}$ , i) 300  $\mu\text{m}$ . Scale bar = 400  $\mu\text{m}$ . ....52

**Figure 2-4** Stretchability, wearability, and durability of the gold-coated textile. a) Normalized change in resistance as a function of stretching strain along the course (black line) and wale (red line) direction. b) Photograph of gold-coated fabric sewn onto the knee section of exercise pants. c) Normalized change in sheet resistance after simulated laundry cycles. ....54

**Figure 2-5** Electroluminescent fabric. a) Schematic of electroluminescent fabric structure. b) Photographs of electroluminescent fabric at 0-40% strain. Wearable electroluminescent fabric photographed alongside a retroreflective strip c) with and d) without an external light source.....56

**Figure 3-1** The ultrasheer knitted fabric coated with gold. Schematic and stereomicroscope images (inset) of the a) uncoated ultrasheer fabric and b) gold-coated ultrasheer fabric. SEM images of c) uncoated ultrasheer fabric and d) gold-coated ultrasheer fabric. e) Close-up SEM image of gold-coated spandex fiber....72

**Figure 3-2** Transmittance of the gold-coated ultrasheer fabric with strain. a) Transmittance measured at 550 nm (black line) and transmittance calculated using the cover factor (CF) (red line) as a function of stretching strain in the wale direction. Optical microscope images of gold-coated ultrasheer fabric stretched in the wale direction at b) 0%, c) 120% and d) 200% strain. e) Transmittance measured at 550 nm (black line) and transmittance calculated using the cover factor (CF) (red line) as a function of stretching strain in the course direction. Optical microscope images

of gold-coated ultrasheer fabric stretched in the course direction at f) 0%, g) 160% and h) 200% strain. .... 75

**Figure 3-3** Resistance of the gold-coated ultrasheer fabric with strain. a) Normalized change in resistance as a function of stretching strain along the wale (black line) and course (red line) direction. b) SEM image of the gold-coated ultrasheer fabric stretched to 40% strain. c) SEM image of a gold-coated spandex fiber removed from ultrasheer fabric and stretched to 40% strain. d) Plot of normalized resistance of gold-coated spandex fibers as a function of stretching strain. .... 78

**Figure 3-4** Light-emitting e-textiles fabricated using gold-coated ultrasheer fabric electrodes. a) Diagram of the device structure. Optical microscope images of b) top-view and c) cross-section of the device. Photographs of light-emitting e-textiles d) at twisted state; e) at 0%, 100%, and 200% strain; f) with large area (3 cm × 5cm) conformal to human arm. g) Normalized change in radiance as a function of stretching strain in wale (black line) and course (red line) direction. h) Transmittance measured at 550 nm of encapsulated gold-coated ultrasheer fabric as a function of stretching in the wale (black line) and course (red line) direction. i) Normalized change in radiance as a function of cycles of 0-50% strain in wale (black line) and course (red line) direction. .... 80

**Figure 3-5** Patterned light-emitting e-Textiles. a) Schematic of the patterning process. Photographs of light-emitting textiles displaying b) the “smiling face” emoji, c) a rectangular spiral, and d) the number 8. .... 83

**Figure 3-6** Patterned light-emitting e-textiles with changeable patterns of light emission. a) Schematic of the pattern changing process. b) Photographs of changeable patterned e-textile worn on a mannequin leg. .... 84

**Figure 4-1** Structure of the warp-knitted velour fabric. Schematic of a) front side, b) back side and c) cross-section of the velour fabric. d) Schematic of the warp-knitted velour fabric stretched in the course direction. SEM images of e) front side, f) back side and g) cross-section of the warp-knitted velour fabric..... 101

**Figure 4-2** Fabrication of the velour fabric LIB electrode. a) Schematic of the velour fabric LIB electrode fabrication process. Cross-sectional optical microscope images of the velour fabric b) before and after c) Au, d) Cu and e) CuS deposition..... 103

**Figure 4-3** Sequential, selective, and conformal deposition of Au, Cu and CuS on the velour fabric. Elemental mapping of the velour fabric after a) Au, b) Cu and c) CuS deposition. [Yellow = Au, Blue = Cu, Purple = S]. SEM images of d) Au-coated cut pile fibers, e) Cu/Au-coated cut pile fibers and f) CuS/Au-coated cut pile fibers. g) High magnification SEM image of the CuS coating on the Au-coated cut pile fiber. h) XRD patterns of the velour fabric after Au (red line) and CuS (black line) deposition. i) EDX of the CuS/Au-coated cut pile fiber. .... 104

**Figure 4-4** Electrochemical performance of the velour fabric LIB electrode. a) CV curves of the velour fabric LIB electrode at 0.1 mV/s. b) Charge-discharge profiles and c) cycling ability of the velour fabric LIB electrode at 0.5 C (1 C = 560 mA/g) at 1.3-2.6 V. d) Rate capability of the velour fabric LIB electrode at sequential current rates. .... 106

**Figure 4-5** Electrical and electrochemical performance of the velour fabric LIB electrode with strain. a) Schematic of stretching the velour fabric LIB electrode. Optical microscope images of the front-side of the velour fabric LIB electrode b) unstretched and c) stretched under 50% strain. Cross-sectional SEM images of the velour fabric LIB electrode d) unstretched and e,f) stretched under 50% strain. g) Normalized change in resistance of the velour fabric LIB electrode as a function of stretching strain. h) Normalized change in resistance of the velour fabric LIB electrode during 1000 cycles of 0 to 50% strain. i) Relative capacity versus charging-discharging cycles of the velour fabric LIB electrode before (black line) and after 1000 stretching-releasing cycles at 50% strain (red line). .... 109

**Figure 5-1** Optical microscope images of uncoated a) ACID<sub>65</sub>/PDMS, b) ACID<sub>58</sub>/PDMS, and c) ACID<sub>52</sub>/PDMS. .... 127

**Figure 5-2** AFM images (left), AFM profile (middle) and high-magnification AFM images (right) of uncoated a,d,g) ACID<sub>65</sub>/PDMS, b,e,h) ACID<sub>58</sub>/PDMS, and c,f,i) ACID<sub>52</sub>/PDMS. .... 127

**Figure 5-3** Optical microscope images (top), SEM images (middle) and high-magnification SEM images (bottom) of the copper film on a-c) ACID<sub>65</sub>/PDMS, d-f) ACID<sub>58</sub>/PDMS, and g-i) ACID<sub>52</sub>/PDMS. .... 129

**Figure 5-4** Optical microscope images showing the evolution of cracks of the Cu film on a-c) ACID<sub>65</sub>/PDMS, e-g) ACID<sub>58</sub>/PDMS, and i-k) ACID<sub>52</sub>/PDMS at 10% (first row), 20% (second row), and 80% (third row) strain. Optical microscope images of uncoated d) ACID<sub>65</sub>/PDMS, h) ACID<sub>58</sub>/PDMS, and l) ACID<sub>52</sub>/PDMS at 80% strain. All the samples were stretched in the horizontal direction..... 131

**Figure 5-5** Plot of normalized resistance as a function of strain for copper films on ACID<sub>65</sub>/PDMS (blue triangles), ACID<sub>58</sub>/PDMS (red circles), and ACID<sub>52</sub>/PDMS (black squares). Inset: plot of normalized resistance as a function of strain from 0% to 30% for copper films on ACID<sub>58</sub>/PDMS (red circles) and ACID<sub>52</sub>/PDMS (black squares). ..... 132

**Figure 5-6** SEM images of the copper film at 20% strain on a,b) ACID<sub>65</sub>/PDMS, c,d) ACID<sub>58</sub>/PDMS and e,f) ACID<sub>52</sub>/PDMS. .... 132

## LIST OF SUPPLEMENTARY FIGURES

<b>Figure S2-1</b> Photographs of a) face and b) back of gold-coated fabric (approximately 3 cm × 3 cm).....	63
<b>Figure S2-2</b> SEM image of the gold-coated textile.....	64
<b>Figure S2-3</b> a) X-ray diffraction patterns and b) energy dispersive X-ray spectroscopy of gold-coated textiles. ....	64
<b>Figure S2-4</b> Optical microscope image of cold wax medium printed on the knitted textile.....	64
<b>Figure S2-5</b> Plots of the width of the resulting a) gold lines and b) linear gaps in gold films as a function of the nominal line width of the stencil mask. ....	65
<b>Figure S2-6</b> Stress strain curve of pristine fabric (black line) and gold-coated fabric (red line) in the a) wale direction and b) course direction. ....	65
<b>Figure S2-7</b> Photographs and optical microscope images of the tape after tape test of gold-coated textiles a,b) with APTES treatment and c,d) without APTES treatment. ....	66
<b>Figure S2-8</b> SEM images of gold-coated textile at 20% strain stretched a,b) in the wale direction and c,d) in the course direction. ....	66
<b>Figure S2-9</b> Normalized resistance of the gold-coated textile over 100 stretch-release cycles of 40% strain a) in the wale direction and b) in the course direction. ....	67
<b>Figure S3-1</b> a) Photograph of uncoated ultrasheer fabric. b) UV-visible spectra of uncoated ultrasheer fabric and gold-coated ultrasheer fabric. ....	90
<b>Figure S3-2</b> Stress strain curve of uncoated ultrasheer fabric (black line) and gold-coated ultrasheer fabric (red line) a) in the wale direction and b) in the course direction. ....	91
<b>Figure S3-3</b> Cross-sectional SEM of gold-coated ultrasheer fabric. ....	91
<b>Figure S3-4</b> a) Energy-dispersive X-ray spectroscopy and b) X-ray diffraction patterns of gold-coated ultrasheer fabric.....	92
<b>Figure S3-5</b> Optical microscope image of the tape surface after tape test of gold-coated ultrasheer fabric with APTES treatment.....	92

<b>Figure S3-6</b> Optical microscope images (top rows) and the corresponding images generated from ImageJ (bottom rows) used for cover factor calculation of gold-coated ultrasheer fabric stretched in the wale direction under different strains. The scale bar at the bottom right is for all the images. ....	93
<b>Figure S3-7</b> Optical microscope images (top rows) and the corresponding images generated from ImageJ (bottom rows) used for cover factor calculation of gold-coated ultrasheer fabric stretched in the course direction under different strains. The scale bar at the bottom right is for all the images. ....	94
<b>Figure S3-8</b> Normalized resistance of gold-coated ultrasheer fabric over 1000 stretch-release cycles of 50% strain a) in the wale direction and b) in the course direction. ....	95
<b>Figure S3-9</b> Photographs of light-emitting e-textiles a) folded into and S-shape inside a vial and b) submerged in water. c) Normalized change in radiance as a function of simulated washing cycles. ....	95
<b>Figure S3-10</b> Photographs of a) seven-segment display fabricated using patterned gold-coated ultrasheer fabric and b) light-emitting textile seven-segment display displaying numbers from 0 to 9. ....	96
<b>Figure S4-1</b> Stress strain curve of the velour fabric in the wale (red line) and course (black line) direction. ....	119
<b>Figure S4-2</b> Optical microscope images of the warp-knitted velour fabric stretched at a) 0% and b) 10% strain in the wale direction and at c) 0%, d) 50% and e) 100% strain in the course direction. ....	119
<b>Figure S4-3</b> Optical microscope image of the backside of the velour fabric LIB electrode. ....	120
<b>Figure S4-4</b> Schematic of the coin cell configuration. ....	120
<b>Figure S4-5</b> Charge-discharge profiles at various current rates. ....	121
<b>Figure S4-6</b> SEM image of velour fabric LIB electrode under 20% strain, showing the cracking of gold coating on spandex fiber. ....	121
<b>Figure S5-1</b> Optical microscope images of uncoated ACID <sub>65</sub> /PDMS under different strains. The sample was stretched in the horizontal direction. ....	140

**Figure S5-2** Optical microscope images of uncoated ACID<sub>58</sub>/PDMS under different strains. The sample was stretched in the horizontal direction. .... 141

**Figure S5-3** Optical microscope images of uncoated ACID<sub>52</sub>/PDMS under different strains. The sample was stretched in the horizontal direction. .... 142

**Figure S5-4** Optical microscope image of the copper film on ACID<sub>65</sub>/PDMS under 40% strain. During ELD of copper on this sample, a bubble or other defect likely prevented the copper deposition on the circular area. The circular area thus reveals the underlying substrate and its response to strain. The sample was stretched in the horizontal direction. .... 142

## LIST OF ABBREVIATIONS/SYMBOLS/UNITS

%	percent
~	approximately
±	plus or minus
>	greater than
×	time
=	equal
°	degree
°C	degree Celsius
μm	micrometer
Ω	ohm
3D	three-dimensional
2D	two-dimensional
1D	one-dimensional
AC	alternating current
ACEL	alternating current electroluminescent
AFM	atomic force microscopy
APTES	3-aminopropyltriethoxysilane
CF	cover factor
cm	centimeter
CV	cyclic voltammetry
DI	deionized
e-beam	electron beam
e-skin	electronic skin
e-textiles	electronic textiles
EDX	energy-dispersive X-ray spectroscopy
ELD	electroless deposition
ENIG	electroless nickel immersion gold
g	gram
GPa	gigapascal



h	hour
IoT	Internet of Thing
kHz	kilohertz
kV	kilovolt
L	liter
LEC	light-emitting electrochemical cell
LED	light-emitting diode
LIB	lithium-ion battery
mA	milliampere
min	minutes
MPa	megapascal
mm	millimeter
OLED	organic light-emitting diode
PDMS	polydimethylsiloxane
PEDOT: PSS	poly(3,4-ethylenedioxythiophene) polystyrene sulfonate
PVD	physical vapor deposition
R	resistance
rpm	rotations per minute
SEM	scanning electron microscopy
sq	square
T	transmittance
UV	ultraviolet
V	volt
v/v	volume/volume ratio
w:w	weight/weight ratio
wt%	weight percent
XRD	X-ray diffraction

**Chapter 1 Introduction**

## 1.1 Development of Electronics: from Rigid to Stretchable

Since the invention of transistors and integrated circuits around the 1950s, the research interest in electronics has sought to increase transistors' switch speeds and density in order to create more electronic functions that can be integrated in limited space.<sup>1</sup> After 70 years of development, modern electronic technologies have matured, and electronic devices and circuits have dramatically miniaturized while maintaining and even improving performance. Electronic systems that are based on silicon wafers have traditionally been built on rigid printed circuit boards and packaged in hard and bulky boxes. Personal computers and smartphones are typical examples of integrated circuits, and they have fundamentally changed human life since the 1980s.

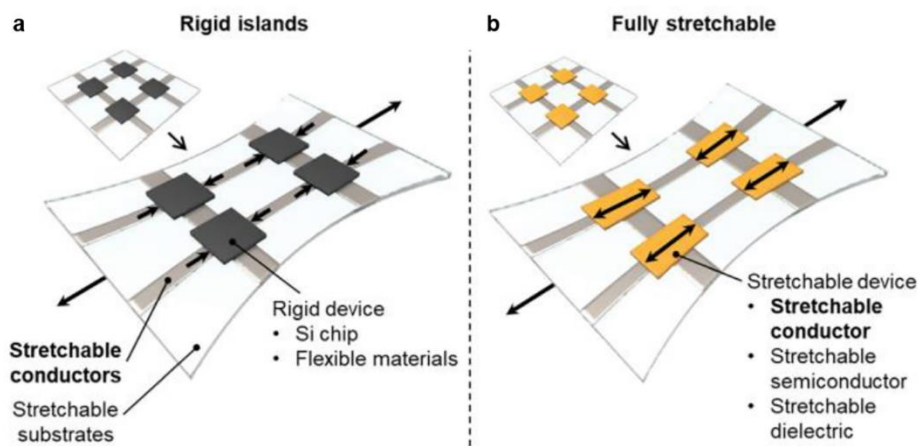
Nowadays, an emerging research frontier of electronics is to develop mechanically unconventional forms of electronics that have superior mechanical attributes while maintaining the functionalities of established electronic technologies. The main characteristics of these types of electronics are stretchability, softness, compliance, and even self-healability, rather than just circuit operating speeds and integration densities. By virtue of these characteristics, these electronics can enable many interesting and innovative applications that are not possible to achieve with conventional electronics alone. These types of electronics, termed stretchable electronics, emerged in the 1990s. With decades of development, the application scope of stretchable electronics has become broad. There are several representative demonstrations of these new conceptual electronic devices, most notably skin-like epidermal health monitors,<sup>2-4</sup> soft biomedical interfaces and implantable circuitry,<sup>5-8</sup> large-area stretchable displays,<sup>9-11</sup> electronic "eyeball" imaging devices,<sup>12-14</sup> stretchable and/or self-healable transistors,<sup>15-17</sup> and electronic textile conformal suit.<sup>18</sup> These flexible, stretchable, conformable, and large-area electronics are expected to revolutionize a wide range of applications in different fields, such as healthcare, communication and entertainment, sports, space exploration, and public safety.

In particular, rendering electronics soft and stretchable by, for example, matching the Young's modulus of human skin, will make electronics more comfortable to wear and accelerate the adoption of wearable electronics into our daily life. Wearable electronics are expected to enrich daily lives and improve the quality of life by providing smart functions or wellness information. They can also accelerate the realization of the "Internet of Things"

(IoT), which integrates and connects people, processes, data, and devices. This new way of connection can particularly aid us to transform our healthcare system and address the challenges coming from population aging. For example, using the IoT platform, the wellness information can be distributed and processed. Then, the data is sent back to the user as bio-feedback. This new healthcare system can help us take better care of older adults.

## 1.2 Strategies to Stretchable Electronics Design

The first step to render electronics stretchable is to replace rigid printed circuit boards with stretchable and soft substrates, such as elastomers and textiles, which have become prevalent substrates for stretchable electronics. Based on stretchable substrates, two design strategies are mainly adopted to implement stretchable electronics. One is to deploy rigid electronic components on stretchable substrates as “islands” bridged by stretchable interconnects (**Figure 1-1a**). Due to the large Young’s modulus contrast within this island-bridge structure, upon stretching, stress is mostly concentrated on the stretchable interconnects; rigid electronic components are thus isolated from the strain. This strategy allows the use of conventional high-performance electronic components but at relatively low coverages. Failures often occur at the interface between soft and hard materials due to stress localization. The other approach is to fabricate a fully stretchable system including substrates and electronic components, such as conductors, dielectrics, and semiconductors (**Figure 1-1b**). The main challenge is the integration of different materials with mechanical mismatches and the simultaneous achievement of excellent mechanical and electronic performance. Innovative material designs and structural mechanics designs have been proposed to meet the challenge by developing intrinsically stretchable materials or configuring traditional non-stretchable electronic materials into certain architectures that can stretch.



**Figure 1-1** A schematic to describe a) "rigid islands" and b) "fully stretchable" approach (adapted with permission from reference [34]).

In both types of stretchable electronic systems discussed above, stretchable conductors are the basic building blocks. They can provide electrical connections between individual devices as interconnects, contact other functional materials as electrodes within stretchable devices or act as active sensing components themselves based on electrical performance change with stimuli. The electrical conductance and the critical strain at which conduction is lost or substrates cannot be stretched any more are the two primary performance parameters for stretchable conductors. Furthermore, they are also expected to sustain reversible stretching.

### 1.3 Elastomer-Based Electronics: e-Skin

Creating stretchable electronics based on elastomers is an important branch of stretchable electronics. These elastomer-based electronics are often referred to as electronic skin (e-skin) since they have potential to mimic functionalities of human skin, such as elasticity, sensing, and self-healing.<sup>19-21</sup> There are wide applications for e-skin, most notably in soft robotics, prosthetics, and health monitoring technologies. For example, they can be attached to human skin as health monitors or function as skin in prosthetics or robotics for autonomous artificial intelligence.

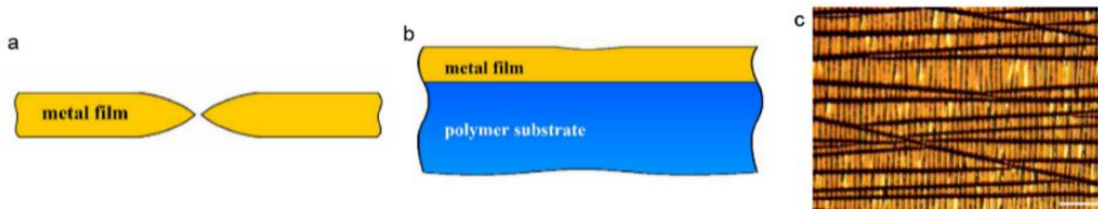
#### 1.3.1 Elastomer Substrates

Elastomers that are characterized by high stretchability, such as polydimethylsiloxane (PDMS),<sup>22</sup> Ecoflex,<sup>23</sup> polyurethane,<sup>24</sup> poly(isobutylene-co-isoprene),<sup>25</sup> and polystyrene-block-poly(ethylene-*ran*-butylene)-block-polystyrene,<sup>26</sup> have

been employed as the supporting substrate for stretchable electronics. PDMS, a commercially available silicone-based elastomer, is the most extensively used due to its excellent physical and chemical properties, such as high stretchability, biocompatibility, optical transparency, and moldability.<sup>27</sup> The repeat unit of PDMS is  $-\text{[SiO(CH}_3\text{)}_2\text{]}-$  and its backbone typically adopts a helical conformation, in which the inner part constitutes siloxane units and the outer part methyl groups.<sup>28</sup> The polymer chains are crosslinked to form a reversibly stretchable network. The methyl groups pointing to the outside render the PDMS surface hydrophobic, which can be modified to be hydrophilic by plasma oxidation,<sup>29</sup> UV/ozone exposure<sup>30</sup> or acid oxidation.<sup>31</sup> The modification usually creates a thin stiff layer on the surface of PDMS.

### 1.3.2 Elastomer-Based Stretchable Conductors

Elastomers are usually nonconductive. To produce elastomer-based stretchable conductors, conductive materials, such as carbon-based nanomaterials, metal films, metallic nanowires, liquid metals, and conducting polymers, have been integrated with elastomers either as thin films to form a bilayer stack or as fillers to form a composite.<sup>32-35</sup> Among the conductive materials, metal films are materials of choice because they are highly conductive and widely used as interconnects in conventional circuits. Deposition of metal films on the surface of PDMS to fabricate stretchable conductors has been extensively studied.<sup>36</sup> Typical free-standing metal thin films cannot extend to high strains; they rupture at  $\sim 1\%$  tensile strain due to localized plastic deformation, such as local thinning (**Figure 1-2a**).<sup>37-39</sup> While finite element simulations have shown that bonding the metal thin film to a substrate can suppress strain localization (**Figure 1-2b**),<sup>40</sup> metal films deposited on PDMS often exhibit detrimental channel cracks under strain due to the huge mechanical mismatch between the metal film (modulus of GPa magnitude) and PDMS substrate (modulus of MPa magnitude) (**Figure 1-2c**).<sup>41-45</sup> The channel cracks, which are perpendicular to the tensile direction, traverse the entire width of the metal film and cut off the flow of current.



**Figure 1-2** Schematic to describe a) the rupture of a freestanding metal film caused by local thinning and b) the suppression of local elongation by the substrate for a metal film well bonded to a substrate (adapted with permission from reference [39]). c) Optical microscope image of evaporated gold film on PDMS under 20% strain. The sample was stretched in the vertical direction. Scale bar = 80  $\mu\text{m}$  (adapted with permission from reference [43]. Copyright [2015] American Chemical Society).

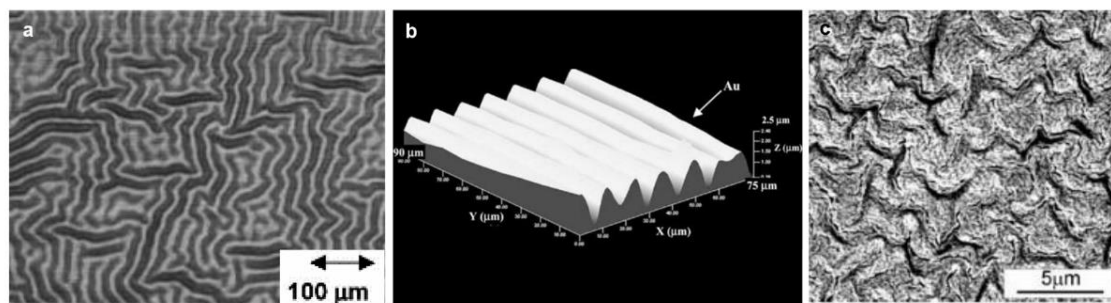
Many approaches have been developed to retain the conductivity of metal films on PDMS under strain. They can be mainly classified into two types of categories. One prevents the cracking of metal films with stretching using structural mechanics designs; the other allows metal films to crack but rationally engineers the cracking patterns.

#### *Using structural mechanics design to prevent metal films from cracking*

Metal in the form of a thin film is not stretchable but has good bendability/flexibility due to the linear decrease in bending strain with thickness and bending curvature. Configuring metal films into wavy structures can enable stretchability because the tensile strain can be accommodated by unbending of curved wavy structures. The underlying mechanism is analogous to a spring or accordion bellows. The achieved stretchability is mainly determined by the wavelength and amplitude of the wavy structures. Wavy structures can be out-of-plane wrinkles or in-plane serpentines.

Out-of-plane wrinkles are mainly generated by buckling through thermal mismatch or mechanical strain mismatch between metal films and stretchable substrates. Depositing thin gold films on PDMS by electron beam (e-beam) evaporation under certain conditions can produce gold films with isotropic wrinkles.<sup>41,46</sup> During the gold film deposition, PDMS thermally expands from the heat which is mainly generated from the e-beam radiation. After cooling down, there is compressive stress built into the gold film due to the large thermal expansion coefficient difference between the gold film and PDMS. The compressive stress induces spontaneous wrinkling of the gold film as shown in **Figure 1-3a**.<sup>41</sup> The wrinkled gold film on PDMS retains electrical conductivity to 22% strain, which is above its fracture strain ( $\sim 1\%$  strain). However, this method heavily depends on the gold film deposition parameters; the wrinkled morphology only occurs under certain

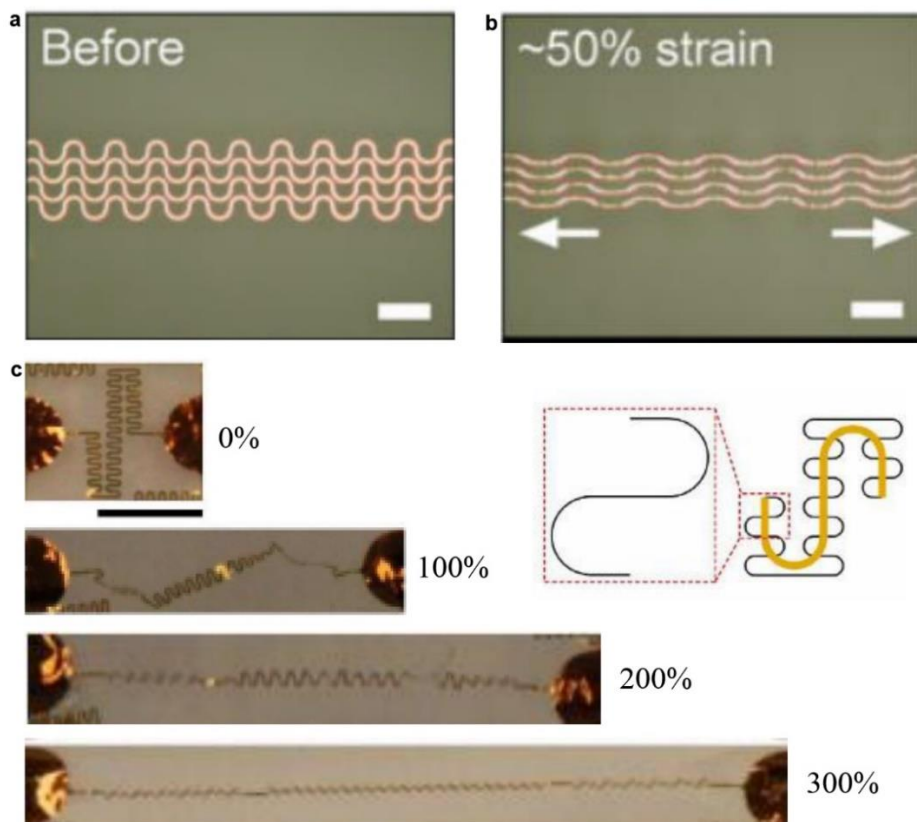
film deposition conditions.<sup>47</sup> The other method to generate out-of-plane wrinkles is to deposit a thin metal film on a prestretched substrate. Releasing the strain in the substrate results in compressive stress in the thin metal film, leading to the formation of wrinkles. Lacour *et al.* used the prestrain method to fabricate stretchable metal conductors by depositing gold films on PDMS that was uniaxially prestretched by 15% strain.<sup>48</sup> The resulting gold film showed a longitudinal wave with  $\sim 8.4 \mu\text{m}$  wavelength and  $\sim 1.2 \mu\text{m}$  amplitude as shown in **Figure 1-3b**. The resistance of the wavy gold films showed a negligible change to 15% strain and rose suddenly to open circuit at  $\sim 28\%$  strain. Between 0 to 15% strain, the gold film gradually flattened and no cracks perpendicular to the stretching direction developed, which accounts for the stable resistance. Above 15% strain, the metal film experienced destructive strain, causing the formation of cracks, and increasing the resistance. The stretchability of the metal films fabricated using the prestrain method is mainly determined by the applied prestrain. To further increase the stretchability, Joyelle *et al.* reported increasing the prestrain to 25% before gold film deposition<sup>49</sup> and Wang *et al.* reported depositing copper films on 100% prestrained PDMS, which was the fracture limit of the PDMS used in this study.<sup>50</sup> While high stretchability is achieved, cracks parallel to the direction of prestrain tend to form during the release process, which are due to the Poisson effect.<sup>48,51</sup> These wrinkled conductors can also only be stretched in the pre-stretch direction. Radially stretching stretchable substrates to develop isotropically wrinkled metal films as shown in **Figure 1-3c** can enable omnidirectional stretchability and alleviate the crack formation from the Poisson effect.<sup>52</sup> However, prestretching and holding the elastomer substrate during fabrication can be technically challenging.



**Figure 1-3** Images of wrinkled gold film induced by a) thermal mismatch (adapted with permission from reference [41]), b) uniaxial strain mismatch (adapted with permission from reference [48], copyright [2004] IEEE) and c) omnidirectional strain mismatch (adapted with permission [52]).



Instead of creating out-of-plane wrinkles, in-plane patterning of metal films into tortuous shapes on stretchable substrates can also enable the stretchability of metal films. Compared to out-of-plane wrinkles, in-plane tortuous metal wires not only unbend, but also tend to deflect and twist out of plane at the peaks to accommodate the strain during stretching. Gray *et al.* fabricated gold serpentine wires on PDMS using standard lithography techniques (**Figure 1-4a**).<sup>53</sup> The narrow serpentine wires can be stretched to ~50% strain while maintaining stable conductivity by the unbending of the tortuous metal wires (**Figure 1-4b**). Brosteaux *et al.* further optimized the patterned shape by changing the serpentine into a horseshoe-like shape, which increased the stretchability to ~70% strain because the experienced stress of horseshoe wires is reduced compared to serpentine wires.<sup>54</sup> Furthermore, Xu *et al.* introduced a “self-similar” design in which serpentine wires are laid out in a hierarchical design.<sup>55</sup> The design leads to hierarchical levels of unbending, allowing stretchability up to 300% strain (**Figure 1-4c**).



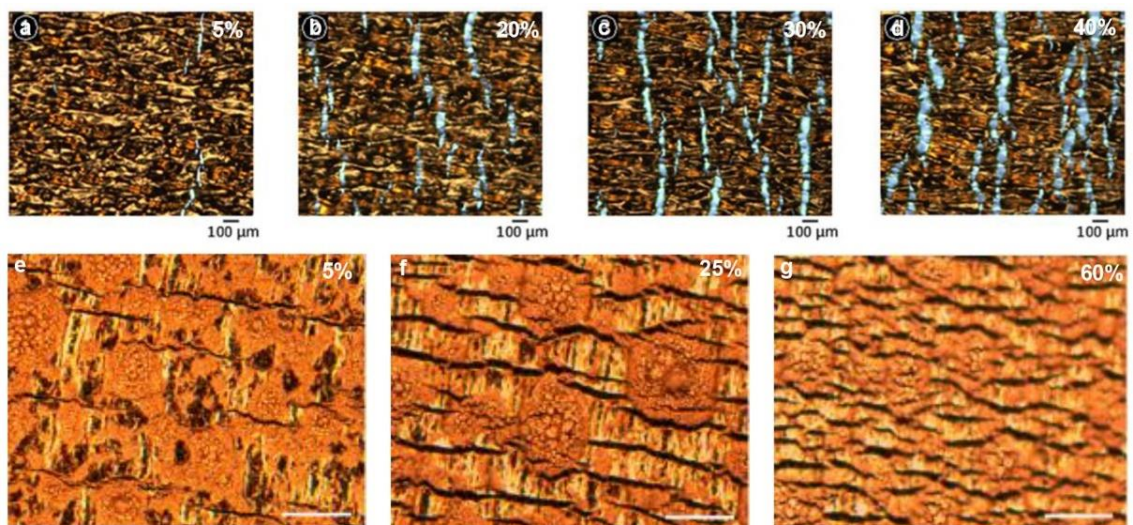
**Figure 1-4** Optical microscope images of serpentine gold wires at a) 0% and b) 50% strain. Scale bar = 100  $\mu\text{m}$  (adapted with permission from reference [53]). c) Optical images of “self-similar” serpentine gold wires stretching at 0-300% strain. Inset: illustration of “self-similar” serpentine geometries. Scale bar = 2 mm (adapted with permission from reference [55]).

### *Inducing engineered cracks*

Stretching metal films on PDMS can cause metal films to crack because of the mechanical mismatch between metals and PDMS. The formation of cracks is necessary to release the strain energy and cracking patterns in metal films greatly affect their electrical conductance. Long channel cracks can cut off the electrical flow; microcracks that are not completely merged in metal films can still preserve electrical conductance through interconnected tortuous metal islands. An analogy is numerous randomly distributed small stones in a creek. The water can easily flow around these small stones; however, a big stone that traverses the creek can greatly block the water flow. By controlling the cracking patterns, we can control the resistance change of metal films with strain. The electrical response with strain can be utilized for different applications, such as dramatic resistance changes with strain for sensitive strain gauges and stable resistance with strain for interconnects.<sup>43</sup> The strategy discussed here is to allow metal films to experience stress from stretching strain, while applying methods to regulate crack initiation and propagation, and thus rationally engineer metal cracking patterns to control the electrical conductance of metal films with strain.

Creating topography on PDMS substrates has been demonstrated as an effective way to control crack initiation and propagation by regulating stress distribution over metal films on PDMS.<sup>43-45,56-59</sup> The uneven surface comprising “peaks” and “valleys” induces an inhomogeneous stress field within a metal film on the PDMS surface. While applying tensile strain, the surface tensile stress is more concentrated at valleys than in other regions.<sup>57,60</sup> Cracks tend to initiate where stress is more concentrated. Therefore, the numerous valleys act as sites for crack initiation/nucleation and peaks act as crack arresters to inhibit propagation. With the increase of strain, the crack density, length, and width gradually increase to release the tensile stress. The topography can be imparted to PDMS by either casting PDMS prepolymers against molds with microstructures<sup>44,45,56-59</sup> or depositing a microstructured polymeric layer on the surface.<sup>43</sup> For example, Lambricht *et al.* reported producing a rough surface by curing PDMS against sand-blasted masters.<sup>45</sup> Metallization of the rough surface with gold produced stretchable conductors with microcrack patterns rather than channel cracks under strain (**Figure 1-5a-d**). Filiatrault *et al.* deposited emulsions of poly(vinyl acetate) glue onto PDMS to create a microstructured

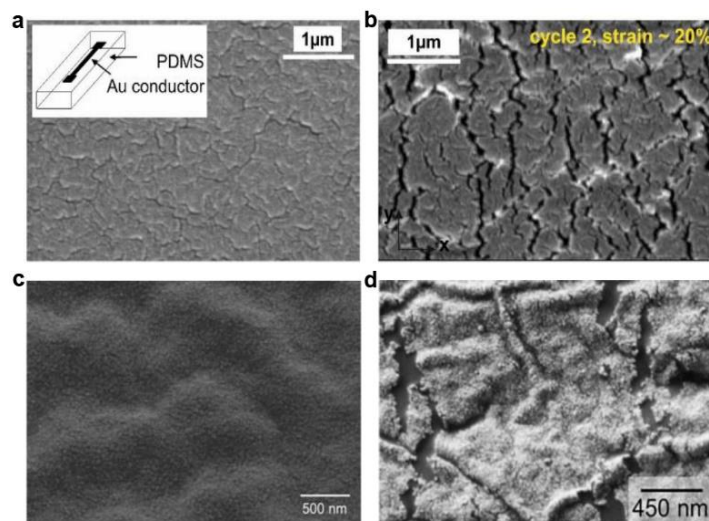
topography with randomly distributed globules.<sup>43</sup> Gold films on the surface of the microstructures exhibited high conductivity to 65% elongation; the globules act as “peaks” to arrest cracks (**Figure 1-5e-g**). While using topographies to engineer crack patterns formed in metal films under strain is effective and straightforward, the high surface roughness of the fabricated stretchable conductors could be problematic when integrating these metal films as electrodes in thin-film devices.



**Figure 1-5** Optical images of a gold film on rough PDMS at a) 5%, b) 20%, c) 30% and d) 40% strain (adapted with permission from reference [45]). Optical images of a gold film on polymer-coated PDMS at e) 5%, f) 25% and g) 60% strain. Scale bar = 40  $\mu\text{m}$  (adapted with permission from reference [43]. Copyright [2015] American Chemical Society).

The morphology and microstructure of metal films on PDMS can also affect how metal films crack. Metallurgical approaches such as manipulating metal deposition conditions and methods to fabricate metal films with specific microstructures have been demonstrated to fabricate stretchable metal films with planar topography.<sup>61-65</sup> For example, Lacour *et al.* showed that gold films deposited on smooth PDMS using e-beam evaporation under certain conditions exhibited microcrack morphology before stretching as shown in **Figure 1-6a**.<sup>61</sup> The presence of these microcracks allowed the metal to stretch by widening of the cracks during stretching (**Figure 1-6b**). This type of gold film remained conductive to 60% strain<sup>42</sup> and showed stable conductivity over 250000 cycles to 20% strain.<sup>66</sup> Matsuhisa *et al.* furthermore controlled the length of initial microcracks of gold films by changing the evaporation rate and film thickness to improve the stretchability and conductance at high strains.<sup>62</sup> They reported that the gold film with longer initial

microcrack lengths showed smaller resistance change under high strains. Besides the metal deposition conditions based on physical vapor evaporation, the morphology of metal films can be also affected by the metal fabrication method. Electroless deposition (ELD) is a solution-based alternative to vapor-based methods for metal films fabrication. ELD is based on an autocatalytic redox reaction without the need to use electricity. A typical ELD process involves first activating the substrate by immobilizing a catalyst, typically a palladium (0) species, onto the surface. The immobilized catalyst subsequently catalyzes the reduction of metal ions in the ELD plating solution onto the surface of the substrate, with metal reduction/deposition continuing autocatalytically as a reducing agent in the ELD solution is consumed.<sup>67</sup> Miller *et al.* reported using ELD to fabricate continuous copper films on smooth PDMS, which remained conductive to ~50%.<sup>65</sup> However, the detailed characterization of morphology and cracking patterns of copper films under strain was not reported. Later on, Chen *et al.* fabricated gold films on smooth PDMS using ELD of Ni followed by immersion gold.<sup>63</sup> The fabricated gold film showed a continuous and heterogeneous crystalline surface morphology (**Figure 1-6c**). The gold film exhibited a nanoscale cracking pattern under strain and remained conductive until the PDMS substrate fractured (**Figure 1-6d**). This unique cracking pattern formation comes from the misoriented grains in the gold film, which act as strong barriers to dislocation movement.



**Figure 1-6** SEM of a gold film on PDMS with microcrack morphology at a) 0% and b) 20% strain (adapted with permission from reference [61]). SEM of a gold film on PDMS prepared using ELD of Ni followed by immersion gold at c) 0% and d) 30% strain (adapted with permission from reference [63]). Copyright [2019] American Chemical Society).

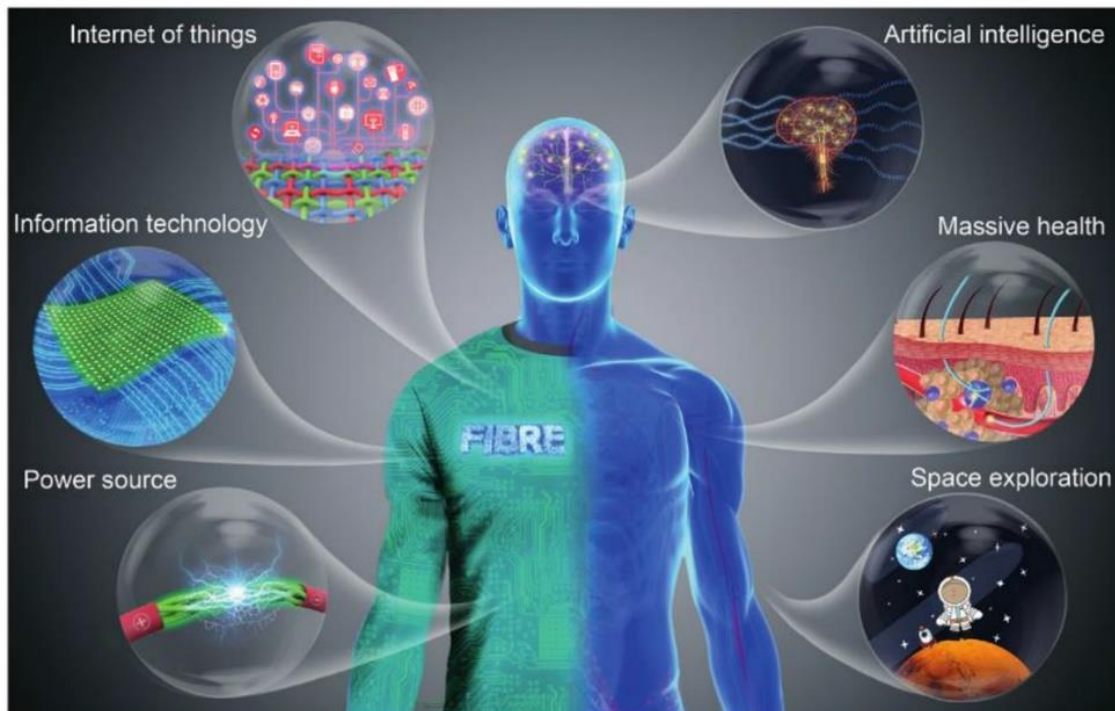
There are also other novel approaches reported to engineer the formation of cracks in the metal film. For example, creating a brittle layer between the two elastomers to alter crack formation through stress transfer have been demonstrated.<sup>68</sup> Creating an interlocking layer between metal and PDMS to change the way of metal films crack by increasing the interfacial adhesion and regulating the strain distribution in the film also has been reported.<sup>69,70</sup>

#### **1.4 Textile-Based Electronics: e-Textiles**

Textiles were first manually made about 26,000 years ago as shown by archaeological evidence and could be contested as humankind's first material invention.<sup>71</sup> After thousands of years' development, they have become an essential and indispensable part of human life by virtue of their drapability, softness, flexibility, stretchability, breathability, and durability. These characteristics make them applicable in a wide range of applications, such as clothing, household articles (e.g. towels, bags, window shades, coverings for tables and beds), medical supplies (e.g. wound dressings and surgical masks), construction materials, and artistic supplies. While ubiquitous and diverse, the core functionalities of textiles have not really changed in thousands of years. The integration of electronics into textiles creates electronic textiles (e-textiles), which can further expand the functionality of textiles ranging from sensing and actuation, energy harvesting and storage, to lighting and display.<sup>72-78</sup> Clothing made from e-textiles can interface routinely with human bodies and is thus an ideal format of wearable and even fashionable electronic devices to bring electronics close to the human body seamlessly and unobtrusively.

Ubiquitous e-textiles will play a key role in the future, making everyday life more convenient, efficient, and safe. For instance, e-textiles with sensing properties will play a ground-breaking role in human health by simultaneously monitoring health conditions, detecting diseases at an early stage, and administering treatments. E-textiles may harvest energy from the environment or human body and store it to power portable and wearable electronic products. E-textiles may also replace everyday electronic products such as cell phones as tools for communication and remote control. E-textiles may enable your shirt to say or display what you feel. They may even adapt to a broad range of temperatures to serve as adaptive spacesuits, thus paving the way for human beings to emigrate to other planets. From these futuristic visions for e-textiles, it is not hard to see that e-textiles will

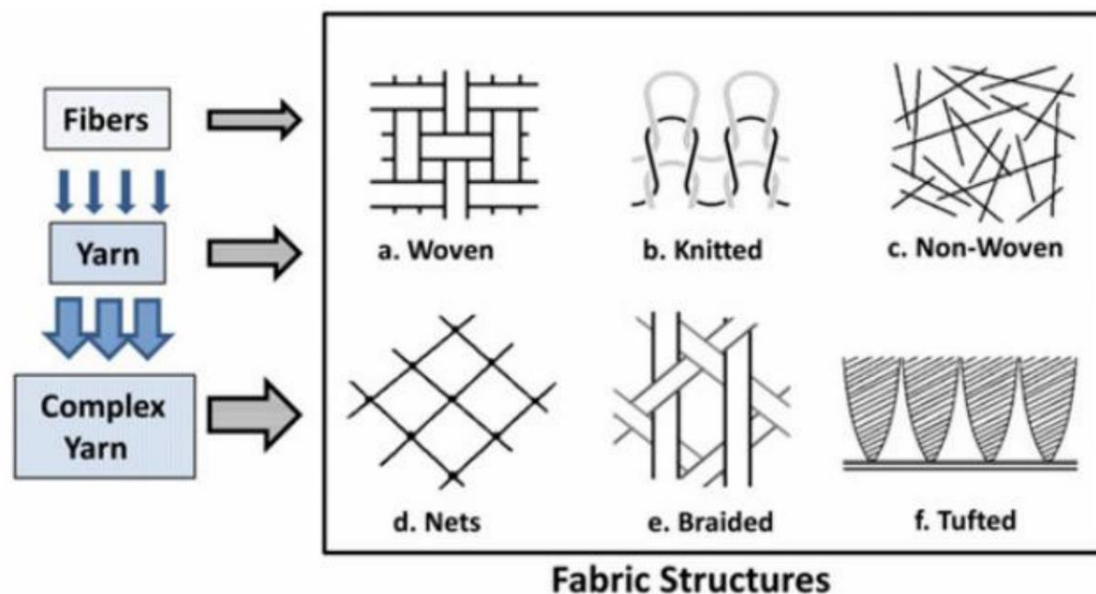
potentially revolutionize many important fields, such as public health, IoT, power sources, information technology, artificial intelligence, and space exploration (**Figure 1-7**).



**Figure 1-7** Illustration to show that electronic textiles can be used for power sources, information technology, the IoT, artificial intelligence, public health, and space exploration (reproduced with permission from reference [78]).

#### 1.4.1 Textile Structures and Properties

Textiles are constructed hierarchically from fibers, which are elementary building blocks. They can be natural fibers, such as cotton, silk, wool, flax, jute, and hemp; they can also be synthetic fibers, such as nylon, polyester, spandex, and acrylic. Multiple fibers are twisted together to form yarns. By using different manufacturing techniques, yarns are interlaced to form textiles with different structures, such as woven, knitted, braided, and tufted (**Figure 1-8**).



**Figure 1-8** Schematic to show the textile hierarchy and structures (adapted with permission from reference [73]).

Different from stretchable elastomer substrates, textiles can be stretchable due to their contexture, which comprises inherently built-in structures with mechanical designs that enable stretchability and drapability of the fabric. For example, knitted fabrics can often sustain high elongation due to the serpentine loops in the knitted structure; woven fabrics are less stretchable but more stable than knitted fabrics because of the strong deformation resistance of the woven structure. The stretchability and strength of knitted fabrics are related to the knitting structure; different knitting structures show different stretchabilities.<sup>79</sup> In addition, stretchable fabrics show J-shaped strain-stiffening behavior, which is well matched to the mechanical properties of natural tissues (skin, arteries, tendons, etc.).<sup>80,81</sup> Textiles are characterized by being soft, flexible, stretchable, lightweight, and breathable. These qualities are mainly attributed to the voids formed in the structure, which provide space for fiber deformation and inter-fiber movement with strain. Meanwhile, the cohesive and frictional forces between fibers and the interlock of yarns under strain endow textiles with certain strength.<sup>82</sup> The combinations of seemingly disparate and conflicting properties (e.g. softness, flexibility, and strength, etc.) are derived from their hierarchical porous structures, which pose challenges in the development of e-textiles as well as opportunities to utilize their unique architectures as advantages to create e-textiles.

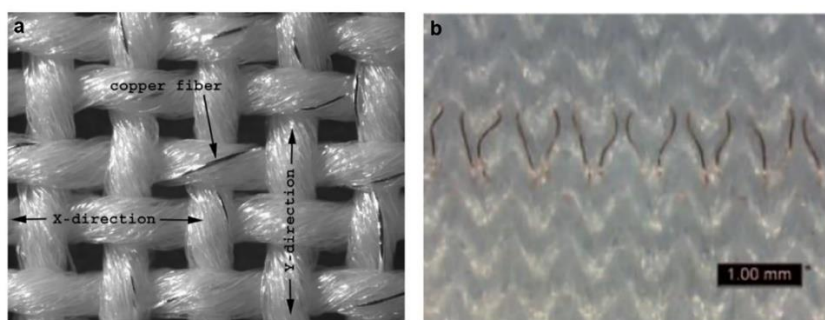
### 1.4.2 Conductive Textiles

The first and fundamental step toward producing e-textiles is to fabricate conductive textiles, which form the basis for e-textile system implementation. For example, conductive textiles can act as electrodes for light-emitting textiles and current collectors for energy storage textiles. E-textiles involve curved fibers and 3D porous textile substrates, which make them conceptually different from flat elastomer-based stretchable electronics, while they have similarities in softness and stretchability. Modern electronic fabrication techniques, such as photolithography, physical vapor deposition, and printing, are well-established typically for 2D planar surfaces, and not applicable to textiles. This issue can be directly circumvented by the planarization of the textile substrate with a polymeric layer.<sup>83,84</sup> This approach can convert porous textile substrates into planar substrates so that they are compatible with conventional electronic fabrication technology; however, planarization also stiffens textiles and diminishes the intrinsic textile characteristics. This effect is due to filling the voids of the fabrics with the planarizing polymer, thereby restricting the yarn mobility, which is key to the unique attributes of textiles.

One way to produce conductive textiles while maintaining the void network is to incorporate conductive fibers within fabric using textile manufacturing techniques, such as embroidering,<sup>85,86</sup> weaving,<sup>87,88</sup> or knitting.<sup>89,90</sup> Metal fibers are the first conductive fibers used within textiles initially for decoration; embroidering metal fibers, such as gold, into textiles, also known as Zardozi, has been used for centuries. For conductivity of e-textiles, Post *et al.* embroidered steel fibers within textiles as interconnects.<sup>86</sup> Copper fibers with polyester fibers were woven together to form conductive traces within fabrics as transmission lines and interconnects (**Figure 1-9a**).<sup>87</sup> Copper fibers were co-knitted with spandex and polyester fibers into the knitted fabric as stretchable interconnects (**Figure 1-9b**).<sup>90</sup> Although metal fibers have superior electrical conductivity, they are stiff and the produced fabrics may have an undesired texture that can cause an uncomfortable skin sensation. Moreover, they are heavier than regular textile fibers, which make them not ideal for large-scale applications. In recent decades, new types of conductive fibers directly spun from conductive materials, such as conductive polymers,<sup>91-93</sup> carbon nanotubes,<sup>94</sup> graphene,<sup>95</sup> and metal particle-based composite,<sup>89</sup> have been developed. In addition to the



development of intrinsically conductive fibers, coating conventional insulating fibers with conductive materials, such as metals,<sup>96-100</sup> conductive polymers,<sup>101-104</sup> and carbon-based materials,<sup>105,106</sup> have also been explored. Even integration of conductive fibers into fabrics to fabricate conductive textiles using conventional textile manufacturing techniques can fully retain textile structures, breakage of conductive fibers during the manufacturing process can occur if the sewability (weavability and knittability) of conductive fibers cannot meet the requirements of industrial textile manufacturing machines.<sup>106,107</sup> The deterioration of electrical performance due to abrasion during the manufacturing process can be a concern as well.

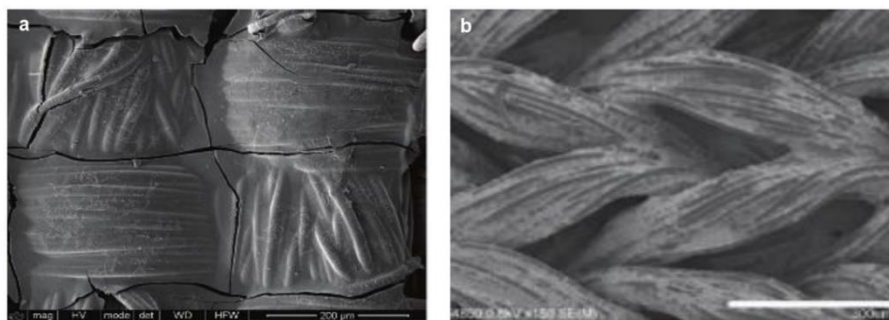


**Figure 1-9** Optical images of metal wires a) woven (adapted with permission from reference [87]) and b) knitted into fabrics (adapted with permission from reference [90]).

Conductive textiles can be also fabricated by directly coating off-the-shelf textiles with conductive materials, which is similar to the dyeing and finishing process in the textile industry. This approach has the advantage of directly converting already manufactured textiles into conductive textiles, eliminating the need to integrate conductive fibers with textiles during textile manufacturing. The coated textiles have conductivity in all directions, giving free tailorability. Major efforts are dedicated to research in developing scalable deposition methods that are compatible with porous, 3D textile substrates so as to maintain the textile structures and not considerably change existing textile properties such as softness, flexural rigidity, and stretchability.

One straightforward way to fabricate conductive textiles is to directly treat textiles with conductive inks through dip coating or printing techniques. The use of conductive inks based on carbon nanotubes,<sup>108,109</sup> Ag nanowires,<sup>110</sup> graphene,<sup>111,112</sup> poly(3,4-ethylenedioxythiophene) polystyrene sulfonate (PEDOT:PSS)<sup>113-116</sup> and Ag flakes or particles<sup>117-120</sup> have all been reported. The properties of ink formulation (such as viscosity

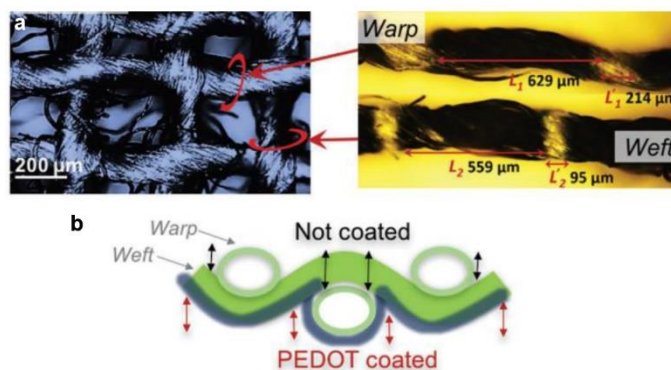
and surface tension) and the properties of the textile (such as porosity and coating factor of the textiles and hydrophilicity of textile fiber materials) control the ink penetration depth into textiles, which has a significant effect on the electrical and mechanical properties of the coated textiles.<sup>116,121-123</sup> For example, Ding *et al.* studied the conductivity of different types of conductive textiles that were fabricated by soaking fabrics in a conductive polymer aqueous dispersion.<sup>116</sup> It was found that the fabric with higher water uptake resulted in higher conductivity because more conductive materials were absorbed inside the textiles. In another example in **Figure 1-10a**, dispersions of the conductive polymer PEDOT:PSS did not penetrate well into woven fabrics and ended up staying on the top of the textile, which stiffens the textiles by filling the voids of the fabrics and restricting the movement of yarns.<sup>114</sup> The resulting conductive fabric composite is also vulnerable to cracking under mechanical deformation. To avoid cracking of conductive coatings and stiffening the textile, Jin *et al.* developed specialized conductive Ag ink formulations to control the permeation of the ink in the textile.<sup>123</sup> By adjusting the evaporation rate of inks using different solvents, the ink fluid transported, permeated and only filled the small gaps between individual fibers, leaving the big gaps between fiber bundles unchanged to retain flexibility and stretchability (**Figure 1-10b**).



**Figure 1-10** SEM images of the a) woven fabric coated with PEDOT:PSS (adapted with permission from reference [114]) and b) knitted fabric printed with the specialized conductive Ag ink. Scale bar = 300  $\mu\text{m}$  (adapted with permission from reference [123]).

Conformally coating textiles with a thin layer of conductive materials using vapor-based deposition methods, such as physical vapor deposition of metals<sup>124,125</sup> and chemical vapor coating of conductive polymers,<sup>126</sup> has a minor effect on the intrinsic fabric structure and mechanical properties, but the conductive textiles fabricated using this approach have limitations in terms of stretchability. Physical vapor deposition, such as sputtering, is a line-of-sight process, which can cause a shadowing issue for 3D fiber and textiles.<sup>125</sup>

Chemical vapor deposition methods, such as atomic layer deposition, are non-line-of-sight methods, which make them suitable to coat nonplanar fiber surfaces with functional materials.<sup>127</sup> However, the diffusion depth of reactants into textile structures needs to be carefully controlled; insufficient penetration of initiators/reactants through textiles can limit deposition to the surface-exposed fibers, resulting in uncoated regions on the underlying fibers of textiles. For example, Zhang *et al.* reported the chemical vapor deposition of PEDOT on a woven textile to fabricate conductive textiles.<sup>126</sup> The broken pattern of the PEDOT coating was observed on individual yarns pulled from the fabric after the vapor coating (**Figure 1-11a**). At the intersection of yarns, the surface of overlaying yarns was coated with PEDOT, but the underlying yarns were uncoated due to the lack of the reach of reactants, producing a discontinuous PEDOT coating with broken conductive pathways (**Figure 1-11b**). Therefore, each yarn is not conductive; the conductance of the overall PEDOT-coated fabric relies on the closely packed woven structure that results in a tight connection of PEDOT coatings at the crossover points. It can be anticipated that for stretchable fabrics, once the yarns start to move due to mechanical deformation, such as bending, twisting, and stretching, the connection will break, leading to the loss of fabric conductivity.



**Figure 1-11** a) Optical images of PEDOT-coated textiles and threads pulled from these fabrics after PEDOT coating. b) An illustration showing that only one side of the fabric is coated with PEDOT (adapted with permission from reference [126]).

Solution-based ELD is a promising method to stretchable conductive textiles. The aqueous ELD plating solution can easily permeate into textiles mostly via the capillary force generated from the gaps between fibers.<sup>128</sup> By virtue of this capillary action, the ELD plating solution has access to each individual fiber and deposits metal films on them, leaving the textile structures intact to retain the intrinsic textile characteristics. There have

been many reports on metalizing fabrics using ELD for different applications, such as using the brilliant appearance of metalized fabrics for textile design,<sup>129</sup> and using the conductivity of metalized fabrics for electromagnetic interference shielding<sup>130-133</sup> and wearable e-textiles fabrication.<sup>134-141</sup> However, research work on metalized fabrics using ELD for e-textile fabrication is mostly based on woven fabrics, which have limited stretchability. For example, using ELD, copper<sup>136</sup> and nickel patterns<sup>138</sup> on woven cotton fabrics and silver patterns<sup>139</sup> on woven polyester fabrics were fabricated as interconnects for electrical circuits. For comfort and wearability, it is necessary to fabricate robust stretchable e-textiles that can deform with the movement of human body. Furthermore, the stability and biocompatibility of materials used for wearables are important for long-term use and safety. So far, the metals demonstrated in these studies can be problematic for wearables due to the tendency of silver and copper to oxidize or corrode,<sup>142</sup> particularly in contact with salt solutions such as human sweat, and possible metal allergy caused by nickel.<sup>143</sup> For wearable applications, gold is an ideal material since it has high electrical conductivity, wide potential windows, long-term stability, and particularly excellent biocompatibility. It has become the prime material of choice for fabrication of wearable and implantable electronics.<sup>144</sup>

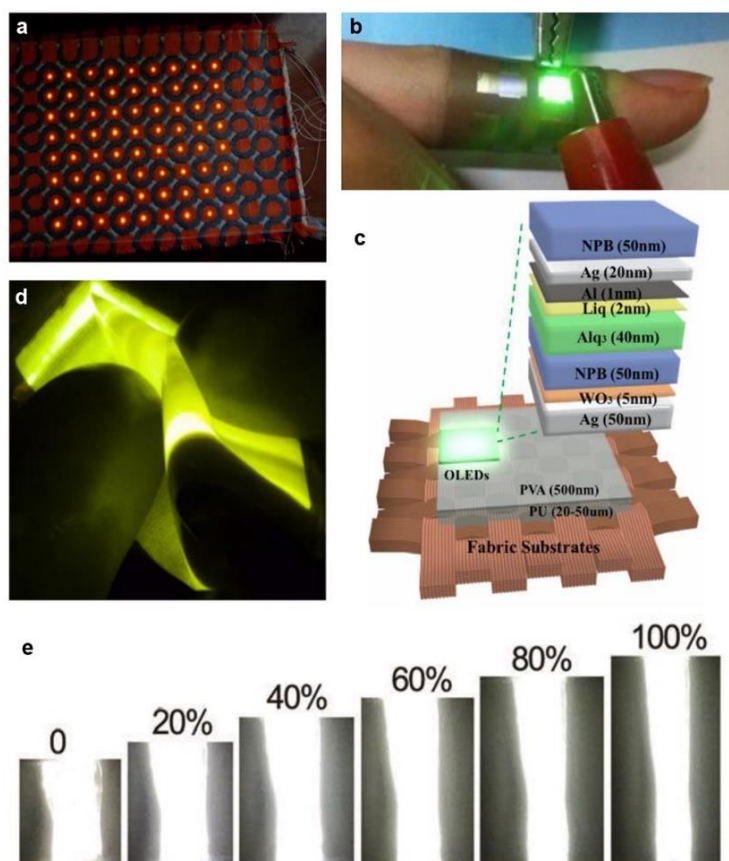
Other methods, such as in-situ polymerization of conductive polymers on the surfaces of textile fibers<sup>145-147</sup> and in-situ carbonization of cellulose-based textiles through high-temperature thermal treatment ( $\sim 1000$  °C)<sup>148,149</sup> have also been explored. While these methods can well retain the fabric structures, the resistivity of these conductive fabrics is relatively high, and the harsh reaction environment required can be detrimental to textiles. For example, the use of strong acidic oxidants for the in-situ polymerization of PEDOT caused the dissolving of nylon fibers during the reaction process.<sup>147</sup> Carbonization processes greatly lower the mechanical strength and stretchability of the original textiles.<sup>148</sup>

### 1.4.3 Light-Emitting Textiles

Endowing light-emitting function to textiles as a new creative dimension can inspire many innovative and exciting applications. For example, light-emitting t-shirts can be designed as a media to express our mood and give messages to people around us. Light-emitting apparel with animated color illumination can increase the entertainment effect for stage performers. Sportswear with light-emitting function can improve the safety of the

wearer at night due to higher visibility. Integrating light-emitting function with hospital gowns can display patients' vital signs, which are monitored by health sensors, or be used as light therapy treatment. Light-emitting textiles can also be used for interior design and visual merchandising.

One approach to fabricate light-emitting textiles is to attach conventional rigid light-emitting diodes (LEDs) to textiles using conductive interconnects<sup>150,151</sup> or adhesive layers.<sup>152</sup> For example, Parkova *et al.* designed a light-emitting textile display in which surface mounted light-emitting diodes were connected to conductive yarns within a piece of textile as shown in **Figure 1-12a**.<sup>150</sup> This method is simple but has the drawback that the rigid components could cause discomfort; discrete LEDs are also limited to discontinuous small-area lighting.



**Figure 1-12** Photograph of a) LED textile display prototype (adapted with permission from reference [150]). b) Photograph and c) schematic diagram of OLEDs fabricated on fabric substrates (adapted with permission from reference [153]). d) Photograph of a flexible LEC textile during deformation between two fingers (adapted with permission from reference [157]). e) Photographs of the stretchable ACEL fabric at 0-100% strain (adapted with permission from reference [163]).

Creating light-emitting textiles directly fabricated from pre-made textile substrates is a promising approach to fabricate comfortable (soft and stretchable) and large-area light-emitting textiles. Different types of light-emitting devices fabricated on textiles, such as organic light-emitting diodes (OLEDs),<sup>153-155</sup> light-emitting electrochemical cells (LECs),<sup>156,157</sup> and alternating current electroluminescent (ACEL) devices<sup>158-163</sup> have been reported. Different types of devices require different modifications of textiles. For example, efficient p-n junction formation is crucial to the performance of OLEDs, so the requirement for the surface smoothness of the substrate is strict. However, the surface of textiles is rough due to their hierarchical porous structures. To solve the roughness problem, Kim *et al.* developed a planarization process to smooth textiles.<sup>153</sup> In this way, they successfully fabricated OLEDs based on textiles as shown in **Figure 1-12b**, but this planarization method can reduce the intrinsic character of textiles and inhibit stretchability as discussed in Chapter 1.4.2. In addition, high-performance OLEDs also require the deposition of multiple layers to match the work functions of the electrodes for efficient electron and hole transfer, which adds to the complexity of fabrication (**Figure 1-12c**). LECs can better tolerate uneven surfaces, are insensitive to work function, and have a simpler device structure since charge injection, transport, and emissive recombination processes can efficiently take place in a single emissive layer. Lanz *et al.* reported LECs based on a conductive fabric consisting of non-conductive fibers interwoven with conductive Ag-coated Cu wires.<sup>157</sup> The fabricated textile-based LEC was flexible as shown in **Figure 1-12d**, but the operation and testing were done inside the glovebox with an inert atmosphere. The stability of LEC emissive layers in the ambient environment is still a concern.

ACEL devices avoid the problems of OLEDs and share the advantages of LECs without the environmental sensitivity, making them the most promising candidate for stretchable and durable light-emitting textiles. ACEL devices can be constructed in a simple sandwich structure: an emissive composite layer is between two electrodes. At least one of the electrodes need to be optically transparent to permit light transmission. ACEL devices produce light mainly through the radiative combination of excitons in the luminescent centers of the emissive layer, which are generated based on the hot-electron impact excitation mechanism.<sup>164</sup> Since the charge carriers that excite excitons in the

luminescent centers are mostly generated from the frequent reversal of strong electric field, the operation of ACEL devices has no harsh requirement on the work functions of the electrodes for energy band matching. The emissive layer is usually a composite of dielectric polymer binder and inorganic phosphor powder, such as ZnS doped with Cu, Mn or Al.<sup>165</sup> Research on textile-based ACEL devices has mostly used flexible woven textiles.<sup>158-162</sup> Hu *et al.* first fabricated flexible ACEL devices based on PEDOT:PSS-coated woven textiles in 2011.<sup>160</sup> However, this light-emitting textile was not stretchable due to the woven textile substrate, the stiffness of the epoxy resin/phosphor composite emissive material, and the brittleness of the transparent electrode. Developing soft and stretchable light-emitting textiles can improve the wearing comfort for a better adoption into the consumer market. In 2015, Wang *et al.* reported mixing phosphor with elastomer to form a stretchable emissive layer for stretchable elastomer-based ACEL devices, which accelerated the development of stretchable textile-based ACEL devices.<sup>166</sup> In 2017, Zhang *et al.* reported stretchable textile-based ACEL devices by using polypyrrole-coated stretchable spandex fabric as the bottom electrode, phosphor/silicone elastomer composite as the emissive layer, and an ionic conductor as the transparent electrode.<sup>163</sup> While this light-emitting textile was highly stretchable and could stretch to 100% strain (**Figure 1-12e**), its durability may be limited by the transparent electrode because of the potential evaporation of the solvent/liquid component of the ionic conductor.

#### 1.4.4 Energy-Storage Textiles

Towards the implementation of e-textile systems, power sources are required to provide power for textile-based electronic devices. Although energy can be directly harvested from solar radiation using solar cells or from human motion via triboelectric nanogenerators, energy storage devices are still needed to ensure stable and lasting power supply for e-textiles since the power output of energy harvesting devices is usually not continuous and largely relies on the ambient environment, such as weather condition or body movement. A promising solution to the e-textile energy supply problem is to integrate both energy-harvesting and energy-storing devices within textiles to work together for a sustainable wearable power unit.

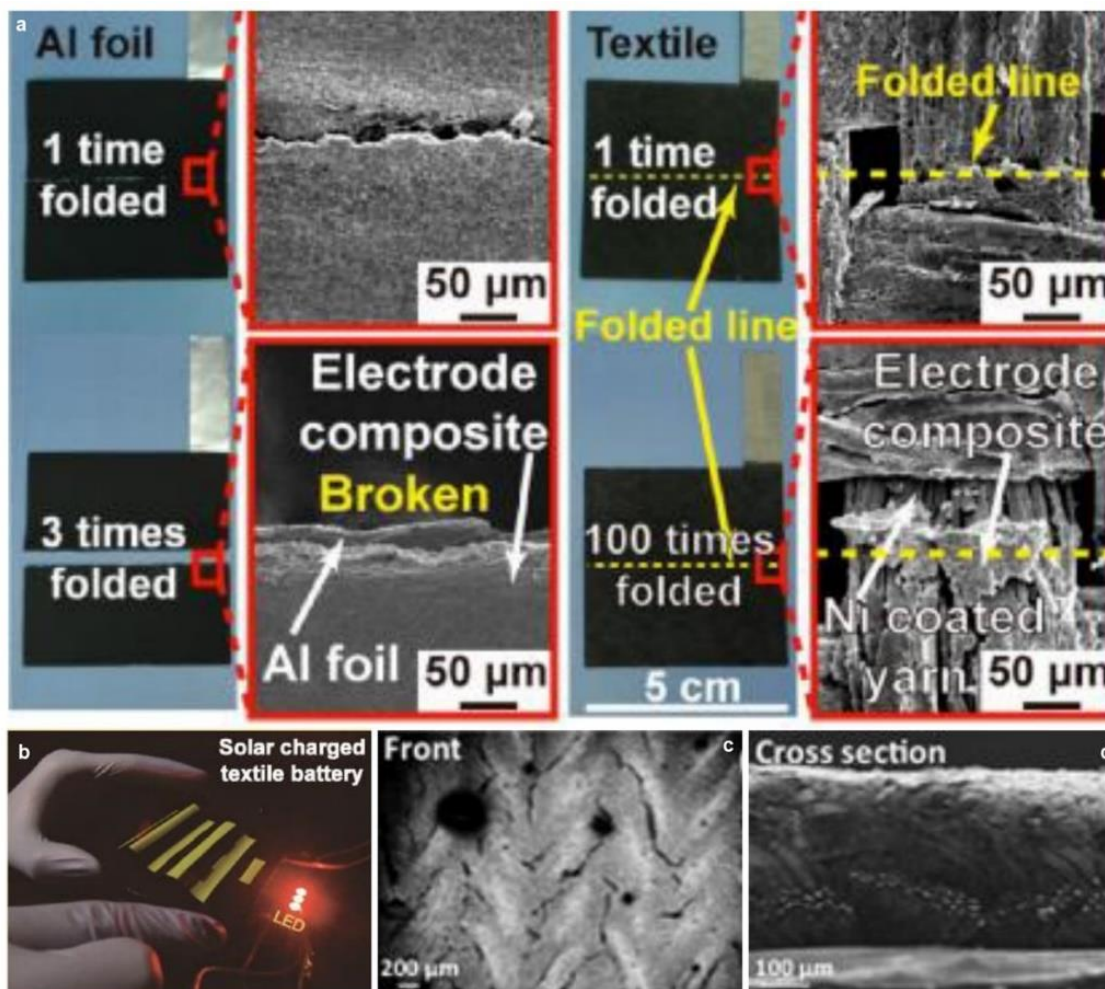
Supercapacitors and batteries are two mainstreams of energy storage devices. Both types of devices have been developed for integration with textiles.<sup>167-170</sup> In general,

supercapacitors have a relatively high power density, while batteries have a relatively high energy density. They are used for different applications based on the power requirements. Among different batteries, lithium-ion batteries (LIBs) are the most promising as power sources for wearables due to their high working voltage, high energy density, long cycle life, low self-discharge, and no memory effect.<sup>171</sup> By virtue of these properties, they have been successfully and widely used to power many types of devices, such as laptops, cell phones, electrical watches, flashlights, and even cars. For wearable applications, they are expected to be flexible and stretchable for comfortable wearing and also maintain stable battery performance under deformation. However, conventional LIBs are usually bulky in size and heavy in weight; they also tend to crack under severe mechanical deformation, leading to performance degradation and poor wearability. Conventional LIBs consist of two electrodes, an electrolyte, and a separator, which are packed together inside rigid metallic or plastic housing in the form of coin cells, pouch cells, or cylindrical cells. To realize flexible and stretchable LIBs, each battery component needs to be functional during mechanical deformation. Particularly, the electrodes require the most significant modification since they largely dictate the mechanical property of the entire LIB. Conventional LIB electrodes are usually fabricated by casting a slurry of electroactive materials, conductive additives, and binder onto a metallic current collector, such as aluminum or copper foil. Electroactive materials are usually brittle metal oxides such as  $\text{LiCoO}_2$ ,  $\text{LiFePO}_4$ , or  $\text{Li}_4\text{Ti}_5\text{O}_{12}$ .<sup>172</sup> Carbonaceous materials, such as carbon black and carbon nanotubes, are usually used as the conductive additive and stiff thermoplastic polymers, such as polyvinylidene difluoride, as binder.

Using conductive textiles to replace metal foils as current collectors is the first step toward developing textile LIBs and also the most distinct feature from conventional LIBs. The efforts in this research field has focused on improving flexibility with flexible conductive fabrics most often being used as current collectors, such as Ni-coated woven<sup>173-175</sup> and nonwoven fabric,<sup>176,177</sup> carbonized woven fabric,<sup>178,179</sup> and carbon fiber woven fabric.<sup>180-184</sup> Compared to conventional battery electrodes based on metal foils, textile battery electrodes showed better tolerance to bending/folding as demonstrated by Lee *et al.*<sup>173</sup> As shown in **Figure 1-13a**, after one cycle of folding-unfolding the battery active layer on the Al foil started to peel off, and after 3 folding-unfolding cycles the Al foil was



broken into two pieces. In contrast, the textile electrode retained mechanical integrity after 100 cycles of the same folding-unfolding. Based on the textile electrode, a flexible textile LIB that was rechargeable by solar cells was demonstrated (**Figure 1-13b**).



**Figure 1-13** a) Photographs and SEM images showing durability between the foil-based conventional electrode and the textile battery electrode and b) photograph of solar-charged textile battery (adapted with permission from reference [173]. Copyright [2013] American Chemical Society). SEM images of c) front and d) cross-section of the LiCoO<sub>2</sub> fabric electrode (adapted with permission from reference [185]).

In addition to flexibility, stretchability is also a desirable property for the comfort and practical applications. However, little research work regarding stretchable fabric LIBs has been done, possibly because of the difficulty of integrating brittle battery materials into soft and stretchable fabrics. Knitted fabrics are intrinsically stretchable due to their serpentine loops. Conductive knitted fabrics can be a promising candidate as current collectors for stretchable textile LIBs. Instead of using flexible conductive fabrics, Ghadi

*et al.* reported using the conventional battery electrode fabrication method to fabricate the textile electrode by casting LiCoO<sub>2</sub> slurry onto a stretchable knitted silver fabric.<sup>185</sup> The SEM images of the LiCoO<sub>2</sub> fabric electrode (**Figure 1-13c,d**) show that the LiCoO<sub>2</sub> slurry filled in the fabric voids, stiffening the fabric and potentially rendering the composite vulnerable to cracking and delamination under strain, which can cause unsatisfactory capacity decay. The electrochemical properties of the LiCoO<sub>2</sub> fabric electrodes under or after strain were not reported. Clearly, while the conventional method to prepare a battery electrode by casting a slurry onto a metal foil is compatible with planar substrates (metal foils), it is insufficient for 3D and porous stretchable textiles. Thus, exploration and development of novel integration methods including material and structure designs to fabricate stretchable textiles LIBs are needed.

### 1.5 Summary and Scope of Dissertation

The primary goal of the research constituting this dissertation is to address the challenges faced in research field of e-textiles and e-skin, in the hope of advancing this field forward. As this introduction has illustrated, the main challenge is the mechanical mismatch between functional materials and stretchable substrates. For textile substrates, we also need to address the challenges posed by 3D, porous structures, and curved fibers. As a result, the ensuing chapters are focused on developing new fabrication methods and integration approaches to integrate functional materials with stretchable substrates, in specific, knitted textiles and PDMS elastomer.

In Chapter 2, we describe the fabrication of patterned gold-coated knitted textiles, in which individual fibers are coated with gold and the void structure is maintained. As a result, the fabricated gold-coated knitted textiles are conductive, stretchable, and durable to wearing, sweating, and washing. The achievement of these desired properties is attributed to the synergy of the knitted structure of textile, the conformal coating, and the inertness and biocompatibility of gold films. We investigate the structure and electrical change of gold-coated knitted textiles with stretching. Based on this stretchable and conductive fabric, we integrate illumination functionality inside the fabric and demonstrate stretchable electroluminescent fabrics.

In Chapter 3, we demonstrate a textile-centric design concept for e-textile fabrication in which the textile structure is used as an integral part of device design.

Specifically, we introduce a gold-coated ultrasheer knitted fabric as the transparent electrode for light-emitting textiles instead of using transparent and conductive thin films, which potentially suffer from low stretchability and durability. The semitransparency and stretchability of the knitted ultrasheer fabric properties are strategically utilized to construct stretchable light-emitting textiles in which the light emission travels through the open space between the gold-coated yarns. The conductivity and transmittance as well as the structure change of the gold-coated ultrasheer fabric with stretching are investigated. We study the emission brightness change of the light-emitting e-textile with stretching and washing.

In Chapter 4, we continue the exploration of retaining and utilizing textile structures as advantages to create e-textiles. We integrate a brittle LIB electrode material with a conductive knitted velour fabric, using the velour fabric structure as a mechanical design to protect the brittle electrode material from strain and subsequent damage. The electrical and electrochemical performance of the velour fabric electrode before and after cyclic stretching is investigated.

In Chapter 5, we introduce the use of the acid-oxidized PDMS as substrates to engineer the cracking patterns of stretchable metal films for e-skin. We use an aqueous acid mixture to oxidize PDMS and create hierarchical topography on the surface. We metallize the acid-oxidized PDMS using ELD and study the effect of the hierarchical substrate topography on the cracking patterns of the overlying metal films and corresponding electrical performance.

In Chapter 6, conclusions and an outlook for the fields of e-textiles and e-skin is discussed.

## 1.6 References

- [1] Moore, G. E. Cramming More Components onto Integrated Circuits. *Electronics* **1965**, *38*, 114-117.
- [2] Liu, Y.; Pharr, M.; Salvatore, G. A Lab-on-Skin: A Review of Flexible and Stretchable Electronics for Wearable Health Monitoring. *ACS Nano* **2017**, *11*, 9614-9635.
- [3] Zhou, W.; Yao, S.; Wang, H.; Du, Q.; Ma, Y.; Zhu, Y. Gas-Permeable, Ultrathin, Stretchable Epidermal Electronics with Porous Electrodes. *ACS Nano* **2020**, *14*, 5798-5805.
- [4] Kim, D.-H.; Lu, N.; Ma, R.; Kim, Y.-S.; Kim, R.-H.; Wang, S.; Wu, J.; Won, S.; Tao, H.; Islam, A.; Yu, K.; Kim, T.-i.; Chowdhury, R.; Ying, M.; Xu, L.; Li, M.; Chung, H.-J.; Keum, H.; McCormick, M.; Liu, P.; Zhang, Y.-W.; Omenetto, F. G.; Huang, Y.; Coleman, T.; Rogers, J. A. Epidermal Electronics. *Science* **2011**, *333*, 838-843.
- [5] Mineev, I. R.; Musienko, P.; Hirsch, A.; Barraud, Q.; Wenger, N.; Moraud, E.; Gandar, J.; Capogrosso, M.; Milekovic, T.; Asboth, L.; Torres, R.; Vachicouras, N.; Liu, Q.; Pavlova, N.; Duis, S.; Larmagnac, A.; Vörös, J.; Micera, S.; Suo, Z.; Courtine, G.; Lacour, S. P. Electronic Dura Mater for Long-Term Multimodal Neural Interfaces. *Science* **2015**, *347*, 159-163.
- [6] Xu, L.; Gutbrod, S. R.; Ma, Y.; Petrossians, A.; Liu, Y.; Webb, C. R.; Fan, J. A.; Yang, Z.; Xu, R.; Whalen, J. J.; Weiland, J. D.; Huang, Y.; Efimov, I. R.; Rogers, J. A. Materials and Fractal Designs for 3D Multifunctional Integumentary Membranes with Capabilities in Cardiac Electrotherapy. *Adv. Mater.* **2015**, *27*, 1731-1737.
- [7] Lacour, S. P.; Courtine, G.; Guck, J. Materials and Technologies for Soft Implantable Neuroprostheses. *Nat. Rev. Mater.* **2016**, *1*, 16063.
- [8] Kim, D.-H.; Lu, N.; Ghaffari, R.; Kim, Y.-S.; Lee, S. P.; Xu, L.; Wu, J.; Kim, R.-H.; Song, J.; Liu, Z.; Viventi, J.; de Graff, B.; Elolampi, B.; Mansour, M.; Slepian, M. J.; Hwang, S.; Moss, J. D.; Won, S.-M.; Huang, Y.; Litt, B.; Rogers, J. A. Materials for Multifunctional Balloon Catheters with Capabilities in Cardiac

- Electrophysiological Mapping and Ablation Therapy. *Nat. Mater.* **2011**, *10*, 316-323.
- [9] Sekitani, T.; Nakajima, H.; Maeda, H.; Fukushima, T.; Aida, T.; Hata, K.; Someya, T. Stretchable Active-Matrix Organic Light-Emitting Diode Display Using Printable Elastic Conductors. *Nat. Mater.* **2009**, *8*, 494-499.
- [10] Filiatrault, H. L.; Porteous, G. C.; Carmichael, S. R.; Davidson, G. J. E.; Carmichael, T. B. Stretchable Light-Emitting Electrochemical Cells Using an Elastomeric Emissive Material. *Adv. Mater.* **2012**, *24*, 2673-2678.
- [11] Wang, J.; Yan, C.; Cai, G.; Cui, M.; Eh, A.; Lee, P. Extremely Stretchable Electroluminescent Devices with Ionic Conductors. *Adv. Mater.* **2016**, *28*, 4490-4496.
- [12] Song, Y.; Xie, Y.; Malyarchuk, V.; Xiao, J.; Jung, I.; Choi, K.-J.; Liu, Z.; Park, H.; Lu, C.; Kim, R.-H.; Li, R.; Crozier, K. B.; Huang, Y.; Rogers, J. A. Digital Cameras with Designs Inspired by the Arthropod Eye. *Nature* **2013**, *497*, 95-99.
- [13] Ko, H.; Stoykovich, M. P.; Song, J.; Malyarchuk, V.; Choi, W.; Yu, C.-J.; Iii, J. B.; Xiao, J.; Wang, S.; Huang, Y.; Rogers, J. A. A Hemispherical Electronic Eye Camera Based on Compressible Silicon Optoelectronics. *Nature* **2008**, *454*, 748-753.
- [14] Jung, I. W.; Xiao, J. L.; Malyarchuk, V.; Lu, C. F.; Li, M.; Liu, Z. J.; Yoon, J.; Huang, Y. G.; Rogers, J. A. Dynamically Tunable Hemispherical Electronic Eye Camera System with Adjustable Zoom Capability. *Proc. Natl. Acad. Sci. U.S.A.* **2011**, *108*, 1788-1793.
- [15] Oh, J. Y.; Rondeau-Gagne, S.; Chiu, Y. C.; Chortos, A.; Lissel, F.; Wang, G. J. N.; Schroeder, B. C.; Kurosawa, T.; Lopez, J.; Katsumata, T.; Xu, J.; Zhu, C. X.; Gu, X. D.; Bae, W. G.; Kim, Y.; Jin, L. H.; Chung, J. W.; Tok, J. B. H.; Bao, Z. N. Intrinsically Stretchable and Healable Semiconducting Polymer for Organic Transistors. *Nature* **2016**, *539*, 411-415.
- [16] Oh, J. Y.; Son, D.; Katsumata, T.; Lee, Y.; Kim, Y.; Lopez, J.; Wu, H. C.; Kang, J.; Park, J.; Gu, X. D.; Mun, J.; Wang, N. G. J.; Yin, Y. K.; Cai, W.; Yun, Y. J.; Tok, J. B. H.; Bao, Z. N. Stretchable Self-Healable Semiconducting Polymer Film for Active-Matrix Strain-Sensing Array. *Sci. Adv.* **2019**, *5*, eaav3097.

- [17] Wang, S. H.; Xu, J.; Wang, W. C.; Wang, G. J. N.; Rastak, R.; Molina-Lopez, F.; Chung, J. W.; Niu, S. M.; Feig, V. R.; Lopez, J.; Lei, T.; Kwon, S. K.; Kim, Y.; Foudeh, A. M.; Ehrlich, A.; Gasperini, A.; Yun, Y.; Murmann, B.; Tok, J. B. H.; Bao, Z. Skin Electronics from Scalable Fabrication of an Intrinsically Stretchable Transistor Array. *Nature* **2018**, *555*, 83-88.
- [18] Wicaksono, I.; Tucker, C. I.; Sun, T.; Guerrero, C. A.; Liu, C.; Woo, W. M.; Pence, E. J.; Dagdeviren, C. A Tailored, Electronic Textile Conformable Suit for Large-Scale Spatiotemporal Physiological Sensing in Vivo. *npj Flex. Electron.* **2020**, *4*, 5.
- [19] Hammock, M. L.; Chortos, A.; Tee, B.; Tok, J.; Bao, Z. 25th Anniversary Article: The Evolution of Electronic Skin (E-Skin): A Brief History, Design Considerations, and Recent Progress. *Adv. Mater.* **2013**, *25*, 5997-6038.
- [20] Yang, J.; Mun, J.; Kwon, S.; Park, S.; Bao, Z.; Park, S. Electronic Skin: Recent Progress and Future Prospects for Skin-Attachable Devices for Health Monitoring, Robotics, and Prosthetics. *Adv. Mater.* **2019**, *31*, 1904765.
- [21] Chortos, A.; Bao, Z. N. Skin-Inspired Electronic Devices. *Mater. Today* **2014**, *17*, 321-331.
- [22] Khang, D. Y.; Jiang, H. Q.; Huang, Y.; Rogers, J. A. A Stretchable Form of Single-Crystal Silicon for High-Performance Electronics on Rubber Substrates. *Science* **2006**, *311*, 208-212.
- [23] Lee, P.; Lee, J.; Lee, H.; Yeo, J.; Hong, S.; Nam, K.; Lee, D.; Lee, S.; Ko, S. Highly Stretchable and Highly Conductive Metal Electrode by Very Long Metal Nanowire Percolation Network. *Adv. Mater.* **2012**, *24*, 3326-3332.
- [24] Shin, M.; Oh, J.; Lima, M.; Kozlov, M. E.; Kim, S.; Baughman, R. H. Elastomeric Conductive Composites Based on Carbon Nanotube Forests. *Adv. Mater.* **2010**, *22*, 2663-2667.
- [25] Vohra, A.; Filiatrault, H. L.; Amyotte, S. D.; Carmichael, S. R.; Suhan, N. D.; Siegers, C.; Ferrari, L.; Davidson, G. J. E.; Carmichael, T. B. Reinventing Butyl Rubber for Stretchable Electronics. *Adv. Funct. Mater.* **2016**, *26*, 5222-5229.
- [26] Xu, J.; Wang, S. H.; Wang, G. J. N.; Zhu, C. X.; Luo, S. C.; Jin, L. H.; Gu, X. D.; Chen, S. C.; Feig, V. R.; To, J. W. F.; Rondeau-Gagne, S.; Park, J.; Schroeder, B.

- C.; Lu, C.; Oh, J. Y.; Wang, Y. M.; Kim, Y. H.; Yan, H.; Sinclair, R.; Zhou, D. S.; Xue, G.; Murmann, B.; Linder, C.; Cai, W.; Tok, J. B. H.; Chung, J. W.; Bao, Z. Highly Stretchable Polymer Semiconductor Films through the Nanoconfinement Effect. *Science* **2017**, *355*, 59-64.
- [27] Wolf, M. P.; Salieb-Beugelaar, G. B.; Hunziker, P. PDMS with Designer Functionalities-Properties, Modifications Strategies, and Applications. *Prog. Polym. Sci.* **2018**, *83*, 97-134.
- [28] de Buyl, F. Silicone Sealants and Structural Adhesives. *Int. J. Adhes. Adhes.* **2001**, *21*, 411-422.
- [29] Bowden, N.; Huck, W. T. S.; Paul, K. E.; Whitesides, G. M. The Controlled Formation of Ordered, Sinusoidal Structures by Plasma Oxidation of an Elastomeric Polymer. *Appl. Phys. Lett.* **1999**, *75*, 2557.
- [30] Efimenko, K.; Wallace, W. E.; Genzer, J. Surface Modification of Sylgard-184 Poly(dimethyl siloxane) Networks by Ultraviolet and Ultraviolet/Ozone Treatment. *J. Colloid Interface Sci.* **2002**, *254*, 306-315.
- [31] Shih, T.-K.; Ho, J.-R.; Chen, C.-F.; Whang, W.-T.; Chen, C.-C. Topographic Control on Silicone Surface Using Chemical Oxidization Method. *Appl. Surf. Sci.* **2007**, *253*, 9381-9386.
- [32] Noh, J. S. Conductive Elastomers for Stretchable Electronics, Sensors and Energy Harvesters. *Polymers* **2016**, *8*, 123.
- [33] Wu, W. Stretchable Electronics: Functional Materials, Fabrication Strategies and Applications. *Sci. Technol. Adv. Mater.* **2019**, *20*, 187-224.
- [34] Matsuhisa, N.; Chen, X. D.; Bao, Z. A.; Someya, T. Materials and Structural Designs of Stretchable Conductors. *Chem. Soc. Rev.* **2019**, *48*, 2946-2966.
- [35] Kim, D. C.; Shim, H. J.; Lee, W.; Koo, J. H.; Kim, D. H. Material-Based Approaches for the Fabrication of Stretchable Electronics. *Adv. Mater.* **2020**, *32*, 1902743.
- [36] Mechael, S. S.; Wu, Y.; Schlingman, K.; Carmichael, T. B. Stretchable Metal Films. *Flex. Print.* **2018**, *3*, 43001.
- [37] Huang, H.; Spaepen, F. Tensile Testing of Free-Standing Cu, Ag and Al Thin Films and Ag/Cu Multilayers. *Acta Mater.* **2000**, *48*, 3261-3269.

- [38] Pashley, W. D. A Study of the Deformation and Fracture of Single-Crystal Gold Films of High Strength inside an Electron Microscope. *Proc. R. Soc. London, Ser. A* **1960**, 255, 218-231.
- [39] Xiang, Y.; Li, T.; Suo, Z.; Vlassak, J. J. High Ductility of a Metal Film Adherent on a Polymer Substrate. *Appl. Phys. Lett.* **2005**, 87, 161910.
- [40] Li, T.; Huang, Z. Y.; Xi, Z. C.; Lacour, S. P.; Wagner, S.; Suo, Z. Delocalizing Strain in a Thin Metal Film on a Polymer Substrate. *Mech. Mater.* **2005**, 37, 261-273.
- [41] Lacour, S.; Wagner, S.; Huang, Z.; Suo, Z. Stretchable Gold Conductors on Elastomeric Substrates. *Appl. Phys. Lett.* **2003**, 82, 2404-2406.
- [42] Lacour, S. P.; Jones, J.; Wagner, S.; Li, T.; Suo, Z. Stretchable Interconnects for Elastic Electronic Surfaces. *Proc. IEEE* **2005**, 93, 1459-1467.
- [43] Filiatrault, H. L.; Carmichael, S. R.; Boutette, R. A.; Carmichael, T. B. A Self-Assembled, Low-Cost, Microstructured Layer for Extremely Stretchable Gold Films. *ACS Appl. Mater. Interfaces* **2015**, 7, 20745-20752.
- [44] Zhao, C.; Jia, X.; Shu, K.; Yu, C.; Min, Y.; Wang, C. Stretchability Enhancement of Buckled Polypyrrole Electrode for Stretchable Supercapacitors via Engineering Substrate Surface Roughness. *Electrochim. Acta* **2020**, 343, 136099.
- [45] Lambricht, N.; Pardoen, T.; Yunus, S. Giant Stretchability of Thin Gold Films on Rough Elastomeric Substrates. *Acta Mater.* **2013**, 61, 540-547.
- [46] Bowden, N.; Brittain, S.; Evans, A. G.; Hutchinson, J. W.; Whitesides, G. M. Spontaneous Formation of Ordered Structures in Thin Films of Metals Supported on an Elastomeric Polymer. *Nature* **1998**, 393, 146-149.
- [47] Graudejus, O.; Görrn, P.; Wagner, S. Controlling the Morphology of Gold Films on Poly(dimethylsiloxane). *ACS Appl. Mater. Interfaces* **2010**, 2, 1927-1933.
- [48] Lacour, S. P.; Jones, J.; Suo, Z.; Wagner, S. Design and Performance of Thin Metal Film Interconnects for Skin-Like Electronic Circuits. *IEEE Electron Device Lett.* **2004**, 25, 179-181.
- [49] Jones, J.; Lacour, S. P.; Wagner, S.; Suo, Z. Stretchable Wavy Metal Interconnects. *J. Vac. Sci. Technol. A* **2004**, 22, 1723-1725.



- [50] Wang, X.; Hu, H.; Shen, Y.; Zhou, X.; Zheng, Z. Stretchable Conductors with Ultrahigh Tensile Strain and Stable Metallic Conductance Enabled by Prestrained Polyelectrolyte Nanoplateforms. *Adv. Mater.* **2011**, *23*, 3090-3094.
- [51] Zhang, Q.; Tang, Y.; Hajfathalian, M.; Chen, C.; Turner, K. T.; Dikin, D. A.; Lin, G.; Yin, J. Spontaneous Periodic Delamination of Thin Films to Form Crack-Free Metal and Silicon Ribbons with High Stretchability. *ACS Appl. Mater. Interfaces* **2017**, *9*, 44938-44947.
- [52] Görrn, P.; Cao, W.; Wagner, S. Isotropically Stretchable Gold Conductors on Elastomeric Substrates. *Soft Matter* **2011**, *7*, 7177-7180.
- [53] Gray, D. S.; Tien, J.; Chen, C. S. High-Conductivity Elastomeric Electronics. *Adv. Mater.* **2004**, *16*, 393-397.
- [54] Brosteaux, D.; Axisa, F.; Gonzalez, M.; Vanfleteren, J. Design and Fabrication of Elastic Interconnections for Stretchable Electronic Circuits. *IEEE Electron Device Lett.* **2007**, *28*, 552-554.
- [55] Xu, S.; Zhang, Y.; Cho, J.; Lee, J.; Huang, X.; Jia, L.; Fan, J. A.; Su, Y.; Su, J.; Zhang, H.; Cheng, H.; Lu, B.; Yu, C.; Chuang, C.; Kim, T.-i.; Song, T.; Shigeta, K.; Kang, S.; Dagdeviren, C.; Petrov, I.; Braun, P. V.; Huang, Y.; Paik, U.; Rogers, J. A. Stretchable Batteries with Self-Similar Serpentine Interconnects and Integrated Wireless Recharging Systems. *Nat. Commun.* **2013**, *4*, 1543.
- [56] Mandlik, P.; Lacour, S. P.; Li, J. W.; Chou, S. Y.; Wagner, S. Fully Elastic Interconnects on Nanopatterned Elastomeric Substrates. *IEEE Electron Device Lett.* **2006**, *27*, 650-652.
- [57] Lee, H. B.; Bae, C. W.; Duy, L.; Sohn, I. Y.; Kim, D. I.; Song, Y. J.; Kim, Y. J.; Lee, N. E. Mogul-Patterned Elastomeric Substrate for Stretchable Electronics. *Adv. Mater.* **2016**, *28*, 3069-3077.
- [58] Guo, R.; Yu, Y.; Zeng, J.; Liu, X.; Zhou, X.; Niu, L.; Gao, T.; Li, K.; Yang, Y.; Zhou, F.; Zheng, Z. Biomimicking Topographic Elastomeric Petals (E-Petals) for Omnidirectional Stretchable and Printable Electronics. *Adv. Sci.* **2015**, *2*, 1400021.
- [59] Wu, C.; Tang, X.; Gan, L.; Li, W.; Zhang, J.; Wang, H.; Qin, Z.; Zhang, T.; Zhou, T.; Huang, J.; Xie, C.; Zeng, D. High-Adhesion Stretchable Electrode via Cross-

- Linking Intensified Electroless Deposition on Biomimetic Elastomeric Micropore Film. *ACS Appl. Mater. Interfaces* **2019**, *11*, 20535-20544.
- [60] Xu, W.; Yang, J. S.; Lu, T. J. Ductility of Thin Copper Films on Rough Polymer Substrates. *Mater. Des.* **2011**, *32*, 154-161.
- [61] Lacour, S. P.; Chan, D.; Wagner, S.; Li, T.; Suo, Z. Mechanisms of Reversible Stretchability of Thin Metal Films on Elastomeric Substrates. *Appl. Phys. Lett.* **2006**, *88*, 204103.
- [62] Matsuhisa, N.; Jiang, Y.; Liu, Z. Y.; Chen, G.; Wan, C. J.; Kim, Y.; Kang, J.; Tran, H.; Wu, H. C.; You, I.; Bao, Z. A.; Chen, X. D. High-Transconductance Stretchable Transistors Achieved by Controlled Gold Microcrack Morphology. *Adv. Electron. Mater.* **2019**, *5*, 1900347.
- [63] Chen, Y.; Wu, Y.; Mechael, S. S.; Carmichael, T. B. Heterogeneous Surface Orientation of Solution-Deposited Gold Films Enables Retention of Conductivity with High Strain-A New Strategy for Stretchable Electronics. *Chem. Mater.* **2019**, *31*, 1920-1927.
- [64] Kim, S.; Lee, S.; Kim, D.; Lee, S.; Cho, K. Omnidirectionally Stretchable Metal Films with Preformed Radial Nanocracks for Soft Electronics. *ACS Appl. Nano Mater.* **2020**, *9*, 41712-41721.
- [65] Miller, M. S.; Davidson, G. J. E.; Sahli, B. J.; Mailloux, C. M.; Carmichael, T. B. Fabrication of Elastomeric Wires by Selective Electroless Metallization of Poly(dimethylsiloxane). *Adv. Mater.* **2008**, *20*, 59-64.
- [66] Graz, I. M.; Cotton, D. P. J.; Lacour, S. P. Extended Cyclic Uniaxial Loading of Stretchable Gold Thin-Films on Elastomeric Substrates. *Appl. Phys. Lett.* **2009**, *94*, 71902.
- [67] *Electroless Plating: Fundamentals and Applications*; G. O. Mal-lory, J. B. H., Ed.; American Electroplaters and Surface Finisher Society: Orlando, 1990.
- [68] Vohra, A.; Schlingman, K.; Carmichael, S. R.; Carmichael, T. B. Membrane-Interface-Elastomer Structures for Stretchable Electronics. *Chem* **2018**, *4*, 1673-1684.

- [69] Liu, Z.; Wang, X.; Qi, D.; Xu, C.; Yu, J.; Liu, Y.; Jiang, Y.; Liedberg, B.; Chen, X. High-Adhesion Stretchable Electrodes Based on Nanopile Interlocking. *Adv. Mater.* **2016**, *29*, 1603382.
- [70] Liu, Z.; Wang, H.; Huang, P.; Huang, J.; Zhang, Y.; Wang, Y.; Yu, M.; Chen, S.; Qi, D.; Wang, T.; Jiang, Y.; Chen, G.; Hu, G.; Li, W.; Yu, J.; Luo, Y.; Loh, X.; Liedberg, B.; Li, G.; Chen, X. Highly Stable and Stretchable Conductive Films through Thermal-Radiation-Assisted Metal Encapsulation. *Adv. Mater.* **2019**, *31*, 1901360.
- [71] Adovasio, J. M.; Soffer, O.; Klíma, B. Upper Palaeolithic Fibre Technology: Interlaced Woven Finds from Pavlov I, Czech Republic, C. 26,000 Years Ago. *Antiquity* **1996**, *70*, 526-534.
- [72] Cherenack, K.; van Pieterse, L. Smart Textiles: Challenges and Opportunities. *J. Appl. Phys.* **2012**, *112*, 91301.
- [73] Castano, L. M.; Flatau, A. B. Smart Fabric Sensors and E-Textile Technologies: A Review. *Smart Mater. Struct.* **2014**, *23*, 53001.
- [74] Stoppa, M.; Chiolerio, A. Wearable Electronics and Smart Textiles: A Critical Review. *Sensors* **2014**, *14*, 11957-11992.
- [75] Weng, W.; Chen, P.; He, S.; Sun, X.; Peng, H. Smart Electronic Textiles. *Angew. Chem. Int. Ed.* **2016**, *55*, 6140-6169.
- [76] Chatterjee, K.; Tabor, J.; Ghosh, T. K. Electrically Conductive Coatings for Fiber-Based E-Textiles. *Fibers* **2019**, *7*, 51.
- [77] Wang, L.; Fu, X.; He, J.; Shi, X.; Chen, T.; Chen, P.; Wang, B.; Peng, H. Application Challenges in Fiber and Textile Electronics. *Adv. Mater.* **2019**, *32*, 1901971.
- [78] Xu, X.; Xie, S.; Zhang, Y.; Peng, H. The Rise of Fiber Electronics. *Angew. Chem. Int. Ed.* **2019**, *131*, 13778-13788.
- [79] Mikucioniene, D.; Ciukas, R.; Mickeviciene, A. The Influence of the Knitting Structure on Mechanical Properties of Weft Knitted Fabrics. *Mater. Sci.* **2010**, *16*, 221-225.

- [80] Ma, Y.; Feng, X.; Rogers, J. A.; Huang, Y.; Zhang, Y. Design and Application of ‘J-Shaped’ Stress–Strain Behavior in Stretchable Electronics: A Review. *Lab on a Chip* **2017**, *17*, 1689-1704.
- [81] Zhalmuratova, D.; Chung, H.-J. Reinforced Gels and Elastomers for Biomedical and Soft Robotics Applications. *ACS Appl. Polym. Mater.* **2020**, *2*, 1073-1091.
- [82] Chatterjee, K.; Ghosh, T. K. 3D Printing of Textiles: Potential Roadmap to Printing with Fibers. *Adv. Mater.* **2019**, *32*, 1902086.
- [83] Yang, K.; Torah, R.; Wei, Y.; Beeby, S.; Tudor, J. Waterproof and Durable Screen Printed Silver Conductive Tracks on Textiles. *Text. Res. J.* **2013**, *83*, 2023-2031.
- [84] Silva, L. N.; Gonçalves, L. M.; Carvalho, H. Deposition of Conductive Materials on Textile and Polymeric Flexible Substrates. *J. Mater. Sci. Mater. Electron.* **2013**, *24*, 635-643.
- [85] Wang, Z.; Zhang, L.; Bayram, Y.; Volakis, J. L. Embroidered Conductive Fibers on Polymer Composite for Conformal Antennas. *IEEE Trans. Antennas Propag.* **2012**, *60*, 4141-4147.
- [86] Post, E. R.; Orth, M.; Russo, P. R.; Gershenfeld, N. E-Broidery: Design and Fabrication of Textile-Based Computing. *IBM Syst. J.* **2000**, *39*, 840-860.
- [87] Cottet, D.; Grzyb, J.; Kirstein, T.; Tröster, G. Electrical Characterization of Textile Transmission Lines. *IEEE Trans. Adv. Packag.* **2003**, *26*, 182-190.
- [88] Locher, I.; Tröster, G. Enabling Technologies for Electrical Circuits on a Woven Monofilament Hybrid Fabric. *Text. Res. J.* **2008**, *78*, 583-594.
- [89] Ma, R.; Lee, J.; Choi, D.; Moon, H.; Baik, S. Knitted Fabrics Made from Highly Conductive Stretchable Fibers. *Nano Lett.* **2014**, *14*, 1944-1951.
- [90] Li, Q.; Tao, X. A Stretchable Knitted Interconnect for Three-Dimensional Curvilinear Surfaces. *Text. Res. J.* **2011**, *81*, 1171-1182.
- [91] Okuzaki, H.; Ishihara, M. Spinning and Characterization of Conducting Microfibers. *Macromol. Rapid Commun.* **2003**, *24*, 261-264.
- [92] Foroughi, J.; Spinks, G. M.; Wallace, G. G.; Whitten, P. G. Production of Polypyrrole Fibres by Wet Spinning. *Synth. Met.* **2008**, *158*, 104-107.

- [93] Seyedin, S.; Razal, J. M.; Innis, P. C.; Jeiranikhameneh, A.; Beirne, S.; Wallace, G. G. Knitted Strain Sensor Textiles of Highly Conductive All-Polymeric Fibers. *ACS Appl. Mater. Interfaces* **2015**, *7*, 21150-21158.
- [94] Li, Y.-L.; Kinloch, I. A.; Windle, A. H. Direct Spinning of Carbon Nanotube Fibers from Chemical Vapor Deposition Synthesis. *Science* **2004**, *304*, 276-278.
- [95] Xu, Z.; Gao, C. Graphene Chiral Liquid Crystals and Macroscopic Assembled Fibres. *Nat. Commun.* **2011**, *2*, 571.
- [96] Schwarz, A.; Hakuzimana, J.; Kaczynska, A.; Banaszczyk, J.; Westbroek, P.; McAdams, E.; Moody, G.; Chronis, Y.; Priniotakis, G.; Mey, G.; Tseles, D.; Langenhove, L. Gold Coated Para-Aramid Yarns through Electroless Deposition. *Surf. Coat. Technol.* **2010**, *204*, 1412-1418.
- [97] Little, B. K.; Li, Y.; Cammarata, V.; Broughton, R.; Mills, G. Metallization of Kevlar Fibers with Gold. *ACS Appl. Mater. Interfaces* **2011**, *3*, 1965-1973.
- [98] Liu, X.; Chang, H.; Li, Y.; Huck, W. T. S.; Zheng, Z. Polyelectrolyte-Bridged Metal/Cotton Hierarchical Structures for Highly Durable Conductive Yarns. *ACS Appl. Mater. Interfaces* **2010**, *2*, 529-535.
- [99] Schwarz, A.; Hakuzimana, J.; Gasana, E.; Westbroek, P.; Langenhove, L. Gold Coated Polyester Yarn. *Adv. Sci. Technol.* **2008**, *60*, 47-51.
- [100] Atwa, Y.; Maheshwari, N.; Goldthorpe, I. A. Silver Nanowire Coated Threads for Electrically Conductive Textiles. *J. Mater. Chem. C* **2015**, *3*, 3908-3912.
- [101] Irwin, M. D.; Roberson, D. A.; Olivas, R. I.; Wicker, R. B.; MacDonald, E. Conductive Polymer-Coated Threads as Electrical Interconnects in E-Textiles. *Fibers Polym.* **2011**, *12*, 904.
- [102] Ryan, J. D.; Mengistie, D.; Gabrielsson, R.; Lund, A.; Müller, C. Machine-Washable PEDOT:PSS Dyed Silk Yarns for Electronic Textiles. *ACS Appl. Mater. Interfaces* **2017**, *9*, 9045-9050.
- [103] Eom, J.; Jaisutti, R.; Lee, H.; Lee, W.; Heo, J.-S.; Lee, J.-Y.; Park, S.; Kim, Y.-H. Highly Sensitive Textile Strain Sensors and Wireless User-Interface Devices Using All-Polymeric Conducting Fibers. *ACS Appl. Mater. Interfaces* **2017**, *9*, 10190-10197.

- [104] Bashir, T.; Skrifvars, M.; Persson, N. K. Synthesis of High Performance, Conductive PEDOT-Coated Polyester Yarns by OCVD Technique. *Polym. Adv. Technol.* **2012**, *23*, 611-617.
- [105] Lin, Z.-I.; Lou, C.-W.; Pan, Y.-J.; Hsieh, C.-T.; Huang, C.-H.; Huang, C.-L.; Chen, Y.-S.; Lin, J.-H. Conductive Fabrics Made of Polypropylene/Multi-Walled Carbon Nanotube Coated Polyester Yarns: Mechanical Properties and Electromagnetic Interference Shielding Effectiveness. *Compos. Sci. Technol.* **2017**, *141*, 74-82.
- [106] Uzun, S.; Seyedin, S.; Stoltzfus, A. L.; Levitt, A. S.; Alhabeab, M.; Anayee, M.; Strobel, C. J.; Razal, J. M.; Dion, G.; Gogotsi, Y. Knittable and Washable Multifunctional Mxene-Coated Cellulose Yarns. *Adv. Funct. Mater.* **2019**, *29*, 1905015.
- [107] Orth, M. Defining Flexibility and Sewability in Conductive Yarns. *Mater. Res. Soc. Symp. Proc.* **2002**, *736*.
- [108] Hu, L.; Pasta, M.; Mantia, F.; Cui, L.; Jeong, S.; Deshazer, H.; Choi, J.; Han, S.; Cui, Y. Stretchable, Porous, and Conductive Energy Textiles. *Nano Lett.* **2010**, *10*, 708-714.
- [109] Ogawa, Y.; Takai, Y.; Kato, Y.; Kai, H.; Miyake, T.; Nishizawa, M. Stretchable Biofuel Cell with Enzyme-Modified Conductive Textiles. *Biosens. Bioelectron.* **2015**, *74*, 947-952.
- [110] Cui, H.-W.; Sukanuma, K.; Uchida, H. Highly Stretchable, Electrically Conductive Textiles Fabricated from Silver Nanowires and Cupro Fabrics Using a Simple Dipping-Drying Method. *Nano Res.* **2015**, *8*, 1604-1614.
- [111] Gan, L.; Shang, S.; Yuen, C.; Jiang, S.-x. Graphene Nanoribbon Coated Flexible and Conductive Cotton Fabric. *Compos. Sci. Technol.* **2015**, *117*, 208-214.
- [112] Cataldi, P.; Ceseracciu, L.; Athanassiou, A.; Bayer, I. S. A Healable Cotton-Graphene Nanocomposite Conductor for Wearable Electronics. *ACS Appl. Mater. Interfaces* **2017**, *9*, 13825-13830.
- [113] Takamatsu, S.; Lonjaret, T.; Crisp, D.; Badier, J.-M.; Malliaras, G. G.; Ismailova, E. Direct Patterning of Organic Conductors on Knitted Textiles for Long-Term Electrocardiography. *Sci. Rep.* **2015**, *5*, 15003.

- [114] Moraes, M. R.; Alves, A. C.; Toptan, F.; Martins, M. S.; Vieira, E. M. F.; Paleo, A. J.; Souto, A. P.; Santos, W. L. F.; Esteves, M. F.; Zille, A. Glycerol/PEDOT:PSS Coated Woven Fabric as a Flexible Heating Element on Textiles. *J. Mater. Chem. C* **2017**, *5*, 3807-3822.
- [115] Guo, Y.; Otley, M. T.; Li, M.; Zhang, X.; Sinha, S. K.; Treich, G. M.; Sotzing, G. A. PEDOT:PSS “Wires” Printed on Textile for Wearable Electronics. *ACS Appl. Mater. Interfaces* **2016**, *8*, 26998-27005.
- [116] Ding, Y.; Invernale, M. A.; Sotzing, G. A. Conductivity Trends of PEDOT-PSS Impregnated Fabric and the Effect of Conductivity on Electrochromic Textile. *ACS Appl. Mater. Interfaces* **2010**, *2*, 1588-1593.
- [117] Matsuhisa, N.; Kaltenbrunner, M.; Yokota, T.; Jinno, H.; Kuribara, K.; Sekitani, T.; Someya, T. Printable Elastic Conductors with a High Conductivity for Electronic Textile Applications. *Nat. Commun.* **2015**, *6*, 7461.
- [118] Kim, Y.; Kim, H.; Yoo, H.-J. Electrical Characterization of Screen-Printed Circuits on the Fabric. *IEEE Trans. Adv. Packag.* **2010**, *33*, 196-205.
- [119] Kazani, I.; Hertleer, C.; May, G.; Schwarz, A.; Guxho, G.; Langenhove, L. Electrical Conductive Textiles Obtained by Screen Printing. *Fibres Text. East. Eur.* **2012**, *20*, 57-63.
- [120] La, T. -G.; Qiu, S.; Scott, D. K.; Bakhtiari, R.; Jonathan, W. P. K.; Mathewson, K. E.; Rieger, J.; Chung, H. -J. Two-Layered and Stretchable e-Textile Patches for Wearable Healthcare Electronics. *Adv. Healthcare Mater.* **2018**, *7*, 1801033.
- [121] Farboodmanesh, S.; Chen, J.; Mead, J. L.; White, K. D.; Yesilalan, H. E.; Laoulache, R.; Warner, S. B. Effect of Coating Thickness and Penetration on Shear Behavior of Coated Fabrics. *J. Elastomers Plast.* **2005**, *37*, 197-227.
- [122] Kim, I.; Shahariar, H.; Ingram, W. F.; Zhou, Y.; Jur, J. S. Inkjet Process for Conductive Patterning on Textiles: Maintaining Inherent Stretchability and Breathability in Knit Structures. *Adv. Funct. Mater.* **2019**, *29*, 1807573.
- [123] Jin, H.; Matsuhisa, N.; Lee, S.; Abbas, M.; Yokota, T.; Someya, T. Enhancing the Performance of Stretchable Conductors for E-Textiles by Controlled Ink Permeation. *Adv. Mater.* **2017**, *29*, 1605848.

- [124] Wei, Q.; Yu, L.; Wu, N.; Hong, S. Preparation and Characterization of Copper Nanocomposite Textiles. *J. Ind. Text.* **2008**, *37*, 275-283.
- [125] Depla, D.; Segers, S.; Leroy, W.; Hove, T.; Parys, M. Smart Textiles: An Explorative Study of the Use of Magnetron Sputter Deposition. *Text. Res. J.* **2011**, *81*, 1808-1817.
- [126] Zhang, L.; Fairbanks, M.; Andrew, T. L. Rugged Textile Electrodes for Wearable Devices Obtained by Vapor Coating Off-the-Shelf, Plain-Woven Fabrics. *Adv. Funct. Mater.* **2017**, *27*, 1700415.
- [127] Brozena, A. H.; Oldham, C. J.; Parsons, N. G. Atomic Layer Deposition on Polymer Fibers and Fabrics for Multifunctional and Electronic Textiles. *J. Vac. Sci. Technol. A* **2016**, *34*, 010801.
- [128] Hollies, N. R. S.; Kaessinger, M. M.; Watson, B. S.; Bogaty, H. Water Transport Mechanisms in Textile Materials. *Text. Res. J.* **1957**, *27*, 8-13.
- [129] Jiang, S. Q.; Newton, E.; Yuen, C. W. M.; Kan, C. W. Chemical Silver Plating and Its Application to Textile Fabric Design. *J. Appl. Polym. Sci.* **2005**, *96*, 919-926.
- [130] Gan, X.; Wu, Y.; Liu, L.; Shen, B.; Hu, W. Electroless Plating of Cu-Ni-P Alloy on PET Fabrics and Effect of Plating Parameters on the Properties of Conductive Fabrics. *J. Alloys Compd.* **2008**, *455*, 308-313.
- [131] Afzali, A.; Mottaghitalab, V.; Motlagh, M.; Haghi, A. The Electroless Plating of Cu-Ni-P Alloy onto Cotton Fabrics. *Korean J. Chem. Eng.* **2010**, *27*, 1145-1149.
- [132] Guo, R. H.; Jiang, S. X.; Zheng, Y. D.; Lan, J. W. Electroless Nickel Deposition of a Palladium-Activated Self-Assembled Monolayer on Polyester Fabric. *J. Appl. Polym. Sci.* **2013**, *127*, 4186-4193.
- [133] Moazzenchi, B.; Montazer, M. Click Electroless Plating of Nickel Nanoparticles on Polyester Fabric: Electrical Conductivity, Magnetic and EMI Shielding Properties. *Colloids Surf. A Physicochem. Eng. Asp.* **2019**, *571*, 110-124.
- [134] Yan, C.; Zheng, Z. The Development of Pad-Dry-Cure Compatible Method for Preparing Electrically Conductive Copper Coated Cotton Woven Fabrics. *J. Fiber Bioeng. Inform.* **2013**, *6*, 117-128.
- [135] Haghdoost, F.; Mottaghitalab, V.; Haghi, A. Comfortable Textile-Based Electrode for Wearable Electrocardiogram. *Sens. Rev.* **2015**, *35*, 20-29.



- [136] Liu, S.; Hu, M.; Yang, J. A Facile Way of Fabricating a Flexible and Conductive Cotton Fabric. *J. Mater. Chem. C* **2016**, *4*, 1320-1325.
- [137] Zhao, H.; Hou, L.; Wu, J. X.; Lu, Y. X. Fabrication of Dual-Side Metal Patterns onto Textile Substrates for Wearable Electronics by Combining Wax-Dot Printing with Electroless Plating. *J. Mater. Chem. C* **2016**, *4*, 7156-7164.
- [138] Taushanoff, S.; Dubin, V. M. Photopatternable, Electrochemically Plated Conductive Fabrics. *ECS Trans.* **2017**, *77*, 877-885.
- [139] Mao, Y.; Zhu, M.; Wang, W.; Yu, D. Well-Defined Silver Conductive Pattern Fabricated on Polyester Fabric by Screen Printing a Dopamine Surface Modifier Followed by Electroless Plating. *Soft Matter* **2018**, *14*, 1260-1269.
- [140] Zhu, C.; Chalmers, E.; Chen, L.; Wang, Y.; Xu, B.; Li, Y.; Liu, X. A Nature-Inspired, Flexible Substrate Strategy for Future Wearable Electronics. *Small* **2019**, *15*, 1902440.
- [141] Lin, X.; Wu, M.; Zhang, L.; Wang, D. Superior Stretchable Conductors by Electroless Plating of Copper on Knitted Fabrics. *ACS Appl. Electron. Mater.* **2019**, *1*, 397-406.
- [142] Sharma, S. P. Atmospheric Corrosion of Silver, Copper, and Nickel-Environmental Test. *J. Electrochem. Soc.* **1978**, *125*, 2005-2011.
- [143] Thyssen, J. P.; Menné, T. Metal Allergy-A Review on Exposures, Penetration, Genetics, Prevalence, and Clinical Implications. *Chem. Res. Toxicol.* **2010**, *23*, 309-318.
- [144] Zhu, B.; Gong, S.; Cheng, W. Softening Gold for Elastronics. *Chem. Soc. Rev.* **2018**, *48*, 1668-1711.
- [145] Wu, J.; Zhou, D.; Too, C. O.; Wallace, G. G. Conducting Polymer Coated Lycra. *Synth. Met.* **2005**, *155*, 698-701.
- [146] Muthukumar, N.; Thilagavathi, G.; Kannaian, T. Analysis of Piezoresistive Behavior of Polyaniline-Coated Nylon Lycra Fabrics for Elbow Angle Measurement. *J. Text. Inst.* **2016**, *108*, 1-8.
- [147] Hong, K.; Oh, K.; Kang, T. Preparation and Properties of Electrically Conducting Textiles by In Situ Polymerization of Poly(3,4-ethylenedioxythiophene). *J. Appl. Polym. Sci.* **2005**, *97*, 1326-1332.

- [148] Wang, C.; Zhang, M.; Xia, K.; Gong, X.; Wang, H.; Yin, Z.; Guan, B.; Zhang, Y. Intrinsically Stretchable and Conductive Textile by a Scalable Process for Elastic Wearable Electronics. *ACS Appl. Mater. Interfaces* **2017**, *9*, 13331-13338.
- [149] Wang, C.; Li, X.; Gao, E.; Jian, M.; Xia, K.; Wang, Q.; Xu, Z.; Ren, T.; Zhang, Y. Carbonized Silk Fabric for Ultrastretchable, Highly Sensitive, and Wearable Strain Sensors. *Adv. Mater.* **2016**, *28*, 6640-6648.
- [150] Parkova, I.; Parkovs, I.; Vilumsone, A. Light-Emitting Textile Display with Floats for Electronics Covering. *Int. J. Cloth. Sci. Tech.* **2015**, *27*, 34-46.
- [151] Cherenack, K.; Zysset, C.; Kinkeldei, T.; Münzenrieder, N.; Tröster, G. Woven Electronic Fibers with Sensing and Display Functions for Smart Textiles. *Adv. Mater.* **2010**, *22*, 5178-5182.
- [152] Choi, W.-S.; Kim, W.; Park, S.-H.; Cho, S.; Lee, J.; Park, J.; Ha, J.-S.; Chung, T.; Jeong, T. Light-Emitting Diodes Fabricated on an Electrical Conducting Flexible Substrate. *Solid State Electron.* **2017**, *127*, 57-60.
- [153] Kim, W.; Kwon, S.; Lee, S.-M.; Kim, J.; Han, Y.; Kim, E.; Choi, K.; Park, S.; Park, B.-C. Soft Fabric-Based Flexible Organic Light-Emitting Diodes. *Org. Electron.* **2013**, *14*, 3007-3013.
- [154] Kim, W.; Kwon, S.; Han, Y.; Kim, E.; Choi, K.; Kang, S. H.; Park, B. C. Reliable Actual Fabric-Based Organic Light-Emitting Diodes: Toward a Wearable Display. *Adv. Electron. Mater.* **2016**, *2*, 1600220.
- [155] Choi, S.; Kwon, S.; Kim, H.; Kim, W.; Kwon, J.; Lim, M.; Lee, H.; Choi, K. Highly Flexible and Efficient Fabric-Based Organic Light-Emitting Devices for Clothing-Shaped Wearable Displays. *Sci. Rep.* **2017**, *7*, 6424.
- [156] Kim, H.; Kwon, S.; Choi, S.; Choi, K. Solution-Processed Bottom-Emitting Polymer Light-Emitting Diodes on a Textile Substrate Towards a Wearable Display. *J. Inf. Disp.* **2015**, *16*, 179-184.
- [157] Lanz, T.; Sandström, A.; Tang, S.; Chabrecek, P.; Sonderegger, U.; Edman, L. A Light-Emission Textile Device: Conformal Spray-Sintering of a Woven Fabric Electrode. *Flex. Print.* **2016**, *1*, 25004.
- [158] Vos, M.; Torah, R.; Tudor, J. Dispenser Printed Electroluminescent Lamps on Textiles for Smart Fabric Applications. *Smart Mater. Struct.* **2016**, *25*, 45016.

- [159] Hu, B.; Li, D.; Manandharm, P.; Fan, Q.; Kasilingam, D.; Calvert, P. CNT/Conducting Polymer Composite Conductors Impart High Flexibility to Textile Electroluminescent Devices. *J. Mater. Chem.* **2011**, *22*, 1598-1605.
- [160] Hu, B.; Li, D.; Ala, O.; Manandhar, P.; Fan, Q.; Kasilingam, D.; Calvert, P. D. Textile-Based Flexible Electroluminescent Devices. *Adv. Funct. Mater.* **2011**, *21*, 305-311.
- [161] Graßmann, C.; Grethe, T.; van Langenhove, L.; Schwarz-Pfeiffer, A. Digital Printing of Electroluminescent Devices on Textile Substrates. *J. Eng. Fibers Fabr.* **2019**, *14*, 1-10.
- [162] de Vos, M.; Torah, R.; Glanc-Gostkiewicz, M.; Tudor, J. A Complex Multilayer Screen-Printed Electroluminescent Watch Display on Fabric. *J. Disp. Technol.* **2016**, *12*, 1757-1763.
- [163] Zhang, Z.; Shi, X.; Lou, H.; Xu, Y.; Zhang, J.; Li, Y.; Cheng, X.; Peng, H. A Stretchable and Sensitive Light-Emitting Fabric. *J. Mater. Chem. C* **2017**, *5*, 4139-4144.
- [164] Wang, L.; Xiao, L.; Gu, H. S.; Sun, H. D. Advances in Alternating Current Electroluminescent Devices. *Adv. Opt. Mater.* **2019**, *7*, 1801154.
- [165] Bredol, M.; Dieckhoff, H. Materials for Powder-Based AC-Electroluminescence. *Materials* **2010**, *3*, 1353-1374.
- [166] Wang, J.; Yan, C.; Chee, K.; Lee, P. Highly Stretchable and Self-Deformable Alternating Current Electroluminescent Devices. *Adv. Mater.* **2015**, *27*, 2876-2882.
- [167] Zhang, C.; Zhu, J.; Lin, H.; Huang, W. Flexible Fiber and Fabric Batteries. *Adv. Mater. Technol.* **2018**, *3*, 1700302.
- [168] Liu, Z.; Mo, F.; Li, H.; Zhu, M.; Wang, Z.; Liang, G.; Zhi, C. Advances in Flexible and Wearable Energy-Storage Textiles. *Small Methods* **2018**, *2*, 1800124.
- [169] Zhai, S.; Karahan, E. H.; Wei, L.; Qian, Q.; Harris, A. T.; Minett, A. I.; Ramakrishna, S.; Ng, A.; Chen, Y. Textile Energy Storage: Structural Design Concepts, Material Selection and Future Perspectives. *Energy Storage Mater.* **2016**, *3*, 123-139.
- [170] Jost, K.; Dion, G.; Gogotsi, Y. Textile Energy Storage in Perspective. *J. Mater. Chem. A* **2014**, *2*, 10776-10787.

- [171] Etacheri, V.; Marom, R.; Elazari, R.; Salitra, G.; Aurbach, D. Challenges in the Development of Advanced Li-Ion Batteries: A Review. *Energy Environ. Sci.* **2011**, *4*, 3243-3262.
- [172] Nitta, N.; Wu, F. X.; Lee, J. T.; Yushin, G. Li-Ion Battery Materials: Present and Future. *Mater. Today* **2015**, *18*, 252-264.
- [173] Lee, Y.-H.; Kim, J.-S.; Noh, J.; Lee, I.; Kim, H.; Choi, S.; Seo, J.; Jeon, S.; Kim, T.-S.; Lee, J.-Y.; Choi, J. Wearable Textile Battery Rechargeable by Solar Energy. *Nano Lett.* **2013**, *13*, 5753-5761.
- [174] Zhu, Y.; Yang, M.; Huang, Q.; Wang, D.; Yu, R.; Wang, J.; Zheng, Z.; Wang, D. V<sub>2</sub>O<sub>5</sub> Textile Cathodes with High Capacity and Stability for Flexible Lithium-Ion Batteries. *Adv. Mater.* **2020**, *32*, 1906205.
- [175] Pu, X.; Li, L.; Song, H.; Du, C.; Zhao, Z.; Jiang, C.; Cao, G.; Hu, W.; Wang, Z. A Self-Charging Power Unit by Integration of a Textile Triboelectric Nanogenerator and a Flexible Lithium-Ion Battery for Wearable Electronics. *Adv. Mater.* **2015**, *27*, 2472-2478.
- [176] Lee, K.; Choi, J.; Lee, H.; Kim, K.; Choi, J. Solution-Processed Metal Coating to Nonwoven Fabrics for Wearable Rechargeable Batteries. *Small* **2017**, *14*, 1703028.
- [177] Kang, C.; Choi, J.; Ko, Y.-J.; Lee, S.; Kim, H.; Kim, J.; Son, S. Thin Coating of Microporous Organic Network Makes a Big Difference: Sustainability Issue of Ni Electrodes on the PET Textile for Flexible Lithium-Ion Batteries. *ACS Appl. Mater. Interfaces* **2017**, *9*, 36936-36943.
- [178] Gao, Z.; Song, N.; Zhang, Y.; Li, X. Cotton-Textile-Enabled, Flexible Lithium-Ion Batteries with Enhanced Capacity and Extended Lifespan. *Nano Lett.* **2015**, *15*, 8194-8203.
- [179] Xu, S.; Cen, D.; Gao, P.; Tang, H.; Bao, Z. 3D Interconnected V<sub>6</sub>O<sub>13</sub> Nanosheets Grown on Carbonized Textile via a Seed-Assisted Hydrothermal Process as High-Performance Flexible Cathodes for Lithium-Ion Batteries. *Nanoscale Res. Lett.* **2018**, *13*, 65.
- [180] Liu, B.; Zhang, J.; Wang, X.; Chen, G.; Chen, D.; Zhou, C.; Shen, G. Hierarchical Three-Dimensional ZnCO<sub>2</sub>O<sub>4</sub> Nanowire Arrays/Carbon Cloth Anodes for a Novel

- Class of High-Performance Flexible Lithium-Ion Batteries. *Nano Lett.* **2012**, *12*, 3005-3011.
- [181] Balogun, M.-S.; Wu, Z.; Luo, Y.; Qiu, W.; Fan, X.; Long, B.; Huang, M.; Liu, P.; Tong, Y. High Power Density Nitridated Hematite ( $\alpha$ -Fe<sub>2</sub>O<sub>3</sub>) Nanorods as Anode for High-Performance Flexible Lithium Ion Batteries. *J. Power Sources* **2016**, *308*, 7-17.
- [182] Ma, K.; Liu, X.; Cheng, Q.; Saha, P.; Jiang, H.; Li, C. Flexible Textile Electrode with High Areal Capacity from Hierarchical V<sub>2</sub>O<sub>5</sub> Nanosheet Arrays. *J. Power Sources* **2017**, *357*, 71-76.
- [183] Ha, S.; Shin, K.; Park, H.; Lee, Y. Flexible Lithium-Ion Batteries with High Areal Capacity Enabled by Smart Conductive Textiles. *Small* **2018**, *14*, 1703418.
- [184] Min, X.; Sun, B.; Chen, S.; Fang, M.; Wu, X.; Liu, Y. g.; Abdelkader, A.; Huang, Z.; Liu, T.; Xi, K.; Kumar, V. R. A Textile-Based SnO<sub>2</sub> Ultra-Flexible Electrode for Lithium-Ion Batteries. *Energy Storage Mater.* **2019**, *16*, 597-606.
- [185] Ghadi, B.; Yuan, M.; Ardebili, H. Stretchable Fabric-Based LiCoO<sub>2</sub> Electrode for Lithium Ion Batteries. *Extreme Mech. Lett.* **2019**, *32*, 100532.

**Chapter 2 Solution Deposition of Conformal Gold Coatings on Knitted Fabric for  
E-Textiles and Electroluminescent Clothing**

## **2.1 Introduction**

Textile-based wearable electronics will unlock a future with a redefined human-computer interaction, in which interacting with devices is as simple as getting dressed. For truly wearable electronics, it is essential to integrate electrical functionality while maintaining the soft, stretchable properties of the textile, and the look and feel the end-user expects. The rapidly developing field of skin-mounted wearable electronics has successfully addressed the fundamental mismatch between conventional hard electronics and soft substrates by developing an impressive range of soft devices on elastomers that can be laminated on the skin, including biosensors,<sup>1</sup> displays,<sup>2</sup> and power sources.<sup>3</sup> Integrating such sophisticated function into textiles, however, is vastly different from fabrication on the flat surfaces of elastomers due to the porous, 3D structure of knitted or woven fabrics. This difference presents special challenges to the field of e-textiles, distinguishing it conceptually from elastomer-based stretchable electronics. A fundamental step toward sophisticated e-textiles involves endowing textiles with electrical conductivity, which forms the basis of two design concepts: The first concept uses conductive wiring integrated in the textile to form a power bus and data network to connect multiple, separate devices, effectively decoupling device fabrication from the textile and enabling the distribution of high-performance devices over different locations in clothing.<sup>4,5</sup> The second concept seeks more intimate merging of devices with textiles by using a conductive textile as a base on which to build up layers of functional materials to form highly integrated, imperceptible devices.<sup>6</sup> Both approaches require highly conductive textiles with stable conductivity under strain for consistent performance, as well as stretchability and flexibility.

Knitted or woven textiles present a unique challenge owing to their complex, porous 3D structure, which consists of an interconnected network of fiber bundles (yarns) separated by a network of voids. These voids are key to the flexibility and stretchability of the fabric by providing space for the yarns to move and slip in response to stress. Creating conductive pathways by filling these voids with conductive inks or pastes, such as conductive polymers,<sup>7</sup> or composites of polymers with graphene,<sup>8</sup> carbon nanotubes,<sup>9</sup> silver nanoparticles,<sup>10</sup> or silver flakes,<sup>11</sup> forms a conductive composite; however, this approach restricts the movement of yarns and stiffens the textile. Such composites are also

vulnerable to cracking under strain.<sup>8</sup> Weaving,<sup>12</sup> knitting<sup>13</sup> or embroidering<sup>14</sup> metal wires or conductive threads into the fabric is one way to add conductivity while maintaining the void network, although this approach can be laborious, and breakage of metal wires during the manufacturing process is a concern.<sup>15</sup> Another tactic has been to develop methods that coat only the individual yarns or fibers of fabric with conductive materials, which leaves the void network unchanged to retain stretchability. For example, Jin *et al.* developed specialized conductive ink formulations to control the permeation of the ink in the textile and maintain the voids.<sup>16</sup> Other approaches use in situ polymerization of conductive polymers<sup>17,18</sup> in the textile or carbonization<sup>19-21</sup> of textiles through thermal treatment; however, the former typically results in low conductivity, and the latter requires cellulose-based textiles that convert to graphite-like materials at very high temperatures (~1000 °C).

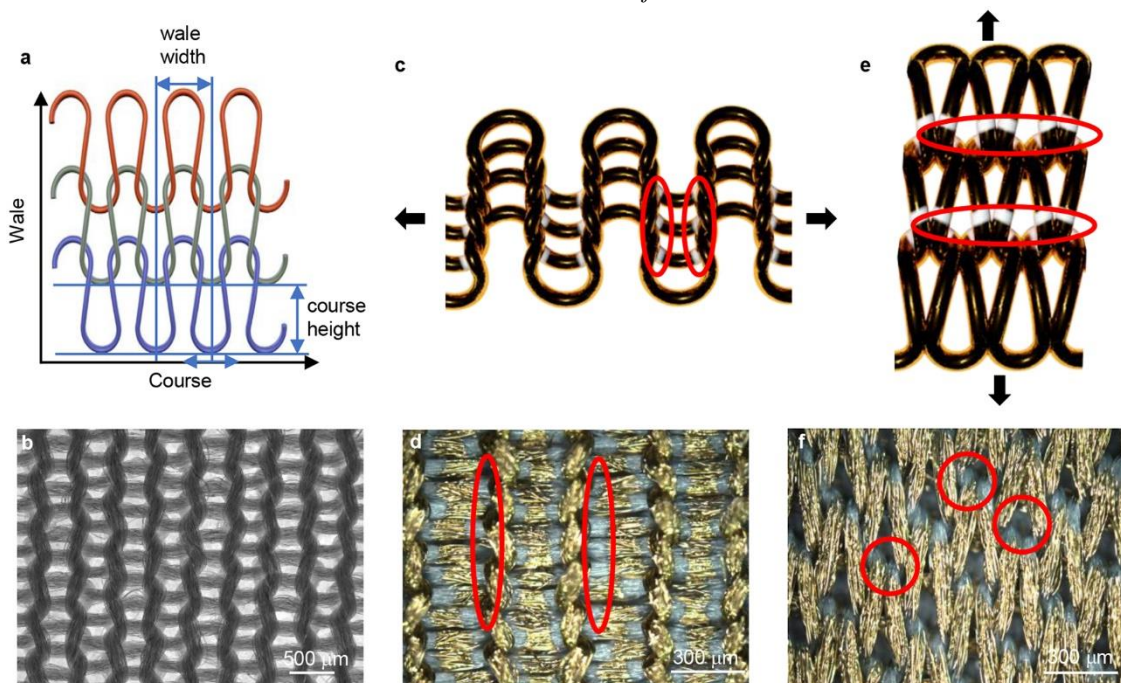
Depositing thin metal coatings on textiles is a promising approach to afford high conductivity while maintaining the void structure necessary for stretchability. Physical vapor deposition (PVD) of metals is a standard method used to prepare metal films; however, its line-of-sight nature is incompatible with the 3D structures of woven or knitted textiles (vide infra). Although PVD methods are suitable for nonwoven fabrics, which are made by binding fibers together in a planar sheet or web, such fabrics are not stretchable.<sup>22</sup> Additional planarization layers, such as polyurethanes, deposited on the fabric can make PVD methods applicable to stretchable knitted or woven fabrics, but this approach fills the void structure and restricts the stretchability.<sup>23,24</sup> Electroless deposition (ELD) is a solution-based alternative to PVD with an important advantage for knitted and woven fabrics: The ELD plating solution can permeate the fabric structure to deposit metal on individual fibers, leaving the void structure intact.<sup>25-31</sup> Metals deposited on woven cotton or nylon textiles using ELD, such as copper,<sup>25,26</sup> silver,<sup>27</sup> and nickel,<sup>28-31</sup> exhibit low sheet resistances (<1  $\Omega/\text{sq}$ ), but the stretchability is limited by the structure of the woven fabric, which consists of interlacing yarns at right angles that restrict stretching to the diagonal direction. Furthermore, the metals demonstrated in these studies are problematic for wearables due to the propensity of silver and copper to oxidize or corrode,<sup>32</sup> particularly in contact with salt solutions like human sweat, and the prevalence of contact dermatitis caused by nickel metal.<sup>33</sup>



Here, we describe the solution deposition of patterned gold coatings on knitted fabric that are conductive, stretchable, wearable, and washable. We chose gold as the metal because it is biocompatible, chemically inert, and not easily oxidized.<sup>34</sup> Our simple, low-cost method uses electroless nickel immersion gold (ENIG) plating, a solution-based technique commonly employed in printed circuit board fabrication.<sup>35</sup> The ENIG process deposits a gold coating over the individual textile fibers, producing a highly conductive textile that retains the softness and stretchability of the knitted fabric. We demonstrate screen printing of a wax resist to pattern the deposition of gold on the fabric, and furthermore employ gold-coated textiles to fabricate stretchable and wearable electroluminescent textiles.

## **2.2 Results and Discussion**

We chose a weft-knitted polyester fabric with a water-resistant polyurethane backing as our substrate. Weft-knitted fabrics consist of wale (column) loops and course (row) loops interlinked with each other (**Figure 2-1a,b**). The polyester fiber of the fabric is not stretchable; rather, the fabric is stretchable due to the serpentine loops in the knitted structure. Stretching along the course direction straightens the curved serpentine yarns, increasing the wale width and decreasing the course height. Stretching along the wale direction increases the course height and decreases the wale width. Using PVD to deposit gold on the weft-knitted textile highlights the complexity of the interlinked structure and, consequently, its incompatibility with the line-of-sight PVD process. Overlying yarns at the interlinked course and wale junctions block gold deposition on the underlying yarns, producing a discontinuous gold coating with broken conductive pathways along the course (**Figure 2-1c,d**) and the wale (**Figure 2-1e,f**) directions.

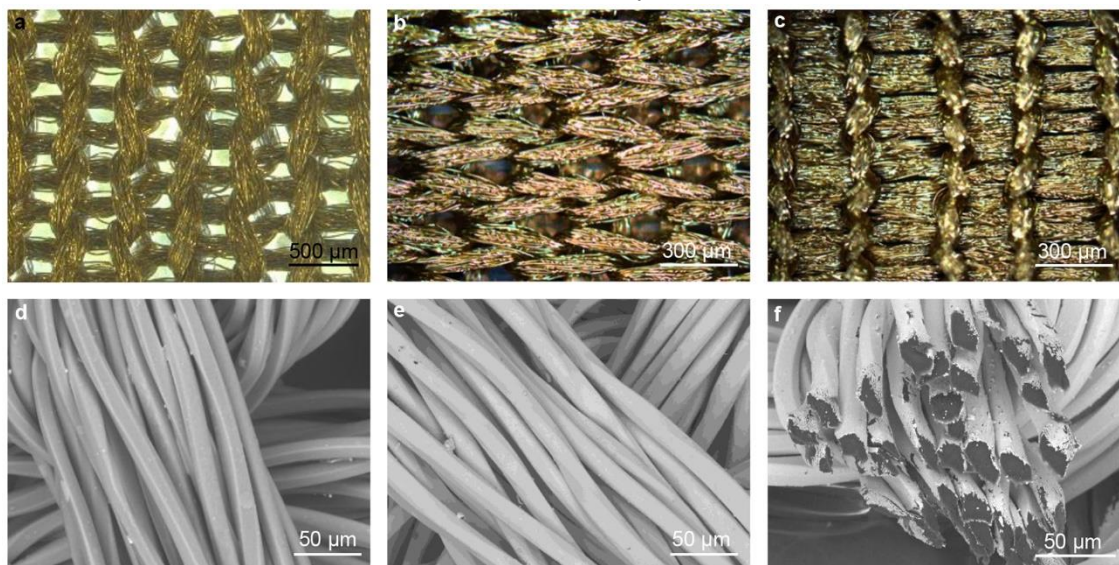


**Figure 2-1** The weft-knitted textile structure. a) Schematic of the weft-knitted textile structure. b) Stereomicroscope image of the pristine textile. Illustrations and optical microscope images of PVD gold-coated textiles stretched in the c,d) course direction and e,f) wale direction, respectively. Red circles show examples of locations where gold deposition was blocked.

We used the solution-based ENIG method to uniformly coat the fibers of the weft-knitted textile with gold and create conductive pathways throughout the textile structure. The ENIG process consists of two solution-based plating steps: ELD of nickel followed by an immersion gold process. The ELD nickel process involves first activating the textile by adsorbing a catalytic species onto its surface. We used a palladium-tin colloidal catalyst, which consists of a palladium-rich core protected from oxidation by a hydrolyzed  $\text{Sn}^{2+}/\text{Sn}^{4+}$  shell, and an associated chloride layer that gives the colloids a negatively charged surface.<sup>36</sup> Pd/Sn colloids can be bound electrostatically to positively charged surfaces through a 3-aminopropyltriethoxysilane (APTES) linker,<sup>37</sup> which we deposited onto the fabric from solution after a plasma oxidation step. Immersing the resulting amine-functionalized textile in the acidic Pd/Sn solution protonates the amino groups of the bound APTES; the resulting positively charged ammonium groups that electrostatically bind the Pd/Sn colloids. Subsequent etching in aqueous HCl removes the Sn shell to expose the Pd core, which initiates ELD by catalyzing the reduction of  $\text{Ni}^{2+}$  ions in the ELD plating solution to nickel metal on the surface of the textile. Nickel deposition is autocatalytic thereafter due to the

dimethylamine borane reducing agent in the nickel ELD solution. In the second ENIG plating step, immersing the nickel-coated textile in a solution of potassium gold cyanide deposits a gold film by galvanic displacement. Ni atoms in the film reduce Au<sup>+</sup> ions from solution, releasing Ni<sup>2+</sup> ions into the solution and depositing a gold metal film on the surface through molecular exchange.<sup>35</sup> Throughout the ENIG process, floating the polyester front face of the fabric on the surface of the plating solutions prevents metallization of the polyurethane-coated backside (**Figure S2-1**), which can facilitate integration into wearable electronics by separating the conductive layer from the body and preventing possible shorts caused by sweat.

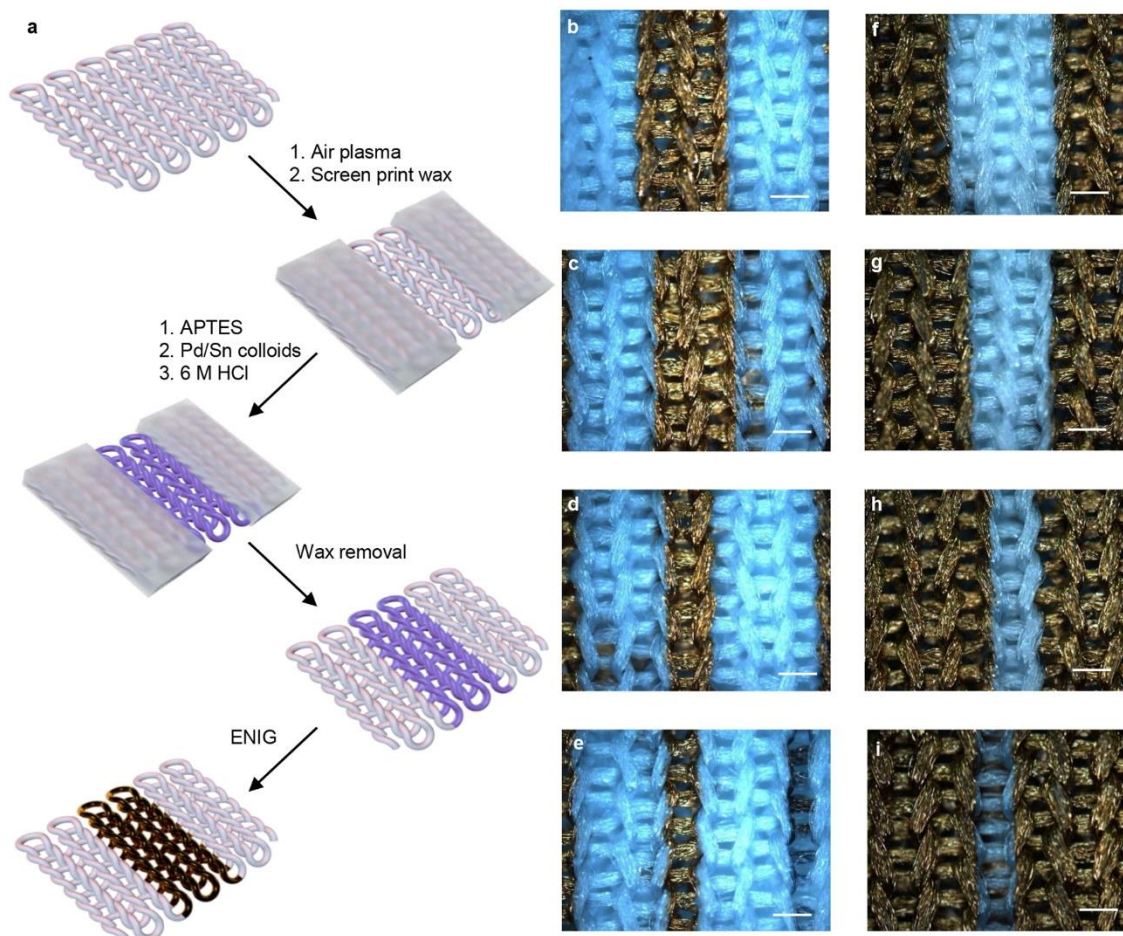
The aqueous solutions used in the ENIG process permeate the fabric to coat the individual fibers with metal, including in the junctions of wale and course yarn, rendering the fabric electrically conductive (**Figure 2-2a-c**). Scanning electron microscopy (SEM) images show the smooth, conformal gold coating on the individual fibers, which appear similar to the pristine fabric due to the uniformity of the coating (**Figure 2-2d,e; Figure S2-2**). Cross-sectional SEM shows that each fiber consists of a core-shell structure, with each polyester fiber core coated with a ~80 nm thick gold shell (**Figure 2-2f**). Analysis of the films using X-ray diffraction and energy dispersive X-ray spectroscopy detected gold, but not nickel, in the gold-coated textile (**Figure S2-3**). The gold-coated textile is highly conductive, with an average sheet resistance in the course direction ( $1.07 \pm 0.23 \text{ } \Omega/\text{sq}$ ) comparable to that of a flat 80 nm thick film of gold deposited by PVD on a glass substrate ( $0.9 \pm 0.1 \text{ } \Omega/\text{sq}$ ). Sheet resistance in the wale direction is slightly higher ( $3.33 \pm 1.49 \text{ } \Omega/\text{sq}$ ), which can be attributed to additional interfiber contact resistance between loops in the wale direction.



**Figure 2-2** The weft-knitted textile coated with gold using ENIG. a) Stereomicroscope image of the gold-coated textile. Optical microscope images of the gold-coated textile stretched b) in the wale direction and c) in the course direction under 50% strain. SEM images of d) pristine and e) gold-coated textile. f) Cross-sectional SEM image of the gold-coated textile.

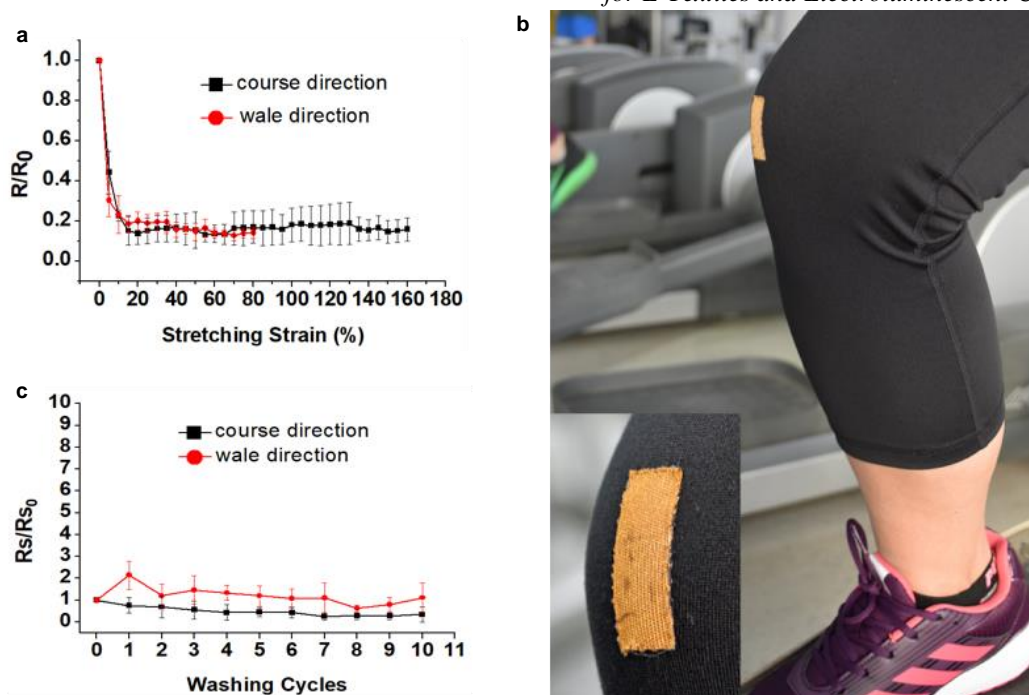
Facile permeation of ENIG solutions into the porous structure of the weft-knitted textile brings the benefit of coating individual fibers with metal; however, this porosity makes it a challenge to pattern the deposition of metal on the textile to create defined conductive features. We used a hydrophobic wax resist to pattern ENIG deposition on the weft-knitted textile (**Figure 2-3a**). Molten wax printing is commonly used to fabricate hydrophobic barriers in applications involving porous substrates, from conventional batik printing to pattern the deposition of dye onto textiles, to defining microfluidic channels in paper-based analytical devices.<sup>38</sup> We used cold wax medium, a beeswax-based paste that is soft, viscous, and suitable for screen printing. Applying the cold wax medium through a stencil mask to plasma-oxidized fabric forms a patterned hydrophobic barrier via the penetration of cold wax medium into the fabric (**Figure S2-4**). The hydrophobic barrier blocks the adsorption of Pd/Sn colloids from solution, thereby rendering these areas of the fabric inactive to ENIG. We then removed the wax resist by dissolution in hexane to leave a pattern of Pd/Sn catalyst on the fabric. Subsequent ENIG processing deposits metal only in these regions to render them conductive, whereas the regions that were masked with the wax resist are non-conductive. We studied the resolution and fidelity of the screen printing process using stencil masks designed to produce two types of features: gold lines (**Figure 2-3b-e**) and linear gaps (**Figure 2-3f-i**) in gold films with widths from 100  $\mu\text{m}$  to 1000  $\mu\text{m}$ .

Plots of the measured feature width as a function of the nominal feature width given by the stencil mask (**Figure S2-5**) yield a linear relationship with slope = 1 for both feature types. Two factors can potentially influence the resolution: Lateral wicking of the cold wax medium into the fabric will cause narrowing of plated metal lines and widening of linear gaps compared to the nominal widths. On the other hand, the metal growth mechanism may cause widening of plated metal lines and narrowing of linear gaps due to accumulation of metal in the x-y plane when longer plating times are used. Nonetheless, we found that our printing and plating conditions produced line and gap features that showed excellent fidelity to feature widths as small as 300  $\mu\text{m}$ , with lateral wicking of the cold wax medium through the fabric preventing the fabrication of smaller lines and gaps.



**Figure 2-3** Patterning gold deposition on the knitted textile by wax screen printing. a) Schematic of the patterning process. Optical microscope images of gold lines with widths b) 1000  $\mu\text{m}$ , c) 800  $\mu\text{m}$ , d) 500  $\mu\text{m}$ , e) 300  $\mu\text{m}$ . Optical microscope images of linear gaps in gold with widths f) 1000  $\mu\text{m}$ , g) 800  $\mu\text{m}$ , h) 500  $\mu\text{m}$ , i) 300  $\mu\text{m}$ . Scale bar = 400  $\mu\text{m}$ .

The gold-coated fabric possesses mechanical and electrical characteristics that make it suitable for applications in wearable electronics. Since ENIG deposits gold conformally on the surfaces of the fabric fibers rather than depositing material in between the yarns, the movement of the loops is not restricted and the stretchability is maintained. The gold-coated fabric largely retains the original mechanical properties of the fabric, although tensile testing before and after metallization showed a slight decrease in tensile strength and breaking load (**Figure S2-6**). This change may be due to the increased interfiber friction caused by the metal coating, which may limit the gliding action of yarns.<sup>39</sup> The gold-coated fabric also retains its conductivity with stretching, a key attribute for using conductive fabric in clothing. We stretched the gold-coated fabric in the course and wale direction and measured the change in resistance with strain (**Figure 2-4a**). In both directions, stretching to 15% strain rapidly decreases the resistance to ~20% of the initial value. This decrease is due to an increase in the contact pressure between adjacent conductive yarns that occurs under tensile strain, which lowers the interfiber contact resistance.<sup>40</sup> The maximum effect of this contact pressure occurs at 15% strain, beyond which the resistance remains consistent even as the fabric is elongated to 80% strain in the wale direction and 160% strain in the course direction. At this point, the loops of the fabric are interlocked, and the fabric can be stretched no further. The difference in the maximum strain in the course and wale directions is due to the anisotropic structure of the textile, which has a larger course height compared to the wale width, causing the interlock to occur at higher elongations in the course direction. The excellent conductivity and stretching performance are likely facilitated by the robust adhesion between the metal and the fabric, which prevents metal delamination and cracking that typically lead to resistance increases and termination of conductivity in metal-on-polymer structures.<sup>41</sup> Mechanical adhesion testing of the gold coating using the tape test showed no visible gold on the tape (**Figure S2-7a,b**), and SEM images of the gold-coated textile at 20% strain show no evidence of metal cracking or peeling (**Figure S2-8**). The APTES molecular layer deposited on the fabric surface is a key contributor to the robust adhesion: Coating the fabric using an ENIG process that omitted the APTES deposition resulted in a gold film poorly adhered to the fabric, and failure of the tape test (**Figure S2-7c,d**).



**Figure 2-4** Stretchability, wearability, and durability of the gold-coated textile. a) Normalized change in resistance as a function of stretching strain along the course (black line) and wale (red line) direction. b) Photograph of gold-coated fabric sewn onto the knee section of exercise pants. c) Normalized change in sheet resistance after simulated laundry cycles.

We further investigated the durability of the gold-coated fabric in wearable electronics by incorporating it into clothing. We sewed  $1.5 \times 3 \text{ cm}^2$  patches of gold-coated textile onto the knee section of a pair of exercise pants (**Figure 2-4b**), and then subjected them to repeated knee bending ( $\sim 40\%$  strain) by wearing the pants for a 5 km running session ( $\sim 3500$  cycles). The resistance of the gold-coated fabric increased  $<10\%$  after running for 5 km (**Table S2-1**). We conducted additional stretch-release experiments by cycling the gold-coated fabric between 0 and 40% strain. We measured the resistance at each 40% elongation and again after each release, allowing the gold-coated textile to relax for 2 minutes before measurement (**Figure S2-9**). The data show that, as expected, the resistance of the gold-coated textile decreases to  $\sim 15\%$  of the initial value at each 40% strain cycle. At each release cycle, however, the resistance does not recover to its initial value, instead returning to  $\sim 50\%$  of the initial value. This recovery is consistent with low resilience of the knitted polyester fabric, which does not incorporate elastic fibers into the knitted structure that are typically used in other fabrics to enable rapid recovery to the original shape. In knitted fabrics that lack elastic fibers, stretching straightens the

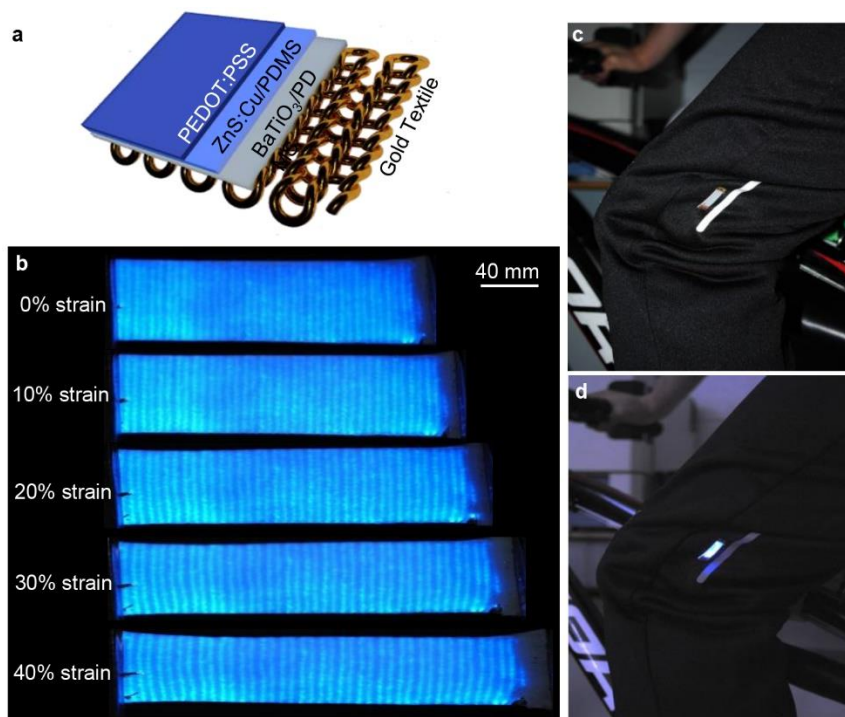
serpentine polyester loops, and recovery requires additional time for the loops to bend back to their original shape. Stretching the gold-coated textile to 40% strain and then allowing the fabric to relax for 12 h enables the recovery of the initial resistance, with a normalized resistance of  $1.01 \pm 0.14$ .

Along with durability to repeated movement, wearable conductors must also be hardy enough to tolerate mild abrasion and laundry cycles. Rapidly rubbing the surface of the gold-coated textile with a gloved finger for 5 min caused minimal changes to the sheet resistance, with normalized values of  $1.03 \pm 0.17$  in the course direction and  $0.83 \pm 0.28$  in the wale direction after the test. We simulated a laundry cycle by stirring the gold-coated textile in an aqueous solution of laundry detergent for 1 h, followed by rinsing with water and drying in a  $60^{\circ}\text{C}$  oven overnight. The sheet resistance of the gold-coated textile varied minimally throughout 10 simulated laundry cycles (**Figure 2-4c**). Wearable electronics worn near human skin must also be tolerant to sweating. We immersed the gold-coated textile in a salt solution to simulate exposure to sweat, and then subjected it a laundry cycle. There was minimal change in resistance after each step: After sweat exposure, the normalized change in sheet resistance in the course and wale directions was  $0.99 \pm 0.31$  and  $0.89 \pm 0.09$ , respectively; after the subsequent laundry cycle, the values in the course and wale directions were  $1.01 \pm 0.11$  and  $0.81 \pm 0.20$ , respectively.

We used the gold-coated textile to fabricate electroluminescent fabric, demonstrating the ultimate integration of device functionality with textiles. The electroluminescent fabric uses the gold-coated textile as the bottom electrode in an alternating current electroluminescent (ACEL) device (**Figure 2-5a**). ACEL devices consist of a light-emitting phosphor material deposited between two electrodes; stretchable ACELs have previously been fabricated by blending ZnS:Cu phosphor microparticles with the elastomer polydimethylsiloxane (PDMS), and using stretchable PDMS-based electrodes.<sup>42</sup> We fabricated a stretchable ACEL on the gold-coated textile by first depositing a stretchable dielectric layer consisting of a blend of barium titanate and PDMS onto the gold-coated textile to smooth the uneven surface of the textile and prevent breakdown of the phosphor under the high field strengths of the device. We deposited a film of ZnS:Cu blended with PDMS, and then completed the device by depositing a film of the conductive polymer poly(3,4-ethylenedioxythiophene) polystyrene sulfonate



(PEDOT:PSS) plasticized with the surfactant Triton X-100<sup>43,44</sup> as the transparent electrode. Operation at 165 V AC and a frequency of 37 kHz produced uniform blue emission from the electroluminescent fabric. The device functionality persisted without degradation to 40% strain (**Figure 2-5b**). Stretching beyond 40% strain caused device failure due to a loss of conductivity of the PEDOT:PSS electrode. The stretchability of the electroluminescent fabric could be improved by using a transparent electrode with high conductivity and stretchability. Nonetheless, electroluminescent functionality from 0 to 40% strain is a workable range<sup>45,46</sup> for applications such as high-visibility safety apparel, which is worn to alert drivers to the presence of a worker, pedestrian, or cyclist in low light or poor visibility conditions. Retroreflective materials used today in safety apparel require an external source of light for visibility, such as car headlights. We integrated the electroluminescent fabric into clothing to demonstrate self-illuminated safety apparel (**Figure 2-5c,d**), which provides consistent visibility regardless of external conditions to enhance the safety of the wearer. A comparison of retroreflective and electroluminescent fabric strips in clothing photographed in light and dark environments shows the superior brightness and visibility of the electroluminescent fabric (**Figure 2-5c,d**).



**Figure 2-5** Electroluminescent fabric. a) Schematic of electroluminescent fabric structure. b) Photographs of electroluminescent fabric at 0-40% strain. Wearable electroluminescent fabric photographed alongside a retroreflective strip c) with and d) without an external light source.

## 2.3 Conclusions

In conclusion, we believe that our simple and scalable ENIG method provides conductive textiles with properties that fit the needs of future wearable electronics. The permeation of ENIG solutions into the porous structure of the weft-knitted polyester textile enables the deposition of a uniform, conformal gold film only on the fabric fibers, preserving the void structure and stretchability of the textile. The adhesion of the gold coating makes this e-textile durable to wearing, sweating, and washing. The stable conductivity of the gold coating to high strains combined with the low-cost screen printing of a wax resist enables the formation of patterned gold textiles that will be useful to electrically connect a network of devices on the body, delivering power and enabling communication. The gold-coated textiles may also be useful in wearable strain sensors over the 0-15% strain range where the resistance decreases with strain.<sup>47</sup> The electroluminescent fabric demonstrated herein demonstrates the merging of devices with fabrics and represents the first steps toward the fabrication of imperceptible, wearable displays. We are currently investigating the use of the ENIG process to metallize other fabrics, such as cotton or nylon, as well as fabrics that incorporate elastic fibers to enable high stretchability and conformability to the human body with high resilience.

## 2.4 Experimental

All chemicals were purchased commercially and used as received.

*ENIG Procedure:* Polyester fabric with ca. 200- $\mu\text{m}$ -diameter threads and polyurethane backing was sonicated in deionized water and isopropyl alcohol for 15 min each, and then exposed to air plasma for 6 min. The patterned fabric was floated on the surface of a 1% v/v solution of APTES in deionized water for 10 min, a Pd/Sn solution (prepared from Cataposit 44 and Cataprep 404 (Shipley) as directed by manufacturer) for 3 min, and aqueous 6 M HCl for 3 min. Samples were rinsed with water in between steps. The fabric was then metallized in nickel ELD bath (21.0 g/L  $\text{NiSO}_4 \cdot 6\text{H}_2\text{O}$ , 37.2 g/L  $\text{Na}_4\text{P}_2\text{O}_7 \cdot 10\text{H}_2\text{O}$  and 4.1 g/L dimethylamine borane in water) for 5 min with sonication. After rinsing with water, the Ni-coated fabric was immersed in Au ELD bath (Gobright TAM-55, Uyemura) for 30 min.

*Patterning of Polyester Fabric:* The fabric was sonicated in deionized water and isopropyl alcohol for 15 min each, and then exposed to air plasma for 6 min. A 0.15 mm stainless steel stencil with the desired pattern was placed on top of the fabric, cold wax medium (Gamblin) was applied to cover the metal stencil, and then a glass microscope slide was used as a squeegee to remove the excess. The ENIG procedure was then performed.

*Washing Durability:* Gold-coated textiles were soaked in 1 wt % solution of Tide Original Liquid Laundry Detergent in DI water with stirring for 1 h, followed by rinsing with water and drying in a 60 °C oven overnight. The sheet resistance was measured before and after each washing cycle using the four-point probe method.

*Electroluminescent Device Fabrication:* The emissive layer was then formed by mixing ZnS:Cu phosphor powder (KPT) with PDMS prepolymer in 1:1 (w:w) ratio, spin-coating on the dielectric layer at 500 rpm for 1 min, and curing in a 60 °C oven overnight. The emissive layer was treated with air plasma for 1 min, and then a PEDOT:PSS aqueous dispersion (Clevious PH1000, Heraeus) with 2 wt% Triton X-100 was spin coated on the emissive layer at 2000 rpm for 1 min and then annealed at 100 °C for 30 min.

*Characterization:* Optical microscopy was performed using an Olympus BX51 microscope equipped with an Olympus Q-Color3 digital camera. A micro-vice stretcher (S.T. Japan, USA, Inc.) was mounted to the microscope stage and samples were clamped in the stretcher to obtain microscope images of stretched samples. Stereomicrographs were taken using Leica m205 FA stereomicroscope with z-stack multi-plane focusing enabled. SEM images and energy dispersive X-ray spectroscopy were taken on an FEI Quanta 200 Environmental SEM. Energy dispersive X-ray spectroscopy was recorded at 20 kV. X-ray diffraction measurements were run on a PROTO AXRD powder diffractometer equipped with a Cu X-ray source, and a Mythen 1K silicon strip detector, operated at 30 kV and 20 mA. Scans were performed using CuK $\alpha$  radiation, a 0.2 mm divergence slit, and a step size of 0.02 degrees 2theta. X-ray diffraction patterns were obtained in the 2 $\theta$  region from 30 to 140°. The XRD pattern for the gold-coated textile showed eight peaks at 38.3°, 44.6°, 64.8°, 77.8°, 82°, 98.8°, 111°, 115.5°, and 135.7°, corresponding to (111), (200), (220), (311), (222), (400), (331), (420), and (442) of fcc Au (JCPDF card 4-0784), respectively. MTS Criterion (model 43) was used for tensile testing under strain rate of 2.5 mm/s. For

electrical characterization under strain, samples were clamped in the micro-vice stretcher and stretched manually in 5% increments while measuring the resistance using a Keithley 2601A Sourcemeter. Textile-based light emitting device was operated at 165 V AC with a frequency of 37 kHz, which was inverted from 5 V DC using an inverter (PCU-554, TDK).

## 2.5 References

- [1] Kudo, H.; Sawada, T.; Kazawa, E.; Yoshida, H.; Iwasaki, Y.; Mitsubayashi, K. A Flexible and Wearable Glucose Sensor Based on Functional Polymers with Soft-MEMS Techniques. *Biosens. Bioelectron.* **2006**, *22*, 558-562.
- [2] Sekitani, T.; Nakajima, H.; Maeda, H.; Fukushima, T.; Aida, T.; Hata, K.; Someya, T. Stretchable Active-Matrix Organic Light-Emitting Diode Display Using Printable Elastic Conductors. *Nat. Mater.* **2009**, *8*, 494-499.
- [3] Xu, S.; Zhang, Y.; Cho, J.; Lee, J.; Huang, X.; Jia, L.; Fan, J. A.; Su, Y.; Su, J.; Zhang, H.; Cheng, H.; Lu, B.; Yu, C.; Chuang, C.; Kim, T.-i.; Song, T.; Shigeta, K.; Kang, S.; Dagdeviren, C.; Petrov, I.; Braun, P. V.; Huang, Y.; Paik, U.; Rogers, J. A. Stretchable Batteries with Self-Similar Serpentine Interconnects and Integrated Wireless Recharging Systems. *Nat. Commun.* **2013**, *4*, 1543.
- [4] Gorlick, M. M. Electric Suspenders: A Fabric Power Bus and Data Network for Wearable Digital Devices. *IEEE* **1999**, 114-121.
- [5] Castano, L. M.; Flatau, A. B. Smart Fabric Sensors and E-Textile Technologies: A Review. *Smart Mater. Struct.* **2014**, *23*, 53001.
- [6] Cherenack, K.; van Pieteron, L. Smart Textiles: Challenges and Opportunities. *J. Appl. Phys.* **2012**, *112*, 91301.
- [7] Moraes, M. R.; Alves, A. C.; Toptan, F.; Martins, M. S.; Vieira, E. M. F.; Paleo, A. J.; Souto, A. P.; Santos, W. L. F.; Esteves, M. F.; Zille, A. Glycerol/PEDOT:PSS Coated Woven Fabric as a Flexible Heating Element on Textiles. *J. Mater. Chem. C* **2017**, *5*, 3807-3822.
- [8] Cataldi, P.; Ceseracciu, L.; Athanassiou, A.; Bayer, I. S. A Healable Cotton-Graphene Nanocomposite Conductor for Wearable Electronics. *ACS Appl. Mater. Interfaces* **2017**, *9*, 13825-13830.

- [9] Wang, S.; Xuan, S.; Liu, M.; Bai, L.; Zhang, S.; Sang, M.; Jiang, W.; Gong, X. Smart Wearable Kevlar-Based Safeguarding Electronic Textile with Excellent Sensing Performance. *Soft Matter* **2017**, *13*, 2483-2491.
- [10] Kazani, I.; Hertleer, C.; May, G.; Schwarz, A.; Guxho, G.; Langenhove, L. Electrical Conductive Textiles Obtained by Screen Printing. *Fibres Text. East. Eur.* **2012**, *20*, 57-63.
- [11] Matsuhisa, N.; Kaltenbrunner, M.; Yokota, T.; Jinno, H.; Kuribara, K.; Sekitani, T.; Someya, T. Printable Elastic Conductors with a High Conductivity for Electronic Textile Applications. *Nat. Commun.* **2015**, *6*, 7461.
- [12] Ryan, J. D.; Mengistie, D.; Gabrielsson, R.; Lund, A.; Müller, C. Machine-Washable PEDOT:PSS Dyed Silk Yarns for Electronic Textiles. *ACS Appl. Mater. Interfaces* **2017**, *9*, 9045-9050.
- [13] Seyedin, S.; Razal, J. M.; Innis, P. C.; Jeiranikhameneh, A.; Beirne, S.; Wallace, G. G. Knitted Strain Sensor Textiles of Highly Conductive All-Polymeric Fibers. *ACS Appl. Mater. Interfaces* **2015**, *7*, 21150-21158.
- [14] Post, E. R.; Orth, M.; Russo, P. R. E-Broidery: Design and Fabrication of Textile-Based Computing. *IBM Syst. J.* **2000**, *39*, 840-860.
- [15] Orth, M. Defining Flexibility and Sewability in Conductive Yarns. *Mater. Res. Soc. Symp. Proc.* **2002**, *736*, D1.4.
- [16] Jin, H.; Matsuhisa, N.; Lee, S.; Abbas, M.; Yokota, T.; Someya, T. Enhancing the Performance of Stretchable Conductors for E-Textiles by Controlled Ink Permeation. *Adv. Mater.* **2017**, *29*, 1605848.
- [17] Zhang, Z.; Shi, X.; Lou, H.; Xu, Y.; Zhang, J.; Li, Y.; Cheng, X.; Peng, H. A Stretchable and Sensitive Light-Emitting Fabric. *J. Mater. Chem. C* **2017**, *5*, 4139-4144.
- [18] Wu, J.; Zhou, D.; Too, C. O.; Wallace, G. G. Conducting Polymer Coated Lycra. *Synth. Met.* **2005**, *155*, 698-701.
- [19] Zhang, M.; Wang, C.; Liang, X.; Yin, Z.; Xia, K.; Wang, H.; Jian, M.; Zhang, Y. Weft-Knitted Fabric for a Highly Stretchable and Low-Voltage Wearable Heater. *Adv. Electron. Mater.* **2017**, *3*, 1700193.

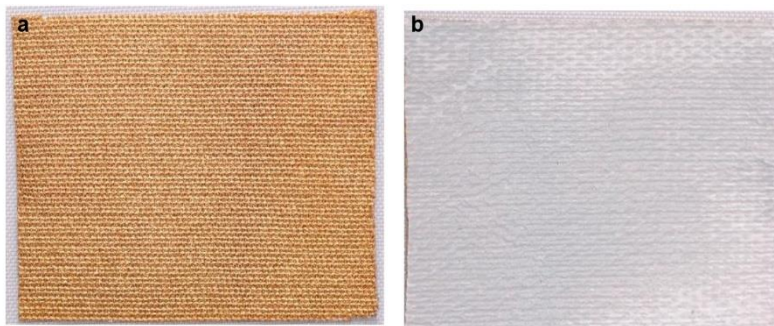
- [20] Wang, C.; Li, X.; Gao, E.; Jian, M.; Xia, K.; Wang, Q.; Xu, Z.; Ren, T.; Zhang, Y. Carbonized Silk Fabric for Ultrastretchable, Highly Sensitive, and Wearable Strain Sensors. *Adv. Mater.* **2016**, *28*, 6640-6648.
- [21] Wang, C.; Zhang, M.; Xia, K.; Gong, X.; Wang, H.; Yin, Z.; Guan, B.; Zhang, Y. Intrinsically Stretchable and Conductive Textile by a Scalable Process for Elastic Wearable Electronics. *ACS Appl. Mater. Interfaces* **2017**, *9*, 13331-13338.
- [22] Wei, Q.; Yu, L.; Wu, N.; Hong, S. Preparation and Characterization of Copper Nanocomposite Textiles. *J. Ind. Text.* **2008**, *37*, 275-283.
- [23] Kim, W.; Kwon, S.; Han, Y.; Kim, E.; Choi, K.; Kang, S. H.; Park, B. C. Reliable Actual Fabric-Based Organic Light-Emitting Diodes: Toward a Wearable Display. *Adv. Electron. Mater.* **2016**, *2*, 1600220.
- [24] Silva, L. N.; Gonçalves, L. M.; Carvalho, H. Deposition of Conductive Materials on Textile and Polymeric Flexible Substrates. *J. Mater. Sci. Mater. Electron.* **2013**, *24*, 635-643.
- [25] Zhao, H.; Hou, L.; Wu, J. X.; Lu, Y. X. Fabrication of Dual-Side Metal Patterns onto Textile Substrates for Wearable Electronics by Combining Wax-Dot Printing with Electroless Plating. *J. Mater. Chem. C* **2016**, *4*, 7156-7164.
- [26] Liu, S.; Hu, M.; Yang, J. A Facile Way of Fabricating a Flexible and Conductive Cotton Fabric. *J. Mater. Chem. C* **2016**, *4*, 1320-1325.
- [27] Zhen, H.; Li, K.; Chen, C.; Yu, Y.; Zheng, Z. Water-Borne Foldable Polymer Solar Cells: One-Step Transferring Free-Standing Polymer Films onto Woven Fabric Electrodes. *J. Mater. Chem. A* **2017**, *5*, 782-788.
- [28] Haghdoost, F.; Mottaghtalab, V.; Haghi, A. Comfortable Textile-Based Electrode for Wearable Electrocardiogram. *Sens. Rev.* **2015**, *35*, 20-29.
- [29] Yang, Y.; Huang, Q.; Niu, L.; Wang, D.; Yan, C.; She, Y.; Zheng, Z. Waterproof, Ultrahigh Areal-Capacitance, Wearable Supercapacitor Fabrics. *Adv. Mater.* **2017**, *29*, 1606679.
- [30] Pu, X.; Liu, M.; Li, L.; Han, S.; Li, X.; Jiang, C.; Du, C.; Luo, J.; Hu, W.; Wang, Z. Wearable Textile-Based In-Plane Microsupercapacitors. *Adv. Energy Mater.* **2016**, *6*, 1601254.

- [31] Guo, R. H.; Jiang, S. X.; Zheng, Y. D.; Lan, J. W. Electroless Nickel Deposition of a Palladium-Activated Self-Assembled Monolayer on Polyester Fabric. *J. Appl. Polym. Sci.* **2013**, *127*, 4186-4193.
- [32] Sharma, S. P. Atmospheric Corrosion of Silver, Copper, and Nickel-Environmental Test. *J. Electrochem. Soc.* **1978**, *125*, 2005-2011.
- [33] Thyssen, J. P.; Menné, T. Metal Allergy-A Review on Exposures, Penetration, Genetics, Prevalence, and Clinical Implications. *Chem. Res. Toxicol.* **2010**, *23*, 309-318.
- [34] *Encyclopedia of World Environment History*; Shepard Krech, J. R. M., Carolyn Merchant, Ed.; Routledge: London, 2004; Vol. 3.
- [35] Liu, H.; Li, N.; Bi, S.; Li, D. Gold Immersion Deposition on Electroless Nickel Substrates Deposition Process and Influence Factor Analysis. *J. Electrochem. Soc.* **2007**, *154*, D662-D668.
- [36] *Electroless Plating: Fundamentals and Applications*; G. O. Mal-lory, J. B. H., Ed.; American Electroplaters and Surface Finisher Society: Orlando, 1990.
- [37] Miller, M. S.; Davidson, G. J. E.; Sahli, B. J.; Mailloux, C. M.; Carmichael, T. B. Fabrication of Elastomeric Wires by Selective Electroless Metallization of Poly(dimethylsiloxane). *Adv. Mater.* **2008**, *20*, 59-64.
- [38] Carrilho, E.; Martinez, A. W.; Whitesides, G. M. Understanding Wax Printing: A Simple Micropatterning Process for Paper-Based Microfluidics. *Anal. Chem.* **2009**, *81*, 7091-7095.
- [39] Mohtaram, F.; Mottaghitalab, V.; Baghersalimi, G. Development and Characterization of Flexible Antenna Based on Conductive Metal Pattern on Polyester Fabric. *J. Text. Inst.* **2017**, *108*, 1888-1898.
- [40] Zhang, H. Flexible Textile-Based Strain Sensor Induced by Contacts. *Meas. Sci. Technol.* **2015**, *26*, 105102.
- [41] Xiang, Y.; Li, T.; Suo, Z.; Vlassak, J. J. High Ductility of a Metal Film Adherent on a Polymer Substrate. *Appl. Phys. Lett.* **2005**, *87*, 161910.
- [42] Wang, J.; Yan, C.; Chee, K.; Lee, P. Highly Stretchable and Self-Deformable Alternating Current Electroluminescent Devices. *Adv. Mater.* **2015**, *27*, 2876-2882.

- [43] Oh, J. Y.; Shin, M.; Lee, J. B.; Ahn, J. H.; Baik, H. K. Effect of PEDOT Nanofibril Networks on the Conductivity, Flexibility, and Coatability of PEDOT:PSS Films. *ACS Appl. Mater. Interfaces* **2014**, *6*, 6954.
- [44] Yoon, S.-S.; Khang, D.-Y. Roles of Nonionic Surfactant Additives in PEDOT:PSS Thin Films. *J. Phys. Chem. C* **2016**, *120*, 29525.
- [45] Wessendorf, A. M.; Newman, D. J. Dynamic Understanding of Human-Skin Movement and Strain-Field Analysis. *IEEE Trans. Biomed. Eng.* **2012**, *59*, 3432-3438.
- [46] Wagner, S.; Lacour, S. P.; Jones, J.; Hsu, P.-h. I.; Sturm, J. C.; Li, T.; Suo, Z. Electronic Skin: Architecture and Components. *Physica E Low Dimens. Syst. Nanostruct.* **2004**, *25*, 326-334.
- [47] Zahid, M.; Papadopoulou, E. L.; Athanassiou, A.; Bayer, I. S. Strain-Responsive Mercerized Conductive Cotton Fabrics Based on PEDOT:PSS/Graphene. *Mater. Des.* **2017**, *135*, 213-222.

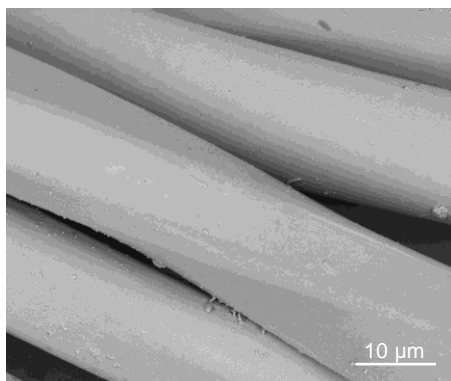
## 2.6 Supporting Information

*Calculation of bending strain at the knee:* To measure bending strain at the knee, we marked two points on the knee and measured the distance between them in the straightened and bent position. We calculated the strain using percent difference between these values.

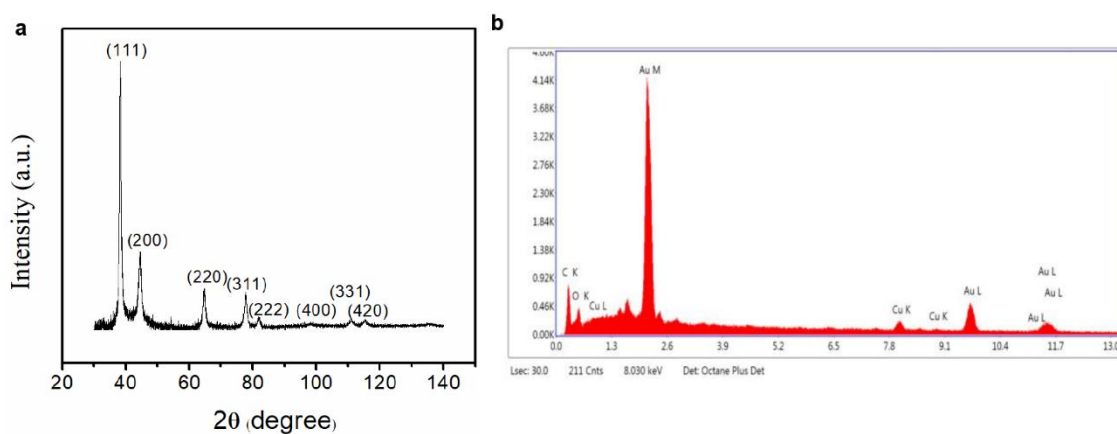


**Figure S2-1** Photographs of a) face and b) back of gold-coated fabric (approximately 3 cm × 3 cm).

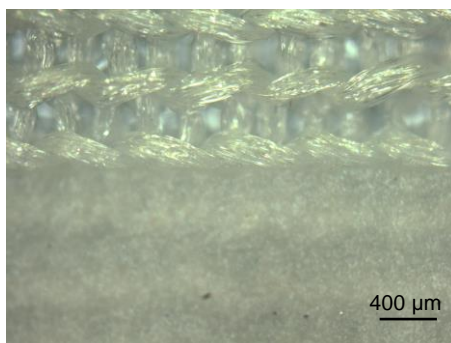




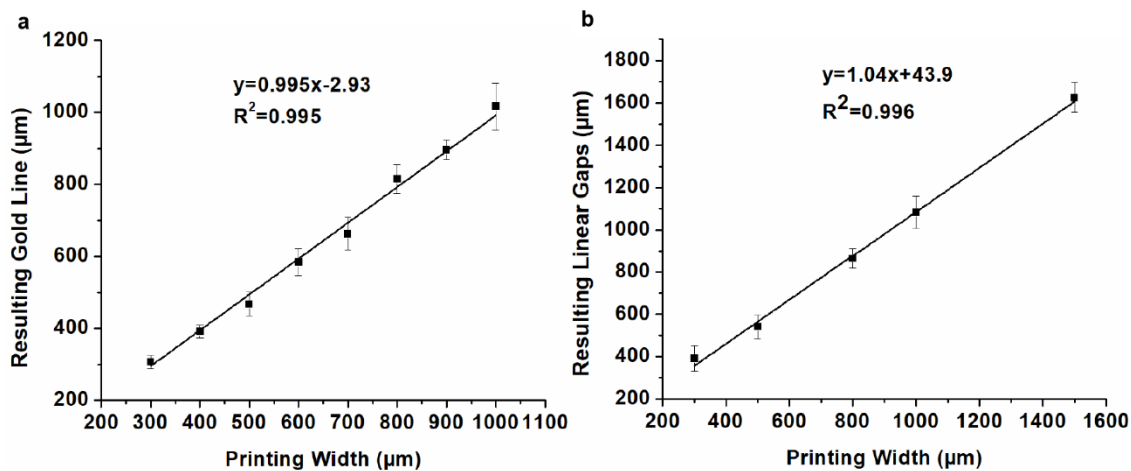
**Figure S2-2** SEM image of the gold-coated textile.



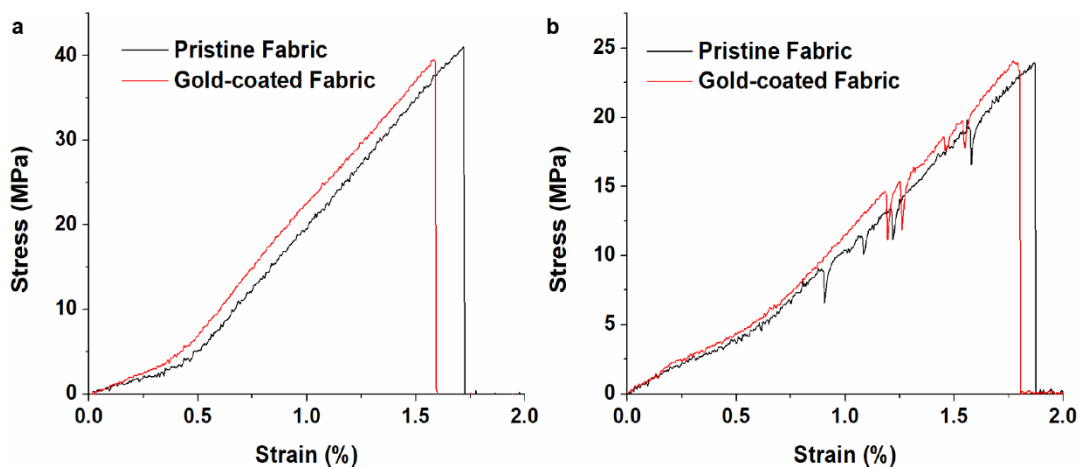
**Figure S2-3** a) X-ray diffraction patterns and b) energy dispersive X-ray spectroscopy of gold-coated textiles.



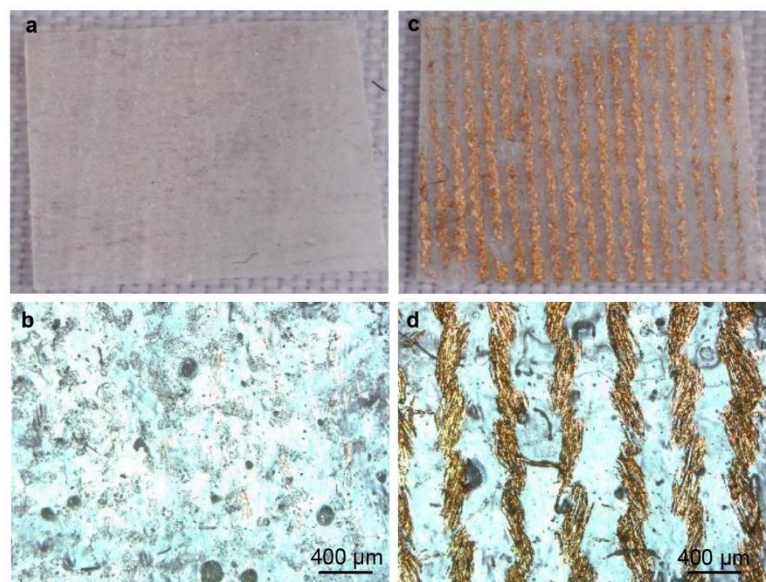
**Figure S2-4** Optical microscope image of cold wax medium printed on the knitted textile.



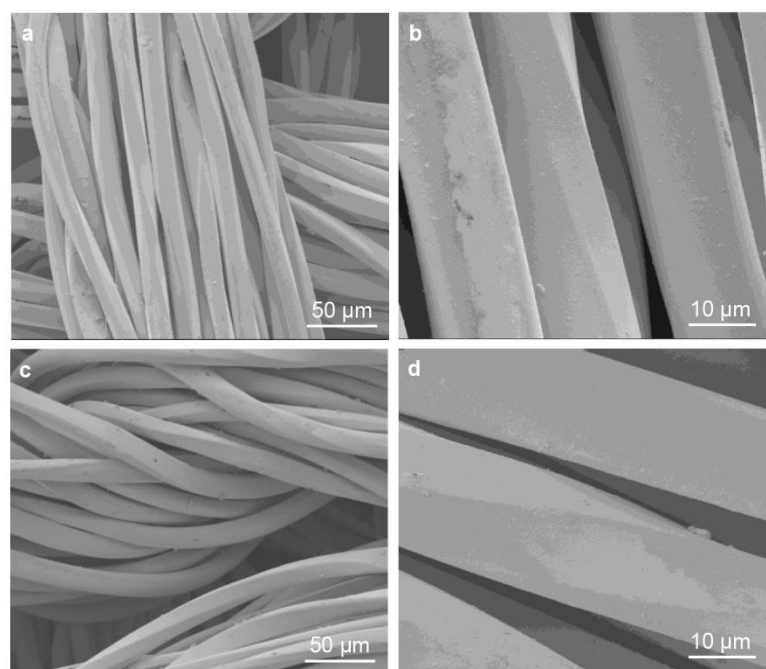
**Figure S2-5** Plots of the width of the resulting a) gold lines and b) linear gaps in gold films as a function of the nominal line width of the stencil mask.



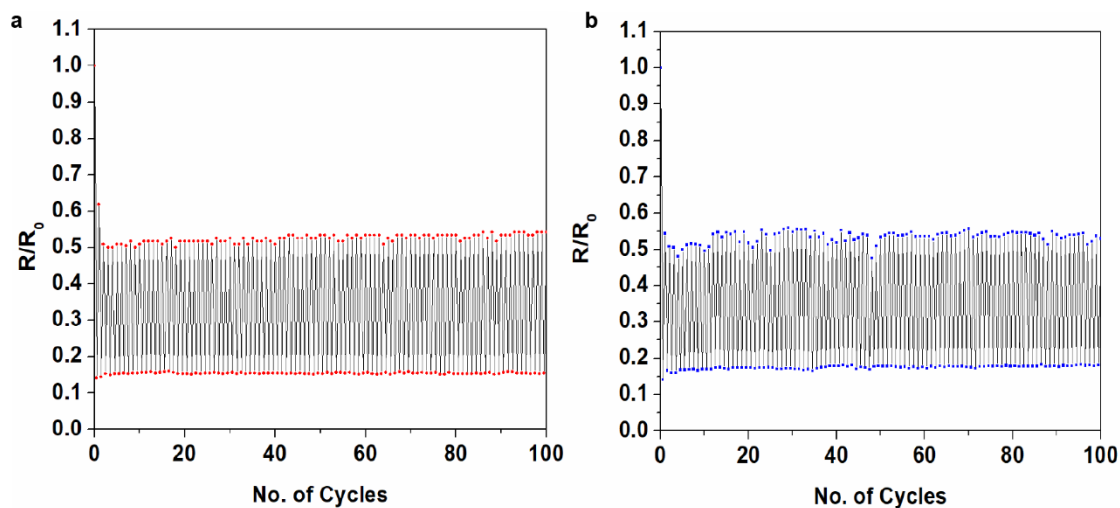
**Figure S2-6** Stress strain curve of pristine fabric (black line) and gold-coated fabric (red line) in the a) wale direction and b) course direction.



**Figure S2-7** Photographs and optical microscope images of the tape after tape test of gold-coated textiles a,b) with APTES treatment and c,d) without APTES treatment.



**Figure S2-8** SEM images of gold-coated textile at 20% strain stretched a,b) in the wale direction and c,d) in the course direction.



**Figure S2-9** Normalized resistance of the gold-coated textile over 100 stretch-release cycles of 40% strain a) in the wale direction and b) in the course direction.

**Table S2-1** Durability of gold-coated fabric to repetitive 40% strain

	Left Leg Resistance <sup>a)</sup> [ $\Omega$ ]	Right Leg Resistance <sup>a)</sup> [ $\Omega$ ]
Before 5 km run	9.3	10.1
After 5 km run	9.6	11.1

<sup>a)</sup>wale direction

**Chapter 3 Stretchable Ultrasheer Fabrics as Semitransparent Electrodes for  
Wearable Light-Emitting e-Textiles with Changeable Display Patterns**

### **3.1 Introduction**

Textiles have been a part of daily life since the beginning of human civilization itself, with centuries of development producing a seemingly endless variety of fabrics made from natural and synthetic materials that are knitted, woven, or braided to form a profusion of textile structures that vary in strength, porosity, durability, and stiffness.<sup>1</sup> The future of textiles is electronic, and will bring new wearable devices integrated into “smart clothing” systems, with sensors<sup>2-5</sup> to detect biometric data; supercapacitors,<sup>6-9</sup> batteries,<sup>10</sup> nanogenerators<sup>11</sup> or solar cells<sup>12-14</sup> as power sources; and light-emitting devices to display data output.<sup>15</sup> Among these e-textile components, light-emitting e-textiles are an especially compelling emerging technology that will also inspire innovations in fashion design, interior design, visual merchandizing, and personal safety. At present, light-emitting textiles are mainly realized by sewing discrete, rigid elements like light-emitting diodes (LEDs) or optical fibers into clothing, which reduces softness, stretchability, and wearability. Smart illuminated clothing that meets the demand for comfort and wearability will require light-emitting devices that are seamlessly integrated with the textile structure. Textiles, however, are difficult substrates for device fabrication. Conventional thin-film device fabrication methods are designed for planar substrates, whereas textiles present complex, 3D structures with non-planar surfaces. This challenge has caused textiles to often be viewed as problematic for device integration. One approach has been to avoid fabrication on the rough textile surface by instead fabricating electroluminescent fibers that are then woven through existing textiles.<sup>16,17</sup> However, with the enormous variety of textile materials and physical structures that are available, reducing the textile element in wearable electronics to an inconvenient substrate is a missed opportunity to truly advance wearable electronics. Here, we present a new, textile-centric design paradigm for wearable electronics that uses a complex textile structure as a fundamental part of wearable device design. We seamlessly integrate new semitransparent and conductive e-textile electrodes with stretchable emissive materials for highly stretchable light-emitting e-textiles.

Previous research on developing light-emitting textiles has most often used flexible woven textiles as substrates, which consist of sets of yarns interlaced at right angles to each other. This fabric structure imparts flexibility, but stretchability is restricted due to the linearity of the yarns and occurs only to a small extent along the diagonal to the square

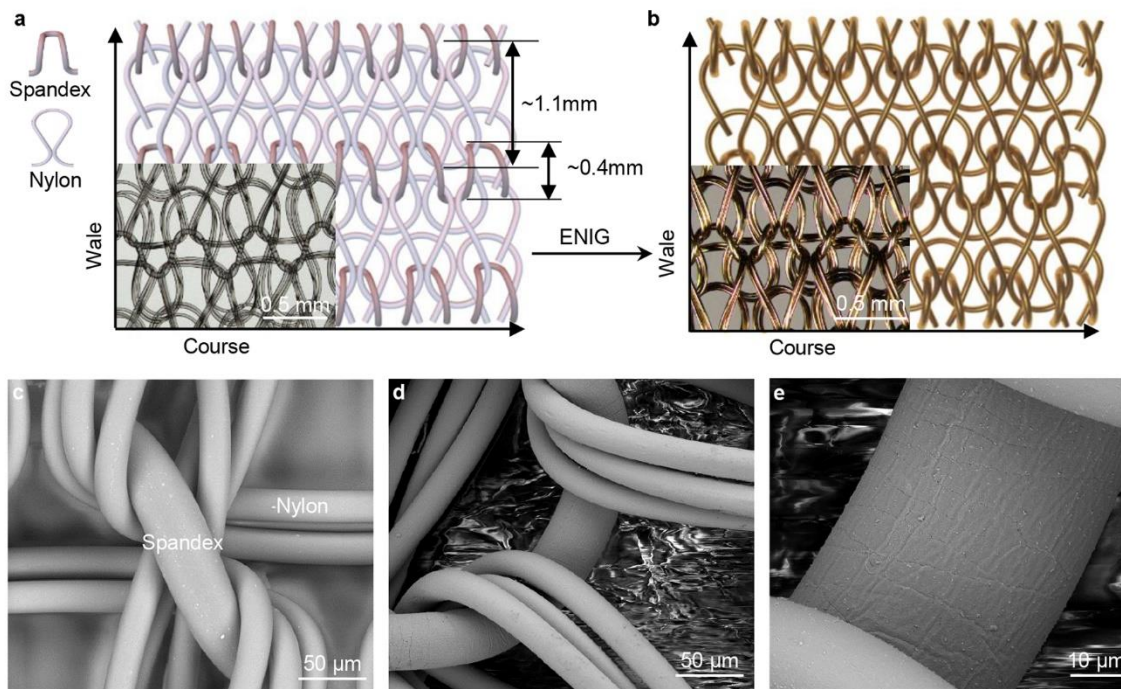
weave pattern. Alternating current electroluminescent (ACEL) devices,<sup>18-20</sup> organic LEDs,<sup>21-23</sup> and light-emitting electrochemical cells<sup>24,25</sup> fabricated on flexible woven fabrics have all been reported. In contrast, knitted textiles present more complex 3D structures with yarns structured into interconnected loops separated by networks of voids, providing space for the yarns to unbend and move in response to stress for high omnidirectional stretchability. Despite numerous reports of conductive knitted textiles that retain conductivity to high elongations,<sup>26</sup> few examples of stretchable light-emitting devices based on knitted textiles have been reported. A central problem with the devices reported to date lies with the limited stretchability and wearability of the transparent electrode, a key component of all light-emitting devices. For example, ACEL light-emitting e-textiles fabricated using a gold-coated knitted textile as the bottom electrode and a thin film of poly(3,4-ethylenedioxythiophene) polystyrene sulfonate (PEDOT:PSS) as the top transparent electrode retain functionality to only 40% strain due to cracking of the PEDOT:PSS electrode, despite the ability of the gold-coated textile electrode to remain conductive to 160% elongation.<sup>27</sup> Using a more stretchable transparent conductor to avoid this cracking problem can produce devices with greater stretchability; however, the essential requirement that new materials be durable enough for wearability can be a challenge. For example, ACEL light-emitting e-textiles fabricated on a conductive knitted bottom electrode that use a film of a stretchable ionic conductor as the transparent electrode produces devices that function to 100% strain,<sup>28</sup> but evaporation of the solvent/liquid component of the ionic conductor limits the durability and wearability of these devices.

Instead of seeking new transparent conductive films that are stretchable as well as wearable, we present a new textile-centric approach for the fabrication of e-textile light-emitting devices whereby we strategically use the open structure of an ultrasheer knitted textile as a framework for the fabrication of stretchable and semitransparent textile-based electrodes using solution-based metallization. Adhering these new textile-based semitransparent electrodes to a stretchable emissive material produces lightweight, wearable, light-emitting e-textiles that function to the strain limit of the textile (200%). Patterning the electrode and incorporating soft-contact lamination in the device fabrication produces light-emitting textiles that exhibit, for the first time, readily changeable patterns of illumination.

### **3.2 Results and Discussion**

In the textile industry, the denier is a unit of measurement used to express the thickness of individual fibers in a textile; low denier fabrics are sheer and semitransparent due to spaces between the fibers. We used a 10-denier ultrasheer knitted fabric to form stretchable and conductive e-textiles with optical transparency. The ultrasheer knitted fabric consists of 87% nylon and 13% spandex fibers knitted together to form interlinked course and wale loops, with nylon fibers of  $\sim 20\ \mu\text{m}$  in diameter forming the knitted structure and spandex fibers of  $\sim 45\ \mu\text{m}$  in diameter running along the course direction (**Figure 3-1a,c**). The open spaces between the fibers constituting the knitted structure permit the transmission of light through the textile (**Figure S3-1a**). The transmittance (T) of the ultrasheer fabric measured using UV-visible spectroscopy is 47% at 550 nm (**Figure S3-1b**). The absorption of 200-230 nm wavelength is due to the peptide bond of the nylon and spandex fibers. The nylon fibers contribute to the strength of the ultrasheer fabric but are not intrinsically stretchable; instead, the knitted structure enables the nylon fibers to move and slip in response to stress, as well as unbending in the course direction. The intrinsically stretchable spandex fibers both unbend and elongate with stretching, providing resilience that returns the fabric to its original shape after stretching. The elastic limit of the fabric occurs at  $\sim 200\%$  strain in both the course and wale direction (**Figure S3-2**).





**Figure 3-1** The ultrasheer knitted fabric coated with gold. Schematic and stereomicroscope images (inset) of the a) uncoated ultrasheer fabric and b) gold-coated ultrasheer fabric. SEM images of c) uncoated ultrasheer fabric and d) gold-coated ultrasheer fabric. e) Close-up SEM image of gold-coated spandex fiber.

We used electroless nickel-immersion gold (ENIG) metallization, a solution-based metal deposition technique commonly employed in printed circuit board fabrication, to produce an ultrasheer e-textile with high conductivity (**Figure 3-1b**). Electroless metallization is a promising technique for the preparation of conductive textiles because the aqueous plating solutions permeate the textile structure to conformally deposit metal on individual fibers, leaving the void structure intact and maintaining the softness and stretchability of the original textile.<sup>27</sup> We chose gold as the metal because it is biocompatible and chemically inert.<sup>29</sup> The ENIG process consists of two solution-based plating steps: electroless deposition (ELD) of nickel followed by an immersion gold process. The ELD nickel process involves first activating the textile by adsorbing a catalytic species onto its surface. We used a palladium-tin colloidal catalyst, which consists of a palladium-rich core protected from oxidation by a hydrolyzed  $\text{Sn}^{2+}/\text{Sn}^{4+}$  shell, and an associated chloride layer that gives the colloids a negatively charged surface that enables electrostatic binding to positively-charged surfaces. We prepared the ultrasheer fabric surface for electrostatic binding of the Pd/Sn colloids by briefly oxidizing the surface using

air plasma, and then chemisorbing 3-aminopropyltriethoxysilane (APTES) from solution. Immersing the resulting amine-functionalized textile in the acidic Pd/Sn colloidal solution protonates the amino groups of the bound APTES; the resulting positively charged ammonium groups electrostatically bind the Pd/Sn colloids. Subsequent etching in aqueous NaOH removes the Sn shell to expose the Pd core, which initiates ELD by catalyzing the reduction of  $\text{Ni}^{2+}$  ions in the ELD plating solution to nickel metal on the surface of the textile. Nickel deposition is autocatalytic thereafter, consuming the dimethylamine borane reducing agent in the nickel ELD solution. In the second ENIG plating step, immersing the nickel-coated textile in a solution of potassium gold cyanide deposits a gold film by galvanic displacement. Ni atoms in the film reduce  $\text{Au}^+$  ions from solution, releasing  $\text{Ni}^{2+}$  ions into the solution and depositing a gold metal film on the surface through molecular exchange.

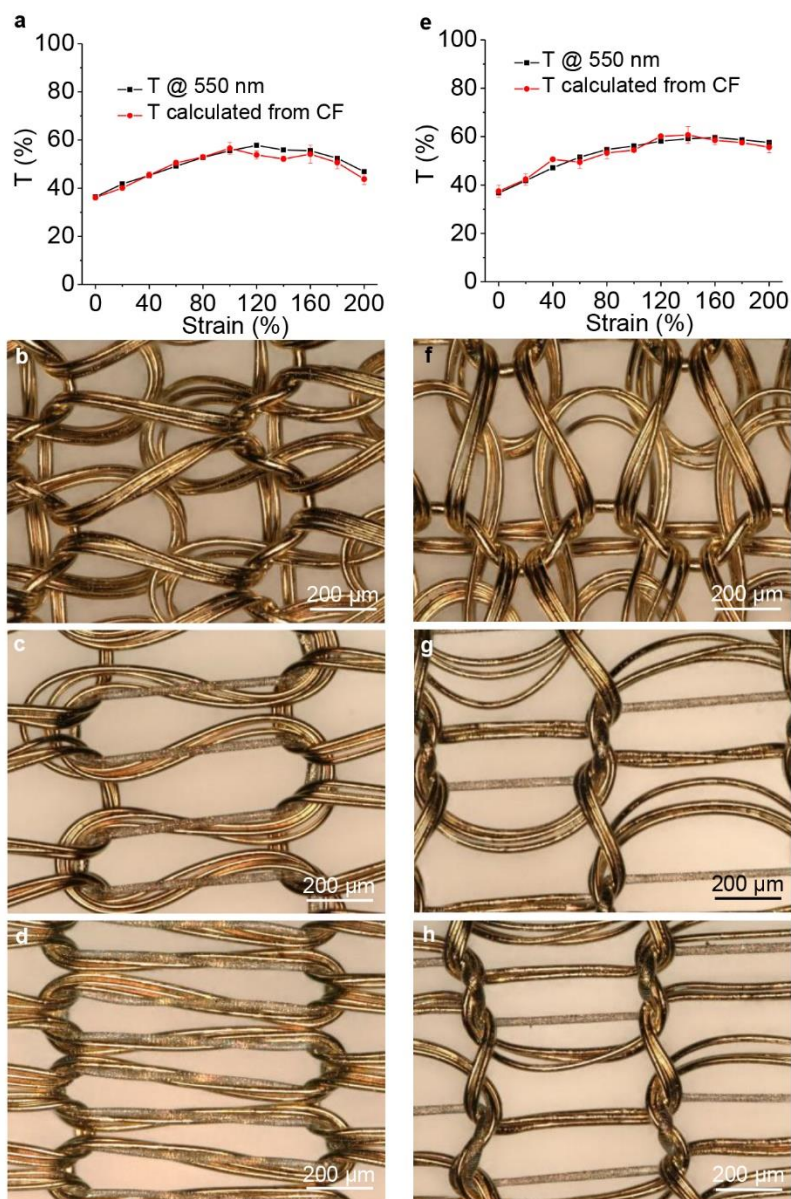
Scanning electron microscopy (SEM) images show that the ENIG process produces uniform gold coatings on both nylon and spandex fibers, with a coating thickness of ~100 nm (**Figure 3-1d,e**; **Figure S3-3**). Small wrinkles and cracks on the surface of gold-coated spandex fibers, but not on the surface of gold-coated nylon fibers, likely originate from thermal expansion of spandex fibers due to the temperature (60 °C) of the immersion gold process (**Figure 3-1e**). Energy-dispersive X-ray spectroscopy of the gold-coated ultrasheer fabric detected gold, but not nickel in the coating (**Figure S3-4a**). Analysis using X-ray diffraction shows diffraction peaks attributed to polycrystalline fcc gold (JCPDS No. 4-0784) (**Figure S3-4b**), with a primary (111) orientation at 38.2° accompanied by peaks at 44.4°, 64.6°, 77.5°, 81.7°, corresponding to (200), (220), (311) and (222) orientations, respectively. This texture is typical of gold films fabricated by electroless deposition.<sup>27,30</sup> Mechanical adhesion testing using the tape test indicates robust adhesion between the gold coating and ultrasheer fabric, showing no visible gold on the tape surface after testing (**Figure S3-5**).

The thin, conformal gold coating on the fibers of the ultrasheer fabric provides electrical conductivity while preserving the softness and stretchability of the original uncoated fabric as well as open spaces in the fabric for optical transmittance. The gold-coated ultrasheer fabric exhibited an average sheet resistance of  $3.6 \pm 0.9 \text{ } \Omega/\text{sq}$ , which is slightly higher than the sheet resistance ( $0.9 \pm 0.1 \text{ } \Omega/\text{sq}$ ) of a continuous, flat gold film of

a similar thickness (100 nm) deposited by physical vapor deposition onto a glass substrate. The slightly higher sheet resistance of the gold-coated ultrasheer fabric can be attributed to contact resistances from interfiber contacts within the knitted fabric structure. The transmittance of the gold-coated ultrasheer fabric (38% at 550 nm) is 10% lower than that of the native ultrasheer fabric (**Figure S3-1b**). The lack of adsorption at 200-230 nm is due to the full coverage of the reflective gold coating on the fabric fibers (**Figure S3-1b**). Tensile testing of ultrasheer fabric before and after gold deposition shows that the ENIG process does not appreciably change the mechanical properties of the ultrasheer fabric, with a slight decrease in tensile strength and a slight increase in breaking load (**Figure S3-2**).

Stretching the gold-coated ultrasheer fabric changes the transmittance in ways that depend on the direction of stretching due to the anisotropic structure of the fabric. We measured the transmittance of the gold-coated ultrasheer fabric with stretching to the elastic limit in the wale direction and course direction. In the wale direction, the transmittance increases steadily with strain to a maximum value 58% at 120% strain, followed by a decrease to 47% at 200% strain (**Figure 3-2a**). In this direction, stretching initially causes the yarns to slip and move and past each other, increasing the open space in the fabric as the wale and course loops eventually become interlocked due to the tension force in the loops. This process increases the transmittance as shown in the optical microscope image of gold-coated ultrasheer fabric at 0% strain (**Figure 3-2b**) with 120% strain (**Figure 3-2c**). Further stretching causes yarns to move toward each other transverse to the stretching direction due to the Poisson effect. This effect decreases the transmittance by decreasing the open area of the ultrasheer fabric, shown in optical microscope images at 200% strain (**Figure 3-2d**). Stretching the gold-coated ultrasheer fabric in the course direction increases the transmittance initially to a maximum value of 60% at 160% strain, followed by a decrease to 58% at 200% strain (**Figure 3-2e**). In this direction, stretching initially unbends the nylon and spandex fibers, widening the course loops to open up the space in the fabric and increase the transmittance. Optical microscope images at 0% (**Figure 3-2f**) and 160% (**Figure 3-2g**) strain show this process. As the strain increases, however, the loops straighten and interlock, and the Poisson effect causes them to move

toward each other transverse to the stretching direction, which decreases the transmittance (Figure 3-2h).



**Figure 3-2** Transmittance of the gold-coated ultrasheer fabric with strain. a) Transmittance measured at 550 nm (black line) and transmittance calculated using the cover factor (CF) (red line) as a function of stretching strain in the wale direction. Optical microscope images of gold-coated ultrasheer fabric stretched in the wale direction at b) 0%, c) 120% and d) 200% strain. e) Transmittance measured at 550 nm (black line) and transmittance calculated using the cover factor (CF) (red line) as a function of stretching strain in the course direction. Optical microscope images of gold-coated ultrasheer fabric stretched in the course direction at f) 0%, g) 160% and h) 200% strain.

To quantitatively validate the correlation between the observed structural changes in the fabric with the measured transmittance change with strain, we used a cover factor (CF) model to calculate a theoretical transmittance value based on optical microscope images of the gold-coated ultrasheer fabric under strain. Calculated light transmittance values using the CF model are based on the assumption that the fibers completely block or absorb light transmission while the spaces between fibers allow complete light transmission:

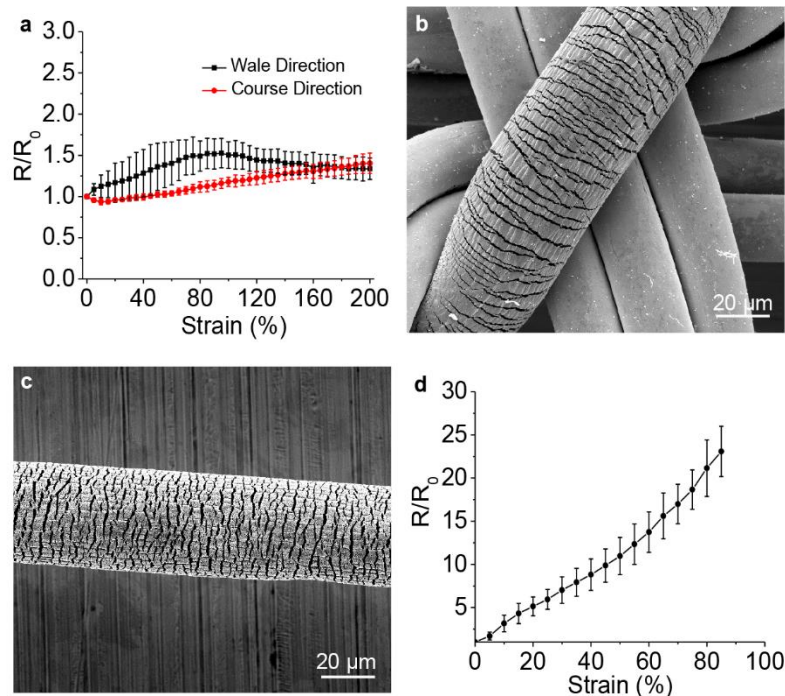
$$\text{CF} = \text{Area covered by fibers} / \text{total area of the fabric} \quad (1)$$

$$\text{T} = 1 - \text{CF} \quad (2)$$

We calculated the CF and theoretical transmittance values using optical images of the gold-coated ultrasheer fabric at different strains in both directions (**Figure S3-6** and **Figure S3-7**). There is excellent agreement between the calculated transmittance values and those measured using UV-visible spectroscopy at 550 nm in both stretching directions (**Figure 3-2a,e**), supporting the idea that the observed opening of the loops with stretching, followed by compression due to the Poisson effect, are the source of the measured transmittance changes.

The resistance of the gold-coated ultrasheer fabric also changes with stretching, due to not only the anisotropic fabric structure but also the combination of gold-coated nylon and spandex fibers in the textile. Conductive knitted textiles made from fibers that are not intrinsically stretchable, such as polyester, typically exhibit an initial decrease, followed by stabilization, of the resistance with stretching. The knitted structure of these textiles causes the yarns to unbend with stretching and also increases the contact pressure between the yarn loops, reducing the contact resistance between adjacent conductive yarns and the overall resistance of the conductive e-textiles.<sup>27,31</sup> In contrast, the resistance of the gold-coated ultrasheer fabric increases with stretching in both the wale and course direction overall (**Figure 3-3a**), which we attribute to a combination of the resistance changes caused by stretching the gold-coated nylon yarns and the intrinsically stretchable gold-coated spandex fibers in the knitted fabric structure. Stretching the gold-coated ultrasheer fabric unbends the nylon yarns as shown in **Figure 3-2** and thus increases the contact pressure between the loops, contributing to reducing the overall resistance of the e-textiles. At the

same time, however, elongation of the intrinsically stretchable spandex fibers within the gold-coated ultrasheer fabric with stretching causes cracks to form in the gold coating on these fibers due to the mechanical mismatch between the metal coating and spandex core (**Figure 3-3b**). These cracks increase the resistance of the gold coating on the spandex fibers and contribute to increasing the overall resistance of the e-textile. To confirm this effect, we pulled individual spandex fibers from the ultrasheer fabric and used the ENIG process to coat them with gold. Stretching gold-coated spandex fibers causes cracks to form in the gold coating (**Figure 3-3c**) that increase the resistance to 23.1-times the initial value at 85% strain; elongating the fiber further resulted in a loss of conductivity (**Figure 3-3d**). The total resistance of the gold-coated ultrasheer fabric with stretching is therefore determined by a combination of the resistance increase from the spandex fibers knitted into the fabric structure and the resistance decrease due to higher contact pressure between the gold-coated nylon fibers. In the wale direction, the resistance increases to 1.53-times the initial value from 0% to 95% strain. Here, the spandex fiber loops elongate perpendicular to the serpentine direction, causing cracks to form in the gold coating. The concomitant increase in resistance dominates the overall resistance of the e-textile. The resistance then gradually decreases to 1.34-times the initial value with further stretching from 95% to 200% strain, consistent with a higher contact pressure between the nylon fibers at these high strains. In the course direction, the resistance initially decreases slightly with stretching from 0% to 15% strain and then gradually increases to 1.40-times the initial value from 15% to 200% strain. This behavior can be attributed to stretching along the serpentine direction of the spandex fibers, which run in the course direction. At low strains, these serpentines merely unbend, converting the stretching strain to bending strain by virtue of the serpentine structure and thus preserving conductivity. At higher strains, however, the serpentines flatten and elongate, forming cracks that increase the overall resistance of the e-textile.



**Figure 3-3** Resistance of the gold-coated ultrasheer fabric with strain. a) Normalized change in resistance as a function of stretching strain along the wale (black line) and course (red line) direction. b) SEM image of the gold-coated ultrasheer fabric stretched to 40% strain. c) SEM image of a gold-coated spandex fiber removed from ultrasheer fabric and stretched to 40% strain. d) Plot of normalized resistance of gold-coated spandex fibers as a function of stretching strain.

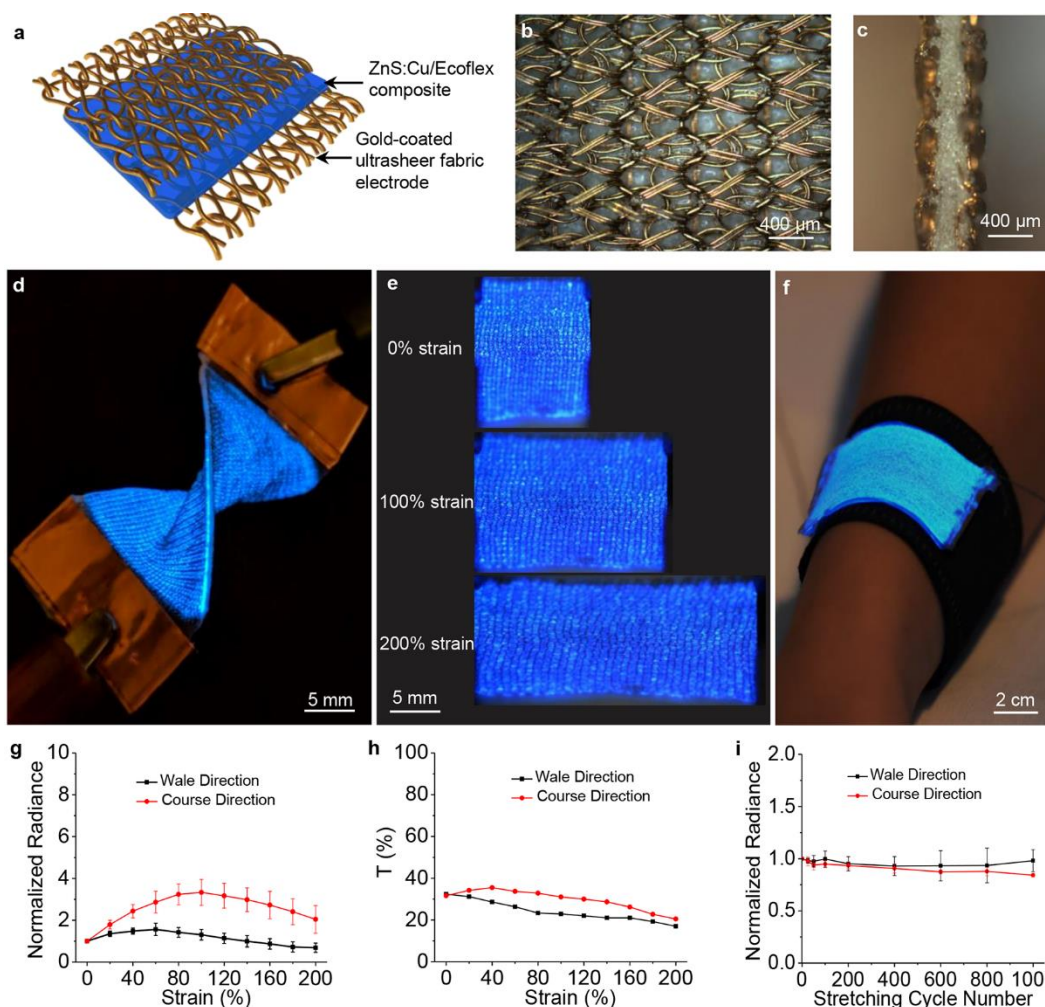
Despite the intricacies of stretching the gold-coated textile due to the anisotropic structure and presence of spandex fibers, the conductivity of the fabric is, overall, remarkably stable to 200% strain in both directions with the change in the normalized resistance remaining within  $\pm 2$ -times the initial value (**Figure 3-3a**). The conductivity also remains stable (within  $\pm 2$ -times the initial value) through 1,000 cycles of 50% strain; after the cycles of strain are complete, the resistance recovers to the initial value in both directions (**Figure S3-8**). The stable conductivity under strain makes gold-coated ultrasheer textiles suitable as wearable wiring and device interconnects; furthermore, the transparency of the e-textile makes this material suitable as a semitransparent electrode in stretchable and wearable light-emitting devices.

There are several important considerations for the fabrication of stretchable and wearable light-emitting devices using e-textiles, which must undergo repeated mechanical deformations and tolerate variable environmental conditions. The stretchability of individual functional layers, the adhesion between the electrodes and emissive layer, and the chemical stability of the emissive layer all contribute to the overall performance. We

fabricated textile-based, highly stretchable ACEL devices using the gold-coated ultrasheer fabric as both top and bottom transparent electrodes with an elastomeric emissive layer sandwiched in between (**Figure 3-4a**). The choice of ACEL device for stretchable light-emitting e-textiles is motivated by previous reports of elastomer-based ACEL devices, which established that the simplicity of the device architecture, utility of elastomeric emissive composites, and insensitivity of these devices to the work function of the electrodes and uniformity of emissive layer are all significant advantages for stretchable devices.<sup>32-34</sup> Although a high operating voltage of >100 V is usually required for ACEL devices to reach practical brightness, the current through the devices is very low. Recent efforts have reduced the operating voltage of these devices by developing new high-permittivity, stretchable dielectric materials, opening the way to practical and safe wearable operation.<sup>35</sup> To fabricate the light-emitting e-textile, we prepared a ~200- $\mu\text{m}$ -thick, uniform film of ZnS:Cu/Ecoflex composite by spin-coating the material onto a temporary carrier substrate. After curing the composite, we spin-coated a thin (~50  $\mu\text{m}$ ) layer of ZnS:Cu/Ecoflex composite on the top surface as an adhesive layer, applied the gold-coated ultrasheer fabric electrode, cured the adhesive layer, and repeated this process on the other side of the emissive layer to complete the device. The total thickness of the device is ~300  $\mu\text{m}$ . This fabrication process partially embeds the gold-coated ultrasheer fabric into the elastomeric emissive layer (**Figure 3-4b,c**), ensuring good adhesion between the layers of the device, which is important for high stretchability and durability of the device. Device operation at 500 V AC and a frequency of 2 kHz produced uniform blue emission through both sides of the device (**Figure 3-4d**) that persisted to the 200% strain limit of the gold-coated ultrasheer fabric (**Figure 3-4e**), making this device the most stretchable light-emitting e-textile fabricated using a textile substrate reported to date and comparable to the stretching performance of light-emitting e-textiles fabricated by weaving stretchable electroluminescent fibers through textile substrates.<sup>17</sup> For the practical wearable operation, we encapsulated both sides of the device with a thin (~300  $\mu\text{m}$ ) protective layer of Ecoflex to prevent possible current leakage when devices are adhered to human skin. After encapsulation, the light-emitting e-textile remains soft (**Figure S3-9a**) and lightweight with a total thickness of 900  $\mu\text{m}$ , a density of ~0.01  $\text{g}/\text{cm}^3$  and a mass per unit area of ~0.1  $\text{g}/\text{cm}^2$ . A large-area device (3 cm  $\times$  5 cm) easily conforms to the human body (**Figure 3-4f**).



The hydrophobicity of the Ecoflex encapsulation layer and chemical stability of inorganic ZnS particles enable the light-emitting e-textiles to function during immersion in water (**Figure S3-9b** and **Video S3-1**) as well as after 10 cycles of stirring in an aqueous solution of laundry detergent, rinsing with water, and drying in a 60 °C oven (**Figure S3-9c**). While these experiments show proof-of-concept of the stability of the light-emitting e-textiles to these aqueous conditions, future work will conduct more extensive washability testing using standard washing conditions such as ISO 105-C06 standard established in textile research to show the practical washability of these wearable light-emitting e-textiles.



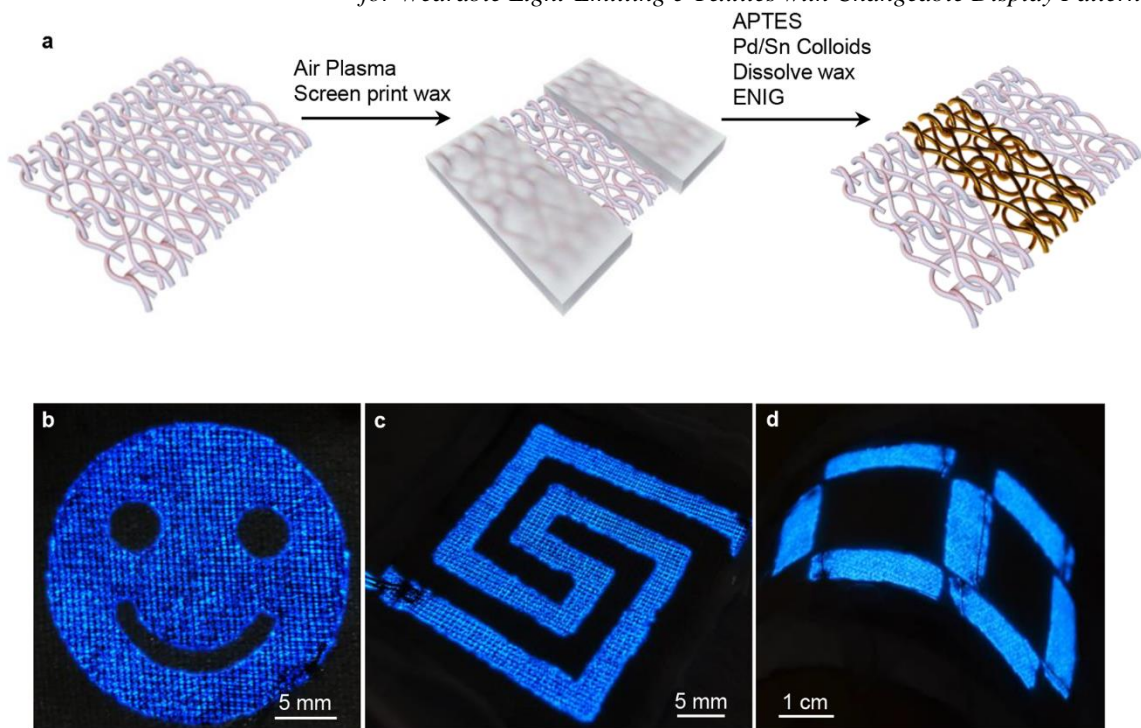
**Figure 3-4** Light-emitting e-textiles fabricated using gold-coated ultrasheer fabric electrodes. a) Diagram of the device structure. Optical microscope images of b) top-view and c) cross-section of the device. Photographs of light-emitting e-textiles d) at twisted state; e) at 0%, 100%, and 200% strain; f) with large area (3 cm × 5cm) conformal to human arm. g) Normalized change in radiance as a function of stretching strain in wale (black line) and course (red line) direction. h) Transmittance measured at 550 nm of encapsulated gold-coated ultrasheer fabric as a function of stretching in the wale (black line) and course (red line) direction. i) Normalized change in radiance as a function of cycles of 0-50% strain in wale (black line) and course (red line) direction.

The emission brightness of the light-emitting e-textile varies with strain, initially increasing in brightness followed by a decrease with additional strain. We quantified the emission performance by measuring the device radiance with stretching in both the wale and course direction and plotting normalized values as a function of strain (**Figure 3-4g**). There are mainly two factors that both contribute to these brightness changes: first, stretching reduces the thickness of the emissive layer, increasing the electric field and contributing to higher brightness; second, the light transmittance of the gold-coated ultrasheer electrodes varies depending on the strain as well as the direction of stretching, thus regulating the emission brightness. Since the gold-coated ultrasheer fabric electrodes are partially embedded into the elastomeric emissive layer of the devices, we created a model electrode by embedding the gold-coated ultrasheer fabric in Ecoflex. The model Ecoflex-embedded electrode exhibits slightly different transmittance values with stretching in the wale and course directions (**Figure 3-4h**) than those of the unembedded gold-coated fabric (**Figure 3-2a,b**), which we attribute to Ecoflex restricting the free slippage of the fabric loops with stretching. The changes in resistance of the gold-coated ultrasheer electrodes with strain, on the other hand, do not play a major role in changing the emission brightness, since ACEL devices are voltage-driven devices and the resistance changes of the gold-coated electrodes with strain are relatively small compared with the resistance of the emissive layer.<sup>36</sup>

In the wale direction, the emission brightness increases as the strain increases from 0 to 60%, ultimately reaching a maximum value of 156%. Since the transmittance of the Ecoflex-embedded e-textile electrode decreases throughout this range, this performance is consistent with the increase in electric field dominating the emission response. At strains >60%, the decrease in transmittance outweighs increases in the electric field, resulting in a decrease in emission brightness that reaches 68% at 200% strain. In the course direction, the transmittance of the Ecoflex-embedded e-textile electrodes initially increases and remains higher than the initial transmittance to 100% strain. This increased transmittance, coupled with the higher electric field in the emissive layer, leads to a rapid increase in emission brightness that reaches a maximum of value of 333% at 100% strain. At strains >100% the transmittance of the e-textile electrodes decreases below its initial value, dominating the emission response and decreasing the emission brightness to 204% at 200%

strain. Along with conformability and stretchability, the light-emitting e-textiles are also highly durable, making them well-suited to applications in wearable electronics. The e-textiles exhibited consistent light emission through 1000 stretch-release cycles of 50% strain (**Figure 3-4i**).

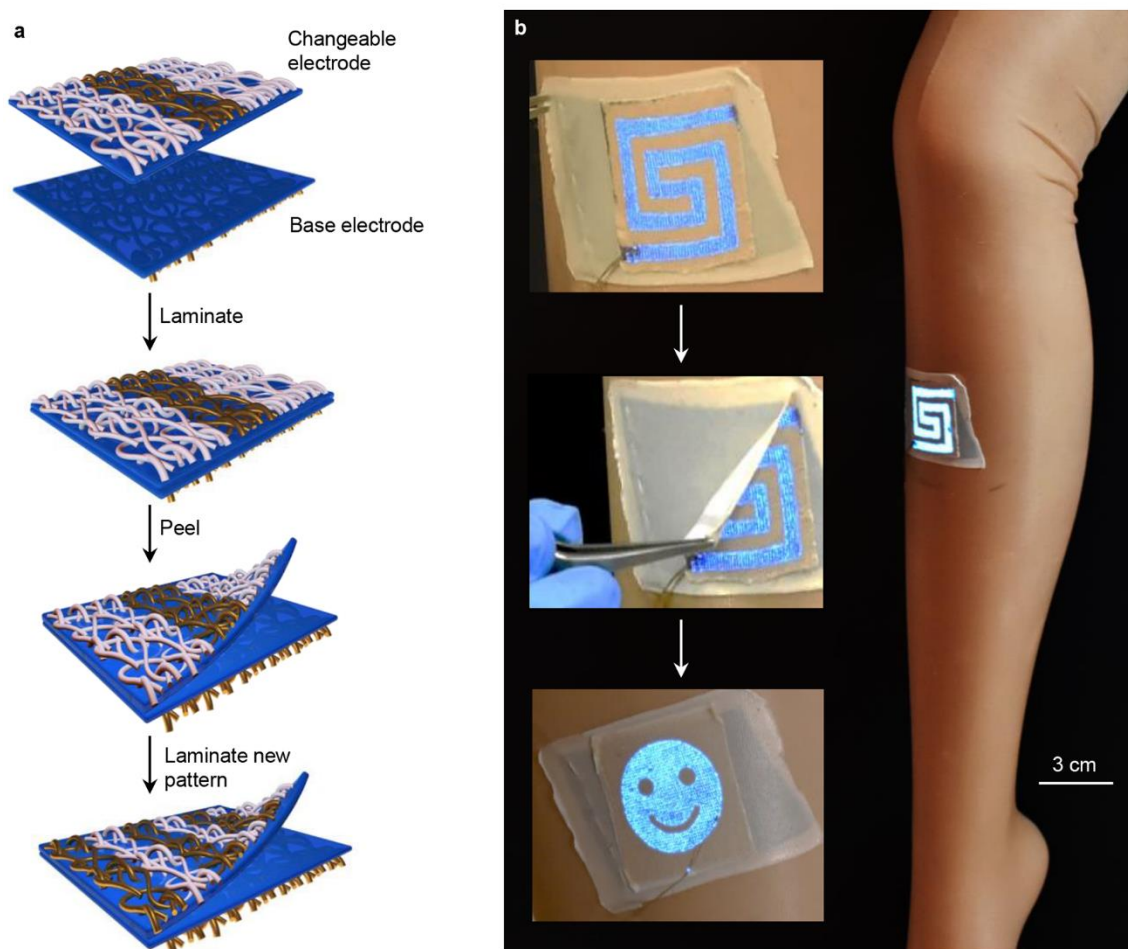
Patterned light emission is important for wearable light-emitting e-textiles to enable information displays and graphics. We used a low-cost stencil-printing method to fabricate patterned e-textile electrodes for patterned light-emitting displays. The patterning process in **Figure 3-5a** is based on stencil printing of cold-wax medium, a soft, viscous, beeswax-based paste. Applying the cold wax medium through a stencil mask onto plasma-oxidized ultrasheer fabric produces a patterned hydrophobic barrier due to penetration of the cold wax medium into the fabric structure. Immersion of the patterned ultrasheer fabric in an aqueous Pd/Sn colloidal dispersion then results in selective uptake of colloids in the regions without wax resist; regions coated in wax resist do not adsorb Pd/Sn colloids and thus remain inactive to ENIG. Dissolving the wax resist using hexane leaves a pattern of Pd/Sn catalyst on the fabric; subsequent ENIG processing deposits metal only in these catalyzed regions. We fabricated patterned light-emitting e-textiles by replacing one of the unpatterned gold-coated ultrasheer textile electrodes in the device with a patterned gold-coated ultrasheer textile electrode. In this way, we fabricated light-emitting textiles displaying the “smiling face” emoji (**Figure 3-5b**) and a rectangular spiral (**Figure 3-5c**). We also used the patterning technique to fabricate a dynamic seven-segment textile display by patterning seven rectangular segments on the ultrasheer fabric (**Figure S3-10a**), and then selectively operating the segments in different combinations to display the numbers from 0 to 9 (**Figure 3-5d**, **Figure S3-10b**).



**Figure 3-5** Patterned light-emitting e-Textiles. a) Schematic of the patterning process. Photographs of light-emitting textiles displaying b) the “smiling face” emoji, c) a rectangular spiral, and d) the number 8.

Soft and wearable electroluminescent clothing has applications in safety apparel, marketing, and fashion. In these domains, the ability to change the illuminated image to suit different situations is more advantageous than requiring the user to change the article of clothing to display a new image. We modified the light-emitting e-textile fabrication process to create multipurpose light-emitting e-textiles by incorporating soft-contact lamination between two e-textile electrodes coated with the emissive material (**Figure 3-6a**). The fabrication process uses two e-textile electrodes: The base electrode, which is integrated into the article of clothing itself, is an unpatterned rectangular ENIG coating. The changeable electrode, which is the top electrode for the light-emitting device, is printed with a desired ENIG pattern. We adhered a thin ( $\sim 150\ \mu\text{m}$ ) layer of the Ecoflex/ZnS:Cu emissive composite to each surface using the process described previously. Simply laminating the emissive surface of the changeable electrode onto the emissive surface of the base electrode adheres the two Ecoflex/ZnS:Cu surfaces together by van der Waals forces, completing the device. **Figure 3-6b** shows a demonstration of this approach, using a base electrode integrated into the leg of a pair of ultrasheer pantyhose and a changeable

electrode laminated over the top. The patterned changeable electrode can be easily peeled off and replaced with an electrode bearing a different pattern, allowing the user to express, for example, different emotional states (**Video S3-2, S3-3, and S3-4**).



**Figure 3-6** Patterned light-emitting e-textiles with changeable patterns of light emission. a) Schematic of the pattern changing process. b) Photographs of changeable patterned e-textile worn on a mannequin leg.

### 3.3 Conclusions

We have demonstrated that the complex, 3D structures of textiles, often viewed as problematic substrates for e-textile fabrication, can instead form the basis for a new design approach whereby the textile structure is a fundamental design component to enable wearable devices. Here, we have shown that the open framework structure of ultrasheer textiles provides a unique way to address the challenging problem of stretchable and wearable transparent electrodes for light-emitting e-textiles. This new textile-centric approach to wearable electronics has enormous potential beyond this present work,

especially considering the incredibly wide range of textiles available for study: natural and synthetic materials that are knitted, woven, tufted, and braided into a variety of structures, all of which vary in fiber density, composition, structure, stiffness, elasticity, weight, water absorbency, water repellence, strength, and durability.

### **3.4 Experimental**

All chemicals were purchased commercially and used as received.

*ENIG Metallization of Knitted Ultrasheer Fabric:* 10-denier knitted ultrasheer fabric (87% nylon and 13% spandex) was sonicated in deionized water and isopropyl alcohol for 15 min each, and then exposed to air plasma for 10 min. The oxidized fabric was immersed in a 1% v/v solution of APTES in deionized water for 30 min, a Pd/Sn solution (prepared from Cataposit 44 and Cataprep 404 (Shipley), as directed by manufacturer) for 2 min, and aqueous 1 M NaOH for 1 min. Samples were rinsed with water in between steps. The fabric was then metallized in a nickel ELD solution (0.08 M NiSO<sub>4</sub>·6H<sub>2</sub>O, 0.14 M Na<sub>4</sub>P<sub>2</sub>O<sub>7</sub>·10 H<sub>2</sub>O and 0.07 M dimethylamine borane in water) for 10 min with sonication. After rinsing with water, the Ni-coated fabric was immersed in Au ELD bath (Gobright TAM-55, Uyemura) for 30 min.

*Patterning of Knitted Ultrasheer Fabric:* The ultrasheer fabric was sonicated in deionized water and isopropyl alcohol for 15 min each, and then exposed to air plasma for 10 min. A 0.15-mm-thick stainless-steel stencil mask with the desired pattern was placed on top of the fabric, cold wax medium (Gamblin) was applied to cover the metal stencil, and then a glass microscope slide was used as a squeegee to remove the excess. The ENIG metallization procedure was then performed.

*Electroluminescent Device Fabrication:* The emissive layer was formed by mixing ZnS:Cu phosphor powder (KPT) with Ecoflex 30 prepolymer (Smooth-on Inc.) in 1:1 (w:w) ratio. This mixture was spin-coated at 500 rpm for 1 min onto a carrier surface comprising a glass substrate covered with a layer of tape, and then curing on a 70 °C hot plate for 5 min. Then, a second layer of ZnS:Cu/Ecoflex was spin-coated on the cured layer at 1000 rpm for 1 min as an adhesive layer, and the gold-coated ultrasheer textile brought into contact with the surface. Curing the adhesive layer at 70 °C for 5 min adhered the gold-coated textile to

the surface. The structure was peeled away from the tape-covered glass, flipped over, and the process was repeated by spin-coating a second adhesive layer of ZnS:Cu/Ecoflex blend, adhering the second gold-coated ultrasheer textile electrode, and curing.

*Washing Durability:* ACEL devices were soaked in 1 wt % solution of Tide Original Liquid Laundry Detergent in DI water with stirring for 1 h, followed by rinsing with water and drying in a 60 °C for 1h.

*Characterization:* Optical microscopy was performed using an Olympus BX51 microscope equipped with an Olympus Q-Color3 digital camera. Stereomicrographs were taken using a Leica m205 FA stereomicroscope with z-stack multi-plane focusing enabled. SEM images and energy dispersive X-ray spectroscopy were taken on an FEI Quanta 200 Environmental SEM. Energy dispersive X-ray spectroscopy was recorded at 15 kV. For samples prepared for cross-sectional SEM, the gold-coated ultrasheer fabric was embedded in PDMS first and then fractured by scalpel after freezing in liquid nitrogen. X-ray diffraction measurements were run on a PROTO AXRD powder diffractometer equipped with a Cu X-ray source, and a Mythen 1K silicon strip detector, operated at 30 kV and 20 mA. Scans were performed using CuK $\alpha$  radiation, a 0.1 mm divergence slit, and a step size of 0.02 degrees 2 theta. X-ray diffraction patterns were obtained in the 2 theta region from 30 to 90°. MTS Criterion (modal 43) was used for tensile testing under strain rate of 300 mm/min. For electrical characterization under strain, samples were clamped in the microvice stretcher (S.T. Japan, USA, Inc.) and stretched manually in 5% increments while measuring the resistance using a Keithley 2601A Sourcemeter. Textile-based light emitting ACEL devices were operated at 500 V AC with a frequency of 2 kHz, which was inverted from 3 V DC using an inverter (Sparkfun). Emission intensity was measured with a calibrated UDT S470 optometer attached to an integrating sphere. Entire samples are put inside the integrating sphere and radiant intensity from 495 nm was measured. A home-made auto-stretching stage (Velmex, Inc) was used for the cyclic stretching test.

### 3.5 References

- [1] Barber, E. J. W.; Princeton University Press: Princeton, 1992.
- [2] Liu, M.; Pu, X.; Jiang, C.; Liu, T.; Huang, X.; Chen, L.; Du, C.; Sun, J.; Hu, W.; Wang, Z. Large-Area All-Textile Pressure Sensors for Monitoring Human Motion and Physiological Signals. *Adv. Mater.* **2017**, *29*, 1703700.
- [3] Atalay, A.; Sanchez, V.; Atalay, O.; Vogt, D. M.; Haufe, F.; Wood, R. J.; Walsh, C. J. Batch Fabrication of Customizable Silicone-Textile Composite Capacitive Strain Sensors for Human Motion Tracking. *Adv. Mater. Technol.* **2017**, *2*, 1700136.
- [4] Coppedè, N.; Tarabella, G.; Villani, M.; Calestani, D.; Iannotta, S.; Zappettini, A. Human Stress Monitoring through an Organic Cotton-Fiber Biosensor. *J. Mater. Chem. B* **2014**, *2*, 5620-5626.
- [5] Zhao, Y.; Zhai, Q.; Dong, D.; An, T.; Gong, S.; Shi, Q.; Cheng, W. A Highly Stretchable and Strain-Insensitive Fiber-Based Wearable Electrochemical Biosensor to Monitor Glucose in the Sweat. *Anal. Chem.* **2019**, *91*, 6569-6576.
- [6] Pu, X.; Liu, M.; Li, L.; Han, S.; Li, X.; Jiang, C.; Du, C.; Luo, J.; Hu, W.; Wang, Z. Wearable Textile-Based In-Plane Microsupercapacitors. *Adv. Energy Mater.* **2016**, *6*, 1601254.
- [7] Yang, Y.; Huang, Q.; Niu, L.; Wang, D.; Yan, C.; She, Y.; Zheng, Z. Waterproof, Ultrahigh Areal-Capacitance, Wearable Supercapacitor Fabrics. *Adv. Mater.* **2017**, 1606679.
- [8] Lee, S. S.; Choi, K. H.; Kim, S. H.; Lee, S. Y. Wearable Supercapacitors Printed on Garments. *Adv. Funct. Mater.* **2018**, *28*, 1705571.
- [9] Hu, L.; Pasta, M.; Mantia, F.; Cui, L.; Jeong, S.; Deshazer, H.; Choi, J.; Han, S.; Cui, Y. Stretchable, Porous, and Conductive Energy Textiles. *Nano Lett.* **2010**, *10*, 708-714.
- [10] Gaikwad, A. M.; Zamarayeva, A. M.; Rousseau, J.; Chu, H.; Derin, I.; Steingart, D. A. Highly Stretchable Alkaline Batteries Based on an Embedded Conductive Fabric. *Adv. Mater.* **2012**, *24*, 5071-5076.
- [11] Xiong, J. Q.; Lee, P. S. Progress on Wearable Triboelectric Nanogenerators in Shapes of Fiber, Yarn, and Textile. *Sci. Technol. Adv. Mater.* **2019**, *20*, 837-857.



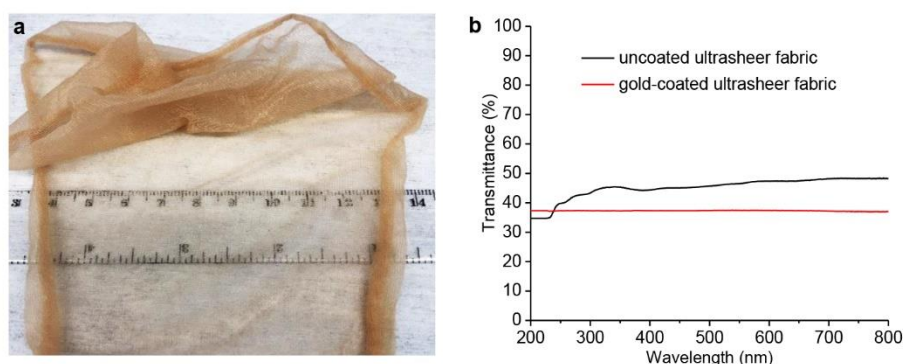
- [12] Pan, S.; Yang, Z.; Chen, P.; Deng, J.; Li, H.; Peng, H. Wearable Solar Cells by Stacking Textile Electrodes. *Angew. Chem. Int. Ed.* **2014**, *53*, 6110-6114.
- [13] Lee, S.; Lee, Y.; Park, J.; Choi, D. Stitchable Organic Photovoltaic Cells with Textile Electrodes. *Nano Energy* **2014**, *9*, 88-93.
- [14] Li, R.; Xiang, X.; Tong, X.; Zou, J.; Materials, L.-Q. Wearable Double-Twisted Fibrous Perovskite Solar Cell. *Adv. Mater.* **2015**, *27*, 3831-3835.
- [15] Cherenack, K.; Zysset, C.; Kinkeldei, T.; Münzenrieder, N.; Tröster, G. Woven Electronic Fibers with Sensing and Display Functions for Smart Textiles. *Adv. Mater.* **2010**, *22*, 5178-5182.
- [16] Kwon, S.; Kim, H.; Choi, S.; Jeong, E.; Kim, D.; Lee, S.; Lee, H.; Seo, Y.; Choi, K. Weavable and Highly Efficient Organic Light-Emitting Fibers for Wearable Electronics: A Scalable, Low-Temperature Process. *Nano Lett.* **2017**, *18*, 347-356.
- [17] Zhang, Z.; Cui, L.; Shi, X.; Tian, X.; Wang, D.; Gu, C.; Chen, E.; Cheng, X.; Xu, Y.; Hu, Y.; Zhang, J.; Zhou, L.; Fong, H.; Ma, P.; Jiang, G.; Sun, X.; Zhang, B.; Peng, H. Textile Display for Electronic and Brain-Interfaced Communications. *Adv. Mater.* **2018**, *30*, 1800323.
- [18] Hu, B.; Li, D.; Ala, O.; Manandhar, P.; Fan, Q.; Kasilingam, D.; Calvert, P. D. Textile-Based Flexible Electroluminescent Devices. *Adv. Funct. Mater.* **2011**, *21*, 305-311.
- [19] Hu, B.; Li, D.; Manandhar, P.; Fan, Q.; Kasilingam, D.; Calvert, P. CNT/Conducting Polymer Composite Conductors Impart High Flexibility to Textile Electroluminescent Devices. *J. Mater. Chem.* **2011**, *22*, 1598-1605.
- [20] Vos, M.; Torah, R.; Tudor, J. Dispenser Printed Electroluminescent Lamps on Textiles for Smart Fabric Applications. *Smart Mater. Struct.* **2016**, *25*, 45016.
- [21] Kim, W.; Kwon, S.; Lee, S.-M.; Kim, J.; Han, Y.; Kim, E.; Choi, K.; Park, S.; Park, B.-C. Soft Fabric-Based Flexible Organic Light-Emitting Diodes. *Org. Electron.* **2013**, *14*, 3007-3013.
- [22] Kim, W.; Kwon, S.; Han, Y.; Kim, E.; Choi, K.; Kang, S.-H.; Park, B.-C. Reliable Actual Fabric-Based Organic Light-Emitting Diodes: Toward a Wearable Display. *Adv. Electron. Mater.* **2016**, *2*, 1600220.

- [23] Choi, S.; Kwon, S.; Kim, H.; Kim, W.; Kwon, J.; Lim, M.; Lee, H.; Choi, K. Highly Flexible and Efficient Fabric-Based Organic Light-Emitting Devices for Clothing-Shaped Wearable Displays. *Sci. Rep.* **2017**, *7*, 6424.
- [24] Kim, H.; Kwon, S.; Choi, S.; Choi, K. Solution-Processed Bottom-Emitting Polymer Light-Emitting Diodes on a Textile Substrate Towards a Wearable Display. *J. Inf. Disp.* **2015**, *16*, 179-184.
- [25] Lanz, T.; Sandström, A.; Tang, S.; Chabreck, P.; Sonderegger, U.; Edman, L. A Light-Emission Textile Device: Conformal Spray-Sintering of a Woven Fabric Electrode. *Flex. Print.* **2016**, *1*, 25004.
- [26] Wang, B.; Facchetti, A. Mechanically Flexible Conductors for Stretchable and Wearable E-Skin and E-Textile Devices. *Adv. Mater.* **2019**, *31*, 1901408.
- [27] Wu, Y.; Mechael, S. S.; Chen, Y.; Carmichael, T. B. Solution Deposition of Conformal Gold Coatings on Knitted Fabric for E-Textiles and Electroluminescent Clothing. *Adv. Mater. Technol.* **2018**, *3*, 1700292.
- [28] Zhang, Z.; Shi, X.; Lou, H.; Xu, Y.; Zhang, J.; Li, Y.; Cheng, X.; Peng, H. A Stretchable and Sensitive Light-Emitting Fabric. *J. Mater. Chem. C* **2017**, *5*, 4139-4144.
- [29] Zhu, B.; Gong, S.; Cheng, W. Softening Gold for Elastronics. *Chem. Soc. Rev.* **2018**, *48*, 1668-1711.
- [30] Chen, Y.; Wu, Y.; Mechael, S. S.; Carmichael, T. B. Heterogeneous Surface Orientation of Solution-Deposited Gold Films Enables Retention of Conductivity with High Strain-A New Strategy for Stretchable Electronics. *Chem. Mater.* **2019**, *31*, 1920-1927.
- [31] Zhang, H. Flexible Textile-Based Strain Sensor Induced by Contacts. *Meas. Sci. Technol.* **2015**, *26*, 105102.
- [32] Shin, H.; Sharma, B. K.; Lee, S.; Lee, J.-B.; Choi, M.; Hu, L.; Park, C.; Choi, J.; Kim, T.; Ahn, J.-H. Stretchable Electroluminescent Display Enabled by Graphene-Based Hybrid Electrode. *ACS Appl. Mater. Interfaces* **2019**, *11*, 14222-14228.
- [33] Wang, J.; Yan, C.; Cai, G.; Cui, M.; Eh, A.; Lee, P. Extremely Stretchable Electroluminescent Devices with Ionic Conductors. *Adv. Mater.* **2016**, *28*, 4490-4496.

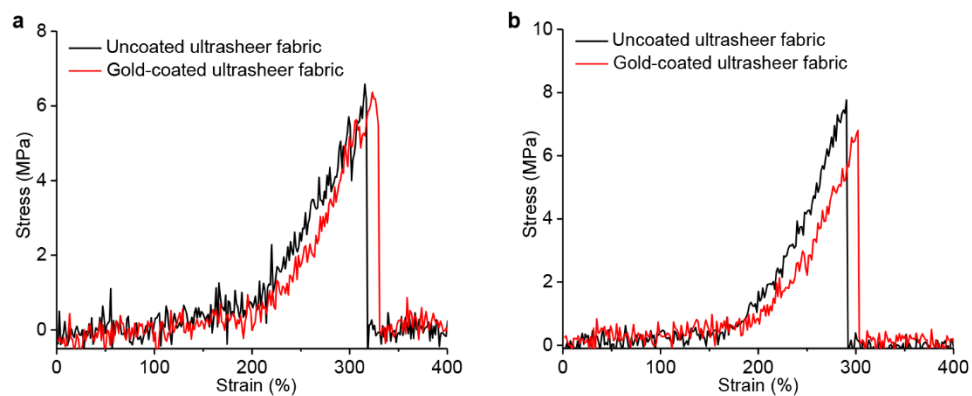
- [34] Wang, J.; Yan, C.; Chee, K.; Lee, P. Highly Stretchable and Self-Deformable Alternating Current Electroluminescent Devices. *Adv. Mater.* **2015**, *27*, 2876-2882.
- [35] Zhou, Y.; Zhao, C.; Wang, J.; Li, Y.; Li, C.; Zhu, H.; Feng, S.; Cao, S.; Kong, D. Stretchable High-Permittivity Nanocomposites for Epidermal Alternating-Current Electroluminescent Displays. *ACS Mater. Lett.* **2019**, 511-518.
- [36] Wang, Z.-g.; Chen, Y.-f.; Li, P.-j.; Hao, X.; Liu, J.-b.; Huang, R.; Li, Y.-r. Flexible Graphene-Based Electroluminescent Devices. *ACS Nano* **2011**, *5*, 7149-7154.

### 3.6 Supporting Information

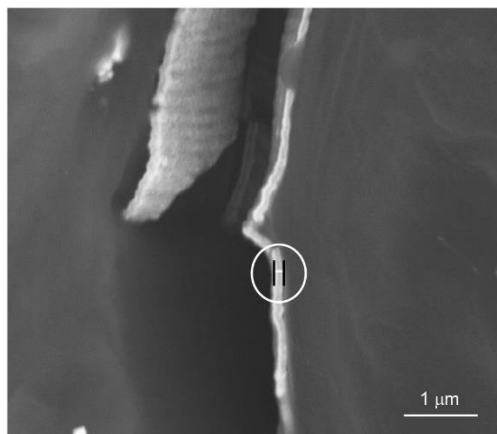
*Cover factor (CF) calculation:* Optical micrographs of gold-coated ultrasheer fabrics under different strains in both stretching directions were first processed using Adobe Photoshop to color the fibers of fabrics in black and the open space in white. Then the processed images were imported into ImageJ to calculate the area percentage of the black color in the image, which is the value of the cover factor according to its definition. **Figure S3-6** and **Figure S3-7** show the selected optical micrographs and corresponding images generated from ImageJ for CF calculation. At least three optical micrographs were taken and used to calculate the cover factor at one stain and the average value was used to calculate the transmittance, which is plotted against strain in **Figure 3-2a,b**.



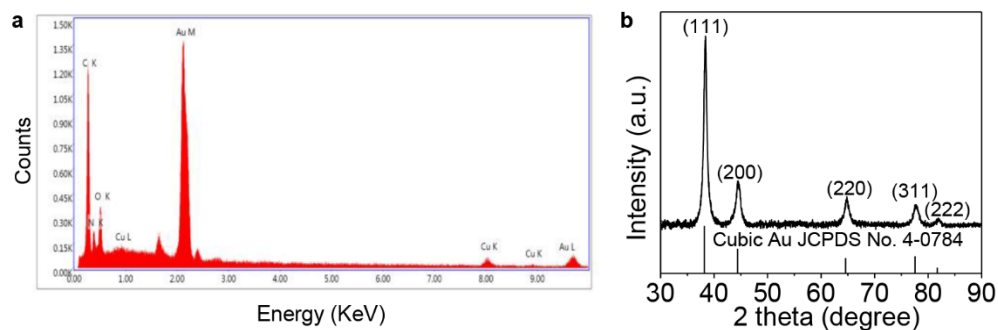
**Figure S3-1** a) Photograph of uncoated ultrasheer fabric. b) UV-visible spectra of uncoated ultrasheer fabric and gold-coated ultrasheer fabric.



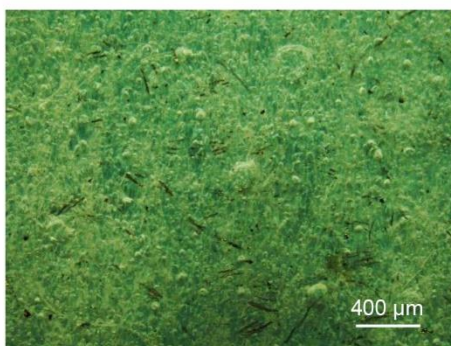
**Figure S3-2** Stress strain curve of uncoated ultrasheer fabric (black line) and gold-coated ultrasheer fabric (red line) a) in the wale direction and b) in the course direction.



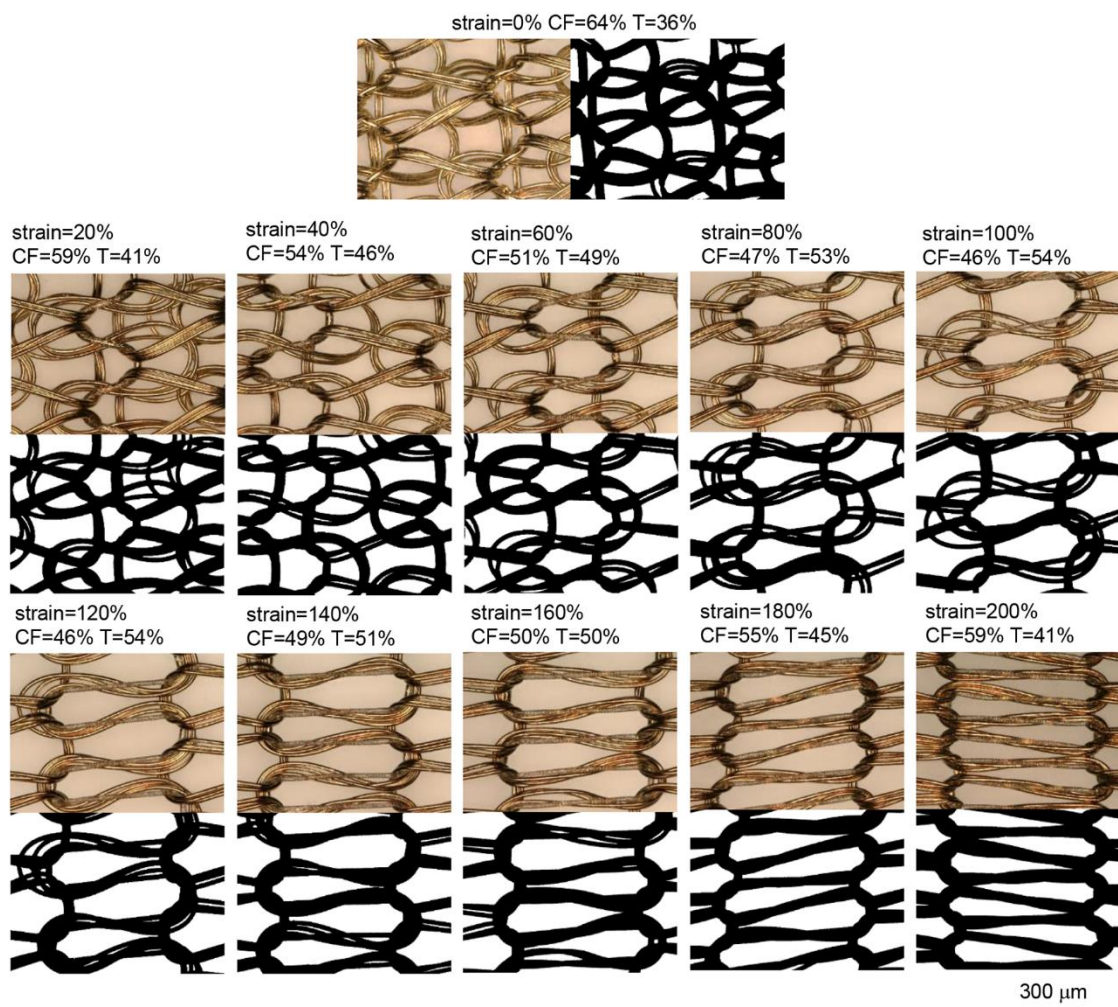
**Figure S3-3** Cross-sectional SEM of gold-coated ultrasheer fabric.



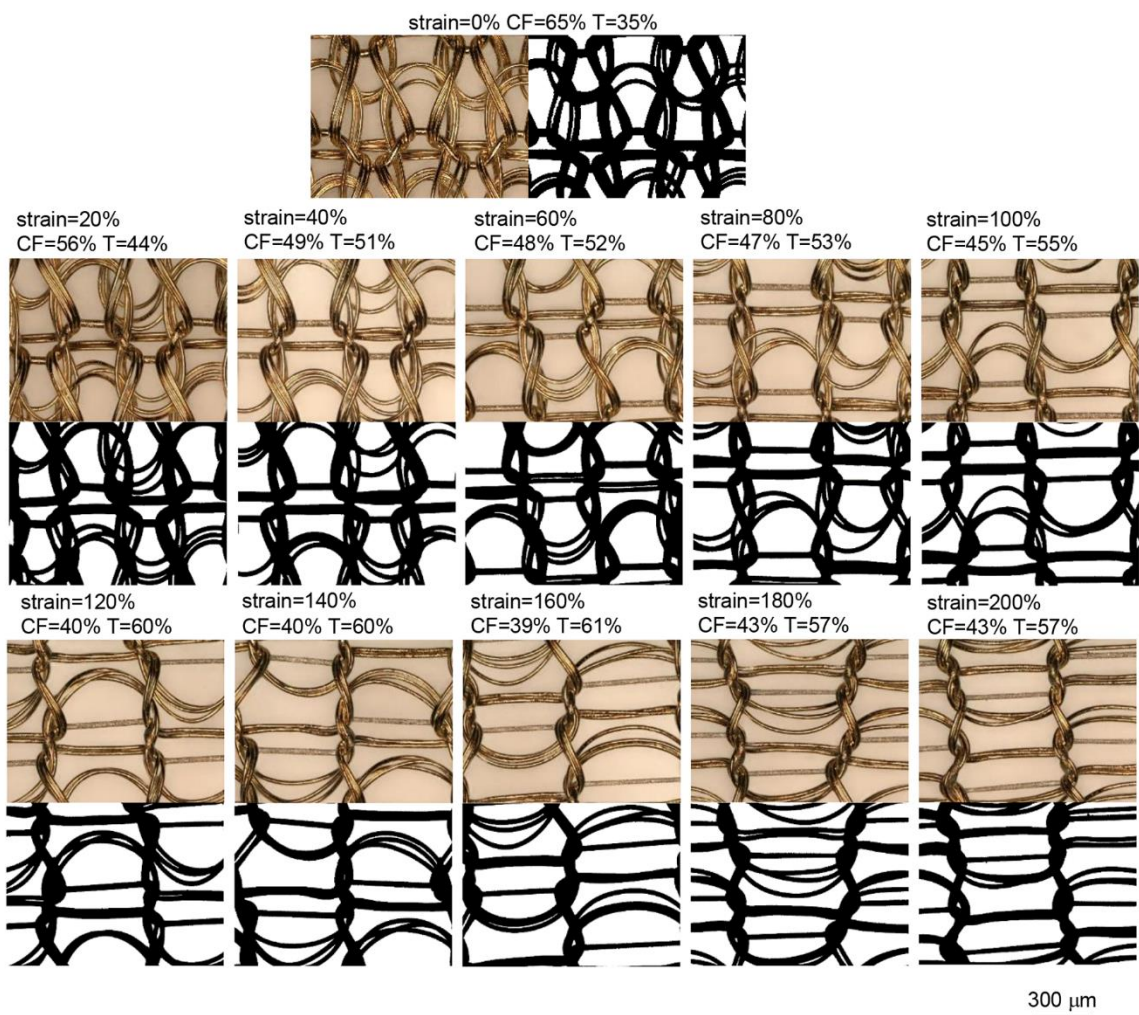
**Figure S3-4** a) Energy-dispersive X-ray spectroscopy and b) X-ray diffraction patterns of gold-coated ultrasheer fabric.



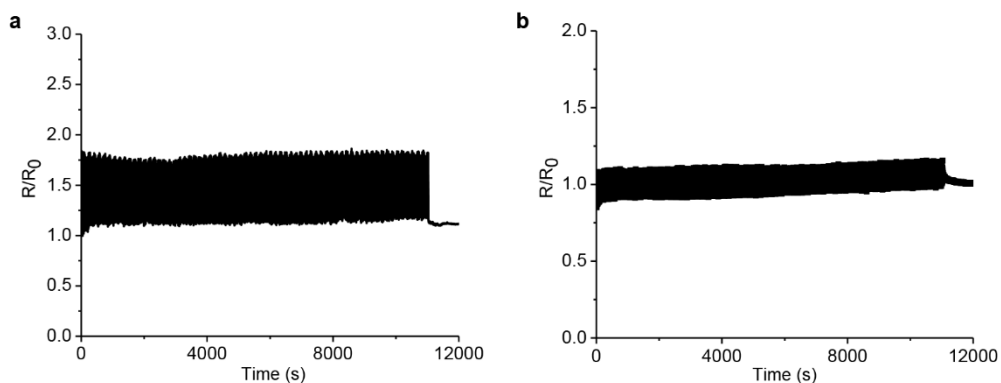
**Figure S3-5** Optical microscope image of the tape surface after tape test of gold-coated ultrasheer fabric with APTES treatment.



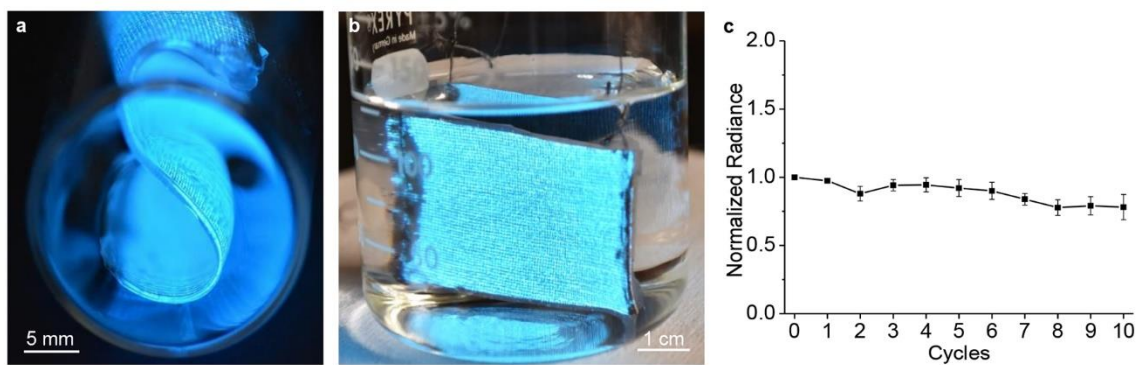
**Figure S3-6** Optical microscope images (top rows) and the corresponding images generated from ImageJ (bottom rows) used for cover factor calculation of gold-coated ultrasheer fabric stretched in the wale direction under different strains. The scale bar at the bottom right is for all the images.



**Figure S3-7** Optical microscope images (top rows) and the corresponding images generated from ImageJ (bottom rows) used for cover factor calculation of gold-coated ultrasheer fabric stretched in the course direction under different strains. The scale bar at the bottom right is for all the images.



**Figure S3-8** Normalized resistance of gold-coated ultrasheer fabric over 1000 stretch-release cycles of 50% strain a) in the wale direction and b) in the course direction.



**Figure S3-9** Photographs of light-emitting e-textiles a) folded into and S-shape inside a vial and b) submerged in water. c) Normalized change in radiance as a function of simulated washing cycles.





**Figure S3-10** Photographs of a) seven-segment display fabricated using patterned gold-coated ultrasheer fabric and b) light-emitting textile seven-segment display displaying numbers from 0 to 9.

**Video S3-1** Light-emitting e-textile operating under water; **Video S3-2** and **S3-3** Peeling off the changeable patterned electrode from light-emitting e-textile; **Video S3-4** Peeling off the patterned electrode from light-emitting e-textiles and replacing with a different patterned electrode can be found online at <https://doi.org/10.1016/j.matt>.

**Chapter 4 Velour Fabric as an Island-Bridge Architectural Design for Stretchable  
Textile-Based Lithium-Ion Battery Electrodes**

## 4.1 Introduction

The future of textiles is electronic, with new wearable electronics integrated into "smart clothing" systems that will incorporate input devices such as sensors to detect biometric data<sup>1-5</sup> and output devices such as light-emitting displays to display data to the user.<sup>6-9</sup> Powering this next generation of smart clothing to enable the continuous function of these wearable devices is of key importance. At present, heavy and bulky "black box" battery packs that do not meet the demand for comfort and wearability are carried as power sources for wearable electronic devices. The development of lightweight and stretchable energy storage devices that are seamlessly integrated with textiles is thus a critically important next step in the development of wearables. The electronic textile (e-textile) community is actively investigating several potential solutions, including textile-based supercapacitors,<sup>10-13</sup> energy generators,<sup>14</sup> and solar cells.<sup>15-17</sup> Lithium-ion batteries (LIBs) are one of the most promising power sources due to relatively high energy density and long cycle life;<sup>18-20</sup> however, conventional LIB materials are mechanically incompatible with soft and stretchable textiles. The battery electrode is the core component that largely dictates the mechanical properties of the entire battery. These electrodes consist of a current collector, such as aluminum or copper foil, coated with a brittle electroactive material composite, such as  $\text{LiCoO}_2$ ,  $\text{LiFePO}_4$  or  $\text{Li}_4\text{Ti}_5\text{O}_{12}$ , mixed with a conductive additive and binder.<sup>21</sup> Each component in this conventional electrode is vulnerable to cracking or delamination in response to mechanical strain during wearing, leading to diminished electrochemical performance. Solving the mechanical mismatch problem between brittle LIB materials and stretchable textiles is thus a key challenge in the development of robust wearable power sources with stable performance under mechanical deformation. Here, we present a textile-based architectural strain-engineering approach, inspired by mechanics designs in elastomeric electronics, to fabricate a stretchable textile-based LIB electrode that protects brittle LIB materials from strain.

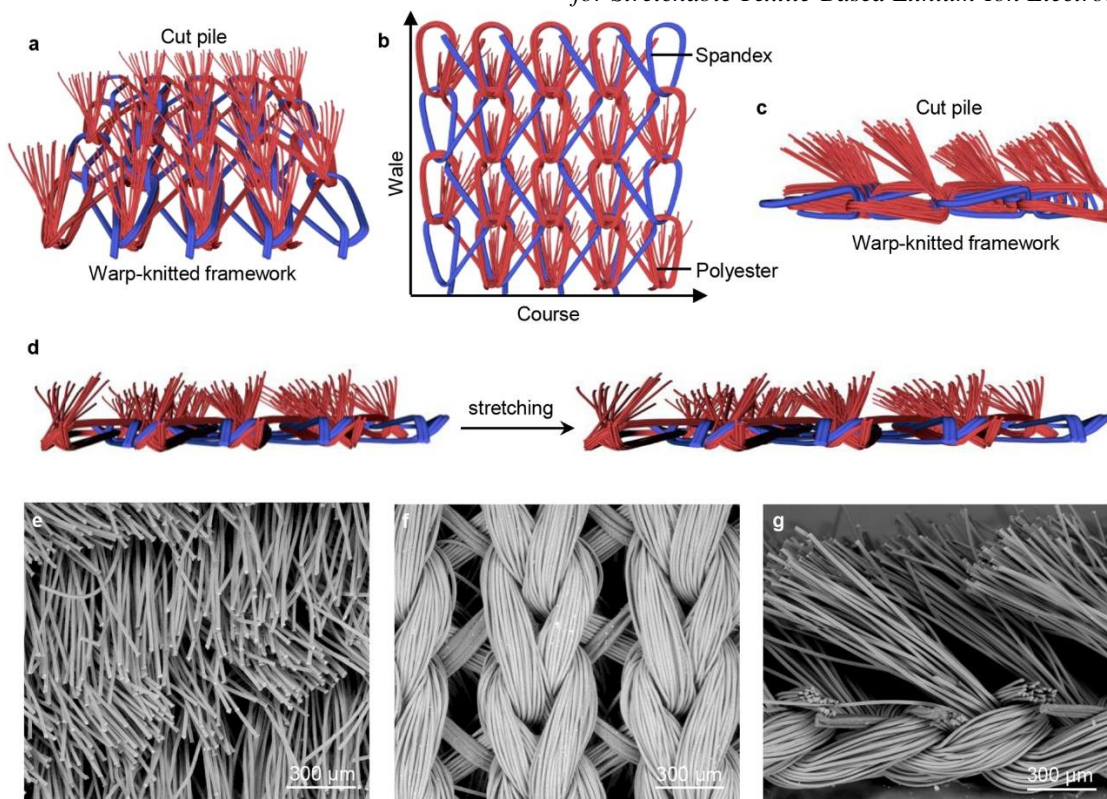
The rapidly developing field of skin-mounted elastomer-based electronics has successfully navigated the mechanical mismatch between rigid, brittle functional materials and soft elastomeric substrates by configuring conventional rigid and brittle materials into mechanics-guided architectures that can stretch.<sup>22</sup> These architectural strain-engineering strategies have successfully converted many types of highly brittle or rigid materials, such

as silicon,<sup>23</sup> gallium arsenide,<sup>24</sup> and metals,<sup>25</sup> into stretchable formats. Configuring these materials into thin, wavy structures such as out-of-plane wrinkles or arches, or in-plane serpentine and meshes, enables tensile strain to be accommodated by converting stretching strains into less destructive bending strains of the wavy and curved structures. Metallic wavy structures have also been deployed to electrically connect arrays of rigid conventional electronic devices on stretchable substrates.<sup>26</sup> In these “island-bridge” structures, the metallic “bridges” unbend to absorb the strain with stretching, protecting the rigid “islands” from strain-induced damage and providing stretchability to the entire circuit. These architectural strain-engineering designs have been applied to fabricate stretchable LIBs on elastomeric substrates, minimizing the strain concentration and alleviating the detrimental effects of strain on the performance of LIB electrodes.<sup>27-33</sup> For example, Wei *et al.* fabricated stretchable LIBs consisting of arched electrodes that unbend with strain, enabling stable electrochemical performance with stretching,<sup>27</sup> whereas Xu *et al.* reported the use of conventional LIBs as rigid islands connected by stretchable serpentine metallic interconnects on an elastomeric substrate.<sup>31</sup>

The strain-engineering architectures developed for elastomer-based electronics do not translate directly to the non-planar, porous, 3D structures of textiles; however, the structures of textiles themselves comprise inherently built-in mechanical designs that enable stretchability, softness, and drapability of the fabric. For example, the interlaced yarn loops in knitted textiles can be thought of as wavy serpentine structures that unbend with stretching. Humankind has furthermore been developing textiles for millennia, providing an extensive variety of textile architectures, including woven, braided, and tufted designs. These different textile architectures have the potential to form the basis for architectural strain-engineering approaches that enable the integration of brittle functional materials with soft textiles to solve the mechanical mismatch problem. Although previous research has used textiles as substrates for LIBs,<sup>34-43</sup> no reports have yet emerged that use textile structures as an architectural strain-engineering strategy. Most of the research on developing textile-based LIBs for wearable power sources has used flexible fabrics as substrates to form electrodes, such as woven carbon cloth,<sup>34-38</sup> woven cotton fabrics,<sup>39</sup> woven polyester fabrics<sup>40</sup> and nonwoven polyester fabrics.<sup>41,42</sup> These textile-based LIB electrodes exhibit excellent electrochemical performance and mechanical flexibility but

lack softness and stretchability. Although the softness and stretchability of knitted textiles makes them a more suitable choice for wearable electronics, the integration of functional LIB materials with knitted structures has proven to be difficult. For example, Ghadi *et al.* reported LIB electrodes by casting a  $\text{LiCoO}_2$  slurry onto a stretchable knitted silver fabric.<sup>43</sup> The slurry filled in the fabric voids, stiffening the fabric, and rendering the composite vulnerable to cracking. The electrochemical performance of the electrode under strain was not reported.

Instead of using textiles simply as substrates for LIB electrodes, we use the architectural features of a warp-knitted velour textile as the basis for an island-bridge architectural strain-engineering strategy to fabricate a stretchable LIB electrode. The velour fabric consists of a warp-knitted framework and a cut pile (**Figure 4-1a-c**). As the textile is stretched, the warp-knitted framework elongates but the cut pile fibers protruding from the framework move horizontally and separate (**Figure 4-1d**). In its mechanical response to stretching, this velour fabric architecture is similar to island-bridge structures: The looped yarns comprising the warp-knitted framework act as “bridges” and unbend with strain, while the cut pile fibers - the “islands” - are not subjected to the strain. By metallizing the warp-knitted velour fabric with gold and then selectively depositing the brittle electroactive material CuS on the cut pile, we integrate the LIB electrode into a single piece of velour fabric, while protecting the brittle CuS from strain and subsequent damage. The electrode exhibited a specific capacity of  $\sim 400$  mAh/g at 0.5 C with no obvious sign of capacity decay for at least 300 cycles. Furthermore, after undergoing 1000 stretching-releasing cycles, the electrode exhibited stable electrochemical performance, demonstrating the success of this architectural strain-engineering approach to textile-based stretchable LIBs.

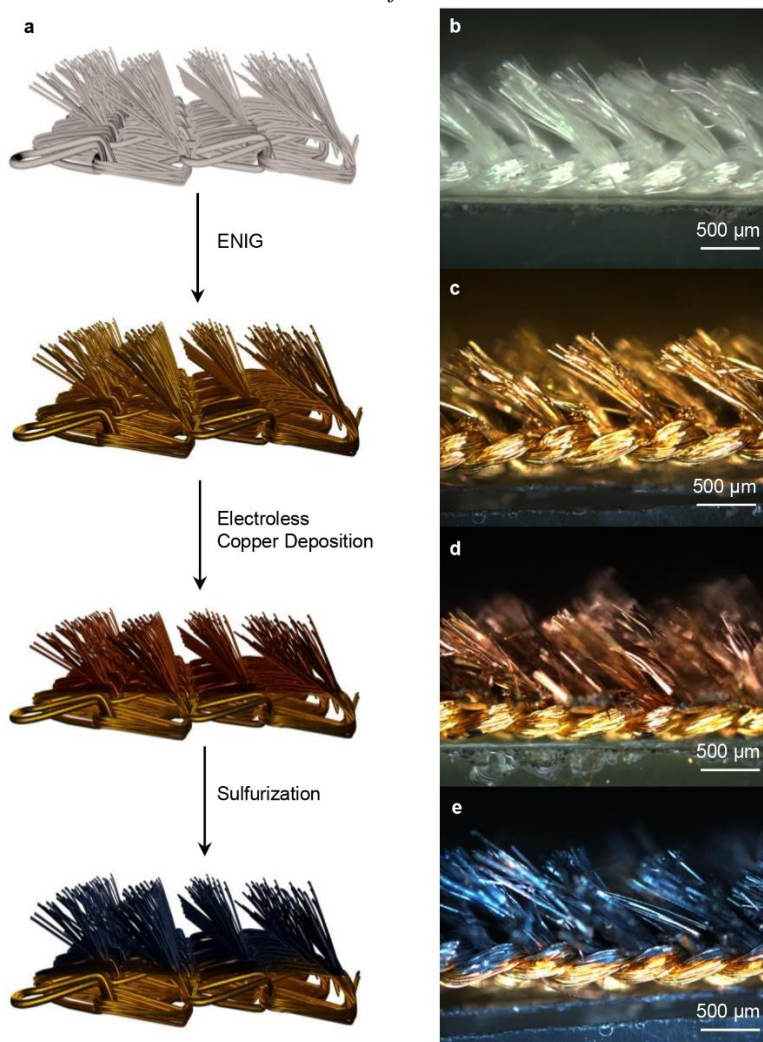


**Figure 4-1** Structure of the warp-knitted velour fabric. Schematic of a) front side, b) back side and c) cross-section of the velour fabric. d) Schematic of the warp-knitted velour fabric stretched in the course direction. SEM images of e) front side, f) back side and g) cross-section of the warp-knitted velour fabric.

## 4.2 Results and discussion

The warp-knitted velour fabric consists of polyester and spandex yarns knitted together to provide a framework for the cut pile (**Figure 4-1f**). The cut pile are polyester fibers that are woven through and protrude from the framework (**Figure 4-1e**). The length of the cut pile protruding from the warp-knitted framework is about 1 mm with an angle of natural inclination of  $\sim 30^\circ$  (**Figure 4-1g**). The warp-knitted structure of the framework provides stretchability to the fabric by unbending of the curved polyester yarns with strain. The presence of the intrinsically stretchable spandex fibers provides resilience, enabling the fabric to return to its original shape after stretching. Tensile testing of the fabric shows that the elastic stretchability in the wale direction is only  $\sim 10\%$  (**Figure S4-1**), at which point the loops of the framework became interlocked (**Figure S4-2**). In contrast, the elastic stretchability in the course direction is  $\sim 130\%$  (**Figure S4-1**). This difference is due to the anisotropic structure of the warp-knitted framework.

We used the warp-knitted velour fabric as an island-bridge architectural design to fabricate stretchable electrochemically active electrodes for use in LIBs by first metallizing the fabric to create the current collector, and then selectively depositing the brittle electroactive material, CuS, only on the cut pile surfaces (**Figure 4-2a**). In the initial step, we used solution-based electroless nickel-immersion gold (ENIG) metallization<sup>6,8,44,45</sup> to deposit a gold coating conformally over the surfaces of both the warp-knitted framework and the cut pile of the velour fabric. The ENIG process consists of four steps: activation of the velour fabric surfaces, catalyst binding, electroless nickel deposition, and galvanic displacement of nickel for gold. Activation of the velour fabric uses oxidation in an air plasma to produce hydroxyl groups on the surface, followed by chemisorption of 3-aminopropyltriethoxysilane (APTES) to form an amine-terminated surface. Catalyst binding occurs by immersion in an acidic solution of a palladium-tin (Pd/Sn) colloidal catalyst, which consists of a palladium-rich core protected from oxidation by a hydrolyzed Sn<sup>2+</sup>/Sn<sup>4+</sup> shell with an associated chloride layer that gives the colloids a negatively charged surface.<sup>46</sup> The acidic Pd/Sn solution protonates the amine groups on the surface of the velour fabric to form an ammonium-terminated surface, enabling electrostatic adsorption of the Pd/Sn colloids.<sup>47</sup> Subsequent etching of the Sn shell in 1 M NaOH exposes the Pd core, which initiates the deposition of a nickel coating in an electroless plating solution, followed by autocatalytic deposition of a nickel coating using a dimethylamine borane reducing agent in the electroless nickel solution. Finally, immersing the nickel-coated velour fabric in a solution of potassium gold cyanide results in molecular exchange of nickel for gold. In this galvanic displacement reaction, Ni atoms in the film reduce Au<sup>+</sup> ions from solution, releasing Ni<sup>2+</sup> ions into the solution. The aqueous solutions used in the ENIG process permeate the velour fabric to deposit gold on the surfaces of both the warp-knitted framework and the cut pile, changing the color of the velour fabric from white to golden (**Figure 4-2b,c**) and rendering it conductive with a sheet resistance of 0.77 ± 0.04 Ω/sq.

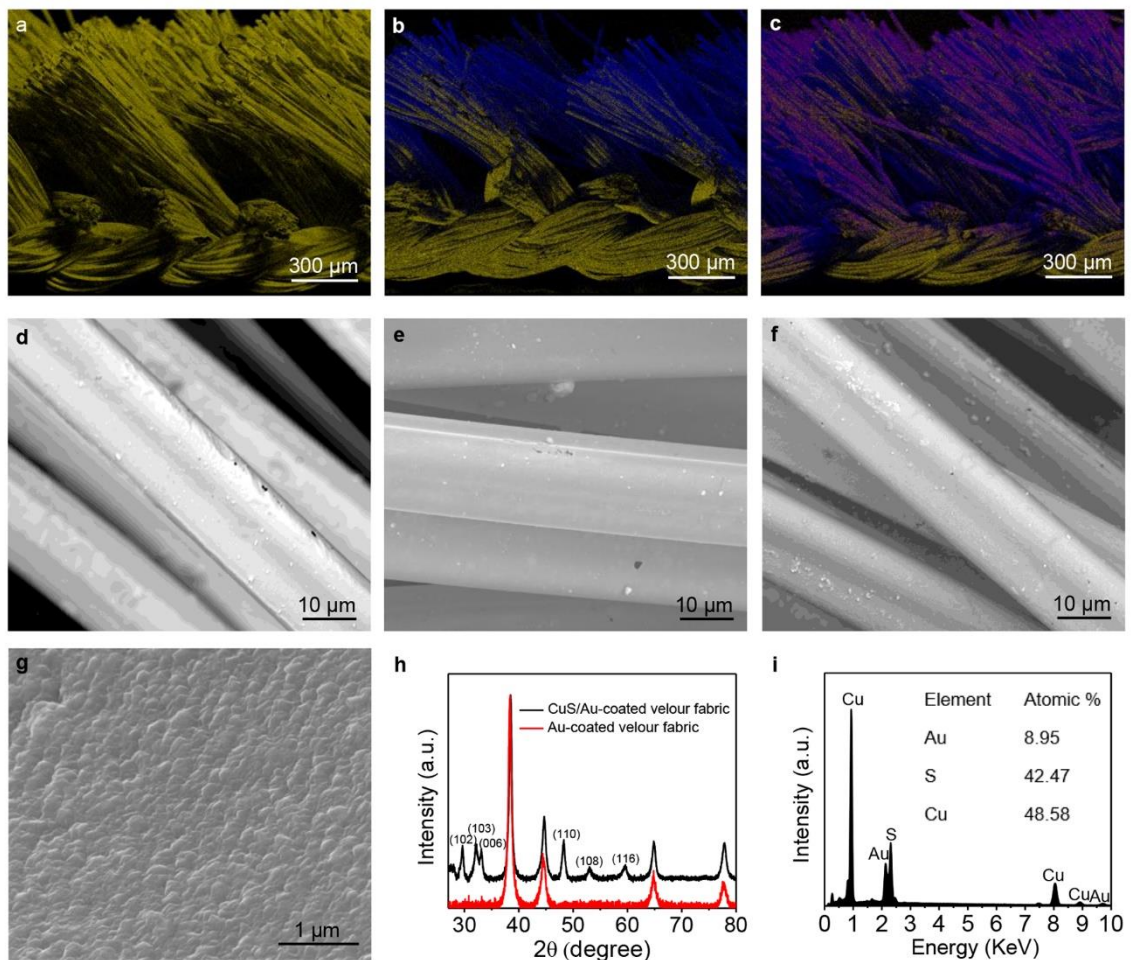


**Figure 4-2** Fabrication of the velour fabric LIB electrode. a) Schematic of the velour fabric LIB electrode fabrication process. Cross-sectional optical microscope images of the velour fabric b) before and after c) Au, d) Cu and e) CuS deposition.

We then deposited the electroactive material, CuS, selectively on the cut pile surfaces using electroless copper deposition and solution sulfurization. We applied Kapton tape to the backside of the velour fabric to prevent deposition on this side of the Au-coated framework current collector. We first deposited a copper coating selectively onto the Au-coated cut pile fibers using an electroless copper plating solution (**Figure 4-2d**). Since gold is catalytic to electroless copper deposition,<sup>48</sup> the copper film could be deposited directly onto the Au-coated cut pile fibers without additional activation or catalyst binding steps. A minor amount of copper deposited on the top side of the current collector, while the back side remained unchanged due to the Kapton tape. Subsequently immersing the velour fabric in a solution of elemental sulfur in carbon disulfide at room temperature forms a CuS



coating on the cut pile surfaces,<sup>49</sup> completing the fabrication of the velour fabric LIB electrode with a CuS loading density of  $\sim 1 \text{ mg/cm}^2$ . The distinct black color of the cut pile after this step is consistent with the conversion of Cu into CuS (**Figure 4-2e**), while the color of the Au-coated framework current collector remained unchanged since gold is inactive to sulfur (**Figure S4-3**).

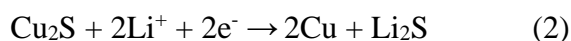
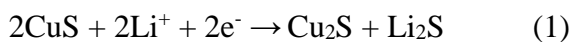


**Figure 4-3** Sequential, selective, and conformal deposition of Au, Cu and CuS on the velour fabric. Elemental mapping of the velour fabric after a) Au, b) Cu and c) CuS deposition. [Yellow = Au, Blue = Cu, Purple = S]. SEM images of d) Au-coated cut pile fibers, e) Cu/Au-coated cut pile fibers and f) CuS/Au-coated cut pile fibers. g) High magnification SEM image of the CuS coating on the Au-coated cut pile fiber. h) XRD patterns of the velour fabric after Au (red line) and CuS (black line) deposition. i) EDX of the CuS/Au-coated cut pile fiber.

We used energy-dispersive X-ray spectroscopy (EDX) of Au, Cu, and S to validate the sequential and selective deposition of Au (**Figure 4-3a**), Cu (**Figure 4-3b**) and CuS (**Figure 4-3c**) on the cut pile of the velour fabric LIB electrode. These images also confirm that the Au-coated framework current collector remains chemically unchanged after the

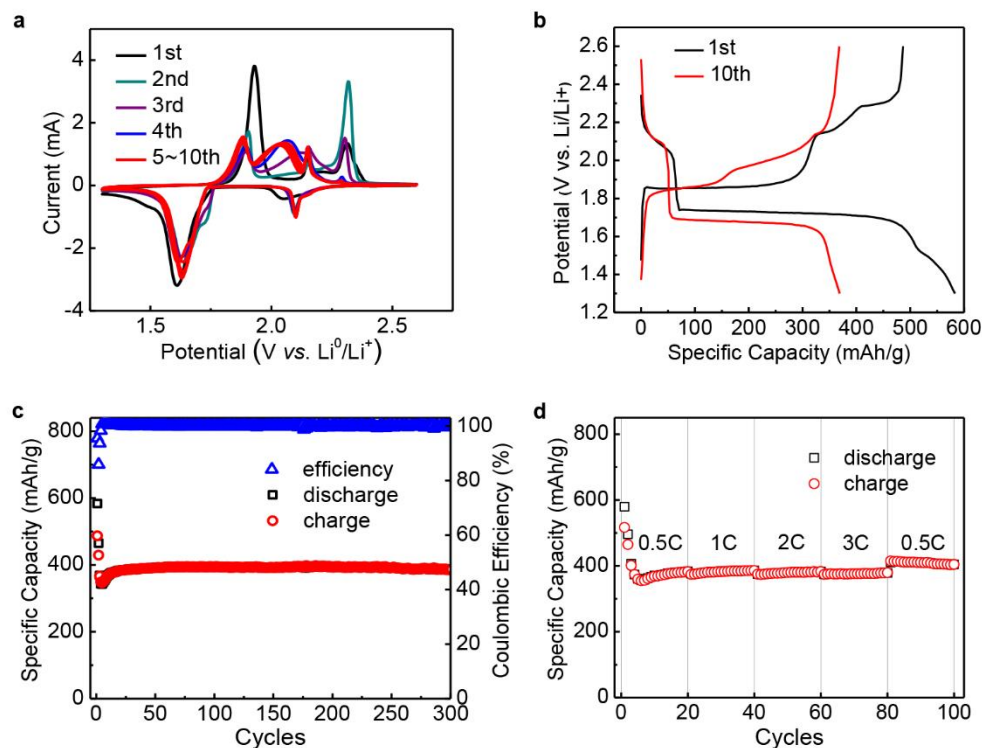
electroless deposition of copper on the cut pile and subsequent reaction with sulfur. The Au-coated framework current collector furthermore maintained high electrical conductivity after these processes with a sheet resistance of  $0.85 \pm 0.06 \Omega/\text{sq}$ , similar to that of the initial Au-coated velour fabric ( $0.77 \pm 0.04 \Omega/\text{sq}$ ). We hypothesize that the slight increase in sheet resistance may be attributed to CuS deposition on the top side of the gold-coated current collector (**Figure 4-2e** and **Figure 4-3c**). SEM images of Au (**Figure 4-3d**), Cu/Au (**Figure 4-3e**) and CuS/Au (**Figure 4-3f**) coatings show that these materials all form conformal coatings over the surfaces of the individual fibers of the cut pile. Higher magnification SEM image shows that the CuS coating on the cut pile fibers is composed of nanograins (**Figure 4-3g**). X-ray diffraction (XRD) analysis revealed that the CuS nanograins possess a hexagonal phase (**Figure 4-3h**). All the identified peaks except the intense diffraction peaks from Au in the XRD pattern can be ascribed to the hexagonal covellite CuS phase (JCPDS No. 06-0464). The EDX spectrum also shows that the atomic ratio of Cu to S was approximately 1:1, agreeing well with the expected stoichiometry of CuS (**Figure 4-3i**).

CuS has been widely investigated as an electrode material for LIBs because of its high theoretical capacity, flat discharge curves, and good conductivity. CuS is furthermore environmentally friendly and elementally abundant on earth.<sup>50-52</sup> It stores lithium ions based on the two-step reversible conversion reaction between CuS and  $\text{Li}^+$ . Reactions are idealized as equation (1) and (2), but are known to be more complex with other types of intermediate products formed besides  $\text{Cu}_2\text{S}$  in reaction (1).<sup>52</sup>



The reaction between CuS and  $\text{Li}^+$  has a high theoretical capacity of 560 mAh/g, which is higher than conventional electrode materials, such as  $\text{LiCoO}_2$  (274 mAh/g) and  $\text{LiFePO}_4$  (170 mAh/g). We investigated the electrochemical properties of the CuS on the cut pile of the velour fabric LIB electrode using a coin-cell type configuration with the velour fabric LIB electrode as the working electrode and a lithium foil as the counter electrode (**Figure S4-4**). Cyclic voltammetry (CV) curves of the cell from 1.3 to 2.6 V at a scan rate of 0.1 mV/s showed the electrode underwent a gradual evolution of oxidation and reduction

processes during the first 4 cycles, stabilizing in the 5th cycle (**Figure 4-4a**). In the first CV curve, there are three oxidation peaks at 1.9 V, 2.2 V, and 2.3 V and two reduction peaks at 1.6 V and 2.0 V, similar to previously reported studies of CuS-based electrodes.<sup>53</sup> After stabilization, the three oxidation peaks shift to 1.9 V, 2.0 V and 2.2 V, and the two well-defined reduction peaks shift to 1.7 V and 2.1 V. The oxidation peaks shift to lower potential and reduction peaks shift to higher potential, resulting in narrower peak intervals that are consistent with the reduced polarization of the velour fabric LIB electrode.<sup>54</sup> The galvanostatic charge and discharge profile measured in the potential range of 1.3 V to 2.6 V (*vs.* Li<sup>0</sup>/Li<sup>+</sup>) at 0.5 C exhibited three charge plateaus and two discharge plateaus well-matched with the peak positions in the CV curves (**Figure 4-4b**). The discharge plateau at 2.1 V corresponds to the Li diffusion into the covellite CuS lattice to form Cu<sub>2</sub>S and Li<sub>2</sub>S (equation (1)), while the plateau at 1.7 V corresponds to further diffusion of lithium resulting in the conversion reaction forming Cu and Li<sub>2</sub>S (equation (2)).

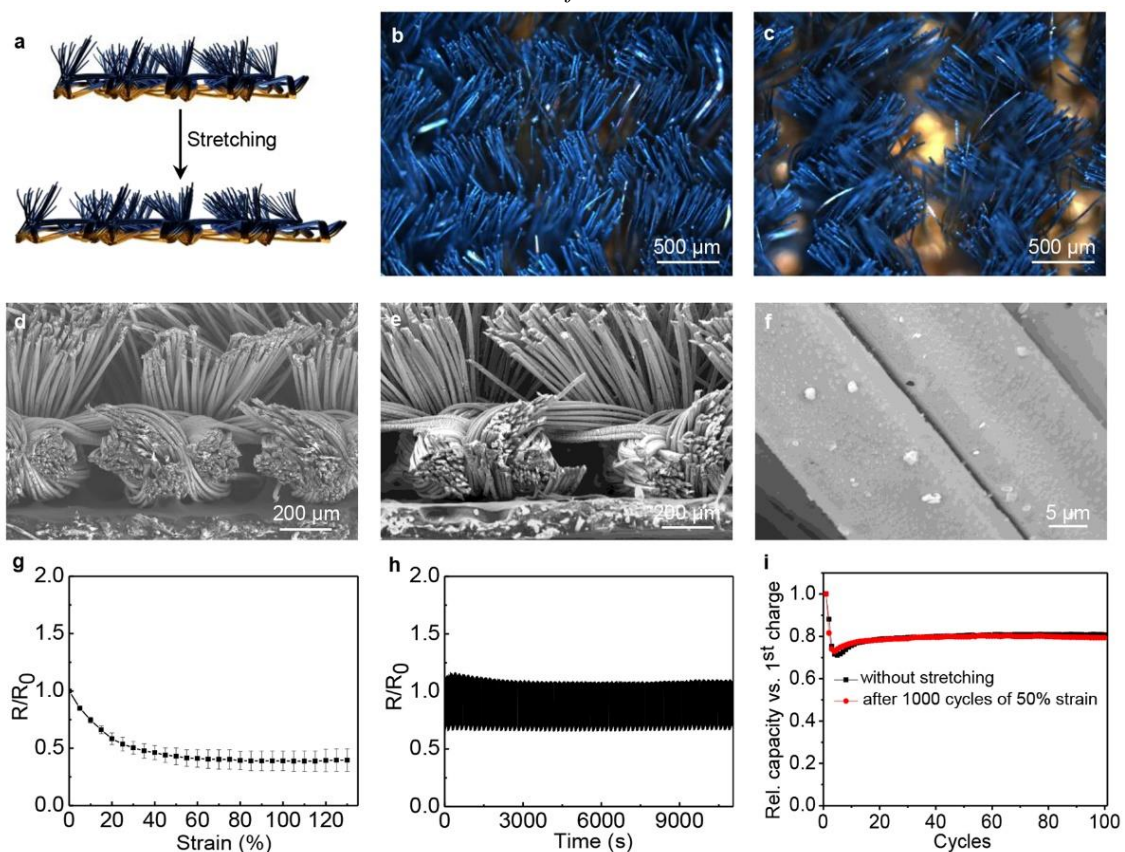


**Figure 4-4** Electrochemical performance of the velour fabric LIB electrode. a) CV curves of the velour fabric LIB electrode at 0.1 mV/s. b) Charge-discharge profiles and c) cycling ability of the velour fabric LIB electrode at 0.5 C (1 C = 560 mA/g) at 1.3-2.6 V. d) Rate capability of the velour fabric LIB electrode at sequential current rates.

The velour fabric LIB electrode exhibited excellent cycling stability, electrochemical reversibility, and rate capability. We assessed the charging-discharging cycling stability at 0.5 C (**Figure 4-4c**). The initial discharge capacity of 583 mAh/g, which was calculated based on the mass loading of CuS, is followed by a decrease and increase, indicating the activation process in the material.<sup>53,55</sup> After activation and stabilization, the electrode exhibited a specific capacity of ~400 mAh/g with no obvious sign of capacity decay for at least 300 cycles. The corresponding Coulombic efficiency was close to 100%, indicating excellent electrochemical reversibility during the charging and discharging process. The specific capacity of the velour fabric LIB electrode is comparable to the previously reported values (~440 mAh/g) for conventional CuS composite electrodes, which were also calculated based on the mass of CuS.<sup>56</sup> The velour fabric LIB electrode shows better cycling stability than that in previous reports, which have shown that CuS suffers from severe capacity decay in the charge-discharge process due to the dissolution of lithium polysulfides into the electrolyte and shuttling away from the electrode.<sup>56-58</sup> We hypothesize that the excellent cycling stability of the velour fabric LIB electrode may be due to favorable chemical interactions between the gold coating on the fabric and the polysulfides.<sup>59</sup> Future work, including a detailed spectroscopic analysis, will focus on a developing a full understanding of the improved cycling stability. The rate performance of the velour fabric LIB electrode at sequential current rates of 0.5 C, 1 C, 2 C, 3 C, and 0.5 C, respectively, is shown in **Figure 4-4d** and **Figure S4-5**. There is a negligible change in capacity and charge-discharge voltage plateau with the increase of current density, indicating excellent rate capability. Directly growing CuS on the Au-coated cut pile fibers, which are connected to the Au-coated framework, provides intimate and stable contact between CuS and the Au-coated framework current collector to facilitate the charge transfer process and enhance the rate capability. The porous structure of the velour fabric also may provide good accessibility of the electrolyte to CuS coating, thereby increasing the electroactive material/electrolyte contact area.

Stretching the velour fabric LIB electrode illustrates the island-bridge strain-engineering architecture. Stretching elongates the Au-coated framework “bridges”, while the CuS/Au-coated cut pile fiber “islands” simply ride along at their anchor points on the framework in the direction of stretching. The CuS/Au-coated cut pile fibers become

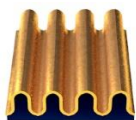

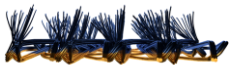
separated from each other with stretching, but they do not experience tensile stress (**Figure 4-5a**). Since the skin at a joint of the human body can stretch to ~50% strain with bending in the longitudinal direction, we used this maximum strain value to characterize the velour fabric electrode.<sup>60</sup> Optical microscope (**Figure 4-5b,c**) and SEM images (**Figure 4-5d,e**) at 0% and 50% strain show this separation of the CuS/Au fibres. High-magnification SEM image of the CuS/Au-coated cut pile fiber at 50% strain also showed no delamination or cracking of CuS coating, consistent with protection from strain (**Figure 4-5f**). Electrical and electrochemical performance metrics during stretching support the proposed functionality of the island-bridge architectural strain-engineering design. The Au-coated framework current collector acts as the “bridge” component of the architecture by remaining conductive as the loops unbend and tighten with strain. The resistance measured from the back side of the Au-coated framework current collector with strain in the course direction decreased to ~50% of the initial resistance at 30% strain and then remained stable to 130% strain (**Figure 4-5g**). The initial decrease in the resistance can be attributed to the increase in contact pressure between adjacent conductive yarns in the framework that occurs with tensile strain, which lowers the interfiber contact resistance. Similar to previous literature reports, the gold coating on spandex fibers developed cracks under strain due to the mechanical mismatch between gold and spandex (**Figure S4-6**).<sup>6</sup> The resistance also remained relatively stable during 1000 cycles of 0 to 50% strain (**Figure 4-5h**). The CuS/Au-coated cut pile fiber “islands” anchored to the Au-coated framework “bridges” exhibit stable electrochemical performance after repetitive stretching, consistent with protection from stress by the island-bridge design. The charge-discharge cycling stability of the velour fabric evaluated in a coin cell after 1000 cycles of stretching at 50% strain was indistinguishable from an unstretched electrode (**Figure 4-5i**).



**Figure 4-5** Electrical and electrochemical performance of the velour fabric LIB electrode with strain. a) Schematic of stretching the velour fabric LIB electrode. Optical microscope images of the front-side of the velour fabric LIB electrode b) unstretched and c) stretched under 50% strain. Cross-sectional SEM images of the velour fabric LIB electrode d) unstretched and e,f) stretched under 50% strain. g) Normalized change in resistance of the velour fabric LIB electrode as a function of stretching strain. h) Normalized change in resistance of the velour fabric LIB electrode during 1000 cycles of 0 to 50% strain. i) Relative capacity versus charging-discharging cycles of the velour fabric LIB electrode before (black line) and after 1000 stretching-releasing cycles at 50% strain (red line).

**Table 4-1** shows the unique strain-engineering architectural design of the velour fabric LIB electrode compared to those of stretchable LIB electrodes fabricated on elastomers. In the velour fabric LIB electrode, the island-bridge comes from the architectural features that are intrinsic to the textile substrate. In contrast, elastomer-based stretchable LIB electrodes impart stretchability by either modification of the elastomer substrate using prestrain, or using lithography to connect rigid LIBs with stretchable interconnects. Performance of all of these systems, however, is suitable for applications in wearable electronics, where the movement of the body typically do not exceed 50% strain.

**Table 4-1** Comparison of strain-engineering designs of stretchable LIB electrodes

Design	Substrate	Electrochemical Performance with Strain	Stretchability	Ref.
 wavy structure	elastomer	unchanged capacity after 500 stretching cycles at a strain of 400%	400%	[27]
 device-level island-bridge structure	elastomer	unchanged galvanostatic charge and discharge profile at 0% and 300% strain	300%	[31]
 electrode-level textile-based island-bridge structure	textile	unchanged charge-discharge cycling stability after 1000 cycles of stretching at 50% strain	130%	This work

### 4.3 Conclusions

Common, everyday fabrics contain built-in architectures that not only provide softness and stretchability to textiles, but also can form the basis for innovative architectural strain-engineering strategies to produce next-generation e-textiles. We have demonstrated that the strategic use of a warp-knitted velour fabric can solve the mechanical mismatch problem between brittle LIB materials and stretchable textiles to produce robust and stretchable textile-based LIB electrodes. The CuS/Au-coated cut pile fibers and Au-coated warp-knitted framework of the velour fabric form an island-bridge strain-engineering structure in which the CuS/Au-coated cut pile fibers are isolated from strain. This work is an important step toward stretchable textile-based LIBs since the battery electrode mainly determines the mechanical properties of the entire battery. Advancing from the stretchable velour fabric LIB electrode to fully stretchable and wearable LIBs will require further development of stretchable separators, solid electrolytes, and packing materials.

This textile-based island-bridge architecture is not exclusive to velour fabrics. These structures are also built into many different tufted fabrics, such as faux fur, plush, and velvet. These textiles comprise diverse materials, densities and lengths of the cut piles, and framework structures. The stable electrical and electrochemical performance of the velour fabric LIB electrode may thus be further improved not only by conventional optimization of the active materials to increase capacity but also by changing the structure of the fabric to increase the density of cut piles, thereby increasing the available surface area and loading of active materials. Furthermore, the great variety of textile structures provide many opportunities to use commonplace textiles as the basis for strain-engineering architectural designs to integrate different functional materials and enable a wide range of e-textile applications.

#### **4.4 Experimental**

*Materials:* Velour fabric was purchased from local textile store (Fabricland). APTES,  $\text{NiSO}_4 \cdot 6\text{H}_2\text{O}$ ,  $\text{Na}_4\text{P}_2\text{O}_7 \cdot 10\text{H}_2\text{O}$ ,  $\text{CuSO}_4 \cdot 5\text{H}_2\text{O}$ ,  $\text{KNaC}_4\text{H}_4\text{O}_6 \cdot 4\text{H}_2\text{O}$ , 37.2% HCHO, and dimethylamine borane were purchased from Sigma Aldrich. All chemicals were used as received. Immersion gold plating solution Gobright TAM-55 was purchased from Uyemura and used as directed by the manufacturer.

*Preparation of Gold-Coated Velour Fabric:* Velour fabric was sonicated in deionized water and isopropyl alcohol for 15 min each, and then exposed to air plasma for 10 min. The cleaned fabric was immersed in a 1% v/v solution of APTES in deionized water for 30 min, a Pd/Sn solution (prepared from Cataposit 44 and Cataprep 404 (Shipley) as directed by manufacturer) for 2 min, and aqueous 1 M NaOH for 1 min. Samples were rinsed with water in between steps. The fabric was then metallized in nickel ELD bath (0.08 M  $\text{NiSO}_4 \cdot 6\text{H}_2\text{O}$ , 0.14 M  $\text{Na}_4\text{P}_2\text{O}_7 \cdot 10\text{H}_2\text{O}$  and 0.07 M dimethylamine borane in water) for 10 min with sonication. After rinsing with water, the Ni-coated fabric was immersed in Au ELD bath (Gobright TAM-55, Uyemura) for 40 min.

*Deposition and Patterning of CuS on Velour Fabric:* Kapton tape was used as the mask to selectively block copper deposition. The gold-coated velour fabric was immersed in the copper ELD bath for 60 min which contains a 10:1 v : v mixture of freshly prepared solution A and B. Solution A consisted of 4.5 g/L  $\text{CuSO}_4 \cdot 5\text{H}_2\text{O}$ , 6.0 g/L NaOH, and 21.0



g/L  $\text{KNaC}_4\text{H}_4\text{O}_6 \cdot 4\text{H}_2\text{O}$ . Solution B was 37.2% HCHO in distilled water. The Au-coated velour fabric with Cu/Au-coated cut pile was then immersed in 100 mg/mL sulfur in carbon disulfide solution for 4 h at room temperature in ambient conditions to convert Cu to CuS. The fabricated velour fabric electrode was dried in vacuum oven at 70 °C overnight. The loading density of the CuS is  $\sim 1 \text{ mg/cm}^2$ , which was calculated based on the weight difference of a gold-coated velour fabric disk with a diameter of 16 mm before and after CuS deposition.

*Electrochemical Measurements:* The electrochemical properties of the velour fabric LIB electrode was tested in standard CR2032 coin cells that were assembled in an Ar-filled glovebox by directly using the velour fabric LIB electrode as the working electrode, a lithium foil as the counter electrode, Celgard 2400 film as the separator, and 1M lithium bis(trifluoromethane sulfonamide) (LiTFSI) in 1:1 v/v 1,3-dioxolane (DOL)/1,2-dimethoxyethane (DME) as the electrolyte. The cells were galvanostatically cycled between 1.3-2.6 V using a LAND battery testing system (CT2001A). Cyclic voltammograms were taken on an electrochemical workstation (Bio-logic) at a scan rate of 0.1 mV/s. All the reported potential values are given versus  $\text{Li}^0/\text{Li}^+$  and the rate is calculated by supposing the whole active material being reduced during the first charge.

*Characterization:* Optical microscopy was performed using an Olympus BX51 microscope equipped with an Olympus Q-Color3 digital camera. SEM images and EDX were taken on an FEI Quanta 200 Environmental SEM. XRD measurement was run on a PROTO AXRD powder diffractometer equipped with a Cu X-ray source, and a Mythen 1K silicon strip detector, operated at 30 kV and 20 mA. XRD patterns were obtained in the  $2\theta$  region from 25 to 80°. For electrical characterization under strain, samples were clamped in the microvice stretcher (S.T. Japan, USA, Inc.) and stretched manually in 5% increments while measuring the resistance using a Keithley 2601A Sourcemeter. A home-made auto-stretching stage was used for the cyclic stretching test.

#### 4.5 References

- [1] Zhao, Y.; Zhai, Q.; Dong, D.; An, T.; Gong, S.; Shi, Q.; Cheng, W. Highly Stretchable and Strain-Insensitive Fiber-Based Wearable Electrochemical Biosensor to Monitor Glucose in the Sweat. *Anal. Chem.* **2019**, *91*, 6569-6576.
- [2] Coppedè, N.; Tarabella, G.; Villani, M.; Calestani, D.; Iannotta, S.; Zappettini, A. Human Stress Monitoring through an Organic Cotton-Fiber Biosensor. *J. Mater. Chem. B* **2014**, *2*, 5620-5626.
- [3] Atalay, A.; Sanchez, V.; Atalay, O.; Vogt, D. M.; Haufe, F.; Wood, R. J.; Walsh, C. J. Batch Fabrication of Customizable Silicone-Textile Composite Capacitive Strain Sensors for Human Motion Tracking. *Adv. Mater. Technol.* **2017**, *2*, 1700136.
- [4] Liu, M.; Pu, X.; Jiang, C.; Liu, T.; Huang, X.; Chen, L.; Du, C.; Sun, J.; Hu, W.; Wang, Z. Large-Area All-Textile Pressure Sensors for Monitoring Human Motion and Physiological Signals. *Adv. Mater.* **2017**, *29*, 1703700.
- [5] Wang, L.; Wang, L. Y.; Zhang, Y.; Pan, J.; Li, S. Y.; Sun, X. M.; Zhang, B.; Peng, H. S. Weaving Sensing Fibers into Electrochemical Fabric for Real-Time Health Monitoring. *Adv. Funct. Mater.* **2018**, *28*, 1804456.
- [6] Wu, Y.; Mechael, S. S.; Lerma, C.; Carmichael, S. R.; Carmichael, T. B. Stretchable Ultrasheer Fabrics as Semitransparent Electrodes for Wearable Light-Emitting e-Textiles with Changeable Display Patterns. *Matter* **2020**, *2*, 882-895.
- [7] Zhang, Z.; Cui, L.; Shi, X.; Tian, X.; Wang, D.; Gu, C.; Chen, E.; Cheng, X.; Xu, Y.; Hu, Y.; Zhang, J.; Zhou, L.; Fong, H.; Ma, P.; Jiang, G.; Sun, X.; Zhang, B.; Peng, H. Textile Display for Electronic and Brain-Interfaced Communications. *Adv. Mater.* **2018**, *30*, 1800323.
- [8] Wu, Y.; Mechael, S. S.; Chen, Y.; Carmichael, T. B. Solution Deposition of Conformal Gold Coatings on Knitted Fabric for E-Textiles and Electroluminescent Clothing. *Adv. Mater. Technol.* **2018**, *3*, 1700292.
- [9] Zhang, Z.; Shi, X.; Lou, H.; Xu, Y.; Zhang, J.; Li, Y.; Cheng, X.; Peng, H. A Stretchable and Sensitive Light-Emitting Fabric. *J. Mater. Chem. C* **2017**, *5*, 4139-4144.

- [10] Hu, L. B.; Pasta, M.; La Mantia, F.; Cui, L. F.; Jeong, S.; Deshazer, H. D.; Choi, J. W.; Han, S. M.; Cui, Y. Stretchable, Porous, and Conductive Energy Textiles. *Nano Lett.* **2010**, *10*, 708-714.
- [11] Pu, X.; Liu, M. M.; Li, L. X.; Han, S. C.; Li, X. L.; Jiang, C. Y.; Du, C. H.; Luo, J. J.; Hu, W. G.; Wang, Z. L. Wearable Textile-Based In-Plane Microsupercapacitors. *Adv. Energy Mater.* **2016**, *6*, 1601254.
- [12] Yang, Y.; Huang, Q. Y.; Niu, L. Y.; Wang, D. R.; Yan, C.; She, Y. Y.; Zheng, Z. J. Waterproof, Ultrahigh Areal-Capacitance, Wearable Supercapacitor Fabrics. *Adv. Mater.* **2017**, *29*, 1606679.
- [13] Levitt, A.; Hegh, D.; Phillips, P.; Uzun, S.; Anayee, M.; Razal, J. M.; Gogotsi, Y.; Dion, G. 3D Knitted Energy Storage Textiles Using Mxene-Coated Yarns. *Mater. Today* **2020**, *34*, 17-29.
- [14] Xiong, J. Q.; Lee, P. S. Progress on Wearable Triboelectric Nanogenerators in Shapes of Fiber, Yarn, and Textile. *Sci. Technol. Adv. Mater.* **2019**, *20*, 837-857.
- [15] Pan, S. W.; Yang, Z. B.; Chen, P. N.; Deng, J.; Li, H. P.; Peng, H. S. Wearable Solar Cells by Stacking Textile Electrodes. *Angew. Chem. Int. Ed.* **2014**, *53*, 6110-6114.
- [16] Lee, S.; Lee, Y.; Park, J.; Choi, D. Stitchable Organic Photovoltaic Cells with Textile Electrodes. *Nano Energy* **2014**, *9*, 88-93.
- [17] Li, R.; Xiang, X.; Tong, X.; Zou, J. Y.; Li, Q. W. Wearable Double-Twisted Fibrous Perovskite Solar Cell. *Adv. Mater.* **2015**, *27*, 3831-3835.
- [18] Etacheri, V.; Marom, R.; Elazari, R.; Salitra, G.; Aurbach, D. Challenges in the Development of Advanced Li-Ion Batteries: A Review. *Energy Environ. Sci.* **2011**, *4*, 3243-3262.
- [19] Tu, F. Z.; Han, Y.; Du, Y. C.; Ge, X. F.; Weng, W. S.; Zhou, X. S.; Bao, J. C. Hierarchical Nanospheres Constructed by Ultrathin MoS<sub>2</sub> Nanosheets Braced on Nitrogen-Doped Carbon Polyhedra for Efficient Lithium and Sodium Storage. *ACS Appl. Mater. Interfaces* **2019**, *11*, 2112-2119.
- [20] Weng, W. S.; Xu, J. Y.; Lai, C. L.; Xu, Z. H.; Du, Y. C.; Lin, J.; Zhou, X. S. Uniform Yolk-Shell Fe<sub>7</sub>S<sub>8</sub>@C Nanoboxes as a General Host Material for the Efficient Storage of Alkali Metal Ions. *J. Alloys Compd.* **2020**, *817*, 152732.

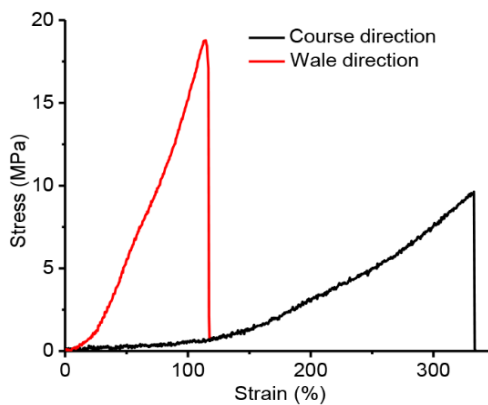
- [21] Nitta, N.; Wu, F. X.; Lee, J. T.; Yushin, G. Li-Ion Battery Materials: Present and Future. *Mater. Today* **2015**, *18*, 252-264.
- [22] Rogers, J. A.; Someya, T.; Huang, Y. Materials and Mechanics for Stretchable Electronics. *Science* **2010**, *327*, 1603-1607.
- [23] Khang, D.-Y.; Jiang, H.; Huang, Y.; Rogers, J. A. A Stretchable Form of Single-Crystal Silicon for High-Performance Electronics on Rubber Substrates. *Science* **2006**, *311*, 208-212.
- [24] Sun, Y.; Choi, W.; Jiang, H.; Huang, Y. Y.; Rogers, J. A. Controlled Buckling of Semiconductor Nanoribbons for Stretchable Electronics. *Nat. Nanotechnol.* **2006**, *1*, 201-207.
- [25] Michael, S. S.; Wu, Y.; Schlingman, K.; Carmichael, T. B. Stretchable Metal Films. *Flex. Print.* **2018**, *3*, 43001.
- [26] Kim, D.-H.; Song, J.; Choi, W.; Kim, H.-S.; Kim, R.-H.; Liu, Z.; Huang, Y. Y.; Hwang, K.-C.; Zhang, Y.-w.; Rogers, J. A. Materials and Noncoplanar Mesh Designs for Integrated Circuits with Linear Elastic Responses to Extreme Mechanical Deformations. *Proc. Natl. Acad. Sci. U.S.A.* **2008**, *105*, 18675-18680.
- [27] Weng, W.; Sun, Q.; Zhang, Y.; He, S.; Wu, Q.; Deng, J.; Fang, X.; Guan, G.; Ren, J.; Peng, H. A Gum-Like Lithium-Ion Battery Based on a Novel Arched Structure. *Adv. Mater.* **2015**, *27*, 1363-1369.
- [28] Liu, W.; Chen, J.; Chen, Z.; Liu, K.; Zhou, G.; Sun, Y.; Song, M. S.; Bao, Z.; Cui, Y. Stretchable Lithium-Ion Batteries Enabled by Device-Scaled Wavy Structure and Elastic-Sticky Separator. *Adv. Energy Mater.* **2017**, *7*, 1701076.
- [29] Gu, T.; Cao, Z.; Wei, B. All-Manganese-Based Binder-Free Stretchable Lithium-Ion Batteries. *Adv. Energy Mater.* **2017**, *7*, 1700369.
- [30] Yu, Y.; Luo, Y.; Wu, H.; Jiang, K.; Li, Q.; Fan, S.; Li, J.; Wang, J. Ultrastretchable Carbon Nanotube Composite Electrodes for Flexible Lithium-Ion Batteries. *Nanoscale* **2018**, *10*, 19972-19978.
- [31] Xu, S.; Zhang, Y.; Cho, J.; Lee, J.; Huang, X.; Jia, L.; Fan, J. A.; Su, Y.; Su, J.; Zhang, H.; Cheng, H.; Lu, B.; Yu, C.; Chuang, C.; Kim, T.-I. I.; Song, T.; Shigeta, K.; Kang, S.; Dagdeviren, C.; Petrov, I.; Braun, P. V.; Huang, Y.; Paik, U.; Rogers,

- J. A. Stretchable Batteries with Self-Similar Serpentine Interconnects and Integrated Wireless Recharging Systems. *Nat. Commun.* **2013**, *4*, 1543.
- [32] Yin, L.; Seo, J.; Kurniawan, J.; Kumar, R.; Lv, J.; Xie, L.; Liu, X.; Xu, S.; Meng, Y. S.; Wang, J. Highly Stable Battery Pack via Insulated, Reinforced, Buckling-Enabled Interconnect Array. *Small* **2018**, *14*, 1800938.
- [33] Wang, L.; Zhang, Y.; Pan, J.; Peng, H. S. Stretchable Lithium-Air Batteries for Wearable Electronics. *J. Mater. Chem. A* **2016**, *4*, 13419-13424.
- [34] Min, X.; Sun, B.; Chen, S.; Fang, M.; Wu, X.; Liu, Y. g.; Abdelkader, A.; Huang, Z.; Liu, T.; Xi, K.; Kumar, V. R. A Textile-Based SnO<sub>2</sub> Ultra-Flexible Electrode for Lithium-Ion Batteries. *Energy Storage Mater.* **2019**, *16*, 597-606.
- [35] Ha, S.; Shin, K.; Park, H.; Lee, Y. Flexible Lithium-Ion Batteries with High Areal Capacity Enabled by Smart Conductive Textiles. *Small* **2018**, *14*, 1703418.
- [36] Ma, K.; Liu, X.; Cheng, Q.; Saha, P.; Jiang, H.; Li, C. Flexible Textile Electrode with High Areal Capacity from Hierarchical V<sub>2</sub>O<sub>5</sub> Nanosheet Arrays. *J. Power Sources* **2017**, *357*, 71-76.
- [37] Balogun, M.-S.; Yu, M.; Huang, Y.; Li, C.; Fang, P.; Liu, Y.; Lu, X.; Tong, Y. Binder-Free Fe<sub>2</sub>N Nanoparticles on Carbon Textile with High Power Density as Novel Anode for High-Performance Flexible Lithium Ion Batteries. *Nano Energy* **2015**, *11*, 348-355.
- [38] Liu, B.; Zhang, J.; Wang, X.; Chen, G.; Chen, D.; Zhou, C.; Shen, G. Hierarchical Three-Dimensional ZnCo<sub>2</sub>O<sub>4</sub> Nanowire Arrays/Carbon Cloth Anodes for a Novel Class of High-Performance Flexible Lithium-Ion Batteries. *Nano Lett.* **2012**, *12*, 3005-3011.
- [39] Zhu, Y.; Yang, M.; Huang, Q.; Wang, D.; Yu, R.; Wang, J.; Zheng, Z.; Wang, D. V<sub>2</sub>O<sub>5</sub> Textile Cathodes with High Capacity and Stability for Flexible Lithium-Ion Batteries. *Adv. Mater.* **2020**, 1906205.
- [40] Lee, Y.-H.; Kim, J.-S.; Noh, J.; Lee, I.; Kim, H.; Choi, S.; Seo, J.; Jeon, S.; Kim, T.-S.; Lee, J.-Y.; Choi, J. Wearable Textile Battery Rechargeable by Solar Energy. *Nano Lett.* **2013**, *13*, 5753-5761.
- [41] Lee, K.; Choi, J.; Lee, H.; Kim, K.; Choi, J. Solution-Processed Metal Coating to Nonwoven Fabrics for Wearable Rechargeable Batteries. *Small* **2017**, *14*, 1703028.

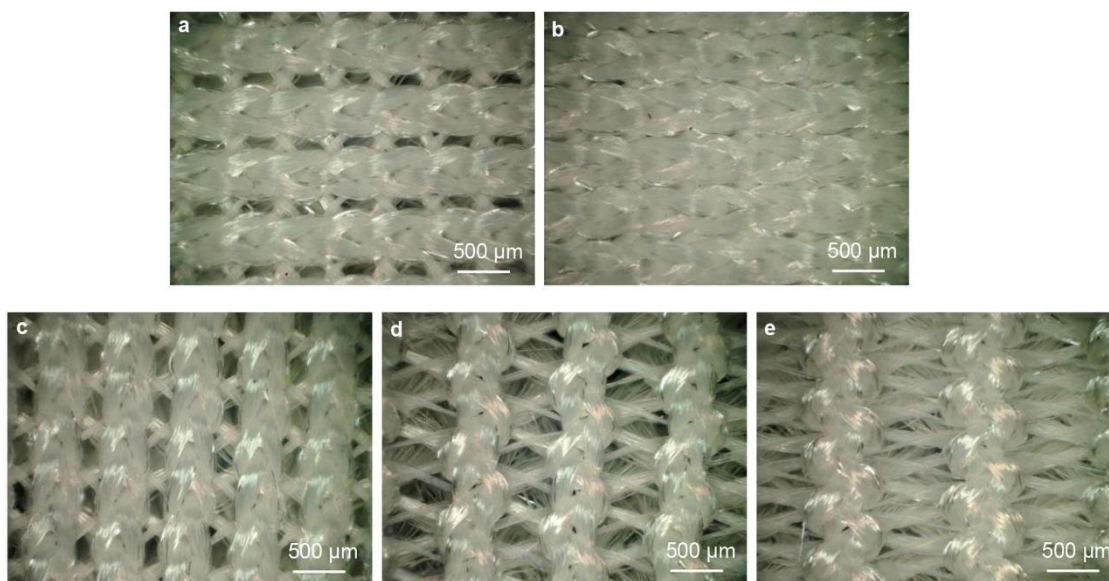
- [42] Kang, C.; Choi, J.; Ko, Y.-J.; Lee, S.; Kim, H.; Kim, J.; Son, S. Thin Coating of Microporous Organic Network Makes a Big Difference: Sustainability Issue of Ni Electrodes on the PET Textile for Flexible Lithium-Ion Batteries. *ACS Appl. Mater. Interfaces* **2017**, *9*, 36936-36943.
- [43] Ghadi, B.; Yuan, M.; Ardebili, H. Stretchable Fabric-Based LiCoO<sub>2</sub> Electrode for Lithium Ion Batteries. *Extreme Mech. Lett.* **2019**, *32*, 100532.
- [44] Chen, Y.; Wu, Y.; Mechael, S. S.; Carmichael, T. B. Heterogeneous Surface Orientation of Solution-Deposited Gold Films Enables Retention of Conductivity with High Strain-A New Strategy for Stretchable Electronics. *Chem. Mater.* **2019**, *31*, 1920-1927.
- [45] Liu, H.; Li, N.; Bi, S.; Li, D. Gold Immersion Deposition on Electroless Nickel Substrates Deposition Process and Influence Factor Analysis. *J. Electrochem. Soc.* **2007**, *154*, D662-D668.
- [46] Osaka, T.; Takematsu, H.; Nihei, K. A Study on Activation and Acceleration by Mixed PdCl<sub>2</sub>-SnCl<sub>2</sub> Catalysts for Electroless Metal-Deposition. *J. Electrochem. Soc.* **1980**, *127*, 1021-1029.
- [47] Miller, M. S.; Davidson, G. J. E.; Sahli, B. J.; Mailloux, C. M.; Carmichael, T. B. Fabrication of Elastomeric Wires by Selective Electroless Metallization of Poly(dimethylsiloxane). *Adv. Mater.* **2008**, *20*, 59-64.
- [48] Baum, T. H. Photochemically Generated Gold Catalyst for Selective Electroless Plating of Copper. *J. Electrochem. Soc.* **1990**, *137*, 252-255.
- [49] Lei, Y.; Jia, H.; Zheng, Z.; Gao, Y.; Chen, X.; Hou, H. A Very Facile, Low Temperature, One-Step Route to In Situ Fabricate Copper Sulfide Nanosheet Thin Films. *CrystEngComm* **2011**, *13*, 6212-6217.
- [50] Zhao, J.; Zhang, Y.; Wang, Y.; Li, H.; Peng, Y. The Application of Nanostructured Transition Metal Sulfides as Anodes for Lithium Ion Batteries. *J. Energy Chem.* **2018**, *27*, 1536-1554.
- [51] Lu, Y.; Li, B.; Zheng, S.; Xu, Y.; Xue, H.; Pang, H. Syntheses and Energy Storage Applications of M<sub>x</sub>S<sub>y</sub> (M = Cu, Ag, Au) and Their Composites: Rechargeable Batteries and Supercapacitors. *Adv. Funct. Mater.* **2017**, *27*, 1703949.

- [52] Jiang, K.; Chen, Z.; Meng, X. CuS and Cu<sub>2</sub>S as Cathode Materials for Lithium Batteries: A Review. *ChemElectroChem* **2019**, *6*, 2825-2840.
- [53] Chen, Y.; Li, J.; Lei, Z.; Huo, Y.; Yang, L.; Zeng, S.; Ding, H.; Qin, Y.; Jie, Y.; Huang, F.; Li, Q.; Zhu, J.; Cao, R.; Zhang, G.; Jiao, S.; Xu, D. Hollow CuS Nanoboxes as Li-Free Cathode for High-Rate and Long-Life Lithium Metal Batteries. *Adv. Energy Mater.* **2020**, *10*, 1903401.
- [54] Li, H.; Wang, Y.; Huang, J.; Zhang, Y.; Zhao, J. Microwave-Assisted Synthesis of CuS/Graphene Composite for Enhanced Lithium Storage Properties. *Electrochim. Acta.* **2017**, *225*, 443-451.
- [55] Du, Y.; Yin, Z.; Zhu, J.; Huang, X.; Wu, X.-J.; Zeng, Z.; Yan, Q.; Zhang, H. A General Method for the Large-Scale Synthesis of Uniform Ultrathin Metal Sulphide Nanocrystals. *Nat. Commun.* **2012**, *3*, 1177.
- [56] Kalimuldina, G.; Taniguchi, I. Electrochemical Properties of Stoichiometric CuS Coated on Carbon Fiber Paper and Cu Foil Current Collectors as Cathode Material for Lithium Batteries. *J. Mater. Chem. A* **2017**, *5*, 6937-6946.
- [57] Chen, Y.; Davoisne, C.; Tarascon, J.-M.; Guéry, C. Growth of Single-Crystal Copper Sulfide Thin Films via Electrodeposition in Ionic Liquid Media for Lithium Ion Batteries. *J. Mater. Chem.* **2012**, *22*, 5295.
- [58] Chung, J. S.; Sohn, H. J. Electrochemical Behaviors of CuS as a Cathode Material for Lithium Secondary Batteries. *J. Power Sources* **2002**, *108*, 226-231.
- [59] Fan, C.-Y.; Xiao, P.; Li, H.-H.; Wang, H.-F.; Zhang, L.-L.; Sun, H.-Z.; Wu, X.-L.; Xie, H.-M.; Zhang, J.-P. Nanoscale Polysulfides Reactors Achieved by Chemical Au-S Interaction: Improving the Performance of Li-S Batteries on the Electrode Level. *ACS Appl. Mater. Interfaces* **2015**, *7*, 27959-27967.
- [60] Kim, S.; Oh, K.; Bahk, J. Electrochemically Synthesized Polypyrrole and Cu-Plated Nylon/Spandex for Electrotherapeutic Pad Electrode. *J. Appl. Polym. Sci.* **2004**, *91*, 4064-4071.

## 4.6 Supporting Information

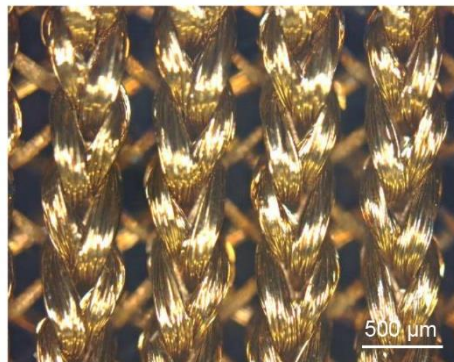


**Figure S4-1** Stress strain curve of the velour fabric in the wale (red line) and course (black line) direction.

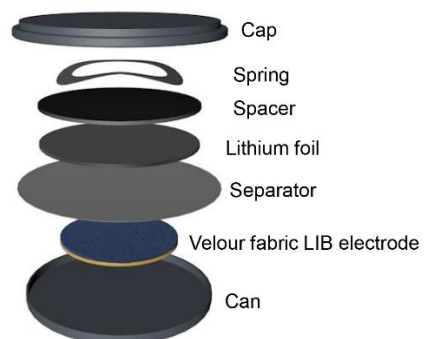


**Figure S4-2** Optical microscope images of the warp-knitted velour fabric stretched at a) 0% and b) 10% strain in the wale direction and at c) 0%, d) 50% and e) 100% strain in the course direction.

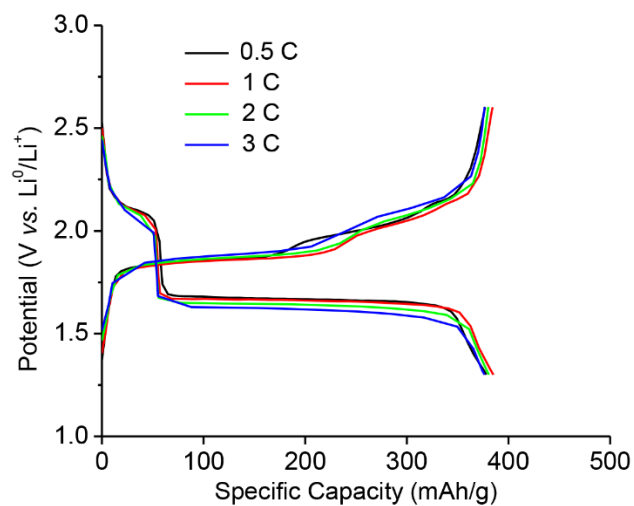




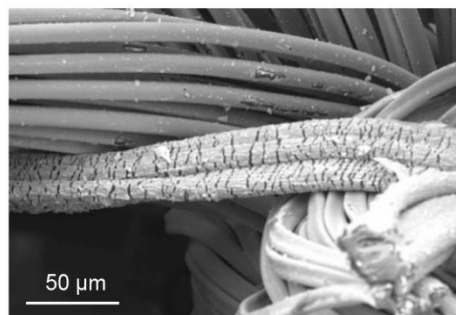
**Figure S4-3** Optical microscope image of the backside of the velour fabric LIB electrode.



**Figure S4-4** Schematic of the coin cell configuration.



**Figure S4-5** Charge-discharge profiles at various current rates.



**Figure S4-6** SEM image of velour fabric LIB electrode under 20% strain, showing the cracking of gold coating on spandex fiber.

**Chapter 5 Engineering the Cracking Patterns in Stretchable Copper Films Using  
Acid-Oxidized Poly(dimethylsiloxane) Substrates**

## **5.1 Introduction**

The new forms of electronics that can tolerate mechanical deformations, such as folding, twisting, and stretching, enable a range of innovative applications unachievable with traditional electronics technology, including skin-like epidermal health monitors,<sup>1-3</sup> soft biomedical interfaces and implantable circuitry,<sup>4-7</sup> large-area stretchable displays<sup>8-10</sup> and stretchable energy storage devices.<sup>11-13</sup> In the stretchable electronics system, stretchable conductors are fundamental and essential components that provide electrical connections between individual devices, contact other functional materials within devices as electrodes, or act as active sensing components based on electrical performance change with stimuli. Depositing metal films on the surface of a polydimethylsiloxane (PDMS) elastomeric substrate using physical vapor deposition (PVD) is one of the earliest approaches used to fabricate stretchable conductors; however, the substantial mechanical mismatch between the metal film and PDMS substrate often results in uncontrolled channel cracks of the metal film, causing a loss of conductivity at low (~20%) strains.<sup>14</sup> Since these early studies, efforts to successfully integrate metal films with elastomers have largely centered on strain-engineering designs that prevent the cracking of metal films. Configuring metal films into wavy structures, such as in-plane serpentes and meshes or out-of-plane wrinkles or arches,<sup>15</sup> convert stretching strains into less destructive bending strains by unbending of the curved structures with strain, preserving conductivity to as high as ~300% strain.<sup>16</sup> However, cracks in metal films are not necessarily bad and can be useful if they are rationally controlled. The resistance of cracked metal films is related to the cracking patterns. Long channel cracks can cut off the electrical flow, whereas microcracks that are not completely merged in metal films can still preserve electrical conductance through interconnected tortuous metal strips. The resistance change of metal films with strain can be manipulated by controlling the evolution of cracking patterns with strain, which can be used as indicators/transducers for different wearable electronics applications. For instance, metal films exhibiting a dramatic resistance change with strain can be used as sensitive strain sensors to monitor human motions with different strain ranges, whereas those with stable resistance with strain are suitable as interconnects or electrodes in stretchable electronic devices.

Creating topography on PDMS substrates has been demonstrated as an effective way to engineer the cracking patterns of metal films.<sup>17-23</sup> Uneven and rough surfaces induce an inhomogeneous stress field over metal films deposited on the PDMS surface, which can be used to manage crack initiation and propagation. Under tensile strain, cracks tend to initiate from “valleys” where the surface tensile stress is most concentrated.<sup>24</sup> Surfaces with randomly distributed and numerous valleys induce the initiation of numerous cracks to distribute strain relief across the metal film, limiting crack propagation and instead forming a reticular cracking pattern with multiple conducting pathways. Creating topography on PDMS by molding PDMS against the rough features of a topographical “master”<sup>17-22</sup> or depositing a microstructured polymeric layer on the surface of PDMS<sup>23</sup> have been used to create microtextured PDMS substrates to engineer cracking patterns in overlying metal films and modulate resistance change with strain. For example, Lambricht *et al.* reported producing rough PDMS substrates by curing PDMS prepolymer against sand-blasted masters fabricated with a range of roughness values.<sup>19</sup> PVD of a gold film onto the rough PDMS surface produced stretchable conductors that exhibited microcracking patterns with strain attributed to the PDMS topography. In this study, the PDMS substrates with the highest roughness created the most favorable microcracking patterns to preserve conductivity to high elongations (40% ~ 50% strain). In contrast, Zhao *et al.* also studied the stretchability of metal films on PDMS substrates with a range of surface roughness values and found that more roughness was not necessarily more beneficial for microcrack formation.<sup>21</sup> PDMS substrates with a range of surface roughness values were produced by curing PDMS prepolymers against sandpaper with different grit sizes. After coating these substrates with gold using PVD, measurements of resistance versus strain showed that the optimal roughness to generate the most favorable microcracking patterns for maximum preservation of electrical conductance was intermediate in the range of roughness values studied. These studies illustrate that although the roughness of the PDMS influences the cracking and resistance response, there is not yet a full understanding of the exact morphologies that give the most optimal cracking pattern in the overlying metal film to preserve conductivity.

Instead of requiring different masters for molding or adding in polymer layers, another method to create topography on PDMS is to alter the surface of a cured PDMS

substrate itself through chemical reaction using an oxidizing acid mixture treatment. Shih *et al.* first reported using an aqueous mixture of sulfuric acid and nitric acid to create a wrinkled topography on the surface of PDMS.<sup>25</sup> The two acids act synergistically to oxidize the methyl groups of PDMS, generating a thin stiff oxidation layer with polar groups on the PDMS surface. Water present in the acid mixture diffuses into the oxidation layer causing swelling, while the bottom of the PDMS substrate is confined to an underlying rigid substrate to restrict this portion from expanding. The difference in volumetric expansion between the stiff oxidation layer and confined elastic PDMS foundation results in compressive force acting on the stiff oxidized layer, causing wrinkling of the stiff oxidation layer. The wrinkles remain even after drying, which has been attributed to cross-linking of the silanol groups during the swelling state that fixes the wrinkled shape.<sup>26</sup> For wrinkles formed in a thin stiff layer on top of an elastic substrate due to the buckling instability, it is known that the wavelength of wrinkles can be expressed as equation (1),<sup>27</sup>

$$\lambda = 2\pi h_f \left( \frac{(1-\nu_f^2)E_f}{3(1-\nu_s^2)E_s} \right)^{1/3} \quad (1)$$

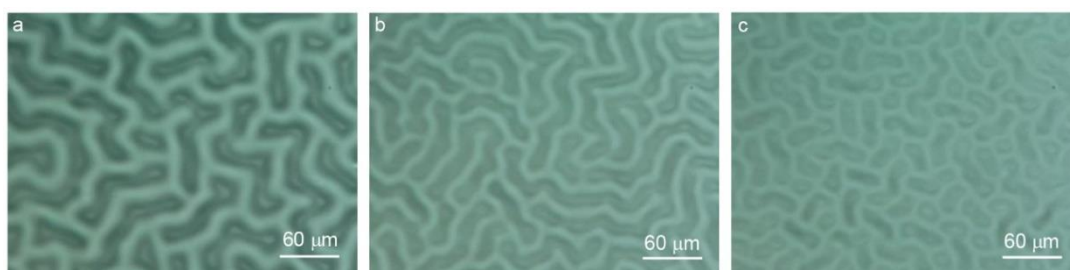
where  $h_f$ ,  $E_f$  and  $\nu_f$  is the thickness, Young's modulus, and Poisson ratio of the thin stiff film, respectively.  $E_s$  and  $\nu_s$  are the Young's modulus and Poisson ratio of the elastic substrate, respectively. According to equation (1), the wavelength of wrinkles can be adjusted by changing the thickness and/or the Young's modulus of the thin stiff layer. Wang *et al.* reported that the wavelength of acid-induced wrinkles decreased by either decreasing the exposure time of PDMS to the acid mixture or by decreasing the volume concentration of sulfuric acid in the acid mixture.<sup>28</sup> This dependence on sulfuric acid concentration indicates that sulfuric acid is the dominant reagent for PDMS oxidation, which is also supported by the fact that concentrated sulfuric acid can oxidize PDMS<sup>29</sup> while concentrated nitric acid has no chemical effect on the surface of PDMS.<sup>30</sup> Acid oxidation and swelling of PDMS also generates secondary fine features along with the wrinkles,<sup>28</sup> which have been attributed to roughening produced from the degradation of the PDMS polymer induced by oxidation.<sup>29</sup> Despite the intriguing hierarchical topography created by acid oxidation, PDMS bearing acid-induced topography has not been explored as substrates to engineer the cracking patterns of stretchable metal films.

Here, we report the use of acid-oxidized PDMS as a substrate to engineer cracking patterns in metal films for stretchable electronics. We use a fully solution-based method to fabricate stretchable metal films by metallization of acid-oxidized PDMS with copper using electroless deposition (ELD). By simply adjusting the composition of acid mixture to change the topography of PDMS, the cracking patterns of ELD copper films with strain can be tuned, which affects the resistance change of metal films. The ELD Cu films with an optimal cracking pattern on acid-treated PDMS retain conductivity to 85% strain with  $R/R_0$  less than 20.

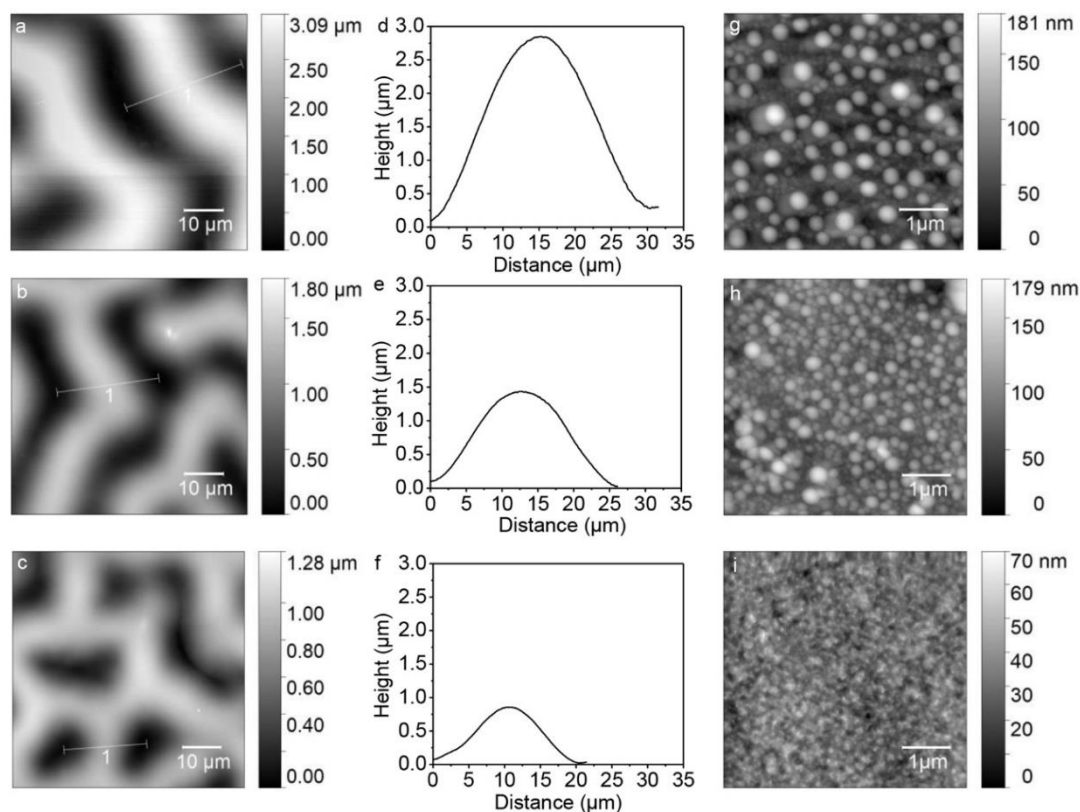
## 5.2 Results and Discussion

To study how the topographical morphology of acid-oxidized PDMS affects the cracking patterns of overlying metal films under strain, we produced three types of topographical features by using three aqueous acid compositions, which vary in the volume concentration of sulfuric acid and thus the oxidation activity. The three aqueous acid compositions were  $V_{\text{H}_2\text{SO}_4}:V_{\text{HNO}_3}:V_{\text{H}_2\text{O}} = 33:12:6$ ,  $33:18:6$ , and  $33:24:6$ , with corresponding volume concentration of sulfuric acid of 65%, 58%, and 52%, respectively. Treating PDMS with the three acid compositions for 1 min produced three PDMS structures referred to as ACID<sub>65</sub>/PDMS, ACID<sub>58</sub>/PDMS, and ACID<sub>52</sub>/PDMS. After acid treatment, labyrinth-like wrinkles formed on the surface of PDMS for all three structures (**Figure 5-1**, **Figure 5-2a-c**). Atomic force microscopy (AFM) profiles reveal that the wavelength and amplitude of the wrinkles on the three structures decreased with decreasing the volume concentration of sulfuric acid in the acid mixture, consistent with previous studies.<sup>28</sup> The acid mixture with the highest volume concentration of sulfuric acid (65%) produced wrinkles with the largest wavelength (30  $\mu\text{m}$ ) and amplitude (2.8  $\mu\text{m}$ ). Decreasing the volume concentration of sulfuric acid to 58% and 52% decreases the wrinkle wavelength to 25  $\mu\text{m}$  and 20  $\mu\text{m}$ , respectively, and the amplitude to 1.5  $\mu\text{m}$  and 0.85  $\mu\text{m}$ , respectively (**Figure 5-2d-f**). According to equation (1), the wrinkle wavelength is proportional to the thickness of the stiff layer and the Young's modulus of the thin stiff layer. Therefore, the decrease of wrinkle wavelength may indicate the decrease of the thickness and/or elastic modulus of the stiff oxidation layer. The acid-oxidized PDMS not only shows microscopic wrinkles but also secondary fine features as shown in high-magnification AFM images (**Figure 5-2g-i**). The fine features on ACID<sub>65</sub>/PDMS comprise spherical features of 100-300 nm in

diameter dispersed over the surface. On ACID<sub>58</sub>/PDMS, the spherical features are more densely packed on the surface and range widely in size with some as large as 300 nm to others <100 nm. ACID<sub>52</sub>/PDMS exhibits a different surface morphology with a fine texture and no discernable spherical features. These secondary fine features on the three types of substrates decrease in size with decreasing the volume concentration of sulfuric acid, thereby decreasing the root-mean-square roughness of the 5 μm × 5 μm acid-oxidized PDMS surface from 25 ± 3 nm for ACID<sub>65</sub>/PDMS to 21 ± 1 nm for ACID<sub>58</sub>/PDMS and 6.3 ± 0.5 nm for ACID<sub>52</sub>/PDMS.



**Figure 5-1** Optical microscope images of uncoated a) ACID<sub>65</sub>/PDMS, b) ACID<sub>58</sub>/PDMS, and c) ACID<sub>52</sub>/PDMS.



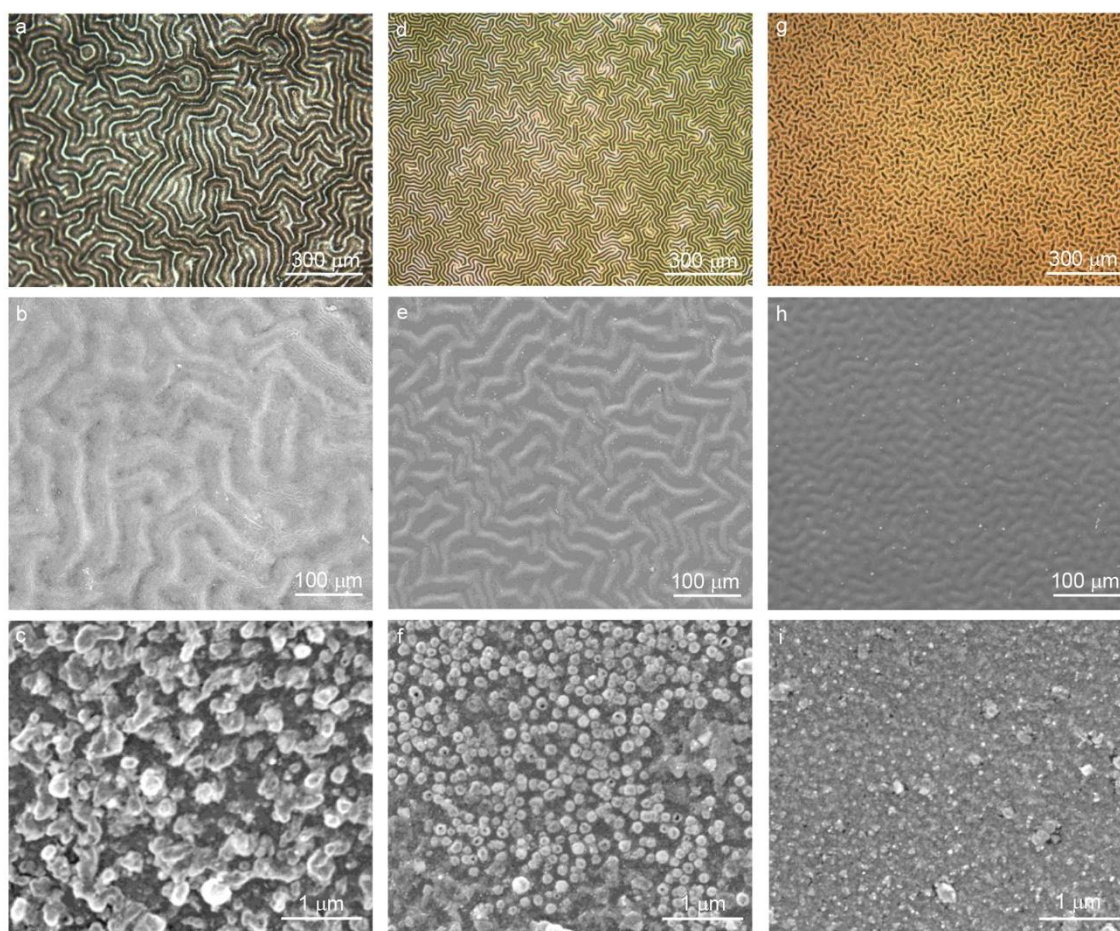
**Figure 5-2** AFM images (left), AFM profile (middle) and high-magnification AFM images (right) of uncoated a,d,g) ACID<sub>65</sub>/PDMS, b,e,h) ACID<sub>58</sub>/PDMS, and c,f,i) ACID<sub>52</sub>/PDMS.



The mechanical properties of the oxidation layers also showed changes corresponding to the volume concentration of sulfuric acid. We measured the crack onset strain to qualitatively evaluate the mechanical properties of oxidation layer on PDMS. Crack onset strain is the point where cracks are large enough to be detected by an optical microscope. We stretched acid-oxidized PDMS and collected optical microscope images at 10% strain increments. The crack onset strain increased according to decreasing sulfuric acid content in the acid mixture: ~20% for ACID<sub>65</sub>/PDMS (**Figure S5-1**), ~30% for ACID<sub>58</sub>/PDMS (**Figure S5-2**) and ~70% for ACID<sub>52</sub>/PDMS (**Figure S5-3**). This result is consistent with a less extensive oxidation process at lower volume concentrations of sulfuric acid. Considering the trend in wrinkle wavelengths of ACID<sub>65</sub>/PDMS > ACID<sub>58</sub>/PDMS > ACID<sub>52</sub>/PDMS, this finding is also consistent with the thickness and/or Young's modulus of the oxidation layers decreasing according to ACID<sub>65</sub>/PDMS > ACID<sub>58</sub>/PDMS > ACID<sub>52</sub>/PDMS. For all substrates, cracks rapidly propagate after the crack onset strain to form channel cracks with additional channel cracks forming to release strain energy. Overall, by changing the acid composition, the three types of oxidation layer on the surface of PDMS vary in the Young's modulus and/or thickness to produce different mechanical properties, wrinkle patterns, and secondary fine features.

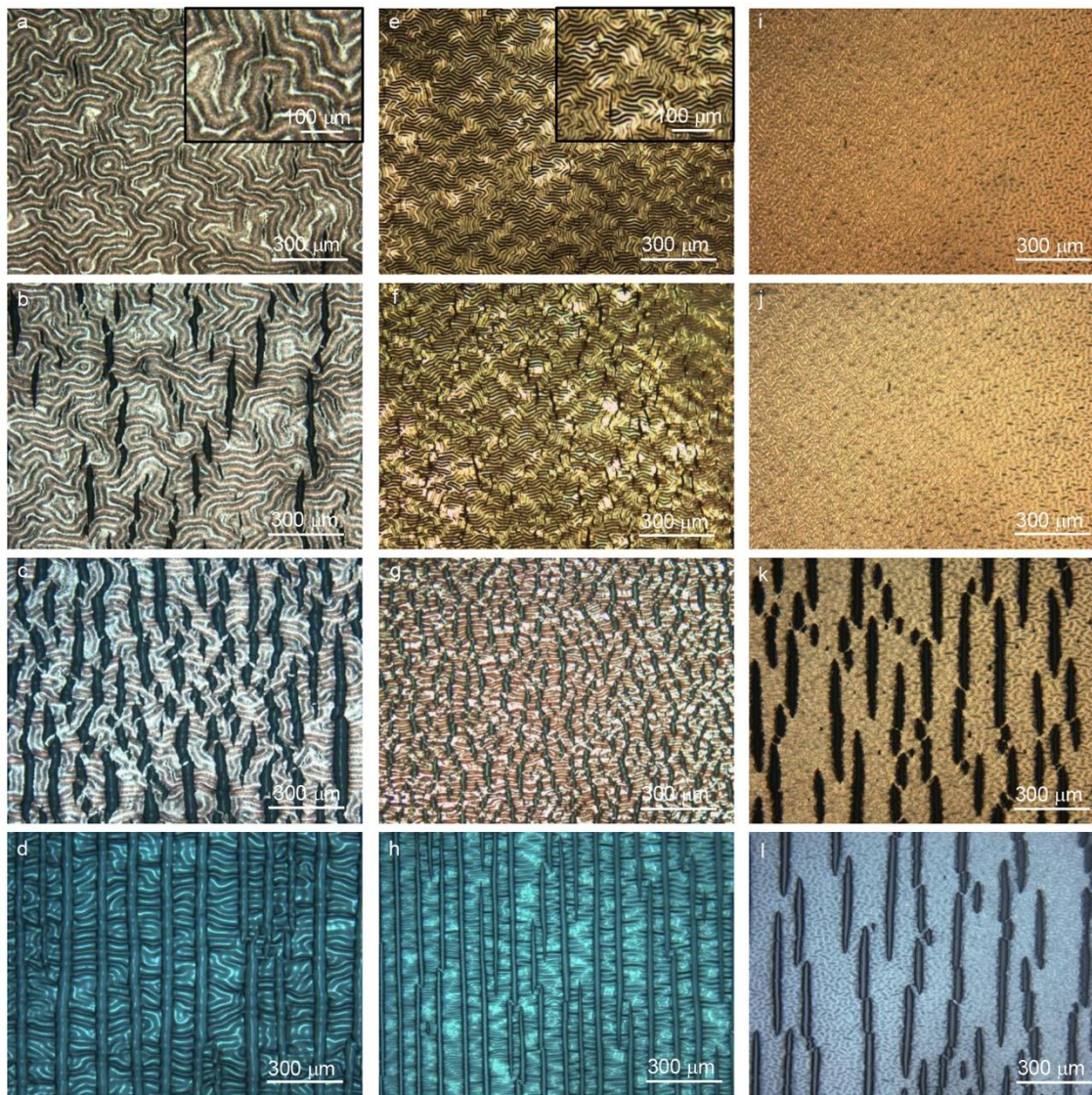
We used ELD to coat the surface of acid-oxidized PDMS with copper to study how the hierarchical topographies on acid-oxidized PDMS substrates affect the cracking patterns of the metal films and corresponding resistance changes with stretching. ELD is a solution-based method to deposit metal films conformally on different surface topographies and can be carried out at room temperature with little damage to the substrate. The ELD copper process involves first activating the acid-oxidized PDMS by adsorbing a catalytic species onto its surface. We used a palladium-tin colloidal catalyst, which consists of a palladium-rich core protected from oxidation by a hydrolyzed Sn<sup>2+</sup>/Sn<sup>4+</sup> shell, and an associated chloride layer that gives the colloids a negatively charged surface. Pd/Sn colloids can be bound electrostatically to positively-charged surfaces through a 3-aminopropyltriethoxysilane (APTES) linker, which we deposited onto the acid-oxidized PDMS surface from solution. Immersing the resulting amine-functionalized PDMS in the acidic Pd/Sn solution protonates the amino groups of the bound APTES; the resulting positively-charged ammonium groups electrostatically bind the negatively charged Pd/Sn

colloids. Subsequent etching in aqueous HCl removes the Sn shell to expose the Pd core, which initiates ELD by catalyzing the reduction of  $\text{Cu}^{2+}$  ions in the ELD plating solution to copper on the surface of the acid-oxidized PDMS. Subsequently, an autocatalytic reaction forms a continuous copper film by consuming the formaldehyde reducing agent in the copper ELD solution. This process deposited conformal copper coatings on the surface of acid-oxidized PDMS with the preservation of both the wrinkled morphology and secondary fine features (**Figure 5-3**). The average sheet resistance of Cu film on ACID<sub>65</sub>/PDMS, ACID<sub>58</sub>/PDMS and ACID<sub>52</sub>/PDMS is  $1.27 \pm 0.24 \text{ } \Omega/\text{sq}$ ,  $1.19 \pm 0.32 \text{ } \Omega/\text{sq}$ , and  $1.18 \pm 0.36 \text{ } \Omega/\text{sq}$ , respectively.

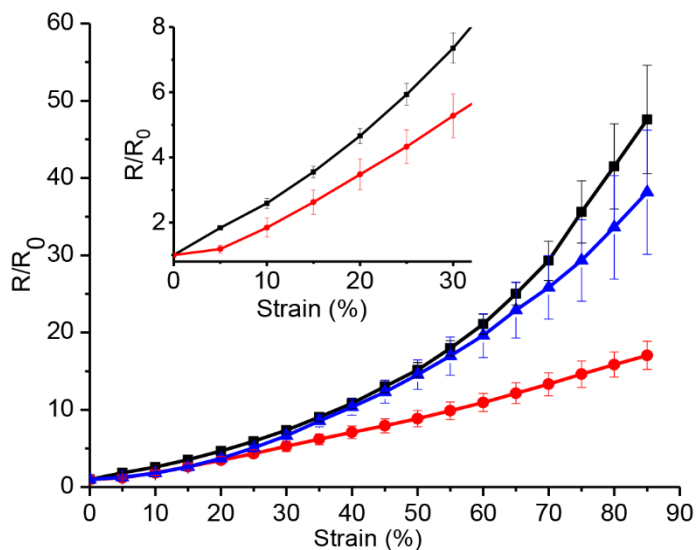


**Figure 5-3** Optical microscope images (top), SEM images (middle) and high-magnification SEM images (bottom) of the copper film on a-c) ACID<sub>65</sub>/PDMS, d-f) ACID<sub>58</sub>/PDMS, and g-i) ACID<sub>52</sub>/PDMS.

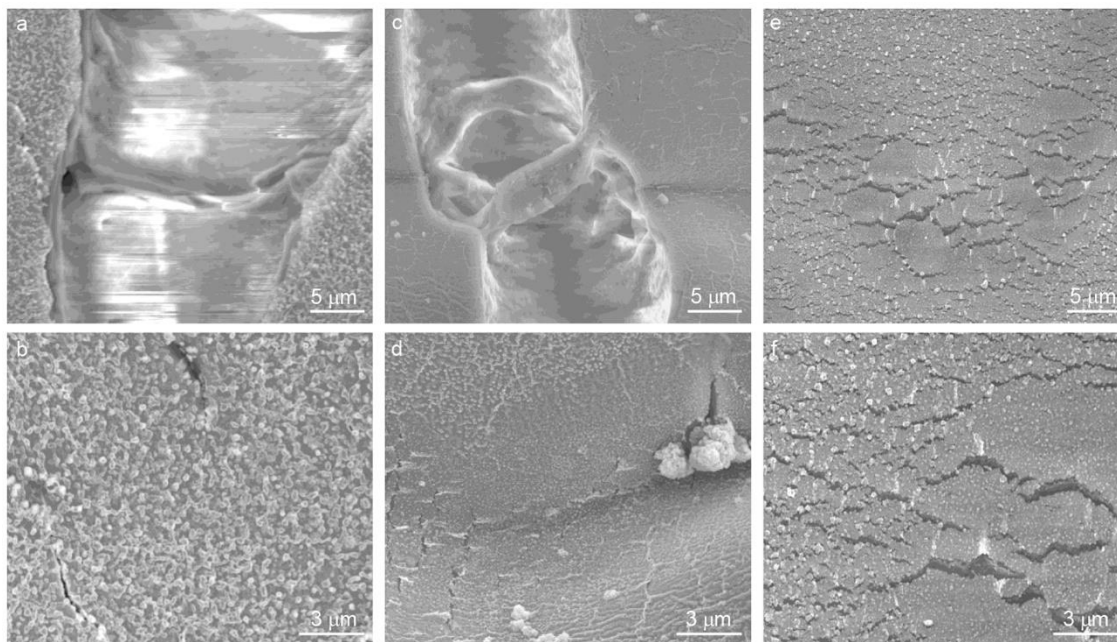
The oxidation layer on PDMS surface induced by acid mixture not only facilitates the ELD process, but profoundly changes the cracking patterns and resistance of metal films under strain. For copper films on ACID<sub>65</sub>/PDMS, at low strain of 10%, cracks are initially microscale in size (~110 μm long and 10 μm wide) and remain confined to the wrinkle valley regions (**Figure 5-4a** and inset). At 20% strain, the microcracks widen and lengthen to relieve strain, forming jagged cracks ~40 μm in width (**Figure 5-4b**). At 80% strain, the cracks become longer, wider (as wide as ~60 μm) and also more numerous, decreasing the width of copper strips between adjacent cracks (**Figure 5-4c**). This progressive evolution of initial microscale cracks to wider cracks with narrower copper strips resulted in the increase of resistance of the copper film (**Figure 5-5**). Even though the cracks are large, they have not channeled all the way through the film. Instead, the cracks create a tortuous, interconnected pattern of copper strips that provides conductive pathways to preserve electrical conductance to 85% strain. Current flow is broken after 85% strain where the acid-treated PDMS substrate fractures. The disconnected reticular microcracks that form in copper films on ACID<sub>65</sub>/PDMS are different from the channel cracks that form in the oxidation layer of acid-oxidized PDMS without the overlying metal film (**Figure 5-4c,d** and **Figure S5-4**). SEM images show that during stretching even at low strains, cracks in the copper film penetrate through the copper film/substrate interface into the ACID<sub>65</sub>/PDMS surface (**Figure 5-6a**), relieving the strain in the oxidized layer of the substrate. This crack penetration is similar to that observed in previous studies of metal films on elastomers under strain.<sup>31-33</sup> Since these metal-induced cracks relieve the strain, there is no need for further strain relief in the oxidation layer of ACID<sub>65</sub>/PDMS via the formation of channel cracks.



**Figure 5-4** Optical microscope images showing the evolution of cracks of the Cu film on a-c) ACID<sub>65</sub>/PDMS, e-g) ACID<sub>58</sub>/PDMS, and i-k) ACID<sub>52</sub>/PDMS at 10% (first row), 20% (second row), and 80% (third row) strain. Optical microscope images of uncoated d) ACID<sub>65</sub>/PDMS, h) ACID<sub>58</sub>/PDMS, and l) ACID<sub>52</sub>/PDMS at 80% strain. All the samples were stretched in the horizontal direction.



**Figure 5-5** Plot of normalized resistance as a function of strain for copper films on ACID<sub>65</sub>/PDMS (blue triangles), ACID<sub>58</sub>/PDMS (red circles), and ACID<sub>52</sub>/PDMS (black squares). Inset: plot of normalized resistance as a function of strain from 0% to 30% for copper films on ACID<sub>58</sub>/PDMS (red circles) and ACID<sub>52</sub>/PDMS (black squares).



**Figure 5-6** SEM images of the copper film at 20% strain on a,b) ACID<sub>65</sub>/PDMS, c,d) ACID<sub>58</sub>/PDMS and e,f) ACID<sub>52</sub>/PDMS.

For the copper film on ACID<sub>58</sub>/PDMS under strain, the crack initiation and propagation processes are similar to those of metal films on ACID<sub>65</sub>/PDMS, but both the dimensions and number of the generated cracks are remarkably different (**Figure 5-4e-g**). At 10% strain, there are microscale cracks similar to those on ACID<sub>65</sub>/PDMS. They appear to be more numerous and largely confined to the valleys of wrinkles although some propagate through wrinkle peaks (**Figure 5-4e** and inset). At 20% strain, cracks evolve to form a fine cracking pattern comprising numerous small, jagged cracks that vary in length and width, but remain < ~100  $\mu\text{m}$  in length and < ~20  $\mu\text{m}$  in width. At 80% strain, the fine cracking pattern evolves to form wider cracks to relieve strain (maximum width of ~50  $\mu\text{m}$ ) but do not appreciably lengthen, preserving a cracking pattern where the copper strips are highly interconnected (**Figure 5-4g**). The formation of this highly interconnected copper film contributes to a smaller resistance change with strain compared to that of ACID<sub>65</sub>/PDMS (**Figure 5-5**). Although copper films on ACID<sub>65</sub>/PDMS also retain interconnections that preserve conductivity, comparing **Figure 5-4c** and **Figure 5-4g** shows that copper films on ACID<sub>58</sub>/PDMS preserve a greater number of interconnections providing more pathways for current flow. The numerous small cracks generated in copper films on ACID<sub>58</sub>/PDMS may be due to the smaller wrinkle wavelength and secondary fine features of the ACID<sub>58</sub>/PDMS compared to that of ACID<sub>65</sub>/PDMS, which provide numerous potential sites for crack nucleation. Initiation of cracks at these sites can lead to numerous incipient cracks that distribute strain relief and limit crack propagation. It is important to note that similar to ACID<sub>65</sub>/PDMS, the cracking pattern of metal films on ACID<sub>58</sub>/PDMS is completely different from the channel cracks that form in the oxidation layer of the substrate without a metal coating (**Figure 5-4g,h**). SEM images show the similar penetration of cracks through the copper film/substrate interface into the ACID<sub>58</sub>/PDMS surface (**Figure 5-6c**) that relieves the strain in the oxidation layer, preventing the formation of channel cracks.

Copper films deposited on ACID<sub>52</sub>/PDMS form distinctly different cracking pattern with strain compared to copper films on ACID<sub>65</sub>/PDMS and ACID<sub>58</sub>/PDMS. The cracks that form in copper films on ACID<sub>52</sub>/PDMS at 10% and 20% strain are too small to be visible in the optical microscope images (**Figure 5-4i,j**). High-magnification SEM images at 20% strain reveal a very fine pattern of numerous nanoscale cracks that vary in size

depending on their location on the wrinkled topography (**Figure 5-6e,f**), with larger cracks (~850 nm at the widest point) occurring in the valleys of the wrinkles and smaller cracks (< ~300 nm in width) distributed over the wrinkle peaks. This pattern of nanoscale cracking at low strains is unique to copper films on ACID<sub>52</sub>/PDMS and does not appear in copper films on ACID<sub>65</sub>/PDMS and ACID<sub>58</sub>/PDMS (**Figure 5-6b,d**). Although SEM images of these films reveal a few small nanoscale cracks, the nanocracks in copper films on ACID<sub>52</sub>/PDMS are much more numerous, indicating the subtle topography of ACID<sub>52</sub>/PDMS is sufficient to initiate distributed nanocracks for strain relief in the copper film. At 80% strain, the copper film on ACID<sub>52</sub>/PDMS shows dramatic large cracks strikingly similar to the channel cracks that form in an uncoated ACID<sub>52</sub>/PDMS under strain (**Figure 5-4k,l**). This surprising result indicates that in copper-coated ACID<sub>52</sub>/PDMS, the nanoscale cracking pattern in the copper film is not sufficient to relieve strain in the oxidation layer on the substrate. Additional strain relief of the substrate in the form of channel cracking thus occurs and transfers to the overlying copper film.

The resistance change with strain that corresponds to the complex cracking pattern of copper films on ACID<sub>52</sub>/PDMS is larger than that of copper films on ACID<sub>58</sub>/PDMS (**Figure 5-5** inset), even at low strains before the onset of channel cracks, where the copper films show smaller but more numerous cracks (**Figure 5-6e,f**). This result indicates that the size and number of cracks have an optimal range for maximum retention of electrical conductance. On both ACID<sub>52</sub>/PDMS and ACID<sub>58</sub>/PDMS, cracks that form in the copper film distribute strain relief and preserve interconnections between the copper strips to retain conductive pathways through the film. The difference between the two is likely the size and number of the copper interconnections that are retained. At low strains (< 30%), copper films on ACID<sub>52</sub>/PDMS preserve narrow, even nanoscale interconnections owing to the numerous nanoscale cracks, which increase the resistance more than the wider interconnections preserved in copper films on ACID<sub>58</sub>/PDMS. At higher strains (> 50%), the channel cracks induced by the substrate amplify the resistance increase further.

### 5.3 Conclusions

In conclusion, we have demonstrated the engineering of cracking patterns of solution-deposited copper films using topography produced from acid oxidation of PDMS. The cracking patterns were greatly affected by the topographical features as well as the

mechanical properties of the surface of the acid-oxidized PDMS. The correlation of resistance change with cracking patterns of copper film reveal that there is an optimal cracking pattern for maximum retention of electrical conductance. A full understanding of the attributes of this cracking pattern and the factors that induce optimal patterns will require a detailed study comprising both experimental and theoretical work. Experimentally, determining the nanomechanical properties of the oxidation layers of acid-oxidized PDMS substrates will provide key data to mechanically model these systems and provide information about the stress distribution. Electrical modelling based on equivalent circuits of cracked metal films is potentially a powerful way to understand and predict optimal cracking patterns to access desired resistance changes with strain.

#### **5.4 Experimental**

All chemicals were purchased commercially and used as received.

*Preparation of PDMS substrates:* PDMS (Dow Corning Sylgard 184) was prepared by mixing elastomer base with curing agent in a 10:1 w:w ratio, followed by degassing under vacuum. The prepolymer mixture was cured at 60 °C overnight in a polystyrene Petri dish.

*Preparation of the Acid Mixture Solution:* Three types of aqueous acid mixtures were prepared by mixing concentrated sulfuric acid, concentrated nitric acid, and distilled water in the ratio of 33: 12: 6, 33: 18: 6 and 33: 24: 6 by volume, respectively. The acid mixtures were stirred in a container that was loosely capped at room temperature for ~1 h until the temperature of the solution decreased to room temperature.

*Acid Oxidation of PDMS Substrates:* A PDMS substrate was cut into rectangular pieces (15 mm × 30 mm × 1 mm), attached to a glass slide via Van der Waals' force, and then immersed into the as-prepared acid solution for 1 min. The sample was then removed from the acid solution and rinsed immediately with distilled water, and then dried in a vacuum desiccator overnight.

*Copper Metallization of PDMS:* The acid-oxidized PDMS substrates were immersed in a 1% APTES solution for 30 min, a Pd/Sn solution (prepared from Cataposit 44 and Cataprep 404 (Shipley) as directed by manufacturer) for 2 min, accelerator solution (6 M HCl) for 1 min, and then metalized in the copper ELD solution for 5-8 min. The copper ELD solution



contains a 10:1 v:v mixture of freshly prepared solution A and B. Solution A consisted of 4.5 g/L  $\text{CuSO}_4 \cdot 5\text{H}_2\text{O}$ , 6.0 g/L NaOH, 21.0 g/L  $\text{KNaC}_4\text{H}_4\text{O}_6 \cdot 4\text{H}_2\text{O}$ . Solution B was 37.2% HCHO in distilled water. Samples were dried using a stream of nitrogen after every step.

*Characterization:* An Olympus BX51 microscope equipped with an Olympus Q-Color3 digital camera, a Digital Instruments Multimode AFM and an FEI Quanta 200 FEG SEM were used to observe the surface morphologies of samples. AFM images were obtained using multimode digital AFM in tapping mode. To determine the linear strain at electrical failure, a Keithley 2601A Sourcemeter was used to measure the resistance under strain by contacting drops of gallium-indium eutectic placed at each of the copper films. Samples were clamped in a micro-vice stretcher (S.T. Japan, USA, Inc.) and stretched manually in 5% increments while monitoring the conductivity until they became non-conductive.

## 5.5 References

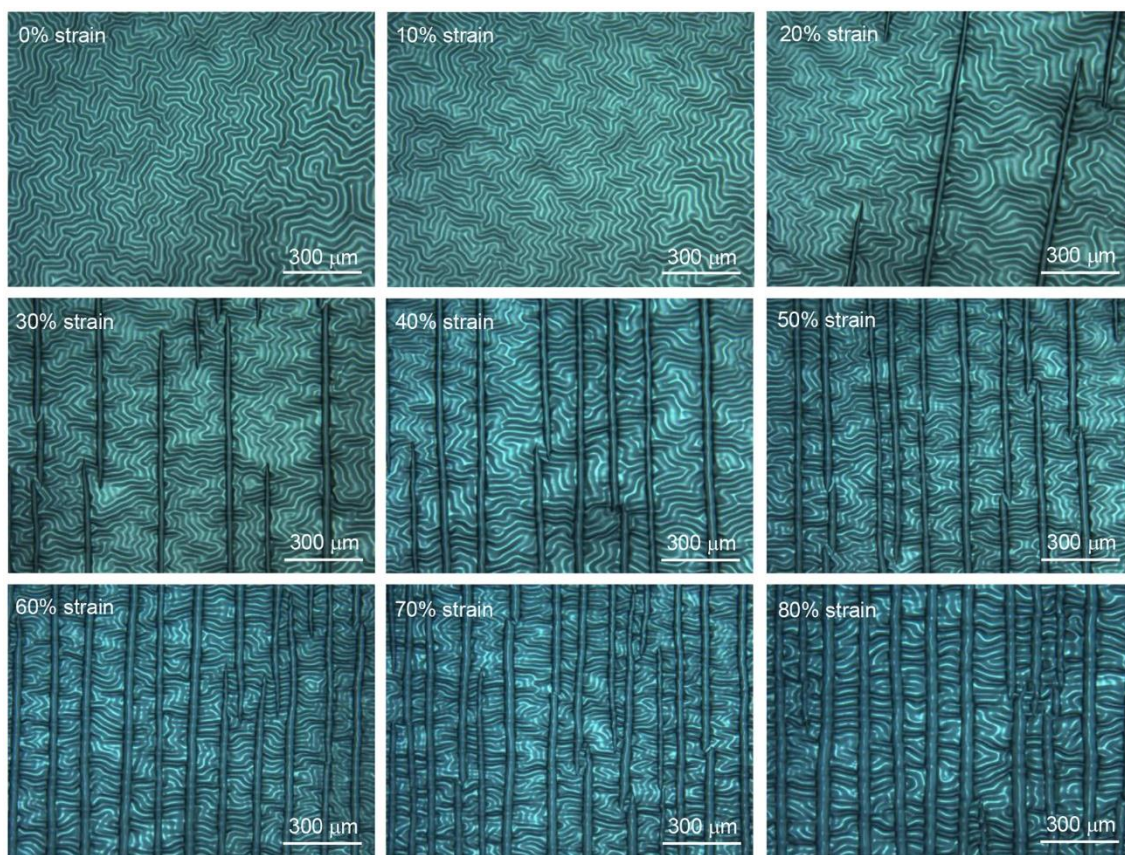
- [1] Liu, Y.; Pharr, M.; Salvatore, G. A Lab-on-Skin: A Review of Flexible and Stretchable Electronics for Wearable Health Monitoring. *ACS Nano* **2017**, *11*, 9614-9635.
- [2] Zhou, W.; Yao, S.; Wang, H.; Du, Q.; Ma, Y.; Zhu, Y. Gas-Permeable, Ultrathin, Stretchable Epidermal Electronics with Porous Electrodes. *ACS Nano* **2020**, *14*, 5798-5805.
- [3] Kim, D.-H.; Lu, N.; Ma, R.; Kim, Y.-S.; Kim, R.-H.; Wang, S.; Wu, J.; Won, S.; Tao, H.; Islam, A.; Yu, K.; Kim, T.-i.; Chowdhury, R.; Ying, M.; Xu, L.; Li, M.; Chung, H.-J.; Keum, H.; McCormick, M.; Liu, P.; Zhang, Y.-W.; Omenetto, F. G.; Huang, Y.; Coleman, T.; Rogers, J. A. Epidermal Electronics. *Science* **2011**, *333*, 838-843.
- [4] Mineev, I. R.; Musienko, P.; Hirsch, A.; Barraud, Q.; Wenger, N.; Moraud, E.; Gandar, J.; Capogrosso, M.; Milekovic, T.; Asboth, L.; Torres, R.; Vachicouras, N.; Liu, Q.; Pavlova, N.; Duis, S.; Larmagnac, A.; Vörös, J.; Micera, S.; Suo, Z.; Courtine, G.; Lacour, S. P. Electronic Dura Mater for Long-Term Multimodal Neural Interfaces. *Science* **2015**, *347*, 159-163.
- [5] Xu, L.; Gutbrod, S. R.; Ma, Y.; Petrossians, A.; Liu, Y.; Webb, C. R.; Fan, J. A.; Yang, Z.; Xu, R.; Whalen, J. J.; Weiland, J. D.; Huang, Y.; Efimov, I. R.; Rogers,

- J. A. Materials and Fractal Designs for 3D Multifunctional Integumentary Membranes with Capabilities in Cardiac Electrotherapy. *Adv. Mater.* **2015**, *27*, 1731-1737.
- [6] Lacour, S. P.; Courtine, G.; Guck, J. Materials and Technologies for Soft Implantable Neuroprostheses. *Nat. Rev. Mater.* **2016**, *1*, 16063.
- [7] Kim, D.-H.; Lu, N.; Ghaffari, R.; Kim, Y.-S.; Lee, S. P.; Xu, L.; Wu, J.; Kim, R.-H.; Song, J.; Liu, Z.; Viventi, J.; de Graff, B.; Elolampi, B.; Mansour, M.; Slepian, M. J.; Hwang, S.; Moss, J. D.; Won, S.-M.; Huang, Y.; Litt, B.; Rogers, J. A. Materials for Multifunctional Balloon Catheters with Capabilities in Cardiac Electrophysiological Mapping and Ablation Therapy. *Nat. Mater.* **2011**, *10*, 316-323.
- [8] Sekitani, T.; Nakajima, H.; Maeda, H.; Fukushima, T.; Aida, T.; Hata, K.; Someya, T. Stretchable Active-Matrix Organic Light-Emitting Diode Display Using Printable Elastic Conductors. *Nat. Mater.* **2009**, *8*, 494-499.
- [9] Filiatrault, H. L.; Porteous, G. C.; Carmichael, S. R.; Davidson, G. J. E.; Carmichael, T. B. Stretchable Light-Emitting Electrochemical Cells Using an Elastomeric Emissive Material. *Adv. Mater.* **2012**, *24*, 2673-2678.
- [10] Wang, J.; Yan, C.; Cai, G.; Cui, M.; Eh, A.; Lee, P. Extremely Stretchable Electroluminescent Devices with Ionic Conductors. *Adv. Mater.* **2016**, *28*, 4490-4496.
- [11] An, T. C.; Cheng, W. L. Recent Progress in Stretchable Supercapacitors. *J. Mater. Chem. A* **2018**, *6*, 15478-15494.
- [12] Song, W. J.; Yoo, S.; Song, G.; Lee, S.; Kong, M.; Rim, J.; Jeong, U.; Park, S. Recent Progress in Stretchable Batteries for Wearable Electronics. *Batteries Supercaps* **2019**, *2*, 181-199.
- [13] Liu, W.; Song, M. S.; Kong, B.; Cui, Y. Flexible and Stretchable Energy Storage: Recent Advances and Future Perspectives. *Adv. Mater.* **2017**, *29*, 1603436.
- [14] Lacour, S.; Wagner, S.; Huang, Z.; Suo, Z. Stretchable Gold Conductors on Elastomeric Substrates. *Appl. Phys. Lett.* **2003**, *82*, 2404-2406.
- [15] Michael, S. S.; Wu, Y.; Schlingman, K.; Carmichael, T. B. Stretchable Metal Films. *Flex. Print.* **2018**, *3*, 43001.

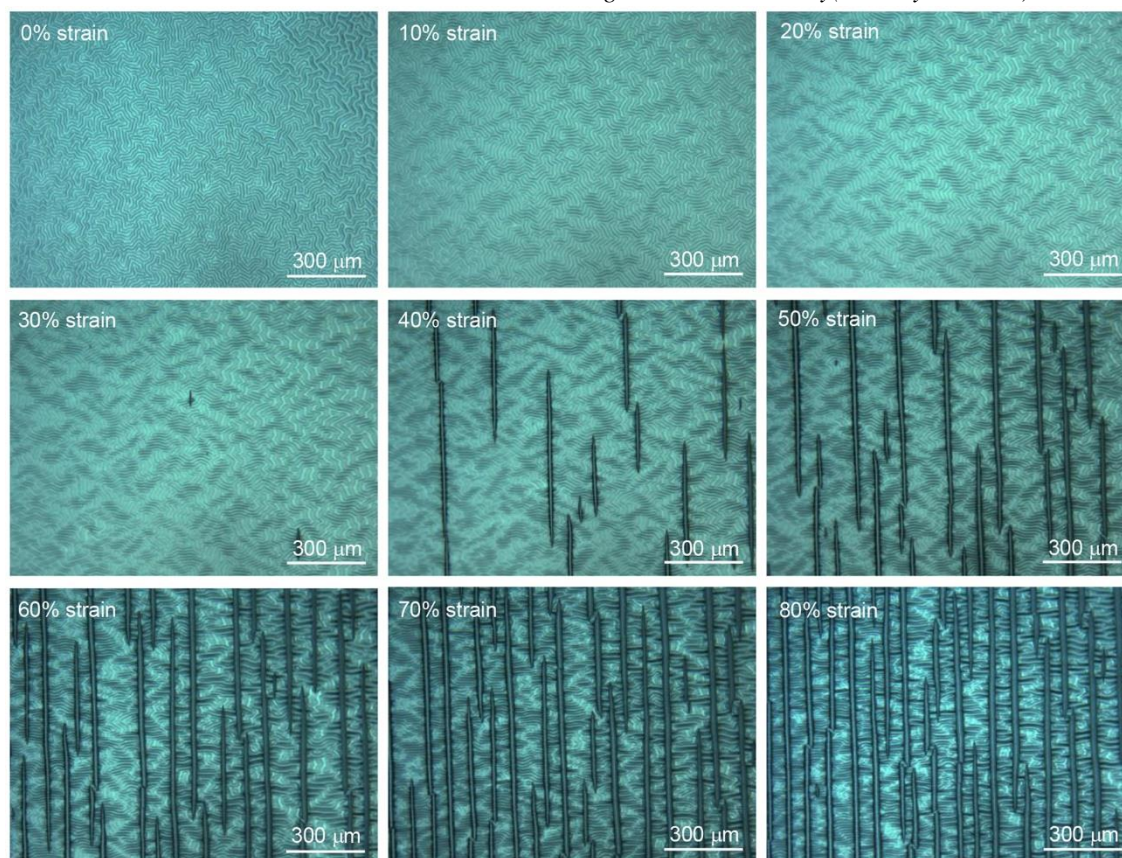
- [16] Xu, S.; Zhang, Y.; Cho, J.; Lee, J.; Huang, X.; Jia, L.; Fan, J. A.; Su, Y.; Su, J.; Zhang, H.; Cheng, H.; Lu, B.; Yu, C.; Chuang, C.; Kim, T.-I. I.; Song, T.; Shigeta, K.; Kang, S.; Dagdeviren, C.; Petrov, I.; Braun, P. V.; Huang, Y.; Paik, U.; Rogers, J. A. Stretchable Batteries with Self-Similar Serpentine Interconnects and Integrated Wireless Recharging Systems. *Nat. Commun.* **2013**, *4*, 1543.
- [17] Mandlik, P.; Lacour, S. P.; Li, J. W.; Chou, S. Y.; Wagner, S. Fully Elastic Interconnects on Nanopatterned Elastomeric Substrates. *IEEE Electron Device Lett.* **2006**, *27*, 650-652.
- [18] Lee, H. B.; Bae, C. W.; Duy, L.; Sohn, I. Y.; Kim, D. I.; Song, Y. J.; Kim, Y. J.; Lee, N. E. Mogul-Patterned Elastomeric Substrate for Stretchable Electronics. *Adv. Mater.* **2016**, *28*, 3069-3077.
- [19] Lambricht, N.; Pardoen, T.; Yunus, S. Giant Stretchability of Thin Gold Films on Rough Elastomeric Substrates. *Acta Mater.* **2013**, *61*, 540-547.
- [20] Guo, R.; Yu, Y.; Zeng, J.; Liu, X.; Zhou, X.; Niu, L.; Gao, T.; Li, K.; Yang, Y.; Zhou, F.; Zheng, Z. Biomimicking Topographic Elastomeric Petals (E-Petals) for Omnidirectional Stretchable and Printable Electronics. *Adv. Sci.* **2015**, *2*, 1400021.
- [21] Zhao, C.; Jia, X.; Shu, K.; Yu, C.; Min, Y.; Wang, C. Stretchability Enhancement of Buckled Polypyrrole Electrode for Stretchable Supercapacitors via Engineering Substrate Surface Roughness. *Electrochim. Acta* **2020**, *343*, 136099.
- [22] Wu, C.; Tang, X.; Gan, L.; Li, W.; Zhang, J.; Wang, H.; Qin, Z.; Zhang, T.; Zhou, T.; Huang, J.; Xie, C.; Zeng, D. High-Adhesion Stretchable Electrode via Cross-Linking Intensified Electroless Deposition on Biomimetic Elastomeric Micropore Film. *ACS Appl. Mater. Interfaces* **2019**, *11*, 20535-20544.
- [23] Filiatrault, H. L.; Carmichael, S. R.; Boutette, R. A.; Carmichael, T. B. A Self-Assembled, Low-Cost, Microstructured Layer for Extremely Stretchable Gold Films. *ACS Appl. Mater. Interfaces* **2015**, *7*, 20745-20752.
- [24] Xu, W.; Yang, J. S.; Lu, T. J. Ductility of Thin Copper Films on Rough Polymer Substrates. *Mater. Des.* **2011**, *32*, 154-161.
- [25] Shih, T.-K.; Ho, J.-R.; Chen, C.-F.; Whang, W.-T.; Chen, C.-C. Topographic Control on Silicone Surface Using Chemical Oxidization Method. *Appl. Surf. Sci.* **2007**, *253*, 9381-9386.

- [26] Watanabe, M.; Mizukami, K. Well-Ordered Wrinkling Patterns on Chemically Oxidized Poly(dimethylsiloxane) Surfaces. *Macromolecules* **2012**, *45*, 7128-7134.
- [27] Genzer, J.; Groenewold, J. Soft Matter with Hard Skin: From Skin Wrinkles to Templating and Material Characterization. *Soft Matter* **2006**, *2*, 310-323.
- [28] Wang, J.-H.; Chen, C.-F.; Ho, J.-R.; Shih, T.-K.; Chen, C.-C.; Whang, W.-T.; Yang, J.-Y. One-Step Fabrication of Surface-Relief Diffusers by Stress-Induced Undulations on Elastomer. *Opt. Laser Technol.* **2009**, *41*, 804-808.
- [29] Gitlin, L.; Schulze, P.; Ohla, S.; Bongard, H. J.; Belder, D. Surface Modification of PDMS Microfluidic Devices by Controlled Sulfuric Acid Treatment and the Application in Chip Electrophoresis. *Electrophoresis* **2015**, *36*, 449-456.
- [30] Yang, Y.; Kim, M.; Park, O. O. Hierarchical Honeycomb-Patterned Polydimethylsiloxane Films with Tunable Nanostructures. *Microelectron. Eng.* **2018**, *195*, 114-120.
- [31] Douville, N. J.; Li, Z. Y.; Takayama, S.; Thouless, M. D. Fracture of Metal Coated Elastomers. *Soft Matter* **2011**, *7*, 6493-6500.
- [32] Seghir, R.; Arscott, S. Controlled Mud-Crack Patterning and Self-Organized Cracking of Polydimethylsiloxane Elastomer Surfaces. *Sci. Rep.* **2015**, *5*.
- [33] Kang, D.; Pikhitsa, P. V.; Choi, Y.; Lee, C.; Shin, S.; Piao, L.; Park, B.; Suh, K.-Y.; Kim, T.-i.; Choi, M. Ultrasensitive Mechanical Crack-Based Sensor Inspired by the Spider Sensory System. *Nature* **2014**, *516*, 222-226.

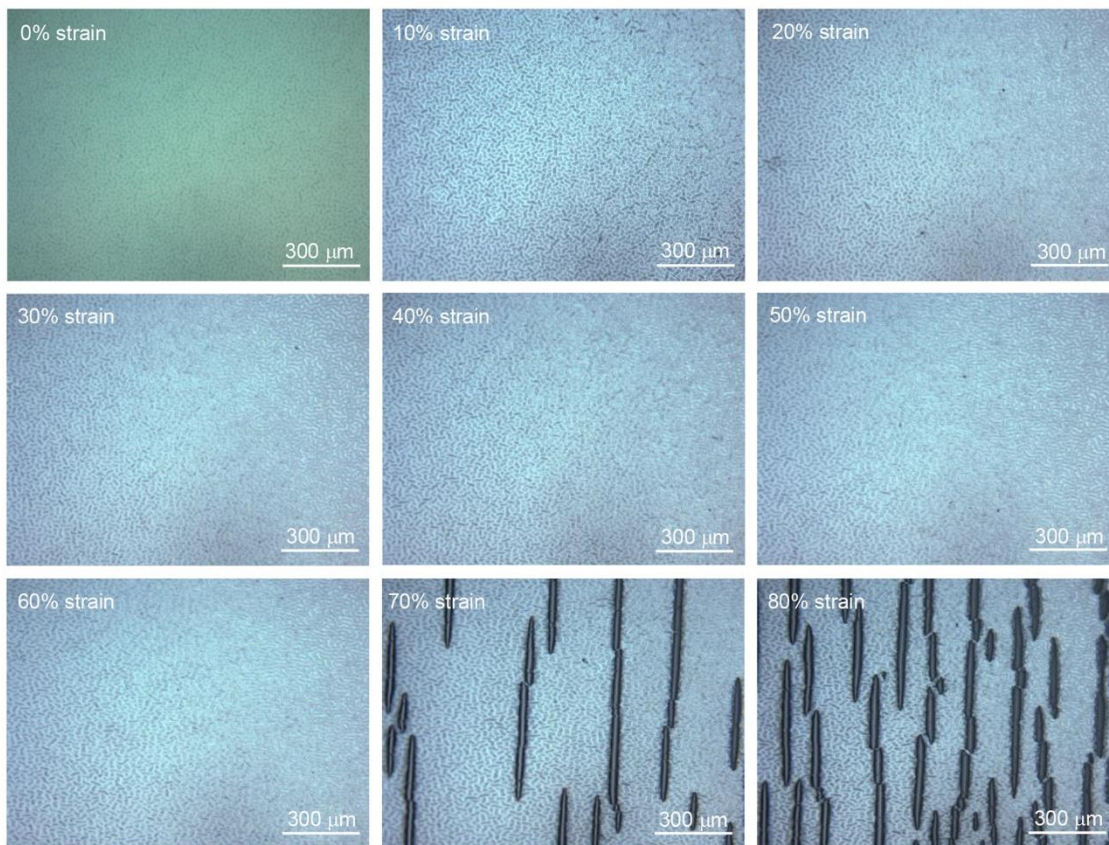
## 5.6 Supporting Information



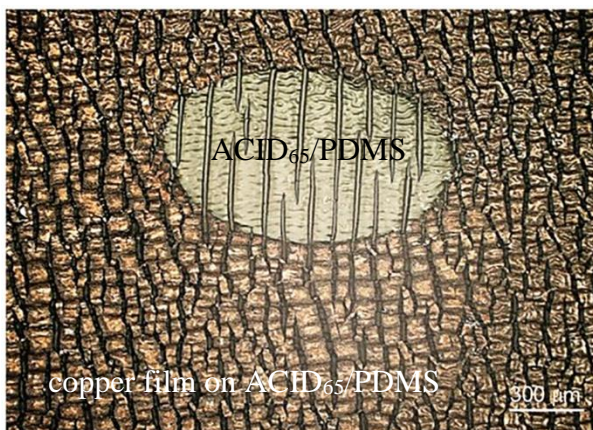
**Figure S5-1** Optical microscope images of uncoated ACID<sub>65</sub>/PDMS under different strains. The sample was stretched in the horizontal direction.



**Figure S5-2** Optical microscope images of uncoated ACID<sub>58</sub>/PDMS under different strains. The sample was stretched in the horizontal direction.



**Figure S5-3** Optical microscope images of uncoated ACID<sub>52</sub>/PDMS under different strains. The sample was stretched in the horizontal direction.



**Figure S5-4** Optical microscope image of the copper film on ACID<sub>65</sub>/PDMS under 40% strain. During ELD of copper on this sample, a bubble or other defect likely prevented the copper deposition on the circular area. The circular area thus reveals the underlying substrate and its response to strain. The sample was stretched in the horizontal direction.

**Chapter 6 Conclusion and Outlook**



One major focus of the research in this dissertation was to advance the e-textile field by developing integration approaches and demonstrating e-textile prototypes, including the design and fabrication of stretchable and conductive textiles, stretchable and durable light-emitting textiles, and stretchable textile battery electrodes. These demonstrations were achieved by conformally depositing functional materials on the textiles using solution-based methods to retain the inherent structure and properties of textiles. The textile structures were further used as an integral part of textile devices rather than just using textiles as substrates. It is worthy to note that the underlying design mechanism that strategically takes advantage of textile architectures for e-textiles fabrication will enrich the methodology/design toolbox for development of e-textiles and possibly inspire additional novel e-textile designs.

While novel integration and fabrication approaches were developed as described in this dissertation to address challenges faced in this emerging research field, e-textile wearables are still in the initial stage and far away from practical applications. Some perspectives on the remaining challenges and future directions in the research field of e-textiles are summarized as follows:

- 1) *Fabrication*: Deposition of functional thin films on textiles can be challenging. For example, depositing thin films on textiles using conventional line-of-sight physical vapor deposition has the shadowing effect due to the 3D and porous structures of textiles, causing discontinuous coatings on the fibers. Printing functional liquid inks onto textiles can stiffen textiles, diminishing softness and wearability. The development of functional materials deposition methods that are compatible with 3D, porous textile structures and also maintain the intrinsic softness and stretchability of the fabric are needed.
- 2) *Performance*: The performance of e-textiles in the relaxed state or under strain is often low. The microstructure of functional materials, the interfacial properties between functional materials and textiles, as well as the device configuration play a big role in device performance. However, the understanding of the underlying mechanisms and rules of high-performance e-textiles is limited. Moreover, it is difficult to compare the performance of e-textiles due to limited characterization standards established for e-textiles. Establishment of standards to characterize e-

textile are needed for comparing and improving the performance of e-textile devices.

- 3) *Durability and safety*: E-textiles are expected to be as durable as our daily clothes are and will have to endure wearing and washing. More studies on the durability of e-textiles in different environmental conditions over long periods, such as washability of e-textiles in standard washing conditions, are needed. The safety of e-textiles also needs to be considered in terms of the biocompatibility of materials and operation of devices since they are mainly used on human bodies. Establishing guidelines for safe biocompatible materials and electrical parameters may be the most important step toward improving the safety of e-textiles.
- 4) *Mass production and commercialization*: Fabrication of large-scale e-textiles is still in the initial stage despite many exciting e-textile prototypes demonstrated by researchers in lab. It will be essential to integrate the e-textile manufacturing process with existing mature textile manufacturing lines for efficient e-textile production. At the current stage, although functionalities like sensing and power have been successfully integrated with textiles, it is still very challenging to fabricate electronic components such as microprocessors and wireless modules based on textiles with performance that is comparable to wafer-based electronics. With the development of silicon-based integrated circuits, electronic devices become smaller and smaller, which makes them easier to integrate with textiles. These can be designed to be located in innocuous locations to eliminate the possible discomfort caused by the rigid components. At the transition stage, a concept that combines wafer-based electronics and textile-based electronics is important to the development of high-performance wearable e-textile systems and will accelerate the speed of e-textiles entering the consumer market. Eventually, we will look forward to the realization of the fully soft and stretchable e-textile system.

Despite many challenges of developing e-textiles, the research efforts in this dissertation contribute to the foundation of this field. Subsequent multidisciplinary efforts are required to address all the challenges for the realization of truly wearable e-textiles which are expected to be robust, high-performance, and comfortable to wear.

Complementary to e-textiles that can be worn on human bodies, e-skin (elastomer-based electronics) can be more intimately integrated with human body, either directly attached on skin or implanted within human bodies. Fabricating elastomer-based metal films for e-skin with desired electrical conductance within different strain ranges is challenging due to the large mechanical mismatch. Creating topography on elastomeric substrates has been used as an approach to engineer cracking patterns of metal films for the desired electrical response. However, the correlation of topography, metal cracking patterns, and resistance change is still not fully understood. The research work of fabricating stretchable metal films using acid-oxidized PDMS substrates in this dissertation will advance this field by providing new different information about how the topography of substrate affects the cracking pattern of the overlying metal film and the corresponding electrical response. Despite this progress, the quantitative relationship between the topography/roughness of substrates, cracking patterns of metal films, and electrical conductance are still not well established; there are also other factors which may play a role in how metal films crack, such as the microstructure of metal films and Young's modulus mismatch ratio, making this system very complex. The vision for this system is that the desired electrical performance will be achieved by rationally designing substrates to induce corresponding cracking patterns of metal films under strain. To achieve this goal, multidisciplinary research will be required including experimental studies to generate empirical data as well as mechanical and electrical modelling studies for better understanding and prediction of this system.

# APPENDICES

## Copyright Permissions

### License Details

This Agreement between Yunyun Wu ("You") and John Wiley and Sons ("John Wiley and Sons") consists of your license details and the terms and conditions provided by John Wiley and Sons and Copyright Clearance Center.

[Print](#) [Copy](#)

License Number	4865020635824
License date	Jul 09, 2020
Licensed Content Publisher	John Wiley and Sons
Licensed Content Publication	Advanced Materials Technologies
Licensed Content Title	Solution Deposition of Conformal Gold Coatings on Knitted Fabric for E-Textiles and Electroluminescent Clothing
Licensed Content Author	Tricia Breen Carmichael, Yiting Chen, Sara S. Mechael, et al
Licensed Content Date	Jan 22, 2018
Licensed Content Volume	3
Licensed Content Issue	3
Licensed Content Pages	7
Type of Use	Dissertation/Thesis
Requestor type	Author of this Wiley article
Format	Print and electronic
Portion	Full article
Will you be translating?	No
Title	New Designs for Wearable Technologies: Stretchable e-Textiles and e-Skin
Institution name	University of Windsor
Expected presentation date	Sep 2020

This is a License Agreement between Yunyun Wu ("You") and Royal Society of Chemistry ("Publisher") provided by Copyright Clearance Center ("CCC"). The license consists of your order details, the terms and conditions provided by Royal Society of Chemistry, and the CCC terms and conditions.

All payments must be made in full to CCC.

Order Date	15-Jul-2020	Type of Use	Republish in a thesis/dissertation
Order license ID	1048680-1	Publisher	ROYAL SOCIETY OF CHEMISTRY
ISSN	1460-4744	Portion	Chart/graph/table/figure

#### LICENSED CONTENT

Publication Title	Chemical Society reviews	Publication Type	e-Journal
Article Title	Materials and structural designs of stretchable conductors.	Start Page	2946
Author/Editor	Royal Society of Chemistry (Great Britain)	End Page	2966
Date	01/01/1972	Issue	11
Language	English	Volume	48
Country	United Kingdom of Great Britain and Northern Ireland	URL	http://www.rsc.org/csr
Rightsholder	Royal Society of Chemistry		

#### REQUEST DETAILS

Portion Type	Chart/graph/table/figure	Distribution	Worldwide
Number of charts / graphs / tables / figures requested	1	Translation	Original language of publication
Format (select all that apply)	Print, Electronic	Copies for the disabled?	Yes
Who will republish the content?	Academic institution	Minor editing privileges?	Yes
Duration of Use	Life of current edition	Incidental promotional use?	Yes
Lifetime Unit Quantity	More than 2,000,000	Currency	CAD
Rights Requested	Main product		

#### NEW WORK DETAILS

Title	New Designs for Wearable Technologies: Stretchable e-Textiles and e-Skin	Institution name	University of Windsor
Instructor name	Prof. Tricia Breen Carmichael	Expected presentation date	2020-09-21

#### ADDITIONAL DETAILS

Order reference number	N/A	The requesting person / organization to appear on the license	Yunyun Wu
------------------------	-----	---	-----------

#### REUSE CONTENT DETAILS

Title, description or numeric reference of the portion(s)	Figure 1	Title of the article/chapter the portion is from	Materials and structural designs of stretchable conductors.
Editor of portion(s)	N/A	Author of portion(s)	Someya, Takao; Bao, Zhenan; Chen, Xiaodong; Matsuhisa, Naoji
Volume of serial or monograph	48	Issue, if republishing an article from a serial	11
Page or page range of portion	2946-2966	Publication date of portion	2019-05-10

## License Details

This Agreement between Yunyun Wu ("You") and AIP Publishing ("AIP Publishing") consists of your license details and the terms and conditions provided by AIP Publishing and Copyright Clearance Center.

[Print](#) [Copy](#)

License Number	4870410763992
License date	Jul 15, 2020
Licensed Content Publisher	AIP Publishing
Licensed Content Publication	Applied Physics Letters
Licensed Content Title	High ductility of a metal film adherent on a polymer substrate
Licensed Content Author	Yong Xiang, Teng Li, Zhigang Suo, et al
Licensed Content Date	Oct 17, 2005
Licensed Content Volume	87
Licensed Content Issue	16
Type of Use	Thesis/Dissertation
Requestor type	Student
Format	Print and electronic
Portion	Figure/Table
Number of figures/tables	1
Title	New Designs for Wearable Technologies: Stretchable e-Textiles and e-Skin
Institution name	University of Windsor
Expected presentation date	Sep 2020
Portions	Figure 1



RightsLink®



Home



Help



Email Support



Yunyun Wu ▾

### A Self-Assembled, Low-Cost, Microstructured Layer for Extremely Stretchable Gold Films



**Author:** Heather L. Filatrault, R. Stephen Carmichael, Rachel A. Boutette, et al

**Publication:** Applied Materials

**Publisher:** American Chemical Society

**Date:** Sep 1, 2015

*Copyright © 2015, American Chemical Society*

#### PERMISSION/LICENSE IS GRANTED FOR YOUR ORDER AT NO CHARGE

This type of permission/license, instead of the standard Terms & Conditions, is sent to you because no fee is being charged for your order. Please note the following:

- Permission is granted for your request in both print and electronic formats, and translations.
  - If figures and/or tables were requested, they may be adapted or used in part.
  - Please print this page for your records and send a copy of it to your publisher/graduate school.
  - Appropriate credit for the requested material should be given as follows: "Reprinted (adapted) with permission from (COMPLETE REFERENCE CITATION). Copyright (YEAR) American Chemical Society." Insert appropriate information in place of the capitalized words.
  - One-time permission is granted only for the use specified in your request. No additional uses are granted (such as derivative works or other editions). For any other uses, please submit a new request.
- If credit is given to another source for the material you requested, permission must be obtained from that source.

[BACK](#)

[CLOSE WINDOW](#)

## License Details

This Agreement between Yunyun Wu ("You") and AIP Publishing ("AIP Publishing") consists of your license details and the terms and conditions provided by AIP Publishing and Copyright Clearance Center.

[Print](#) [Copy](#)

License Number	4865660042701
License date	Jul 10, 2020
Licensed Content Publisher	AIP Publishing
Licensed Content Publication	Applied Physics Letters
Licensed Content Title	Stretchable gold conductors on elastomeric substrates
Licensed Content Author	Stéphanie Périchon Lacour, Sigurd Wagner, Zhenyu Huang, et al
Licensed Content Date	Apr 14, 2003
Licensed Content Volume	82
Licensed Content Issue	15
Type of Use	Thesis/Dissertation
Requestor type	Student
Format	Print and electronic
Portion	Figure/Table
Number of figures/tables	1
Title	New Designs for Wearable Technologies: Stretchable e-Textiles and e-Skin
Institution name	University of Windsor
Expected presentation date	Sep 2020
Order reference number	4
Portions	Figure 1



### Design and performance of thin metal film interconnects for skin-like electronic circuits

Author: S.P. Lacour  
Publication: IEEE Electron Device Letters  
Publisher: IEEE  
Date: April 2004

Copyright © 2004, IEEE

#### Thesis / Dissertation Reuse

The IEEE does not require individuals working on a thesis to obtain a formal reuse license, however, you may print out this statement to be used as a permission grant:

*Requirements to be followed when using any portion (e.g., figure, graph, table, or textual material) of an IEEE copyrighted paper in a thesis:*

- 1) In the case of textual material (e.g., using short quotes or referring to the work within these papers) users must give full credit to the original source (author, paper, publication) followed by the IEEE copyright line © 2011 IEEE.
- 2) In the case of illustrations or tabular material, we require that the copyright line © [Year of original publication] IEEE appear prominently with each reprinted figure and/or table.
- 3) If a substantial portion of the original paper is to be used, and if you are not the senior author, also obtain the senior author's approval.

*Requirements to be followed when using an entire IEEE copyrighted paper in a thesis:*

- 1) The following IEEE copyright/ credit notice should be placed prominently in the references: © [year of original publication] IEEE. Reprinted, with permission, from [author names, paper title, IEEE publication title, and month/year of publication]
- 2) Only the accepted version of an IEEE copyrighted paper can be used when posting the paper or your thesis on-line.
- 3) In placing the thesis on the author's university website, please display the following message in a prominent place on the website: In reference to IEEE copyrighted material which is used with permission in this thesis, the IEEE does not endorse any of [university/educational entity's name goes here]'s products or services. Internal or personal use of this material is permitted. If interested in reprinting/republishing IEEE copyrighted material for advertising or promotional purposes or for creating new collective works for resale or redistribution, please go to [http://www.ieee.org/publications\\_standards/publications/rights/rights\\_link.html](http://www.ieee.org/publications_standards/publications/rights/rights_link.html) to learn how to obtain a License from RightsLink.

If applicable, University Microfilms and/or ProQuest Library, or the Archives of Canada may supply single copies of the dissertation.

This is a License Agreement between Yunyun Wu ("You") and Royal Society of Chemistry ("Publisher") provided by Copyright Clearance Center ("CCC"). The license consists of your order details, the terms and conditions provided by Royal Society of Chemistry, and the CCC terms and conditions.

All payments must be made in full to CCC.

<b>Order Date</b>	15-Jul-2020	<b>Type of Use</b>	Republish in a thesis/dissertation
<b>Order license ID</b>	1048693-1	<b>Publisher</b>	ROYAL SOCIETY OF CHEMISTRY
<b>ISSN</b>	1744-6848	<b>Portion</b>	Chart/graph/table/figure

#### LICENSED CONTENT

<b>Publication Title</b>	Soft matter	<b>Publication Type</b>	e-Journal
<b>Article Title</b>	Isotropically stretchable gold conductors on elastomeric substrates	<b>Start Page</b>	7177
<b>Author/Editor</b>	Royal Society of Chemistry (Great Britain)	<b>End Page</b>	7180
<b>Date</b>	06/01/2005	<b>Issue</b>	16
<b>Language</b>	English	<b>Volume</b>	7
<b>Country</b>	United Kingdom of Great Britain and Northern Ireland	<b>URL</b>	http://www.rsc.org/Publishing/Journals/s...
<b>Rightholder</b>	Royal Society of Chemistry		

#### REQUEST DETAILS

<b>Portion Type</b>	Chart/graph/table/figure	<b>Distribution</b>	Worldwide
<b>Number of charts / graphs / tables / figures requested</b>	1	<b>Translation</b>	Original language of publication
<b>Format (select all that apply)</b>	Print, Electronic	<b>Copies for the disabled?</b>	Yes
<b>Who will republish the content?</b>	Academic institution	<b>Minor editing privileges?</b>	Yes
<b>Duration of Use</b>	Life of current edition	<b>Incidental promotional use?</b>	Yes
<b>Lifetime Unit Quantity</b>	More than 2,000,000	<b>Currency</b>	CAD
<b>Rights Requested</b>	Main product		

#### NEW WORK DETAILS

<b>Title</b>	New Designs for Wearable Technologies: Stretchable e-Textiles and e-Skin	<b>Institution name</b>	University of Windsor
<b>Instructor name</b>	Prof. Tricia Breen Carmichael	<b>Expected presentation date</b>	2020-09-21

#### ADDITIONAL DETAILS

<b>Order reference number</b>	N/A	<b>The requesting person / organization to appear on the license</b>	Yunyun Wu
-------------------------------	-----	--	-----------

#### REUSE CONTENT DETAILS

<b>Title, description or numeric reference of the portion(s)</b>	Figure 3	<b>Title of the article/chapter the portion is from</b>	Isotropically stretchable gold conductors on elastomeric substrates
<b>Editor of portion(s)</b>	N/A	<b>Author of portion(s)</b>	Wagner, Sigurd; Cao, Wenzhe; Görrn, Patrick
<b>Volume of serial or monograph</b>	7	<b>Issue, if republishing an article from a serial</b>	16
<b>Page or page range of portion</b>	7177-7180	<b>Publication date of portion</b>	2011-07-05



## License Details

This Agreement between Yunyun Wu ("You") and John Wiley and Sons ("John Wiley and Sons") consists of your license details and the terms and conditions provided by John Wiley and Sons and Copyright Clearance Center.

[Print](#) [Copy](#)

License Number	4866050815854
License date	Jul 11, 2020
Licensed Content Publisher	John Wiley and Sons
Licensed Content Publication	Advanced Materials
Licensed Content Title	High-Conductivity Elastomeric Electronics
Licensed Content Author	D. S. Gray, J. Tien, C. S. Chen
Licensed Content Date	Feb 18, 2004
Licensed Content Volume	16
Licensed Content Issue	5
Licensed Content Pages	5
Type of Use	Dissertation/Thesis
Requestor type	University/Academic
Format	Print and electronic
Portion	Figure/table
Number of figures/tables	1
Will you be translating?	No
Title	New Designs for Wearable Technologies: Stretchable e-Textiles and e-Skin
Institution name	University of Windsor
Expected presentation date	Sep 2020
Order reference number	5
Portions	Figure 3

## License Details

This Agreement between Yunyun Wu ("You") and Springer Nature ("Springer Nature") consists of your license details and the terms and conditions provided by Springer Nature and Copyright Clearance Center.

[Print](#) [Copy](#)

License Number	4866051412619
License date	Jul 11, 2020
Licensed Content Publisher	Springer Nature
Licensed Content Publication	Nature Communications
Licensed Content Title	Stretchable batteries with self-similar serpentine interconnects and integrated wireless recharging systems
Licensed Content Author	Sheng Xu et al
Licensed Content Date	Feb 26, 2013
Type of Use	Thesis/Dissertation
Requestor type	academic/university or research institute
Format	print and electronic
Portion	figures/tables/illustrations
Number of figures/tables/illustrations	1
High-res required	no
Will you be translating?	no
Circulation/distribution	50000 or greater
Author of this Springer Nature content	no
Title	New Designs for Wearable Technologies: Stretchable e-Textiles and e-Skin
Institution name	University of Windsor
Expected presentation date	Sep 2020
Order reference number	6
Portions	Figure 2

## License Details

This Agreement between Yunyun Wu ("You") and Elsevier ("Elsevier") consists of your license details and the terms and conditions provided by Elsevier and Copyright Clearance Center.

[Print](#) [Copy](#)

License Number	4866060571968
License date	Jul 11, 2020
Licensed Content Publisher	Elsevier
Licensed Content Publication	Acta Materialia
Licensed Content Title	Giant stretchability of thin gold films on rough elastomeric substrates
Licensed Content Author	N. Lambrecht, T. Pardoën, S. Yunus
Licensed Content Date	Jan 1, 2013
Licensed Content Volume	61
Licensed Content Issue	2
Licensed Content Pages	8
Type of Use	reuse in a thesis/dissertation
Portion	figures/tables/illustrations
Number of figures/tables/illustrations	1
Format	both print and electronic
Are you the author of this Elsevier article?	No
Will you be translating?	No
Title	New Designs for Wearable Technologies: Stretchable e-Textiles and e-Skin
Institution name	University of Windsor
Expected presentation date	Sep 2020
Portions	Figure 3

## License Details

This Agreement between Yunyun Wu ("You") and AIP Publishing ("AIP Publishing") consists of your license details and the terms and conditions provided by AIP Publishing and Copyright Clearance Center.

[Print](#) [Copy](#)

License Number	4866061182559
License date	Jul 11, 2020
Licensed Content Publisher	AIP Publishing
Licensed Content Publication	Applied Physics Letters
Licensed Content Title	Mechanisms of reversible stretchability of thin metal films on elastomeric substrates
Licensed Content Author	Stéphanie P. Lacour, Donald Chan, Sigurd Wagner, et al
Licensed Content Date	May 15, 2006
Licensed Content Volume	88
Licensed Content Issue	20
Type of Use	Thesis/Dissertation
Requestor type	Student
Format	Print and electronic
Portion	Figure/Table
Number of figures/tables	2
Title	New Designs for Wearable Technologies: Stretchable e-Textiles and e-Skin
Institution name	University of Windsor
Expected presentation date	Sep 2020
Portions	Figure 1 and Figure 2

## Heterogeneous Surface Orientation of Solution-Deposited Gold Films Enables Retention of Conductivity with High Strain—A New Strategy for Stretchable Electronics



**Author:** Yiting Chen, Yunyun Wu, Sara S. Mechael, et al

**Publication:** Chemistry of Materials

**Publisher:** American Chemical Society

**Date:** Mar 1, 2019

Copyright © 2019, American Chemical Society

### PERMISSION/LICENSE IS GRANTED FOR YOUR ORDER AT NO CHARGE

This type of permission/license, instead of the standard Terms & Conditions, is sent to you because no fee is being charged for your order. Please note the following:

- Permission is granted for your request in both print and electronic formats, and translations.
  - If figures and/or tables were requested, they may be adapted or used in part.
  - Please print this page for your records and send a copy of it to your publisher/graduate school.
  - Appropriate credit for the requested material should be given as follows: "Reprinted (adapted) with permission from (COMPLETE REFERENCE CITATION). Copyright (YEAR) American Chemical Society." Insert appropriate information in place of the capitalized words.
  - One-time permission is granted only for the use specified in your request. No additional uses are granted (such as derivative works or other editions). For any other uses, please submit a new request.
- If credit is given to another source for the material you requested, permission must be obtained from that source.

### License Details

This Agreement between Yunyun Wu ("You") and John Wiley and Sons ("John Wiley and Sons") consists of your license details and the terms and conditions provided by John Wiley and Sons and Copyright Clearance Center.

[Print](#)
[Copy](#)

License Number	4866071023036
License date	Jul 11, 2020
Licensed Content Publisher	John Wiley and Sons
Licensed Content Publication	Angewandte Chemie International Edition
Licensed Content Title	The Rise of Fiber Electronics
Licensed Content Author	Huisheng Peng, Ye Zhang, Songlin Xie, et al
Licensed Content Date	Jul 17, 2019
Licensed Content Volume	58
Licensed Content Issue	39
Licensed Content Pages	11
Type of Use	Dissertation/Thesis
Requestor type	University/Academic
Format	Print and electronic
Portion	Figure/table
Number of figures/tables	1
Will you be translating?	No
Title	New Designs for Wearable Technologies: Stretchable e-Textiles and e-Skin
Institution name	University of Windsor
Expected presentation date	Sep 2020
Portions	Figure 4

This is a License Agreement between Yunyun Wu ("You") and IOP Publishing, Ltd ("Publisher") provided by Copyright Clearance Center ("CCC"). The license consists of your order details, the terms and conditions provided by IOP Publishing, Ltd, and the CCC terms and conditions.

All payments must be made in full to CCC.

Order Date	16-Jul-2020	Type of Use	Republish in a thesis/dissertation
Order license ID	1048872-1	Publisher	IOP Publishing
ISSN	0964-1726	Portion	Chart/graph/table/figure

#### LICENSED CONTENT

Publication Title	Smart Materials and Structures	Rightholder	IOP Publishing, Ltd
Article Title	Smart fabric sensors and e-textile technologies: a review	Publication Type	Journal
Author/Editor	Institute of Physics (Great Britain), American Institute of Physics., Society of Photo-optical Instrumentation Engineers.	Start Page	053001
Date	01/01/1992	Issue	5
Language	English	Volume	23
Country	United Kingdom of Great Britain and Northern Ireland		

#### REQUEST DETAILS

Portion Type	Chart/graph/table/figure	Distribution	Worldwide
Number of charts / graphs / tables / figures requested	1	Translation	Original language of publication
Format (select all that apply)	Print, Electronic	Copies for the disabled?	Yes
Who will republish the content?	Academic institution	Minor editing privileges?	Yes
Duration of Use	Life of current edition	Incidental promotional use?	No
Lifetime Unit Quantity	More than 2,000,000	Currency	CAD
Rights Requested	Main product		

#### NEW WORK DETAILS

Title	New Designs for Wearable Technologies: Stretchable e-Textiles and e-Skin	Institution name	University of Windsor
Instructor name	Prof. Tricia Breen Carmichael	Expected presentation date	2020-09-21

#### ADDITIONAL DETAILS

Order reference number	N/A	The requesting person / organization to appear on the license	Yunyun Wu
------------------------	-----	---	-----------

#### REUSE CONTENT DETAILS

Title, description or numeric reference of the portion(s)	Figure 1	Title of the article/chapter the portion is from	Smart fabric sensors and e-textile technologies: a review
Editor of portion(s)	N/A	Author of portion(s)	Castano, Lina M; Flatau, Alison B
Volume of serial or monograph	23	Issue, if republishing an article from a serial	5
Page or page range of portion	053001	Publication date of portion	2014-04-01



### Electrical characterization of textile transmission lines

Author: D. Cottet  
Publication: Advanced Packaging, IEEE Transactions on  
Publisher: IEEE  
Date: May 2003

Copyright © 2003, IEEE

#### Thesis / Dissertation Reuse

The IEEE does not require individuals working on a thesis to obtain a formal reuse license, however, you may print out this statement to be used as a permission grant:

*Requirements to be followed when using any portion (e.g., figure, graph, table, or textual material) of an IEEE copyrighted paper in a thesis:*

- 1) In the case of textual material (e.g., using short quotes or referring to the work within these papers) users must give full credit to the original source (author, paper, publication) followed by the IEEE copyright line © 2011 IEEE.
- 2) In the case of illustrations or tabular material, we require that the copyright line © [Year of original publication] IEEE appear prominently with each reprinted figure and/or table.
- 3) If a substantial portion of the original paper is to be used, and if you are not the senior author, also obtain the senior author's approval.

*Requirements to be followed when using an entire IEEE copyrighted paper in a thesis:*

- 1) The following IEEE copyright/ credit notice should be placed prominently in the references: © [year of original publication] IEEE. Reprinted, with permission, from [author names, paper title, IEEE publication title, and month/year of publication]
- 2) Only the accepted version of an IEEE copyrighted paper can be used when posting the paper or your thesis on-line.
- 3) In placing the thesis on the author's university website, please display the following message in a prominent place on the website: In reference to IEEE copyrighted material which is used with permission in this thesis, the IEEE does not endorse any of [university/educational entity's name goes here]'s products or services. Internal or personal use of this material is permitted. If interested in reprinting/republishing IEEE copyrighted material for advertising or promotional purposes or for creating new collective works for resale or redistribution, please go to [http://www.ieee.org/publications\\_standards/publications/rights/rights\\_link.html](http://www.ieee.org/publications_standards/publications/rights/rights_link.html) to learn how to obtain a License from RightsLink.

If applicable, University Microfilms and/or ProQuest Library, or the Archives of Canada may supply single copies of the dissertation.



Home



Help



Email Support



Yunyun Wu ▾



#### A stretchable knitted interconnect for three-dimensional curvilinear surfaces

Author: Qiao Li, Xiaoming Tao  
Publication: Textile Research Journal  
Publisher: SAGE Publications  
Date: 07/01/2011

Copyright © 2011, © SAGE Publications

#### Gratis Reuse

Permission is granted at no cost for use of content in a Master's Thesis and/or Doctoral Dissertation, subject to the following limitations. You may use a single excerpt or up to 3 figures/tables. If you use more than those limits, or intend to distribute or sell your Master's Thesis/Doctoral Dissertation to the general public through print or website publication, please return to the previous page and select 'Republish in a Book/Journal' or 'Post on intranet/password-protected website' to complete your request.

[BACK](#)

[CLOSE WINDOW](#)

This is a License Agreement between Yunyun Wu ("You") and Royal Society of Chemistry ("Publisher") provided by Copyright Clearance Center ("CCC"). The license consists of your order details, the terms and conditions provided by Royal Society of Chemistry, and the CCC terms and conditions.

All payments must be made in full to CCC.

<b>Order Date</b>	16-Jul-2020	<b>Type of Use</b>	Republish in a thesis/dissertation
<b>Order license ID</b>	1048887-1	<b>Publisher</b>	Royal Society of Chemistry
<b>ISSN</b>	2050-7534	<b>Portion</b>	Chart/graph/table/figure

#### LICENSED CONTENT

<b>Publication Title</b>	Journal of materials chemistry. C, Materials for optical and electronic devices	<b>Publication Type</b>	e-Journal
<b>Article Title</b>	Glycerol/PEDOT:PSS coated woven fabric as a flexible heating element on textiles Electronic supplementary information (ESI) available: Additional information about the set-up of the electrochemical cell and Joule heating experiments. SEM and EDS images of the plasma treated polyamide 6,6. Additional discussion, XRD and SEM about the effect of the temperature on the current drop at high voltages. See DOI: Web: 10.1039/c7tc00486a	<b>Start Page</b>	3807
<b>Author/Editor</b>	Royal Society of Chemistry (Great Britain)	<b>End Page</b>	3822
<b>Date</b>	01/01/2013	<b>Issue</b>	15
<b>Language</b>	English	<b>Volume</b>	5
<b>Country</b>	United Kingdom of Great Britain and Northern Ireland	<b>URL</b>	<a href="http://pubs.rsc.org/en/journals/journaliss...">http://pubs.rsc.org/en/journals/journaliss...</a>
<b>Rightsholder</b>	Royal Society of Chemistry		

#### REQUEST DETAILS

<b>Portion Type</b>	Chart/graph/table/figure	<b>Distribution</b>	Worldwide
<b>Number of charts / graphs / tables / figures requested</b>	1	<b>Translation</b>	Original language of publication
<b>Format (select all that apply)</b>	Print, Electronic	<b>Copies for the disabled?</b>	Yes
<b>Who will republish the content?</b>	Academic institution	<b>Minor editing privileges?</b>	Yes
<b>Duration of Use</b>	Life of current edition	<b>Incidental promotional use?</b>	Yes
<b>Lifetime Unit Quantity</b>	More than 2,000,000	<b>Currency</b>	CAD
<b>Rights Requested</b>	Main product		

#### NEW WORK DETAILS

<b>Title</b>	New Designs for Wearable Technologies: Stretchable e-Textiles and e-Skin	<b>Institution name</b>	University of Windsor
<b>Instructor name</b>	Prof. Tricia Breen Carmichael	<b>Expected presentation date</b>	2020-09-21

#### ADDITIONAL DETAILS

<b>Order reference number</b>	N/A	<b>The requesting person / organization to appear on the license</b>	Yunyun Wu
-------------------------------	-----	--	-----------

#### REUSE CONTENT DETAILS

<b>Title, description or numeric reference of the portion(s)</b>	Figure 6	<b>Title of the article/chapter the portion is from</b>	Glycerol/PEDOT:PSS coated woven fabric as a flexible heating element on textiles
<b>Editor of portion(s)</b>	N/A	<b>Author of portion(s)</b>	Zille, Andrea; Esteves, Maria F.; Santos, Washington L. F.; Souto, Antonio P.; Paleo, Antonio J.; Vieira, Eliana M. F.; Martins, Marcos S.; Toptan, Fatih; Alves, Alexandra C.; Moraes, Maria R.
<b>Volume of serial or monograph</b>	5	<b>Issue, if republishing an article from a serial</b>	15
<b>Page or page range of portion</b>	3807-3822	<b>Publication date of portion</b>	2017-03-23

## License Details

This Agreement between Yunyun Wu ("You") and John Wiley and Sons ("John Wiley and Sons") consists of your license details and the terms and conditions provided by John Wiley and Sons and Copyright Clearance Center.

[Print](#) [Copy](#)

License Number	4866110711540
License date	Jul 11, 2020
Licensed Content Publisher	John Wiley and Sons
Licensed Content Publication	Advanced Materials
Licensed Content Title	Enhancing the Performance of Stretchable Conductors for E-Textiles by Controlled Ink Permeation
Licensed Content Author	Takao Someya, Tomoyuki Yokota, Mohammad Abbas, et al
Licensed Content Date	Mar 29, 2017
Licensed Content Volume	29
Licensed Content Issue	21
Licensed Content Pages	8
Type of Use	Dissertation/Thesis
Requestor type	University/Academic
Format	Print and electronic
Portion	Figure/table
Number of figures/tables	1
Will you be translating?	No
Title	New Designs for Wearable Technologies: Stretchable e-Textiles and e-Skin
Institution name	University of Windsor
Expected presentation date	Sep 2020
Portions	Figure 3

## License Details

This Agreement between Yunyun Wu ("You") and John Wiley and Sons ("John Wiley and Sons") consists of your license details and the terms and conditions provided by John Wiley and Sons and Copyright Clearance Center.

[Print](#) [Copy](#)

License Number	4866111079797
License date	Jul 11, 2020
Licensed Content Publisher	John Wiley and Sons
Licensed Content Publication	Advanced Functional Materials
Licensed Content Title	Rugged Textile Electrodes for Wearable Devices Obtained by Vapor Coating Off-the-Shelf, Plain-Woven Fabrics
Licensed Content Author	Trisha L. Andrew, Marianne Fairbanks, Lushuai Zhang
Licensed Content Date	May 2, 2017
Licensed Content Volume	27
Licensed Content Issue	24
Licensed Content Pages	9
Type of Use	Dissertation/Thesis
Requestor type	University/Academic
Format	Print and electronic
Portion	Figure/table
Number of figures/tables	1
Will you be translating?	No
Title	New Designs for Wearable Technologies: Stretchable e-Textiles and e-Skin
Institution name	University of Windsor
Expected presentation date	Sep 2020
Portions	Figure 4

## License Details

This Agreement between Yunyun Wu ("You") and Emerald Publishing Limited ("Emerald Publishing Limited") consists of your license details and the terms and conditions provided by Emerald Publishing Limited and Copyright Clearance Center.

[Print](#) [Copy](#)

License Number	4867060269739
License date	Jul 13, 2020
Licensed Content Publisher	Emerald Publishing Limited
Licensed Content Publication	International Journal of Clothing Science and Technology
Licensed Content Title	Light-emitting textile display with floats for electronics covering
Licensed Content Author	Inese Parkova, Ivars Parkovs, Ausma Vilumsone
Licensed Content Date	Mar 2, 2015
Licensed Content Volume	27
Licensed Content Issue	1
Type of Use	Dissertation/Thesis
Requestor type	Academic
Are you the author of the requested content?	No
Format	Print and electronic
Geographic Rights	World rights
Portion	Figures/table/illustration
Number of figures/tables	1
Will you be translating?	No
Title	New Designs for Wearable Technologies: Stretchable e-Textiles and e-Skin
Institution name	University of Windsor
Expected presentation date	Sep 2020
Portions	Figure 6

## License Details

This Agreement between Yunyun Wu ("You") and Elsevier ("Elsevier") consists of your license details and the terms and conditions provided by Elsevier and Copyright Clearance Center.

[Print](#) [Copy](#)

License Number	4866120292107
License date	Jul 11, 2020
Licensed Content Publisher	Elsevier
Licensed Content Publication	Organic Electronics
Licensed Content Title	Soft fabric-based flexible organic light-emitting diodes
Licensed Content Author	Woohyun Kim, Seonil Kwon, Sung-Min Lee, Jin Yeong Kim, Yunchool Han, Eungtaek Kim, Kyung Cheol Choi, Sungmee Park, Byoung-Cheul Park
Licensed Content Date	Nov 1, 2013
Licensed Content Volume	14
Licensed Content Issue	11
Licensed Content Pages	7
Type of Use	reuse in a thesis/dissertation
Portion	figures/tables/illustrations
Number of figures/tables/illustrations	1
Format	both print and electronic
Are you the author of this Elsevier article?	No
Will you be translating?	No
Title	New Designs for Wearable Technologies: Stretchable e-Textiles and e-Skin
Institution name	University of Windsor
Expected presentation date	Sep 2020
Portions	Figure 1



This is a License Agreement between Yunyun Wu ("You") and Royal Society of Chemistry ("Publisher") provided by Copyright Clearance Center ("CCC"). The license consists of your order details, the terms and conditions provided by Royal Society of Chemistry, and the CCC terms and conditions.

All payments must be made in full to CCC.

Order Date	16-Jul-2020	Type of Use	Republish in a thesis/dissertation
Order license ID	1048987-1	Publisher	Royal Society of Chemistry
ISSN	2050-7534	Portion	Chart/graph/table/figure

#### LICENSED CONTENT

Publication Title	Journal of materials chemistry. C, Materials for optical and electronic devices	Publication Type	e-Journal
Article Title	A stretchable and sensitive light-emitting fabric Electronic supplementary information (ESI) available. See DOI: Web: 10.1039/c6tc05156a	Start Page	4139
Author/Editor	Royal Society of Chemistry (Great Britain)	End Page	4144
Date	01/01/2013	Issue	17
Language	English	Volume	5
Country	United Kingdom of Great Britain and Northern Ireland	URL	http://pubs.rsc.org/en/journals/journaliss...
Rightsholder	Royal Society of Chemistry		

#### REQUEST DETAILS

Portion Type	Chart/graph/table/figure	Distribution	Worldwide
Number of charts / graphs / tables / figures requested	1	Translation	Original language of publication
Format (select all that apply)	Print, Electronic	Copies for the disabled?	Yes
Who will republish the content?	Academic institution	Minor editing privileges?	Yes
Duration of Use	Life of current edition	Incidental promotional use?	Yes
Lifetime Unit Quantity	More than 2,000,000	Currency	CAD
Rights Requested	Main product		

#### NEW WORK DETAILS

Title	New Designs for Wearable Technologies: Stretchable e-Textiles and e-Skin	Institution name	University of Windsor
Instructor name	Prof. Tricia Breen Carmichael	Expected presentation date	2020-09-21

#### ADDITIONAL DETAILS

Order reference number	N/A	The requesting person / organization to appear on the license	Yunyun Wu
------------------------	-----	---	-----------

#### REUSE CONTENT DETAILS

Title, description or numeric reference of the portion(s)	Figure 3	Title of the article/chapter the portion is from	A stretchable and sensitive light-emitting fabric
Editor of portion(s)	N/A	Author of portion(s)	Zhang, Zhitao; Shi, Xiang; Lou, Huiqing; Xu, Yifan; Zhang, Jing; Li, Yiming; Cheng, Xunliang; Peng, Huisheng
Volume of serial or monograph	5	Issue, if republishing an article from a serial	17
Page or page range of portion	4139-4144	Publication date of portion	2017-01-05

#### Wearable Textile Battery Rechargeable by Solar Energy

Author: Yong-Hee Lee, Joo-Seong Kim, Jonghyeon Noh, et al

Publication: Nano Letters

Publisher: American Chemical Society

Date: Nov 1, 2013

Copyright © 2013, American Chemical Society



#### PERMISSION/LICENSE IS GRANTED FOR YOUR ORDER AT NO CHARGE

This type of permission/license, instead of the standard Terms & Conditions, is sent to you because no fee is being charged for your order. Please note the following:

- Permission is granted for your request in both print and electronic formats, and translations.
- If figures and/or tables were requested, they may be adapted or used in part.
- Please print this page for your records and send a copy of it to your publisher/graduate school.
- Appropriate credit for the requested material should be given as follows: "Reprinted (adapted) with permission from (COMPLETE REFERENCE CITATION). Copyright (YEAR) American Chemical Society." Insert appropriate information in place of the capitalized words.
- One-time permission is granted only for the use specified in your request. No additional uses are granted (such as derivative works or other editions). For any other uses, please submit a new request.
- If credit is given to another source for the material you requested, permission must be obtained from that source.

## License Details

This Agreement between Yunyun Wu ("You") and Elsevier ("Elsevier") consists of your license details and the terms and conditions provided by Elsevier and Copyright Clearance Center.

[Print](#) [Copy](#)

License Number	4866131499247
License date	Jul 11, 2020
Licensed Content Publisher	Elsevier
Licensed Content Publication	Extreme Mechanics Letters
Licensed Content Title	Stretchable fabric-based LiCoO <sub>2</sub> , electrode for lithium ion batteries
Licensed Content Author	Bahar Moradi Ghadi, Mengying Yuan, Haleh Ardebili
Licensed Content Date	Oct 1, 2019
Licensed Content Volume	32
Licensed Content Issue	n/a
Licensed Content Pages	1
Type of Use	reuse in a thesis/dissertation
Portion	figures/tables/illustrations
Number of figures/tables/illustrations	1
Format	both print and electronic
Are you the author of this Elsevier article?	No
Will you be translating?	No
Title	New Designs for Wearable Technologies: Stretchable e-Textiles and e-Skin
Institution name	University of Windsor
Expected presentation date	Sep 2020
Portions	Figure 2

## IOP Publishing, Ltd - License Terms and Conditions

This is a License Agreement between Yunyun Wu ("You") and IOP Publishing, Ltd ("Publisher") provided by Copyright Clearance Center ("CCC"). The license consists of your order details, the terms and conditions provided by IOP Publishing, Ltd, and the CCC terms and conditions.

All payments must be made in full to CCC.

Order Date	18-Jul-2020	Type of Use	Republish in a thesis/dissertation
Order license ID	1049235-1	Publisher	Institute of Physics Publishing Ltd.
ISSN	2058-8585	Portion	Excerpt (up to 400 words)

### LICENSED CONTENT

Publication Title	Flexible and Printed Electronics	Country	United Kingdom of Great Britain and Northern Ireland
Date	01/01/2016	Rightsholder	IOP Publishing, Ltd
Language	English	Publication Type	e-Journal

### REQUEST DETAILS

Portion Type	Excerpt (up to 400 words)	Distribution	Worldwide
Number of excerpts	1	Translation	Original language of publication
Format (select all that apply)	Print, Electronic	Copies for the disabled?	Yes
Who will republish the content?	Academic institution	Minor editing privileges?	Yes
Duration of Use	Life of current edition	Incidental promotional use?	No
Lifetime Unit Quantity	More than 2,000,000	Currency	CAD
Rights Requested	Main product		

### NEW WORK DETAILS

Title	New Designs for Wearable Technologies: Stretchable e-Textiles and e-Skin	Institution name	University of Windsor
Instructor name	Prof. Tricia Breen Carmichael	Expected presentation date	2020-09-21

### ADDITIONAL DETAILS

Order reference number	N/A	The requesting person / organization to appear on the license	Yunyun Wu
------------------------	-----	---	-----------

### REUSE CONTENT DETAILS

Title, description or numeric reference of the portion(s)	excerpt from "5. Stretchable metals fabricated using solution-based methods" section	Title of the article/chapter the portion is from	Stretchable metal films
Editor of portion(s)	N/A	Author of portion(s)	Sara S Mechael; Yunyun Wu; Kory Schlingman; Tricia Breen Carmichael
Volume of serial or monograph	3	Issue, if republishing an article from a serial	4
Page or page range of portion	043001	Publication date of portion	2018-11-22

## VITA AUCTORIS

**NAME** Yunyun Wu

**PLACE OF BIRTH** Anhui, China

**EDUCATION** Ph.D. Chemistry, 2015-2020  
University of Windsor, Windsor, Ontario, Canada

B.Sc. Solid-State Electronic Engineering, 2011-2015  
University of Electronic Science and Technology of China  
(UESTC), Chengdu, Sichuan, China

**EXPERIENCE**

**Graduate Research Assistant** 2015 - 2020  
Carmichael Lab, University of Windsor, Canada

**Graduate Teaching Assistant** 2015 - 2020  
Department of Chemistry and Biochemistry, University of Windsor, Canada

**Undergraduate Globalink Research Intern** 2014 Summer  
Carmichael Lab, University of Windsor, Canada

**Undergraduate Research Assistant** 2013 Summer  
State Key Lab of Electronic Films and Integrated Devices, UESTC, China

**AWARDS**

- Research Training Award, Mitacs 2020
- Going Above and Beyond in Research Award, University of Windsor 2020
- Mitacs Globalink Research Award, Mitacs 2019
- New Energy Research Prize, University of Windsor 2019
- Oral Presentation Award, 102<sup>nd</sup> Canadian Chemistry Conference 2019
- Ontario Graduate Scholarship 2019 - 2020
- Poster Presentation Award, 100<sup>th</sup> Canadian Chemistry Conference 2017
- W.A. Redmond Memorial Fund, University of Windsor 2017
- Doctoral International Entrance Scholarship, University of Windsor 2016 - 2020
- Master's International Entrance Scholarship, University of Windsor 2015 - 2016
- Mitacs Globalink Graduate Fellowship, Mitacs 2015 - 2018

- National Scholarship, UESTC 2012 - 2014
- National Encouragement Scholarship, UESTC 2011

## PUBLICATIONS

1. **Yunyun Wu**, Sara S. Mechael, Cecilia Lerma, R. Stephen Carmichael and Tricia Breen Carmichael. Stretchable Ultrasheer Fabrics as Semitransparent Electrodes for Wearable Light-emitting e-Textiles with Changeable Display Patterns. *Matter* **2020**, 2, 882-895.
2. Yiting Chen, **Yunyun Wu**, Sara S. Mechael and Tricia Breen Carmichael. Heterogeneous Surface Orientation of Solution-Deposited Gold Films Enables Retention of Conductivity with High Strain - A New Strategy for Stretchable Electronics. *Chemistry of Materials* **2019**, 31, 1920-1927.
3. **Yunyun Wu**, Sara S. Mechael, Yiting Chen, Tricia Breen Carmichael. Solution Deposition of Conformal Gold Coatings on Knitted Fabric for E-textiles and Electroluminescent Clothing. *Advanced Materials Technologies* **2018**, 3, 1700292.
4. Sara S. Mechael, **Yunyun Wu**, Kory Schlingman and Tricia Breen Carmichael. Stretchable Metal Films. *Flexible and Printed Electronics* **2018**, 3, 043001.
5. Xu, Xu, Yuqi Li, Zhongqiang Xiong, Jin Yang, Lulu Pan, **Yunyun Wu**, Chun Wei, and Shaorong Lu. Preparation and Model of High-Performance Shape-Memory Polyurethane with Hydroxylated Perylene Bisimide. *RSC Advances* **2016**, 6, 110329-110336.
6. Junda Zhong, **Yunyun Wu** and Houbiao Li. Application of Matlab-GUI in Traveling Route Optimization Design. *Experiment Science and Technology* **2013**, 11, 39-41.

## PRESENTATIONS

1. **Yunyun Wu**, Tricia Breen Carmichael. "CuS/Au-Coated Velour Fabric Composite Electrodes – A New Architecture for Stretchable and Wearable Energy Storage." Poster presentation at **2019 Materials Research Society (MRS) Fall Meeting and Exhibit**, Boston, Massachusetts, US.
2. **Yunyun Wu**, Sara S. Mechael, Yiting Chen, Tricia Breen Carmichael. "Low-Cost, Solution-Based Fabrication of Conductive and Stretchable Textiles for Wearable

- Electronics." Poster presentation at **2019 LGBTQ+ STEM Conference**, Windsor, Ontario, Canada.
3. **Yunyun Wu**, Sara S. Mechael, Tricia Breen Carmichael. "Gold-Coated Sheer Fabric Electrodes for Stretchable and Wearable Light-Emitting Textiles." Oral presentation at **2019 Canadian Chemistry Conference and Exhibition (CCCE)**, Quebec City, Quebec, Canada.
  4. **Yunyun Wu**, Sara S. Mechael, Yiting Chen, Tricia Breen Carmichael. "Solution Deposition of Conformal Gold Coatings on Knitted Fabric for E-textiles and Electroluminescent Clothing." Oral presentation at **2018 IEEE International Flexible Electronics Technology Conference (IFETC)**, Ottawa, Ontario, Canada.
  5. **Yunyun Wu**, Sara S. Mechael, Yiting Chen, Tricia Breen Carmichael. "Fabrication of Conductive and Stretchable E-textiles for Wearable Electronics." Oral presentation at **2017 International Mechanical Engineering Congress and Exposition (IMECE)**, Tampa, Florida, US.
  6. **Yunyun Wu**, Sara S. Mechael, Yiting Chen, Tricia Breen Carmichael. "Low-cost, Solution-based Fabrication of Conductive and Stretchable Textiles for Wearable Electronics." Poster presentation at **2017 Canadian Chemistry Conference and Exhibition (CCCE)**, Toronto, Ontario, Canada.